

TABLE OF CONTENTS

CHAPTER 1 INTRODUCTION	1
CHAPTER 2 THEORY BACKGROUND	3
2.1 Introduction	3
2.2 A Three-Layer Waveguide Example	4
2.2.1 Transfer Matrix Method (TMM)	4
2.2.2 Numerical Method Consideration	6
2.3 Theory Introduction	7
2.3.1 Far field and near field	7
2.3.2: Confinement Factor	10
2.4 Running the program	14
2.4.1 Description of layer structure	15
2.4.2 Construction of an input file	16
2.4.3 Description of output parameters and output files.	23
REFERENCES:	30
CHAPTER 3 – MATSYS AND WAVEGUIDE INPUT/OUTPUT PARAMETERS	31
3.1 Introduction	31
3.2 Material System MATSYS	31
3.2.1.1 Al(x)Ga(1-x)As 1	37
3.2.1.2 Al(x)Ga(1-x)As 2	37
3.2.1.5 Al(X)Ga(1-X)In(Y)As(1-Y) 2	37
3.2.1.6 Al(X)Ga(1-X)P(Y)Sb(1-Y) 3.2.1.7 Al(X)Ga(1-X)As(Y)Sb(1-Y)	37
3.2.1.8 Al(X)In(1-X)As(Y)Sb(1-Y)	37
3.2.1.9 Ga(X)In(1-X)P(Y)Sb(1-Y)	38
3.2.1.10 AlAs(X)Sb(1-X)	38
3.2.1.11 Al(x)Ga(1-x))0.5In(0.5)P	38
3.2.1.12 In(1-x)Ga(x)As [matched to InP]	38
3.2.1.13 In(1-x)Ga(x)As [matched to GaAs]	38

3.2.1.15	InGaAsP using PL [matched to InP]	38
3.2.1.16	InGaAsP [matched to InP]	38
3.4	Program Parameters	39
3.4.1	Input Parameters	39
3.4.2	Output Parameters	49
3.5	Summary	50
	References	50
 CHAPTER 4 DISPERSION FOR GLASS SLAB WAVEGUIDES		 52
4.1	Introduction	52
4.1.1	Chromatic dispersion	52
4.1.2	Material System	53
4.2	Calculation of Material Dispersions	53
4.2.1	Formulation	54
4.2.2	Dispersion plot	54
4.3	Calculation of waveguide dispersion	56
4.3.1	Formulation	56
4.3.2	Input file	58
4.3.3	Dispersion plot	59
4.4	Chromatic dispersion from WAVEGUIDE	59
4.4.1	Input file	59
4.4.2	Dispersion plot	60
4.5	Simulation	61
4.5.1	Results	62
4.6	Conclusion	64
	Reference	64
 CHAPTER 5 SYMMETRIC – WAVEGUIDE DIRECTIONAL COUPLER		 65
5.1	Structure of Symmetric-Waveguide Directional Coupler	65

5.2 WAVEGUIDE Simulation of Symmetric-Waveguide Directional Coupler Structure	66
5.2.1 Mode Finding and Propagation Constant Calculation of Single Mode, Two-guide Directional Coupler	67
5.2.2 Field Distribution of Single Mode, Two-guide Directional Coupler	73
5.2.3 Coupling length of Symmetric-waveguide Directional Coupler	77

CHAPTER 6 – INGAAS/ALGAAS/GAAS STRUCTURE WITH GRINSCH AND ALGAAS/ALGAAS/GAAS STRUCTURE WITH MULTIPLE QW EXAMPLES 85

6.1 Introduction	85
6.2 MATSYS Options for AlGaAs/GaAs	85
6.3 Single Quantum Well Structure with GRINSCH at 980 nm	86
6.4 Multiple Quantum Well AlGaAs/AlGaAs/GaAs Structure at 820 nm	103
6.5 Summary	112

CHAPTER 7 INGAASP/INGAASP/INP LASERS 113

7.1 InGaAsP/InGaAsP/InP (1310nm)	113
7.1.1 Introduction	113
7.1.2 Initial input file	113
7.1.3 QZMR looping and modes searching	116
7.1.4. Thickness of SCH layer (SCH-TL) looping	120
7.1.5 Thickness of the p-cladding layer (p-cladding-TL) looping	124
7.1.6 Simulation results	128
7.1.7. The Refractive Index Profile	131
7.2 InGaAsP/InGaAsP/InP (1550nm)	132
7.2.1 Introduction	132
7.2.2 The Initial Input File	133
7.2.3. Searching the Fundamental Mode, Looping for QZMR	135
7.2.4. Looping the SCH layers to find the proper thickness for fundamental mode confinement.	136
7.2.5. Making the Full Structure and Including Loss parameters	138
7.2.6. Output Parameters and Plots	141
7.2.7. The Refractive Index Profile	144

CHAPTER 8	ALINGAAS / INP LASERS	146
8.1	TM-mode 1550-nm Semiconductor Laser Design	147
8.1.1	Introduction	147
8.1.2	The Initial Input File	147
8.1.3	Searching the Fundamental Mode, Looping for QZMR	149
8.1.4	Fundamental Mode Confinement and GRIN Looping	151
8.1.5	Building the Full Structure with Loss Parameters	153
8.1.6	Inner Cladding Optimization to Minimize Loss	155
8.1.7	Cladding Optimization to Minimize Loss	156
8.1.8	Output Parameters and Plots	157
8.2	TE-mode 1310 nm Semiconductor Laser Design	159
8.2.1	Introduction	159
8.2.2.	The Initial Input File	160
8.2.3.	Searching the Fundamental Mode, Looping for QZMR	160
8.2.4.	Looping the SCH layers to find the proper thickness for the fundamental mode confinement.	162
8.2.5.	Making the Full Structure and Including Loss parameters	164
8.2.6.	Output Parameters and Plots	166
8.2.7.	The Refractive Index Profile	169
REFERENCES:		170
CHAPTER 9	TE-MODE, 635-NM RED LASER OPTIMIZATION	171
9.1	The Initial Input File and Layer Parameters	171
9.2	Modes Searching, Looping for QZMR	173
9.3	SCH Thickness Determination to Achieve Desired Quantum Well Confinement Factor (GAMMA) and Full-Width-Half-Power Far Field (FWHPF)	175
9.4	Cladding Thickness Determination to Minimize the Loss	179
CHAPTER 10	ASYMMETRIC WAVEGUIDE NITRIDE LASERS	184
10.1	Introduction	184
10.1.1	Asymmetric Waveguide Structure	185
10.2	Structure Analysis	186

10.2.1	Material System	187
10.2.2	Semi-infinite cladding layer	187
10.2.3	Finite n-cladding layer	191
10.3	Output Plots	197
10.3.1	Near field	197
10.3.2	Confinement factor for semi- ∞ and finite cladding layer	198
10.4	Conclusion	200
	Reference	200

CHAPTER 11 DESIGN A RIDGE WAVEGUIDE LASER USING WAVEGUIDE PROGRAM **201**

11.1	Outline and explanations of the design	202
11.1.1	Design a basic waveguide laser	202
11.1.2	Position of an etch stop layer: Δn_{eff} vs. p-spacer thickness	204
11.1.3	Determine ridge width and channel width.	205
11.2	Simulations details for the design of a ridge waveguide laser using WAVEGUIDE program	208
11.2.1	Design of a basic waveguide laser	209
11.2.2	Position of an etch stop layer, Δn_{eff} vs. p-spacer thickness	216
11.2.3	Determine ridge width and channel width.	222
11.2.4	Summary	232
11.3	Summary of the chapter	234
	REFERENCES:	234

CHAPTER 12 POLYMER WAVEGUIDE INTEGRATED ISOLATORS **235**

12.1	Statement of the problem	235
12.2	The RLE Concept	237
12.3	Input File for the Quartz Waveguide Isolator	238
12.4	Quartz Waveguide Isolator	241
12.5	Quartz Waveguide Polarizer	245

12.6 Quartz Waveguide Wavelength Filter	248
---	-----

CHAPTER 13 FURTHER APPLICATION OF WAVEGUIDE MODES CALCULATION	----LEAKY	251
--	------------------	------------

13.1 Introduction	251
-------------------	-----

13.2 Calculation of a Three-Layer Waveguide	252
---	-----

13.2.1 Input file	253
-------------------	-----

13.2.2 Output file	255
--------------------	-----

13.2.3 Loss Calculation	257
-------------------------	-----

13.3 Calculation of a Five-Layer Waveguide	258
--	-----

REFERENCES:	262
-------------	-----

CHAPTER 14. EFFECTS OF METAL COVER ON SEMICONDUCTOR LASERS	263
---	------------

14.1. Metal covered slab waveguide in semiconductor lasers	263
--	-----

14.1.1. Introduction	263
----------------------	-----

14.1.2. The input file for wing region	263
--	-----

14.1.3. Result of evaluation	264
------------------------------	-----

14.1.4. Fundamental mode in wing region	265
---	-----

14.1.5. Fundamental mode in ridge region	266
--	-----

14.1.6. Result analysis	268
-------------------------	-----

14.1.6. Result analysis	268
-------------------------	-----

14.2 Ridge waveguide with metal covers	268
--	-----

14.3 Counterpart ridge waveguide without metal cover	270
--	-----

14.3.1 Fundamental mode in wing region	270
--	-----

14.3.2 Fundamental mode in ridge region	271
---	-----

14.3.3 Fundamental mode in non-metal covered ridge waveguide	272
--	-----

14.3.4 Result discussion	273
--------------------------	-----

REFERENCES:	274
-------------	-----

CHAPTER 15 FIELD OVERLAPPING INTEGRAL CALCULATION	275
--	------------

15.1 Introduction	275
15.2 Input File Creation	276
15.3 Fields Overlap Analysis with WAVEGUIDE	280

APPENDIX SUBPROGRAMS FOR REFRACTIVE INDICES CALCULATION 285

Al(x)Ga(1-x)As 1	285
Al(x)Ga(1-x)As 2	286
Al(X)Ga(1-X)In(Y)As(1-Y) 2	295
Al(X)Ga(1-X)P(Y)Sb(1-Y)	296
Al(X)Ga(1-X)As(Y)Sb(1-Y)	298
Al(X)In(1-X)As(Y)Sb(1-Y)	299
Ga(X)In(1-X)P(Y)Sb(1-Y)	301
AlAs(X)Sb(1-X)	303
Al(x)Ga(1-x)0.5In(0.5)P	304
In(1-x)Ga(x)As [matched to InP]	305
In(1-x)Ga(x)As [matched to GaAs]	307
InGaAsP using PL [matched to InP]	310
InGaAsP [matched to InP]	311

Chapter 1 Introduction

WAVEGUIDE is a computer-aid design (CAD) analysis tool that can simulate and study a variety of optoelectronic devices. The first software was developed with Fortran 77, and recently has been updated by Taha Masood and Michael Marley. To master photonic design by WAVEGUIDE, one would better to understand physical principles and develop a fair amount of expertise in using the software. Therefore, the purpose of this book is to brief theory and describe how WAVEGUIDE is used to analyze photonic devices, more important, to outline how WAVEGUIDE is used in the process of design itself.

Transfer Matrix Method (TMM) is used to find eigen modes in a multi-layer slab waveguide structure. Transfer matrices of each layer is calculated, and eigen values of the effective refractive indices are found by solving eigen functions numerically; furthermore, the effective refractive index could be a complex value, indicating that WAVEGUIDE can find leaky modes or eigen modes in a lossy material. In addition, optical confinement factor in a specified layer, waveguide coupling, near field, far field, and other optical parameters can also be calculated and plotted.

WAVEGUIDE is a Windows version software with a user-friendly interface. Using the software helps users to understand the electromagnetic theory behind designed devices. WAVEGUIDE is a powerful tool in analyzing active or passive photonic devices, and some devices designed in our group will be used to demonstrate how to use WAVEGUIDE, especially users can refer to the corresponding chapter to design their own devices.

The book is organized as follow: Chapter 2 discusses the fundamental principles and general procedures for designing a 3-layer semiconductor laser, followed by a description of parameters in input files and out files, as well as refractive index calculation for semiconductor materials in chapter 3. In chapter 4, the chromatic dispersion of a 3-layer glass waveguide (an optical fiber) is studied. Chapter 5 demonstrates basic concepts and design of a directional coupler. We present design of different kind of multiple quantum well (MQW) semiconductor lasers in the followed 5 chapters. InGaAs/AlGaAs/GaAs (980nm and 808nm), InGaAsP/InP (1310nm and 1550nm), InGaAlAs/InP (1310nm and

1550nm), AlInGaP/GaAs (650nm), and InGaN (415nm) are demonstrated in chapter 6,7,8,9, and 10, respectively. In addition, chapter 11 describes the design of a ridge-guided laser structure, and the lateral confinement behavior will be simulated. A novel integrated isolator is investigated in the chapter 12. Finally, leaky mode properties in semiconductor material and metal are studied in the chapter 13 and 14, respectively.

Chapter 2 Theory Background

2.1 Introduction

This chapter includes the theoretic overview on some major waveguide/laser parameters and detailed description on how to run the WAVEGUIDE program with the demonstration of 3-layer slab waveguide.

Section 2.1 briefly introduces the concepts of confinement factor, far field and near field, and the formulas utilized in the WAVEGUIDE software for calculating those parameters. Section 2.2 provides general idea on how the WAVEGUIDE software solves the complex mode. Numerical methods that used by the WAVEGUIDE software to solve the propagation constant are also covered in this part. Section 2.3 provides step-by-step explanations on how to construct and evaluate an input file with WAVEGUIDE software; followed by the illustration of how to analyze the generated data and plots to obtain useful information of waveguide structure.

2.2 A Three-Layer Waveguide Example

This section gives a basic introduction of how the WAVEGUIDE solves complex modes for a three layer slab waveguide. First part of this section introduces the 2×2 matrix which is used by WAVEGUIDE for solving the propagation constant of three layer waveguide. Numerical methods are mentioned in the second part to give readers a general idea of how those numerical answers are found.

2.2.1 Transfer Matrix Method (TMM)

A three-layer slab waveguide is represented in Figure 2.2.1 (a). In this section, we will give a formulation example for a three-layer slab waveguide. However, WAVEGUIDE can handle arbitrary multi-layer waveguides. Assuming for the plane wave and from Maxwell's equations, we can get a scalar wave equation for each i^{th} layer as follows:

$$\frac{\partial^2}{\partial x^2} \varphi_i + (k_0^2 \epsilon_i + \gamma^2) \varphi_i = 0 \quad (2.1)$$

where φ_i is E_y for TE mode at i^{th} layer and H_y for TM mode,

γ is the modal propagation constant ($= \alpha + j\beta$), and

k_0^2 is $\omega^2 \mu_0 \epsilon_0$.

For TE modes, the boundaries need to have φ_i and $\partial \varphi_i / \partial x$ be continuous over different layers. If we consider the bounded mode and no loss or gain, which means ϵ_i and γ are real, for a three-layer waveguide, we can get a coupled equation in matrix form for the inner layer:

$$\begin{bmatrix} \varphi_i \\ \frac{\partial \varphi_i}{\partial x} \end{bmatrix} = \begin{bmatrix} \cos(h_i x) & \sin(h_i x) \\ -h_i \sin(h_i x) & h_i \cos(h_i x) \end{bmatrix} \begin{bmatrix} A_i \\ B_i \end{bmatrix} \quad (2.2)$$

where h_i is $\sqrt{|k_0^2 \epsilon_i + \gamma^2|}$ and $|\gamma^2| > |k_0^2 \epsilon_i|$.

The outer layer has the matrix form:

2.2 A Three Layer Waveguide Example

$$\begin{bmatrix} \varphi_i \\ \frac{\partial \varphi_i}{\partial x} \end{bmatrix} = \begin{bmatrix} 1 & h_{1orL} \end{bmatrix} \begin{bmatrix} A_o \\ A_o \end{bmatrix} \quad (2.3)$$

where h_{1orL} is $\sqrt{\gamma^2 - k_0^2 \epsilon_{1orL}}$, h_1 is for 1st layer and negative ($-h_L$) for Lth layer,

A_0 is A_1 for 1st layer and A_L for the last layer.

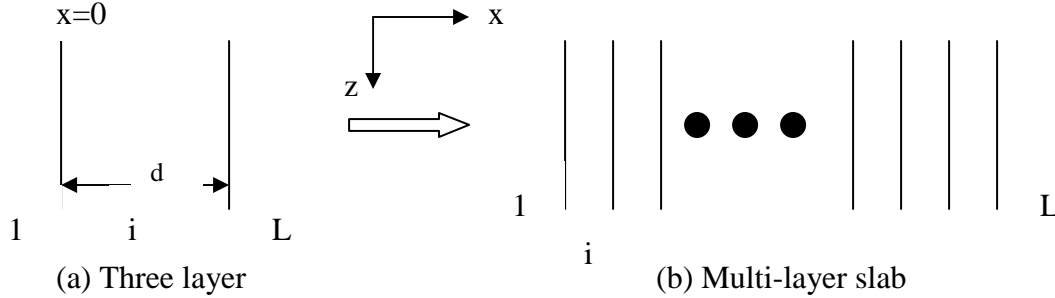


Figure 2.2.1 Slab waveguide

After we match the boundary conditions at each layer, we can get the following matrix form for the whole waveguide structure:

$$\begin{bmatrix} A_L \\ -h_L A_L \end{bmatrix} = T \begin{bmatrix} A_1 \\ h_1 A_1 \end{bmatrix} \quad (2.4)$$

where $T = \begin{bmatrix} T_{11} & T_{12} \\ T_{21} & T_{22} \end{bmatrix} = \begin{bmatrix} \cos(h_i d) & \frac{\sin(h_i d)}{h_i} \\ -h_i \sin(h_i d) & \cos(h_i d) \end{bmatrix}$.

From equation (2.4), we further to get the characteristic equation as the following:

$$T_{21} + T_{22} h_1 + h_L (T_{11} + T_{12} h_1) = 0 \quad (2.5)$$

For multi-layer waveguides, like shown in Figure 2.2.1 (b), the overall T will become a multiplication of matrices T with different h and d in the matrix entries. However, the final characteristic equation is the same as (2.5). The only difference is the final T, which is a 2×2 matrix. The whole idea of TMM is to get the characteristic equation in 2×2 matrix operation. This simple example gives readers a basic idea of how TMM works. WAVEGUIDE can solve more complex cases. In general, WAVEGUIDE

uses complex representations for the matrix elements in T . For other complex cases, like TM-mode case and gain or loss consideration, readers can refer to [1] and [2] for more details.

2.2.2 Numerical Method Consideration

WAVEGUIDE can handle complex modes in the present of loss and gain in different layers. Therefore, the boundary condition is different for complex modes. The field solutions are restricted to the solution in the semi-infinite layers. The choice of branch specification for transverse constant in the inner layer does not affect the complex root search because of no singularity in the finite plane. On the other hand, the principle branch specification for transverse propagation constants in the outer layers is important in WAVEGUIDE for eigenmode problem.

The mode characteristics in the semi-infinite layers determine whether it is a proper or an improper mode. The mode characteristics, the phase propagation and exponential behavior can be determined from transverse propagation constant plane. For bounded modes, the eigenvalue problem is well defined and all the roots are physically acceptable. When searching the complex root for a complex mode, the branch specification is helpful to lead the problem to a well-defined and single-valued characteristic function. For complex mode search, WAVEGUIDE use an arbitrary branch cut in the square of modal propagation constant plane instead of real axis line for proper mode search. In this way, the bound and leaky mode can appear on the same branch.

The Muller-Traub method for complex plane is used in WAVEGUIDE to find a complex root. Readers can refer to [1] for the details. The program uses three kinds of convergence tests. If any one test is satisfied, the last iteration is accepted. Users can set up the maximum iteration number. WAVEGUIDE can generate initial guess, but this can only work well with simple structure and for lower order modes. For a large imaginary part in modal propagation constant, it is better for users to input an initial guess value.

2.3 Theory Introduction

This section gives simple introduction of the most basic theory. Far field, near field and confinement factor are briefly introduced in the section 2.3.1 and 2.3.2 respectively.

2.3.1 Far field and near field

Near field and far field are two of the important characteristics of an emitted optical field. Near field refers to the spatial intensity distribution of the emitted light near the waveguide end face. And the angular intensity distribution far from the endface is known as the far field. Detailed discussion about near field and far field can be referred to some texts ^{[3], [4], [5]}.

Far field is important in determining the coupling efficiency. Mathematically, the far-field pattern can be approximated by taking the Fourier transform of the near field intensity distribution. However, this method is not very accurate for dielectric waveguide, though it is applicable in antenna area. Our software WAVEGUIDE induces the idea of ‘‘obliquity factor’’ during the calculation of far field ^[6]. Here, we use a 3-layer waveguide to exemplify the calculation process. We assume the mode fields to be independent of y direction (lateral direction) if the width of the waveguide is large comparing with the thickness of the waveguide. Then the spatial distribution of the optical field is just associated with the transverse mode $\psi(x)$ that can be solved from the wave equation and boundary condition. For TE mode, the electric field can be written in the following form:

$$E_y = F \psi(x) e^{j(\alpha x - \beta z)} \quad (2.6)$$

And the modal distribution $\psi(x)$ that propagates along z direction has different form at each of the 3 layers:

$$\psi(x) = \begin{cases} C e^{-px} & (x \geq d) \\ A \cos(qx) + B \sin(qx) & (d \geq x \geq 0) \\ D e^{r(x+d)} & (x \leq d) \end{cases} \quad (2.7)$$

Where, p, q and r are wavenumbers at each layer and they satisfy the following conditions that relate with propagation constant at z direction:

Chapter 2 Theory Background

$$\begin{cases} p^2 + \epsilon_1 k_0^2 = \beta^2 \\ -q^2 + \epsilon_2 k_0^2 = \beta^2 \\ r^2 + \epsilon_3 k_0^2 = \beta^2 \end{cases} \quad (2.8)$$

When combining with boundary condition, (i.e. tangential fields and their derivatives are continuous at the interface) and normalizing them, we can solve out the values of p, q, r and coefficients A, B, C and D . Thus $\psi(x)$ can be known.

Write $\psi(x)$ in terms of plane waves by Fourier Transform theory,

$$\bar{\psi}(s) = \frac{1}{\sqrt{2\pi}} \int_{-\infty}^{\infty} \psi(x) e^{jsx} dx \quad (2.9)$$

Where s is the propagation constant at x direction.

Then electric field is in the following form:

$$E_y(x) = \frac{1}{\sqrt{2\pi}} F \int_{-\infty}^{\infty} \bar{\psi}(s) e^{j(\omega t - sx - \beta z)} ds \quad (2.10)$$

When the light radiates from the endface of the waveguide, both reflection and transmission happen and the transmitted field is:

$$E_y(x)^{trans} = \tau F' \int_{-\infty}^{\infty} \bar{\psi}(s) e^{j(\omega t - sx - \beta z)} ds \quad (2.11)$$

Where τ is the transmission coefficient

$$\tau = \frac{2\eta_{air}}{\eta_{air} + \eta_{waveguide}} = \frac{2\beta}{(k_0^2 - s^2)^{1/2} + \beta} \quad (2.12)$$

Consider the coordinate system shown in Fig 2.3.1, where the electromagnetic field is radiated into the air. We have the following relationships:

$$\begin{aligned} x &= r \sin \theta & z &= r \cos \theta \\ s &= k_0 \sin \phi & ds &= k_0 \cos \phi d\phi \end{aligned} \quad (2.13)$$

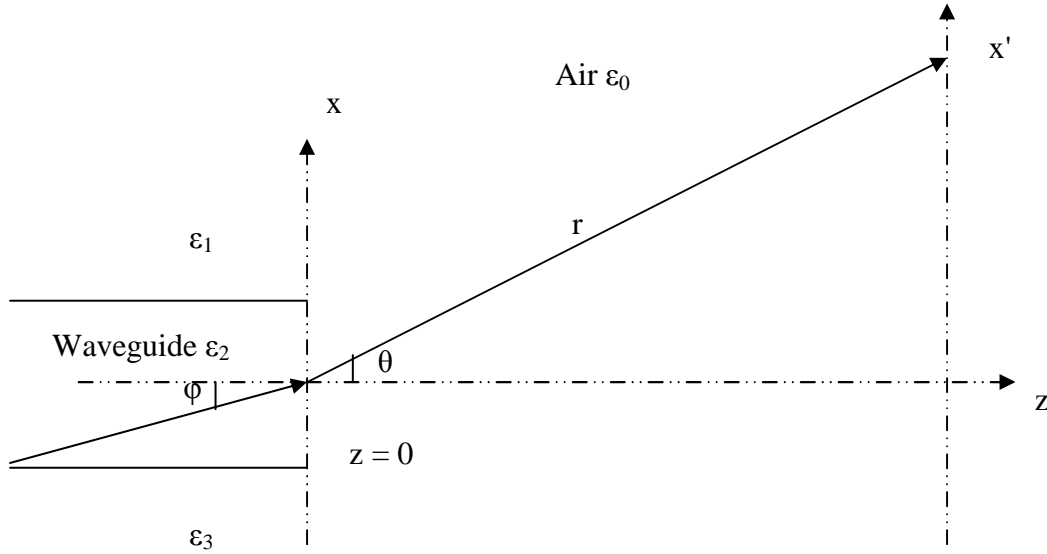


Figure 2.3.1 Schematic coordinate system of the far field of 3-layer waveguide

Then the total field intensity at (r, θ) changes to: (ignore the time term $e^{j\omega t}$)

$$E(r, \theta) = F' \int_{-\infty}^{\infty} \frac{2\beta}{k_0 \cos \phi + \beta} \bar{\psi}(k_0 \sin \phi) e^{-jk_0 r \cos(\theta - \phi)} k_0 \cos \phi d\phi \quad (2.14)$$

And then the “saddle point method”^[7] is used to approximate the value of $E(r, \theta)$ for large distance. The “saddle point method” is shown below:

$$\int_{-\infty}^{\infty} g(x) e^{kh(x)} dx \approx g(a) e^{kh(a)} \sqrt{\frac{-2\pi}{kh''(a)}} \quad (2.15)$$

where a is from

$$h'(x) = 0,$$

in our case, $\sin(\theta - \phi) = 0 \Rightarrow \theta = \phi$ and $\sqrt{\frac{-2\pi}{kh''(a)}} = \sqrt{\frac{-2\pi}{-jk_0r(-\cos(\theta - \phi))}} = \sqrt{\frac{2\pi}{k_0r}}$

$$(2.16)$$

Therefore the calculation equation for far field distribution is:

$$E(r, \theta) = F' \sqrt{\frac{2\pi}{k_0r}} \frac{2\beta}{k_0 \cos \theta + \beta} k_0 \cos \theta \bar{\psi}(k_0 \sin \theta) e^{-jk_0r} \quad (2.17)$$

and the intensity of the far field is

$$I(\theta) = |E(r, \theta)|^2 = I_0 \frac{\cos^2 \theta}{|k_0 \cos \theta + \beta|^2} |\bar{\psi}(k_0 \sin \theta)|^2 \quad (2.18)$$

We call $\cos \theta$ "Huygen obliquity factor" and $\cos^2 \theta$ the "intensity obliquity factor".

In WAVEGUIDE, a coefficient $g(\theta)$ [6] is used to combine all Huygen obliquity factor terms and the effective index of refraction calculated from previous steps contributes here to find the value of $g(\theta)$.

$$g(\theta) = 2 \cos \theta \frac{\frac{\beta}{k_0} + \sqrt{n_{eff}^2 - \sin^2 \theta}}{\cos \theta + \sqrt{n_{eff}^2 - \sin^2 \theta}} \quad (2.19)$$

Then the far field intensity in WAVEGUIDE is calculated as following:

$$I(\theta) = I_0 |\bar{\psi}(k_0 \sin \theta)|^2 g(\theta)^2 \quad (2.20)$$

In addition, WAVEGUIDE normalized the entire far field so that the maximum value is 1 for $\theta = 0^\circ$.

2.3.2: Confinement Factor

The conception and the use of confinement or filling factor Γ will be introduced in this section. Physically the confinement factor accounts for the reduction in gain that occurs because of the spreading of the optical mode beyond the active region, it represents the fraction of the mode energy contained in the active region. The briefly

confinement factor calculation of waveguide will be introduced as transverse modes and lateral modes respectively by the refer to [8].

First let's study the wave equation to get the transverse field distribution and lateral field distribution.

2.3.2.1 Confinement factor calculation

From the Maxwell's equations, we can get the time-independent wave equation:

$$\nabla^2 E + \varepsilon k_0^2 E = 0 \quad (2.21)$$

Where ε is the complex dielectric constant:

$$\varepsilon = \varepsilon' + \varepsilon'' \quad (2.22)$$

Where k_0 is the vacuum wave number:

$$k_0 = \omega / c = 2\pi / \lambda \quad (2.23)$$

Where E is the electric field:

$$E \cong \hat{e} \phi(y; x) \psi(x) \exp(i\beta z) \quad (2.24)$$

Here β is the propagation constant, \hat{e} is the unit vector and z is the propagation direction distance.

By substituting Eq. (2.24) in Eq. (2.21), we obtain:

$$\frac{1}{\psi} \frac{\partial^2 \psi}{\partial x^2} + \frac{1}{\phi} \frac{\partial^2 \phi}{\partial y^2} + [\varepsilon(x, y) k_0^2 - \beta^2] = 0 \quad (2.25)$$

From the above equation (2.25), we can get the transverse field distribution $\phi(y; x)$ by solving:

$$\frac{\partial^2 \phi}{\partial y^2} + [\varepsilon(x, y) k_0^2 - \beta_{eff}^2(x)] \phi = 0 \quad (2.26)$$

Where $\beta_{eff}(x)$ is the effective propagation constant for a fixed value of x.

Chapter 2 Theory Background

From the above equation (2.25), we can also get the lateral field distribution $\psi(x)$ by solving:

$$\frac{\partial^2 \psi}{\partial x^2} + [\beta_{eff}^2(x) - \beta^2] \psi = 0 \quad (2.27)$$

Now let's introduce the confinement factor as transverse modes and lateral modes.

(a): Transverse Modes

The transverse modes depend on the thicknesses and refractive indices of the various layers used to fabricate a semiconductor lasers. Generally it is necessary to consider four or five layers for a reasonably accurate description of the transverse modes. However, the basic concepts involved in dielectric waveguide can be understood by using a symmetric three-layer slab waveguide.

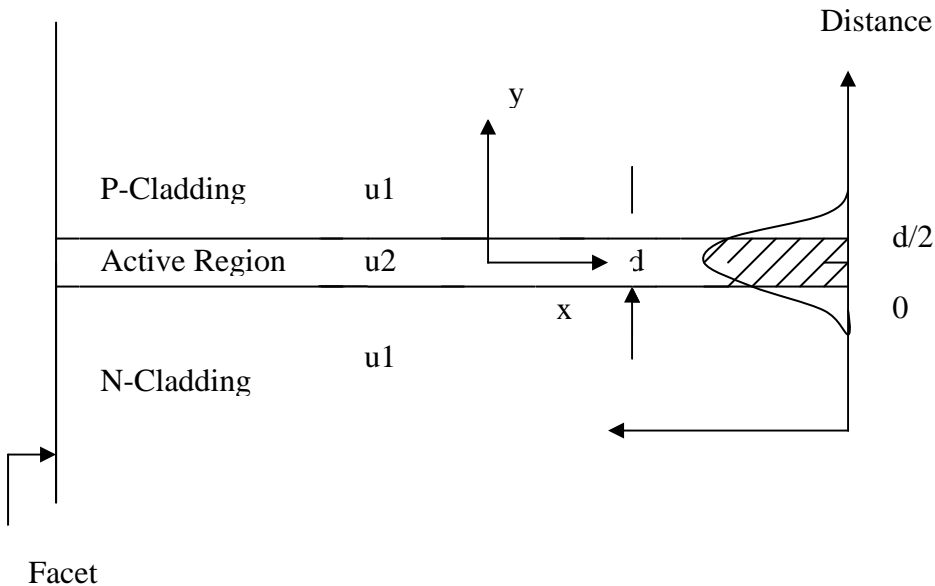


Fig 2.3.2: Three-layer slab-waveguide model.

The above figure shows the three-layer slab-waveguide model of a semiconductor laser with refractive indices such that $u_2 > u_1$. The intensity distribution of the fundamental waveguide mode is also shown. The hatched region represents the fraction of the mode with the active region.

Now the transverse confinement factor can be given as:

$$\Gamma_T = \frac{\int_{-d/2}^{d/2} \phi^2(y) dy}{\int_{-\infty}^{+\infty} \phi^2(y) | dy} \quad (2.28)$$

Where:

Γ_T : transverse confinement factor.

$\phi(y)$: transverse field distribution, can be solved from the Eq. (2.26).

d: the active layer thickness.

(b): Lateral Modes

The lateral-mode behavior in semiconductor lasers is different depending on whether gain guiding or index guiding is used to confine the lateral modes.

$$\Gamma_L = \frac{\int_{-w/2}^{w/2} |\psi^2(x)| dy}{\int_{-\infty}^{+\infty} |\psi^2(x)| dy} \quad (2.29)$$

Where:

Γ_L : lateral confinement factor.

$\psi(x)$: lateral field distribution, can be solved from the Eq. (2.27).

w: central region width.

(c): Total confinement factor

In the waveguide description,

$$\Gamma = \Gamma_T * \Gamma_L \quad (2.30)$$

For typically used $w \cong 2\mu m$, $\Gamma_L \cong 1$ and Γ_T can be used for Γ .

2.3.2.2 The use of the confinement factor in the waveguide software

In waveguide software, the confinement factor (γ) calculation is always turned on. See the website: http://www.edunotes.org/notes/waveguide_man.html#inli for the use of γ in WAVEGUIDE.

2.4 Running the program

This section gives users a brief overview of how to run WaveGuide program to obtain useful information about waveguide structures such as propagation constant of the fundamental mode and far-field profile. The detailed explanation of input and output parameters and files will be provided in Chapter 6 and the simulations of complicated waveguide structures will be discussed in later chapters

The first step in running WaveGuide program is to create an input file with information of the layer structures, input and output commands, looping parameters, free space wavelength, and other program variables such as maximum iteration times and tolerances. Next, the input file is evaluated and output files are generated according to the output commands specified in the input file. Third, data in the output files are analyzed by either the plot command of WaveGuide program or spreadsheet editors.

In the following subsections, the above-motioned steps of running the WaveGuide program will be demonstrated using an three-layer waveguide example in an ordered and straight forward way.

2.4.1 Description of layer structure

As shown in Figure 2.4.1, the three-layer waveguide is a symmetric waveguide with a 2- μm thick dielectric layer of refractive index 3.60 sandwiched by two dielectric layers of refractive index 3.55. The thicknesses of the two outermost layers are deemed infinity in WaveGuide program. In the example, the waveguide is assumed to be lossless for simplicity.

As discussed in the previous sections of this chapter, the WaveGuide program will solve the wave equations and match the boundary conditions, obtain the wave function of interested mode, calculate the confinement factors, near field and far field of the mode, and loop particular parameters such as layer thicknesses and wavelengths.

The WaveGuide also has powerful plot features, and its user-interface allows users to easily select the x-axis variables and y-axis variables and modify graph properties such as color, line type, and graph title.

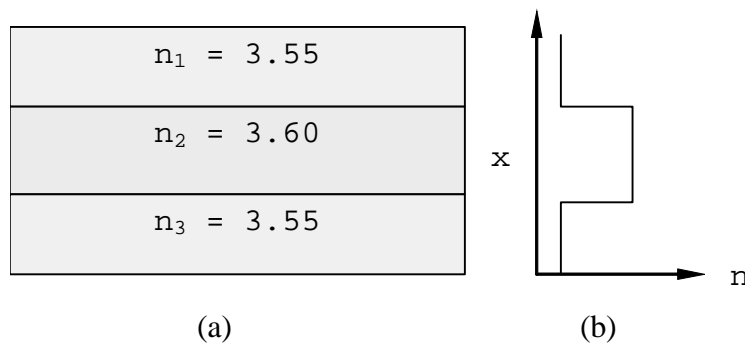


Figure 2.4.1 (a) diagram and (b) index profile of the three-layer waveguide

2.4.2 Construction of an input file

An input file contains all the information of a waveguide structure and input output commands. It can be generated in the “Waveguide Input File Editor” (WIFE) or word editors including notepad. A new user is advised to use WIFE to create input files before getting familiar with WaveGuide commands.

After installation of WaveGuide program, start the program by selecting Photodigm WaveGuide\WaveGuide Beta 0.9 in the start menu. When WaveGuide is running, WaveGuide main screen shown in Figure 2.4.2 pops up.

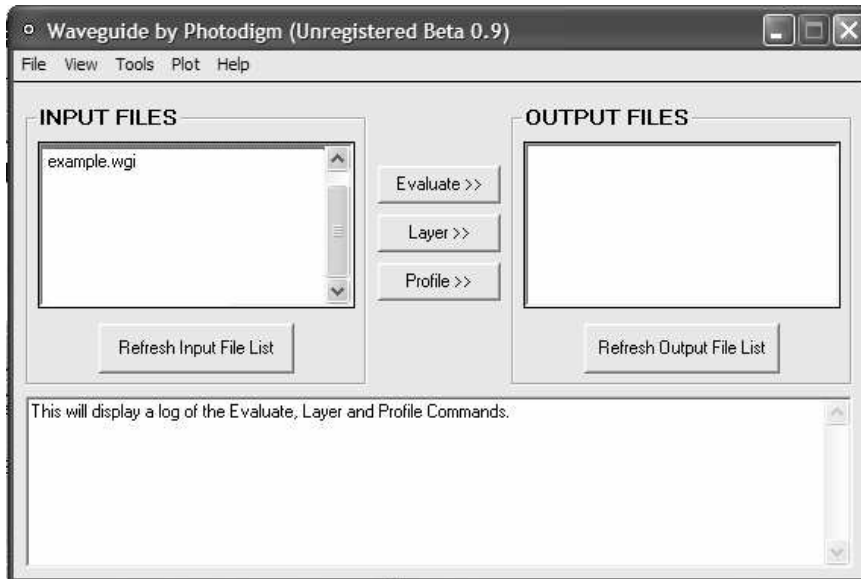


Figure 2.4.2 WaveGuide main screen

Next, activate the WIFE by selecting “Create New Input File” in the pull down menu “File”. As shown in Figure 2.4.3, all the parameters and commands are divided into categories and listed in the tabs; an input file is created by completing all the tabs. Although all the options have default values, it is suggested that users review and fill all the tabs carefully according to structures to be simulated. The construction of an input

2.4 Running the program

file for the three-layer waveguide using WIFE is explained by completing the tabs in an order from left to right in the rest of the section.

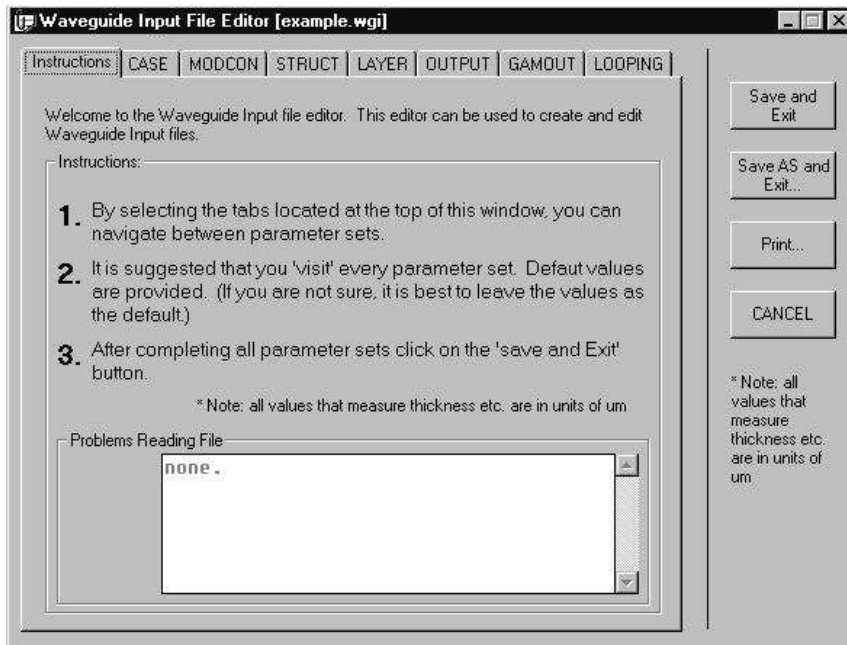


Figure 2.4.3 WaveGuide Input File Editor

1) Tab “Instructions” and “Case”

The first tab “Instructions” contains basic operation instructions and can be taken as a general guide. The second tab “Case” sets general program variables and flags. The detailed explanation of the program variables and flags will be discussed in Chapter 6. For the three-layer waveguide example, as illustrated in Figure 2.4.4, first click the “Case” tab and type “WaveGuide Example File” into the “Description” blank as a brief description of the purpose of the file. Then enter “12.6” in “QZMR” which is the initial guess of effective refractive indices of modes in the waveguide. As can be see from Figure 2.4.4, all the default values of the other program variables and flags are already filled in the blanks automatically. The default values are used in our example, so leave the blanks as they are.

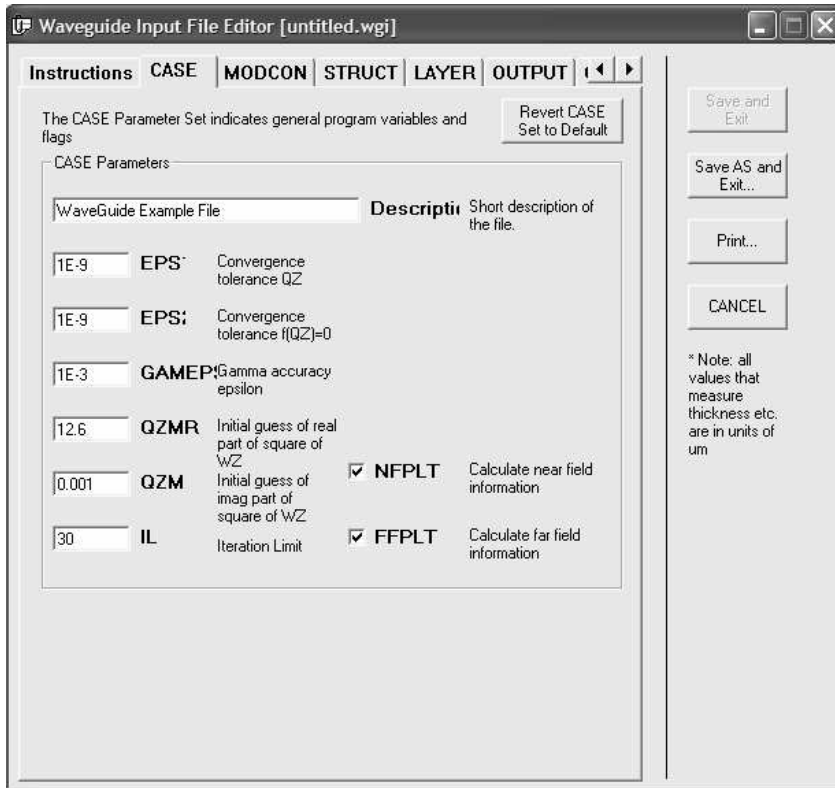


Figure 2.4.4 Illustration of tab “CASE” in WaveGuide Input File Editor

2) Tab “MODCON” and “STRUUCT”

Next, click “MODCON” tab, review and use all the default values as revealed in Figure 2.4.5 (a). After that, click “STRUUCT” tab to specify the free space wavelength of the modes in the waveguide, which is 0.82 μm in our three-layer waveguide example. At the same time, as shown in Figure 2.4.5 (b), leave the default values as they are.

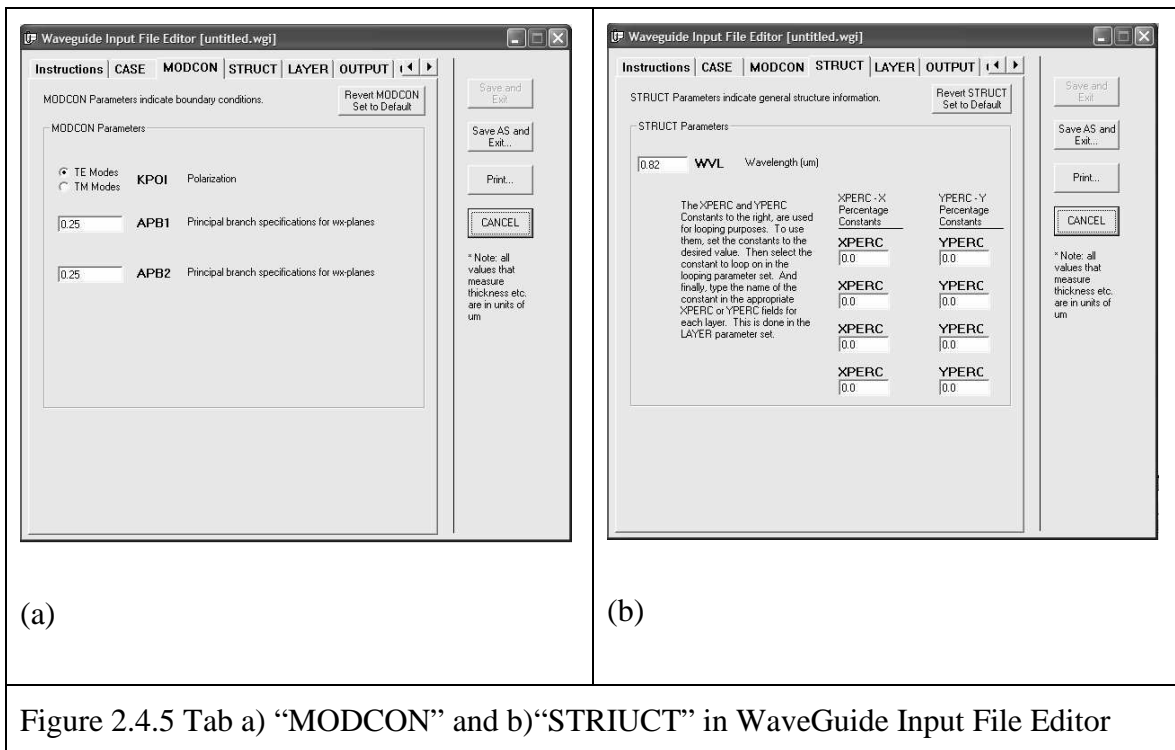


Figure 2.4.5 Tab a) “MODCON” and b)“STRUICT” in WaveGuide Input File Editor

3) Tab “LAYER”

Click the “LAYER” tab as displayed in Figure 2.4.6, specify the total number of layers to be 3 and input characteristic parameters of each layer. When entering the parameters of the layers, users are allowed to choose either entering the refractive indices and loss of the layers or entering material compositions of select material systems for the layers. In this example, we choose the former method. The first and third layers have refractive indices of 3.55 and infinite thickness, while the middle layer has a refractive index of 3.55 and a thickness of 2 um. You may realize that the default values have been set to the three-layer waveguide example, so just scroll down and review the choices and leave the inputs as they are.

Chapter 2 Theory Background

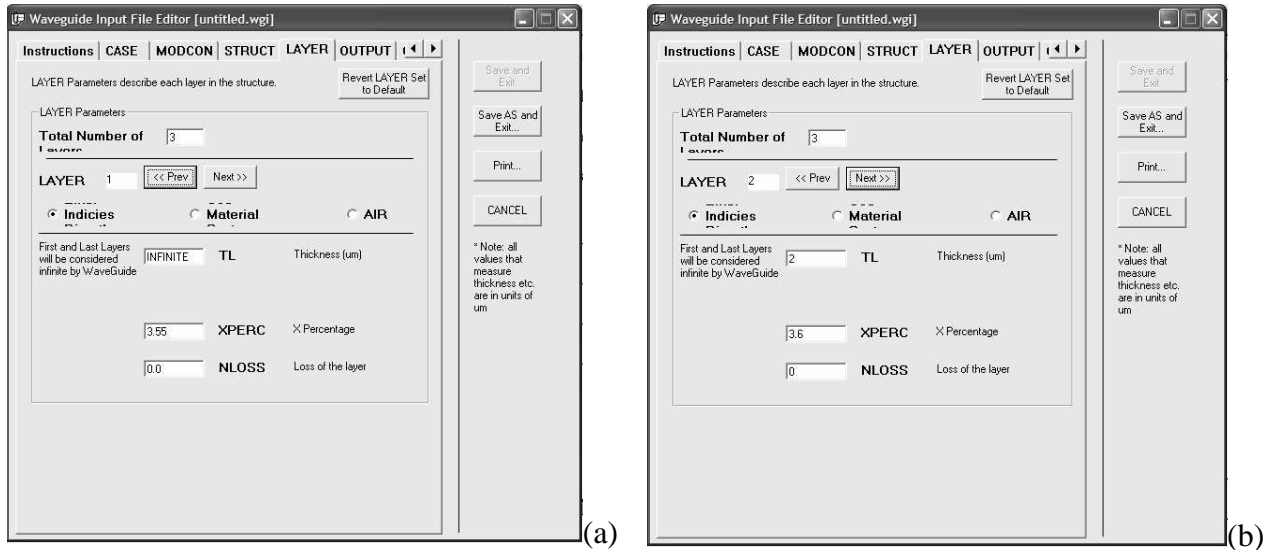


Figure 2.4.6 Layer structure inputs for a) layer 1 and b) layer 2 in tab “LAYER”

4) Tab “OUTPUT” and “GAMOUT”

The next step is to select output of the WaveGuide program, and in this example, check all output as illustrated in Figure 2.4.7. Then in “GAMOUT” tab shown in Figure 2.4.8, enter “2” in the “LAYGAM” blank indicating the program will calculate and output the confinement factor of the layer 2 and leave the “COMGAM” and “GAMALL” unchecked.

2.4 Running the program

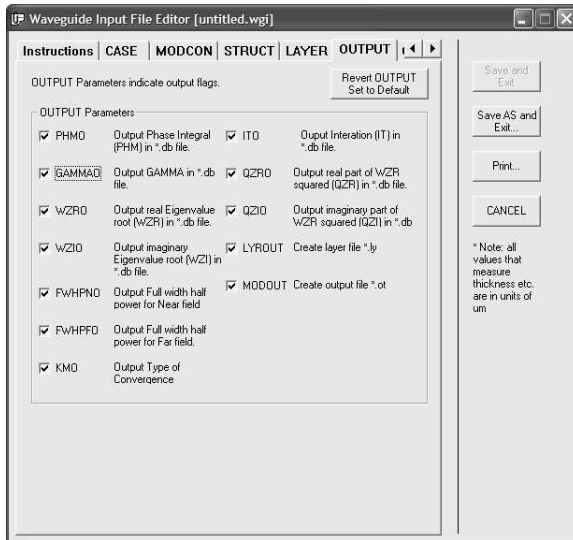


Figure 2.4.7 Tab “OUTPUT” in WIFE

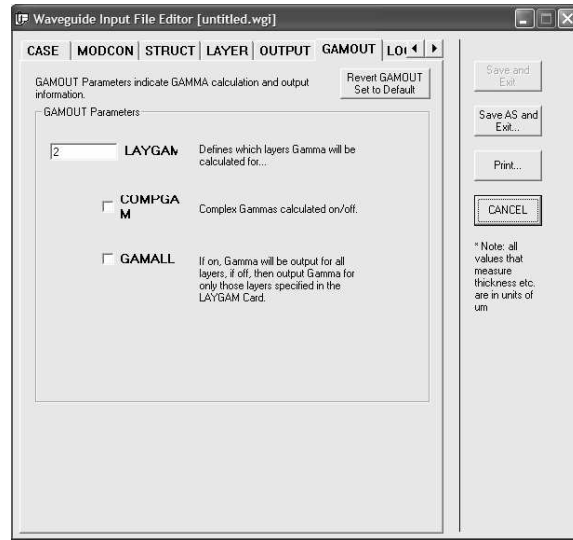


Figure 2.4.8 Tab “GAMOUT” in WIFE

5) Tab “LOOPING”

Finally, click the “LOOPING” tab shown in Figure 2.4.9. WaveGuide program can vary different variables of the waveguide through LOOPX and LOOPZ commands. Usually LOOPX is used to varying the layer thickness and LOOPZ is used to varying effective refractive index guess (square root of “QZMR”) and free space wavelength “WVL”. In the three-layer waveguide, we first need find the effective refractive index, so we check “LOOPZ” to loop “QZMR”.

As discussed in the previous sections in Chapter 2, the values of effective indices of modes in three-layer waveguide are between the highest and lowest refractive indices of all the layers. Therefore, enter the final value of “QZMR” to be the square of the refractive index of layer 2, which is 12.96 in this example, and then enter the increment 0.01. The initial value of “QZMR” was already set to be the square of the lowest refractive index 12.6 in tab “CASE” described in step 1). The WaveGuide program will

Chapter 2 Theory Background

loop the QZMR from 12.6 to 12.96 with an increment 0.01 until it finds the QZMR's that satisfy the wave equations and boundary conditions.

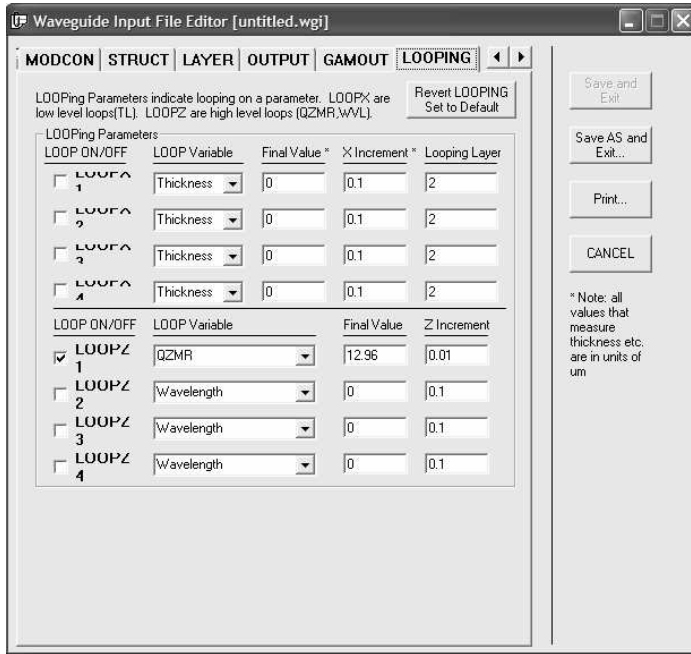


Figure 2.4.9 Tab “LOOPING” in WaveGuide Input File Editor

6) Save and Edit Input File

After going through all the tabs, we complete the input file by clicking the button “Save As and Exit” and saving the input file in the default directory “C:\Waveguide\work\input\” as “example.wgi”. Waveguide can only work under this directory, so make sure the input files are saved in this directory. Table 2.4.1 shows the text form of the input file created by WIFE through step 1) to 5). Users may have noticed that in WaveGuide input file, texts starting with “!” are word description rather than commands.

Table 2.4.1 Input file of three-layer waveguide generated through WIFE.

2.4 Running the program

```
!WIF generated by WIFE (Waveguide Input File Editor)
!-----
!FILENAME:      C:\Waveguide\work\input\example.wgi
!DESCRIPTION:   WaveGuide Example File
!Last Modified: 3/28/2004 10:34:26 PM
!-----

!CASE Parameter Set
CASE KASE=WIFE
CASE EPS1=1E-9 EPS2=1E-9 GAMEPS=1E-3 QZMR=12.60 QZMI=0.001
CASE PRINTF=1 INITGS=0 AUTOQW=0 NFPLT=1 FFPLT=1 IL=30

!MODCON Parameter Set
MODCON KPOL=1 APB1=0.25 APB2=0.25

!STRUCT Parameter Set
STRUCT WVW=0.82
STRUCT XPERC1=0.0 XPERC2=0.0 XPERC3=0.0 XPERC4=0.0
STRUCT YPERC1=0.0 YPERC2=0.0 YPERC3=0.0 YPERC4=0.0

!LAYER Parameter Set
LAYER NREAL=3.55 NLOSS=0.0 TL=1.0
LAYER NREAL=3.6 NLOSS=0 TL=2
LAYER NREAL=3.55 NLOSS=0 TL=1

!OUTPUT Parameter Set
OUTPUT PHMO=1 GAMMAO=1 WZRO=1 WZIO=1 QZRO=1 QZIO=1
OUTPUT FWHPNO=1 FWHPFO=1 KMO=1 ITO=1
OUTPUT SPLTFL=0 MODOUT=1 LYROUT=1

!GAMOUT Parameter Set
GAMOUT LAYGAM=2 COMPGAM=0 GAMALL=0

!LOOPX Parameter Set
LOOPX1 ILX=0 FINV=0 XINC=0.1 LAYCH=2
LOOPX2 ILX=0 FINV=0 XINC=0.1 LAYCH=2
LOOPX3 ILX=0 FINV=0 XINC=0.1 LAYCH=2
LOOPX4 ILX=0 FINV=0 XINC=0.1 LAYCH=2

!LOOPZ Parameter Set
LOOPZ1 ILZ=17 FINV=12.96 ZINC=0.01
LOOPZ2 ILZ=0 FINV=0 ZINC=0.1
LOOPZ3 ILZ=0 FINV=0 ZINC=0.1
LOOPZ4 ILZ=0 FINV=0 ZINC=0.1

END
```

2.4.3 Description of output parameters and output files.

1) Evaluation of an input file

An input file can be evaluated by first selecting the input file, “example.wgi” in our example, and click the button “Evaluate >>”. In our example, an error message window pops up as shown in Figure 2.4.10 when evaluating “example.wgi”, indicating that some guess values of QZMR didn’t converge within 30 iterations. But by checking the output file “example.db”, users can find that not all guess values didn’t converge. Usually in spite of the warning message, roots are still able to be found in the output file.

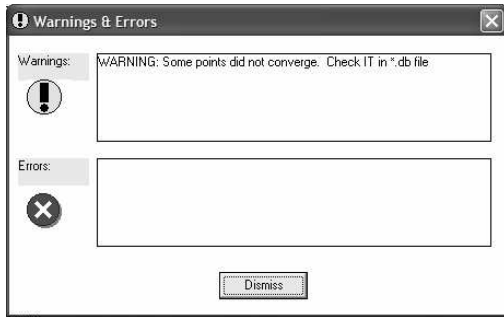


Figure 2.4.10 Error message box appears in evaluation of input file “example.wgi”

2) Effective refractive index of the fundamental mode

As displayed in Figure 2.4.11, after evaluation of the input file, all the output files are listed in the right window of the WaveGuide main screen with the same file name but different extensions such as “example.db” and “example.ff”. The detailed explanation of the output files are offered in Chapter 6, and in this section, a brief overview of the output files will be introduced.

In order to find QZMR of fundamental mode, open the “example.db” by right clicking and selecting “View SELECTED file”. The file “example.db” is opened in Notepad as listed in Table 2.4.2, containing columns of data. The detailed explanation of the parameters in “example.db” will be provided in Chapter 6. In this section, general definitions and criteria to find fundamental mode are introduced. The key parameters to find QZMR of a fundamental mode are PHM, KM, and IT. PHM is phase integral; KM is a computation flag showing QZM quality or type; IT is iteration times. For a fundamental mode, PHM is smaller than 1; KM is 6 or 7, indicating roots of good quality; IT is smaller than 30, which was set in the “CASE” tab of WIFE as discussed before.

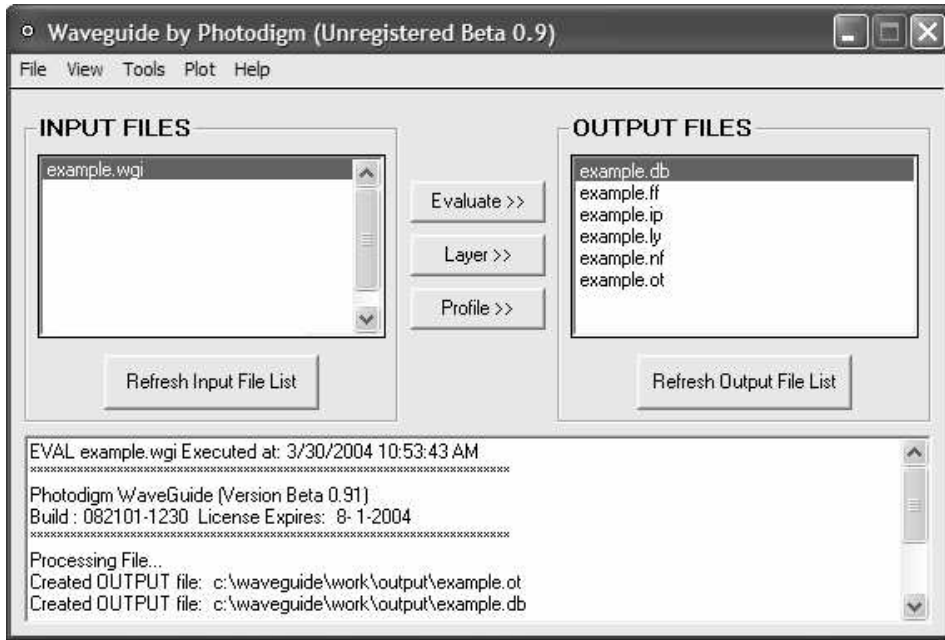


Figure 2.4.11 WaveGuide main screen showing all the output files after evaluation of the input file “example.wgi”.

Therefore, in the output file “example.db” listed in Table 2.4.2, we look for the QZMR’s that meet the criteria for a fundamental mode, which are highlighted to be bold and italic. You will notice that those QZMR’s have the same values of WZR and QZR, which are effective refractive index and the square of WZR respectively. Therefore, we found the effective refractive index of the fundamental mode in the three-layer waveguide to be 3.596.

Table 2.4.2 The output file “example.db” containing QZMR

QZMR	PHM	GAMMA(2)	WZR	WZI	QZR	QZI	FWHPN	
1.260000E+01	2.870376E+00	0.000000E+00	3.551592E+00	1.201351E-03	1.261381E+01	8.533418E-03	0.000000E+00	0.
1.261000E+01	2.914060E+00	0.000000E+00	3.550111E+00	2.056171E-03	1.260328E+01	1.459927E-02	0.000000E+00	0.
1.262000E+01	2.916458E+00	0.000000E+00	3.550031E+00	2.205307E-03	1.260272E+01	1.565782E-02	0.000000E+00	0.
1.263000E+01	2.917461E+00	0.000000E+00	3.550001E+00	2.378989E-03	1.260250E+01	1.689082E-02	0.000000E+00	0.
1.264000E+01	2.916111E+00	0.000000E+00	3.550052E+00	2.568497E-03	1.260286E+01	1.823660E-02	0.000000E+00	0.
1.265000E+01	2.388969E+00	8.149874E-01	3.566533E+00	8.531513E-17	1.272016E+01	6.085584E-16	4.317830E-01	1.
1.266000E+01	2.388969E+00	8.149874E-01	3.566533E+00	5.155953E-18	1.272016E+01	3.677775E-17	4.317830E-01	1.
1.267000E+01	2.388969E+00	8.149874E-01	3.566533E+00	3.047152E-19	1.272016E+01	2.173553E-18	4.317830E-01	1.
1.268000E+01	2.388969E+00	8.149874E-01	3.566533E+00	4.758875E-13	1.272016E+01	3.394537E-12	4.317830E-01	1.
1.269000E+01	2.388969E+00	8.149874E-01	3.566533E+00	1.862216E-14	1.272016E+01	1.328331E-13	4.317830E-01	1.
1.270000E+01	2.388969E+00	8.149874E-01	3.566533E+00	9.581314E-17	1.272016E+01	6.834414E-16	4.317830E-01	1.
1.271000E+01	2.388969E+00	8.149874E-01	3.566533E+00	1.605356E-12	1.272016E+01	1.145111E-11	4.317830E-01	1.
1.272000E+01	2.388969E+00	8.149874E-01	3.566533E+00	4.144338E-13	1.272016E+01	2.956183E-12	4.317830E-01	1.
1.273000E+01	2.388969E+00	8.149874E-01	3.566533E+00	2.510751E-12	1.272016E+01	1.790935E-11	4.317830E-01	1.
1.274000E+01	2.388969E+00	8.149874E-01	3.566533E+00	8.819416E-16	1.272016E+01	6.290947E-15	4.317830E-01	1.
1.275000E+01	2.388969E+00	8.149874E-01	3.566533E+00	5.547851E-13	1.272016E+01	3.957319E-12	4.317830E-01	1.
1.276000E+01	2.388969E+00	8.149874E-01	3.566533E+00	1.159238E-17	1.272016E+01	8.268922E-17	4.317830E-01	1.
1.277000E+01	2.388969E+00	8.149874E-01	3.566533E+00	3.427408E-15	1.272016E+01	2.444793E-14	4.317830E-01	1.
1.278000E+01	2.388969E+00	8.149874E-01	3.566533E+00	2.160358E-13	1.272016E+01	1.540998E-12	4.317830E-01	1.
1.279000E+01	2.388969E+00	8.149874E-01	3.566533E+00	2.182583E-19	1.272016E+01	1.556851E-18	4.317830E-01	1.
1.280000E+01	1.624044E+00	9.346155E-01	3.584572E+00	1.199020E-13	1.284916E+01	8.595949E-13	6.180778E-01	1.
1.281000E+01	1.624044E+00	9.346155E-01	3.584572E+00	1.580543E-18	1.284916E+01	1.133114E-17	6.180778E-01	1.
1.282000E+01	1.624044E+00	9.346155E-01	3.584572E+00	3.056372E-17	1.284916E+01	2.191157E-16	6.180778E-01	1.
1.283000E+01	1.624044E+00	9.346155E-01	3.584572E+00	1.411470E-17	1.284916E+01	1.011903E-16	6.180778E-01	1.
1.284000E+01	1.624044E+00	9.346155E-01	3.584572E+00	1.095169E-12	1.284916E+01	7.851422E-12	6.180778E-01	1.
1.285000E+01	1.624044E+00	9.346155E-01	3.584572E+00	-4.088430E-12	1.284916E+01	-2.931055E-11	6.180778E-01	1.
1.286000E+01	1.624044E+00	9.346155E-01	3.584572E+00	1.760407E-18	1.284916E+01	1.262061E-17	6.180778E-01	1.
1.287000E+01	1.624044E+00	9.346155E-01	3.584572E+00	2.511560E-13	1.284916E+01	1.800573E-12	6.180778E-01	1.
1.288000E+01	1.624044E+00	9.346155E-01	3.584572E+00	1.930753E-16	1.284916E+01	1.384185E-15	6.180778E-01	1.
1.289000E+01	1.624044E+00	9.346155E-01	3.584572E+00	7.334633E-13	1.284916E+01	5.258304E-12	6.180778E-01	1.
1.290000E+01	1.624044E+00	9.346155E-01	3.584572E+00	1.825410E-16	1.284916E+01	1.308663E-15	6.180778E-01	1.
1.291000E+01	8.188365E-01	9.853043E-01	3.596084E+00	-2.207374E-17	1.293182E+01	-1.587581E-16	1.224312E+00	2.
1.292000E+01	8.188365E-01	9.853043E-01	3.596084E+00	2.817344E-15	1.293182E+01	2.026281E-14	1.224312E+00	2.
1.293000E+01	8.188365E-01	9.853043E-01	3.596084E+00	-4.097716E-16	1.293182E+01	-2.947147E-15	1.224312E+00	2.
1.294000E+01	8.188365E-01	9.853043E-01	3.596084E+00	2.286669E-17	1.293182E+01	1.644611E-16	1.224312E+00	2.
1.295000E+01	8.188365E-01	9.853043E-01	3.596084E+00	1.958452E-17	1.293182E+01	1.408552E-16	1.224312E+00	2.
1.296000E+01	8.188365E-01	9.853043E-01	3.596084E+00	-9.814521E-17	1.293182E+01	-7.058769E-16	1.224312E+00	2.

3) Far field, near field, and confinement factor of the fundamental mode

The far field, near field, and confinement factor of the modes allowed in waveguides can be simulated in the WaveGuide program. In this section, the fundamental mode propagating in the three-layer waveguide will be simulated to demonstrate how to obtain the information using WAVEGUIDE program .

To simulate the fundamental mode, first, we need to modify the input file “example.wgi” by WIFE or word editor. By selecting the input file “example.wgi” and right clicking on it, the pull-down menu is displayed, in which “Edit SELECTED file” is used to activate WIFE and “View SELECTED file” views the selected file in Notepad. In this example, “View SELECTED file” is clicked to illustrate how to modify an input file using word editor.

We have simulated that the effective refractive index of the fundamental mode is 3.596, and QZR, which is the square of WZR, is 12.932. So we need to first modify the input file by setting QZMR to 12.932, and then put exclamation mark “!” in front of the the “LOOPZ” command which was used to find QZMR. The new input file is listed in Table 2.4.3, and the modified parts are bold and italic.

Table 2.4.3 Input file for simulation of the fundamental mode

```

!WIF generated by WIFE (Waveguide Input File Editor)
!-----
!FILENAME:      C:\Waveguide\work\input\example.wgi
!DESCRIPTION:  WaveGuide Example File
!Last Modified: 3/28/2004 10:34:26 PM
!-----

!CASE Parameter Set
CASE KASE=WIFE
CASE EPS1=1E-9 EPS2=1E-9 GAMEPS=1E-3 QZMR=12.932 QZMI=0.001
CASE PRINTF=1 INITGS=0 AUTOQW=0 NFPLT=1 FFPLT=1 IL=30

!MODCON Parameter Set
MODCON KPOL=1 APB1=0.25 APB2=0.25

!STRUCT Parameter Set
STRUCT WVL=0.82
STRUCT XPERC1=0.0 XPERC2=0.0 XPERC3=0.0 XPERC4=0.0
STRUCT YPERC1=0.0 YPERC2=0.0 YPERC3=0.0 YPERC4=0.0

!LAYER Parameter Set
LAYER NREAL=3.55 NLOSS=0.0 TL=1.0
LAYER NREAL=3.6 NLOSS=0 TL=2
LAYER NREAL=3.55 NLOSS=0 TL=1

!OUTPUT Parameter Set
OUTPUT PHMO=1 GAMMAO=1 WZRO=1 WZIO=1 QZRO=1 QZIO=1
OUTPUT FWHPNO=1 FWHPFO=1 KMO=1 ITO=1

```

Chapter 2 Theory Background

```

OUTPUT SPLTFL=0 MODOUT=1 LYROUT=1

!GAMOUT Parameter Set
GAMOUT LAYGAM=2 COMPGAM=0 GAMALL=0

!LOOPX Parameter Set
LOOPX1 ILX=0 FINV=0 XINC=0.1 LAYCH=2
LOOPX2 ILX=0 FINV=0 XINC=0.1 LAYCH=2
LOOPX3 ILX=0 FINV=0 XINC=0.1 LAYCH=2
LOOPX4 ILX=0 FINV=0 XINC=0.1 LAYCH=2

!LOOPZ Parameter Set
!LOOPZ1 ILZ=17 FINV=12.96 ZINC=0.01
LOOPZ2 ILZ=0 FINV=0 ZINC=0.1
LOOPZ3 ILZ=0 FINV=0 ZINC=0.1
LOOPZ4 ILZ=0 FINV=0 ZINC=0.1

END

```

Second, select the input file and click the “Evaluate” button to evaluate it. Among the output files, “example.db” contains simulation results as shown in Table 2.4.4. GAMMA (2) in the output file is the confinement factor of the layer 2 of the waveguide, 0.9853; WZR is the real part of the effective refractive index of the mode; WZI is the imaginary of the effective refractive index of the mode; QZR is the square of WZR; QZI is the square of WZI; FWHPN is the near field divergence full width half power, 1.22°; FWHPF is far field divergence full width half power, 20.91°.

Table 2.4.4 Output file “example.db”

PHM	GAMMA(2)	WZR	WZI	QZR	QZI
FWHPN	FWHPF	KM	IT		
8.188365E-01	9.853043E-01	3.596084E+00	-2.244844E-20	1.293182E+01	-1.614529E-19
1.224312E+00	2.090706E+01	7	3		

Far field and near field information is contained in output files “example.ff” and “example.nf” respectively. To plot far field intensity, click “Plot” of the pull-down menu and select “Plot Far Field (*.ff)”, and then in the window that pops up, check “FFIELD” and click “Plot” as illustrated in Figure 2.4.12. Figure 2.4.13 shows the far field intensity graph. Similarly, the near field intensity is plotting by clicking “Plot Near Field (*.nf)” in the pull-down menu, which is shown in Figure 2.4.14. The graph properties such as chart types and color can be modified in the plot window.

2.4 Running the program

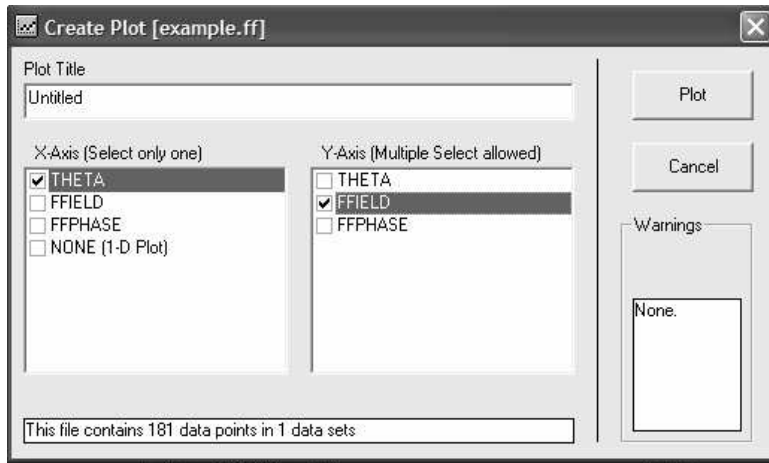


Figure 2.4.12 Plot window allows users to choose X and Y-Axis data.

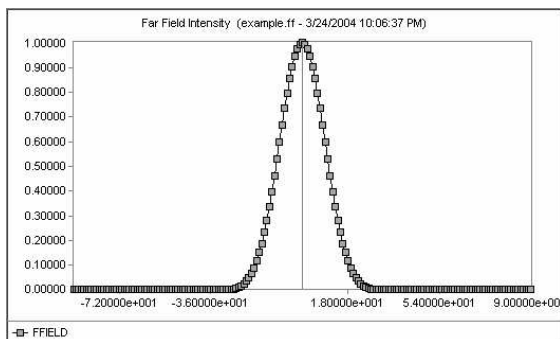


Figure 2.4.13 Far field intensity plot

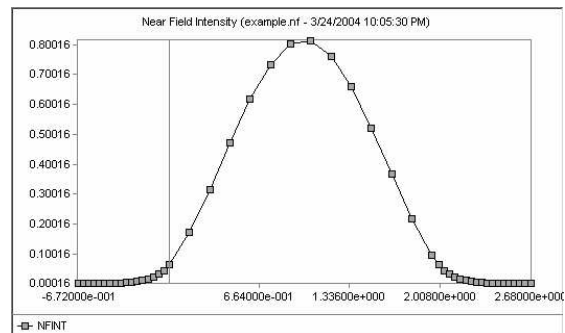


Figure 2.4.14 Near field intensity plot

In summary, a three-layer waveguide example is used to demonstrate how to use WAVEGUIDE program for simulations of waveguide structures. A brief introduction of input file is provided and discussed in this section. Output files are explained or/and plotted including Effective refractive indices of modes, confinement factors of the layers, far field, and near field. The detailed explanation of the input and output files are provided in Chapter 6, and the simulations of complicated waveguide structures are discussed in later chapters.

REFERENCES:

[1] Robert B. Smith, "Calculation of complex propagating modes in arbitrary, plane-layered, complex dielectric structures, I. Analytic formulation, II. Fortran program MODEIG", 1977.

[2] Chao-Suan Yeh, "Theoretical and experimental investigation of slab waveguides with periodical grating layer", 1992.

[3]. H. Kressel, J.K. Butler "Semiconductor Lasers and Heterojunction LEDs", Academic Press, New York, (1977)

[4]. T. Tamir "Integrated Optics", Springer Verlag, Berlin (1976)

[5]. N.S. Kapany "Optical Waveguides", Academic Press, New York, (1972)

[6]. G.A. Hockam, "Radiation from a solid state laser," Electronics Letters, vol. 9, no. 17, pp. 389-391, 1973.

[7]. A. Papoulis "The Fourier Integral and its Application", Mcgraw-hill, New York, (1962)

[8]. G.P.Agrawal, and N.K.Dutta. Long-Wavelength Semiconductor Lasers, Chap. 2. New York: Van Nostrand Reinhold Company Inc, 1986.

Chapter 3 – MATSYS and WAVEGUIDE INPUT/OUTPUT Parameters

3.1 Introduction

This chapter serves as a reference to the program parameters available in WAVEGUIDE. These parameters include a material system feature called MATSYS and program input and output variables. Examples of using MATSYS and changing the program input and output variables are shown in the other chapters of this user guide.

3.2 Material System MATSYS

Typical III-V structures can be entered in WAVEGUIDE layer by layer using menu selections: File, Create new input file, and LAYER tab. After filling in the total number of layers, enter the layer number being defined in the box marked LAYER.

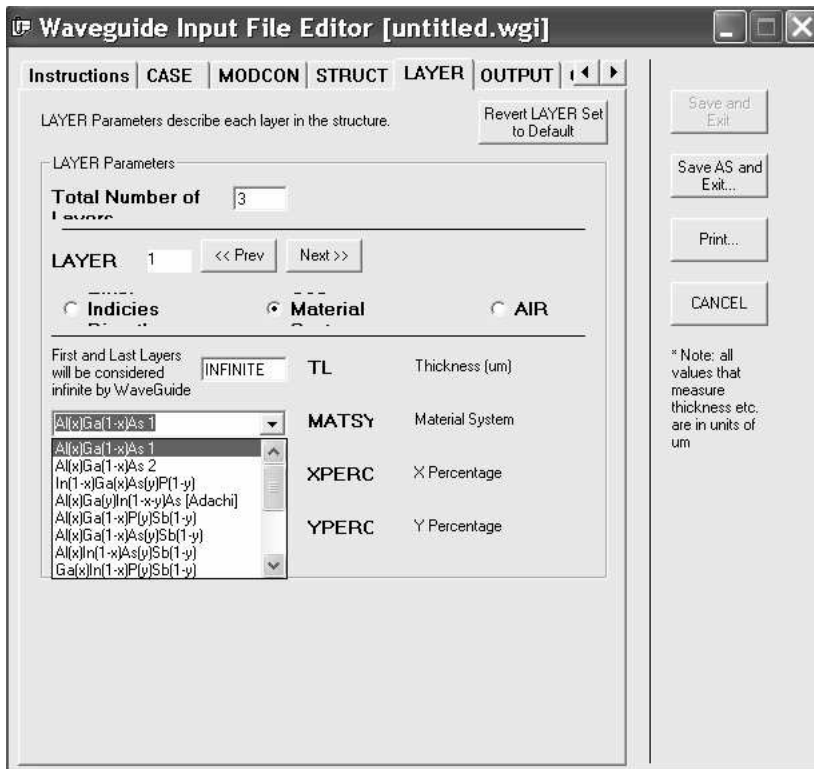


Figure 3.2.1 This is the layer input screen.

There are two ways to input the refractive index. You can enter the refractive index directly by selecting the “Indices” button or you can have the MATSYS feature calculate the refractive index by selecting the “Material” button. In both cases the refractive index value is assigned to the input parameter NREAL corresponding to that layer.

If you use the MATSYS feature, you will see a drop down list of available material compositions to choose from (Figure 3.2.1). Once a specific composition is selected, parameters XPERC and YPERC become available to enter the percent of the element with index “x” and the percent of element with index “y.” For example, in Figure 3.2.2 we have selected the second layer composition to be Al(x)Ga(1-x)As. The percent of Al in this layer is 35%. (The software automatically calculates the percent of Ga as 65%.) You can enter 0 for YPERC since this composition does not have this variable. If you want to enter GaAs with 0% Al, you can enter 0 for XPERC.

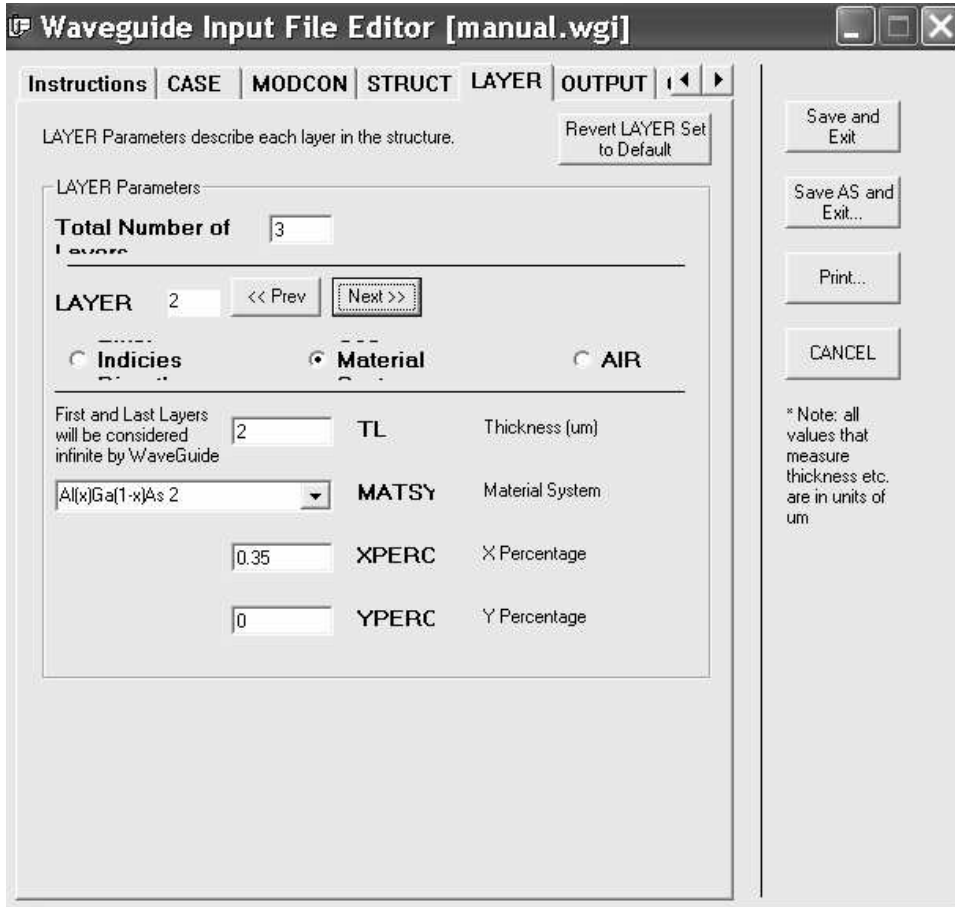


Figure 3.2.2 Layer 2 composition is entered with 35% Al.

The LAYER portion of the input file corresponding to 3 layers (GaAs, Al(0.35)GaAs, GaAs) entered using MATSYS are listed below. The middle layer shows XPERC is set to 35%. The parameter MATSYS corresponds to a code assigned to the Al(x)Ga(1-x)As₂ material composition we selected.

```
!LAYER Parameter Set

LAYER MATSYS=0.1 XPERC=0 YPERC=0.0 TL=1.0

LAYER MATSYS=0.1 XPERC=0.35 YPERC=0 TL=2

LAYER MATSYS=0.1 XPERC=0 YPERC=0 TL=1.0
```

Chapter 3 MATSYS and WAVEGUIDE INPUT/OUTPUT Parameters

The layer output file shows the program's calculated refractive indices (NREAL) based on the input layers:

```
# of layers =          3
LAYER01  NLOSS= 0.00000    NREAL= 3.52903    TL=  1.00000
LAYER02  NLOSS= 0.00000    NREAL= 3.32472    TL=  2.00000
LAYER03  NLOSS= 0.00000    NREAL= 3.52903    TL=  1.00000
```

Note that the structure's wavelength must be entered prior to running the program in order for MATSYS to properly calculate the refractive indices. You can enter the structure wavelength on the STRUCT tab (Figure 3.2.3) or you can modify the input file parameter WV L directly in the input file. For example, if we enter .98 μm for the structure wavelength the input file parameter WV L will look like this:

```
!STRUCT Parameter Set
STRUCT WV L=0.98
```

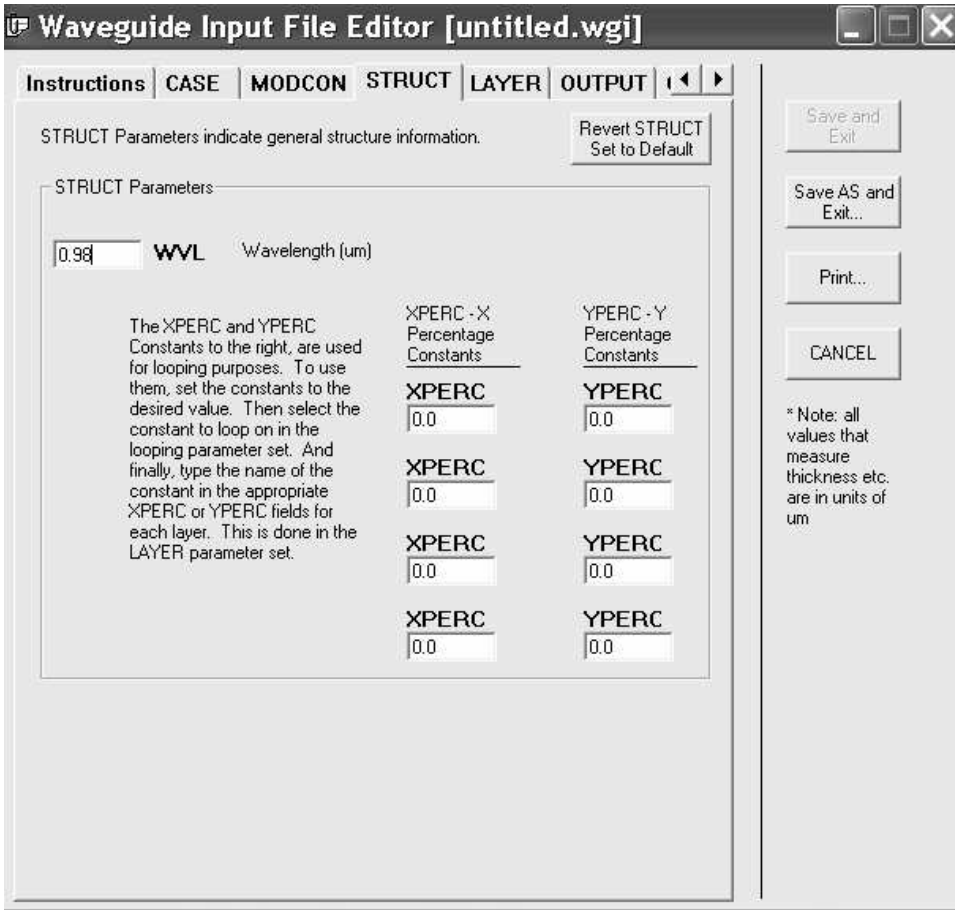


Figure 3.2.3 The wavelength of the light propagating in the structure must be entered before using MATSYS.

The available compositions in MATSYS, the MATSYS code, and whether XPERC and YPERC are required are listed in Table 3.2.1. For the InGaAsP [matched to InP] composition instead of entering the composition percentages, MATSYS uses the photoluminescence (PL) to calculate the refractive index. The PL corresponds to the bandgap and assumes the material is lattice matched.

Table 3.2.1 MATSYS Compositions

Material System	Reference	MATSYS	XPERC	YPERC

Chapter 3 MATSYS and WAVEGUIDE INPUT/OUTPUT Parameters

			Required?	Required?
Al(X)Ga(1-X)As 1	[1]	0.0	YES	Not Used
Al(X)Ga(1-X)As 2	[2]	0.1	YES	Not Used
In(1-X)Ga(X)As(Y)P(1-Y)		1.0	YES	YES
Al(X)Ga(Y)In(1-X-Y)As		2.0	YES	YES
Al(X)Ga(1-X)P(Y)Sb(1-Y)		3.0	YES	YES
Al(X)Ga(1-X)As(Y)Sb(1-Y)		4.0	YES	YES
Al(X)In(1-X)As(Y)Sb(1-Y)		5.0	YES	YES
Ga(X)In(1-X)P(Y)Sb(1-Y)		6.0	YES	YES
AlAs(X)Sb(1-X)		7.0	YES	Not Used
Al(x)Ga(1-x)0.5In(0.5)P		8.0	YES	Not Used
In(1-x)Ga(x)As [matched to InP]		9.0	YES	Not Used
In(1-x)Ga(x)As [matched to GaAs]		10.0	YES	Not Used
Ga(x)In(1-x)P [matched to GaAs]		11.0	YES	Not Used
InGaAsP [matched to InP]	[8]	12.0	Not Used – Enter PL λ	Not Used
AlGaInAs		13.0	YES	YES

MATSYS computations for each composition are based on Adachi's work and the equations are listed below. (Note: The equations are in the process of being added and

some or all of the sections may not yet have the equations listed.) We have included the source code in the appendix for completeness. If you find an error, please let us know so we may update the code!

3.2.1.1 Al(x)Ga(1-x)As 1

3.2.1.2 Al(x)Ga(1-x)As 2

3.2.1.3 In(1-X)Ga(X)As(Y)P(1-Y)

3.2.1.4 Al(X)Ga(Y)In(1-X-Y)As

3.2.1.5 Al(X)Ga(1-X)In(Y)As(1-Y) 2

3.2.1.6 Al(X)Ga(1-X)P(Y)Sb(1-Y)

3.2.1.7 Al(X)Ga(1-X)As(Y)Sb(1-Y)

3.2.1.8 Al(X)In(1-X)As(Y)Sb(1-Y)

3.2.1.9 Ga(X)In(1-X)P(Y)Sb(1-Y)

3.2.1.10 AlAs(X)Sb(1-X)

3.2.1.11 Al(x)Ga(1-x)0.5In(0.5)P

3.2.1.12 In(1-x)Ga(x)As [matched to InP]

3.2.1.13 In(1-x)Ga(x)As [matched to GaAs]

3.2.1.14 Ga(x)In(1-x)P [matched to GaAs]

3.2.1.15 InGaAsP using PL [matched to InP]

3.2.1.16 InGaAsP [matched to InP]

3.4 Program Parameters

WAVEGUIDE has input and output parameters that can be defined when creating a new file or by manually modifying the input file. The following sections provide a list of all possible parameters and their function.

3.4.1 Input Parameters

- CASE - General program variables and flags
- MODCON - Boundary conditions
- STRUCT - General structure information
- LAYER - Specific structure (layer) information
- GAMOUT - Confinement factor (Gamma) calculation/output info
- LOOPX_n - Low-level looping (Nreal, Nloss, Tl) [n=loop #]
- LOOPZ_n - High-level looping (Wvl, Grw, Qw) [n=loop #]
- OUTPUT - Output flags

3.4.1.1 CASE Parameters

- DTHETA - Increment for the far field angle theta (1.0)
- DXIN - Dx used for fine detail in near field (0.1)
- EPS1 - Epsilon for convergence test on delta QZ root search (1E-8)
- EPS2 - Epsilon for convergence test on magnitude of eigen equation function (1E-8)
- FFPLT - Far field calculation flag (0)
- GAMEPS - Confinement factor (Gamma) accuracy epsilon (1E-3)
- IDEN - Density of points in X for field calculations per rad or 1/E (10)
- IL - Iteration limit maximum number for each root search (30)
- IMAX - Maximum number of points in each layer for field calculations (not applicable if DXIN is used) (15)
- INFX - number of rad or 1/e dist into semi-infinite layers for field calculations (3)
- INITGS - Initial guess generation routine flag (0)
- INTHM - Half maximum intensity level (0)
- KASE - WAVEGUIDE case number (yy/mm/dd)
- KCI - Complex frequency factor for normalized KO (imag part) (0.0)
- KCR - Complex frequency factor for normalized KO (real part) (1.0)
- KDOF - Subroutine Fields flag: (1)
0 = No field calculations made
1 = Tangential fields at boundaries only calculated
2 = Fields as a function of X calculated if and only if (iff) KOUT=4
- KEIF - control type of eigen equation used for root searching:
1 = unmodified eigen equation from SM matrix

2 = eigeqf renormalized to R.M.S. magnitude of the 4 possible eigeqf

3 = Eigeqf multiplied by WT function to bias search toward intended MM.

Weight function is WFMP times squared difference between phase integral index and intended mode index.

Warning: 2&3 are non-analytic functions and can greatly slow root search

- KFI - Explicit complex frequency factor (imaginary (imag) part)
- KFR - Explicit complex frequency factor (real part)
- KGCZ - Control use of guesses in complex root search for all QZ. Used to set KM= KGCZ for all guesses. (KGSS >2)

=0 guesses not used, initial iterates about point (1.0,0.0)

=1,2,3 initial iterates at radius of $0.1 \cdot KGCZ$ about each guess.

Only converged and iteration limited roots divided out.

=4,5,6,7 radius of $0.1 \cdot KGCZ$, all other guesses and roots divided out

Warning: Use KGCZ.ge.4 iff guesses are good approximate and distinct.

Do not use if all guesses the same (KGSS=2) or poor input guess.

If good guesses, KGCZ.ge.4 greatly speeds root search convergence.

- KGCZY - Option to control use of estimates for y-modes (3)
(similar in use to KGCZ)

- KGSS - Control type of initial guesses for QZ root search. (3)

=1 QZM(M) and KM(M) from input or previous case used for guesses, =2 all guesses the same (QR max of inner layers),

=3 individual guesses from simple quadratic approximation for real(QZ) vs. phase integral. intended mode indices $MM = MO + M$.

- KGSSY - Option for obtaining estimates for y-roots (see KGSS)
- KM(M) - Index showing QZM quality or type. (5)

Chapter 3 MATSYS and WAVEGUIDE INPUT/OUTPUT Parameters

input value used only if KGSS=1.

=0 to 7, see KGCZ

=8 QZM used as fixed known root, no search, divided out for others

(for output and previous case KM= 5,6,7, shows type of convergence).

- KMDO - Modes are output and fields calculated only for $KM > KMDO$ (5)
- KO - Free-space propagation constant for normalization purposes.

(calculated quantity rather than input)

$KO = 2\pi/WVL$ used to normalize all propagation constants. See KC below.

Effective values of WVL and KO altered by use of non-unity KC.

- KOUE - Flag to control output from subroutine Eigeqf 1-4 (0)
- KOUF - Flag to control output from subroutine Fields 1-4 (3)
- KOUFY - Option for outputting fields as function of y (3)
- KOUJ - Flag to control output from subroutine Putsin 1-4 (1)
- KOUS - Flag to control output from subroutine Search 1-4 (3)
- KOUZ - Flag to control output from subroutine Czerom 1-4 (3)
- KXTL - Control to specify that XL or TL are expected as input (0).

≤ 0 if XL expected as input, TL calculated. (default)

≥ 1 if TL expected as input, XL calculated. $XL(1) = 0$.

- LAYER - Finite layer over which numerate integral is performed (2)

in fldint (active layer). Modified 9/85.

Numerator integral is now performed for all finite layers.

Layer now just represents the active layer used in cxmode.

- LCUTOF(M)- Field cutoff criterion for left margin for mode M (-1.0e10).

$f_y(x) = 0$ for x .lt. LCUTOF(M) or for x .get XCUTOF(M).

3.4 Program Parameters

- MN - Number of x-modes to be searched for or calculations made (1) maximum number of modes presently dimensioned for is 10.
- MO - Bias for mode indexing of intended modes. $MM=MO+M$ (-1).
- NBARFF - N bar used in the far field calculations (3.45).
- NFPLT - = 1 to plot near field, = 0 otherwise. (0).
- PEROPT - Option for specifying PER(l) and PEI(l): (0)
if = 0, then PER(l) and PEI(l) are input directly
if = 1, then PER(l) and PEI(l) are computed from the input quantities NREAL(l), NLOSS(l), and GAIN0.
- PFIELD - Field power used to normalize the field $f_y(x)$ (1.0)
- PMFR - Fractional part for phase integral (phase shift at outer body) assumed in generating guesses. Units of pi. (0.3).
- PMI(1) - Relative permeability, imaginary part, all layers (0.0).
- PMR(1) - Relative permeability, real part, all layers (1.0).
- PRINTF - Control for printing table of fields, intensities, and phases (0).
- QCNT - Mode index used for the input of multiple mode initial guesses (QZMR(QCNT)= ...) (1).
- QZMR - Input set of complex QZ values (x-modes) $M=1, MN$ QZMI see KGSS=1.0 used for guesses for root search, or for field calc, no search. Preset to special real values from default case solutions.
(use QCNT for multiple input)
- QZNI - Imaginary part of QZ for generation of initial guesses (-1.0e-4).
- QZNR - Real part of QZ for generation of initial guesses (0.9).
- XAXLEN - X-axis length (inches) (10.0).
- XCUTOF(M) - Field cutoff criterion for right margin for mode M (1.0e10).

Chapter 3 MATSYS and WAVEGUIDE INPUT/OUTPUT Parameters

- XU - Unit of length implied for all dimensions (meters) (1E-6).
- YAXLEN - Y-axis length (inches) (5.0).

3.4.1.2 MODCON Parameters

- APB1 - Principal branch specification for wx-planes.
- APB2 – Angle into WX half plane for outer layers L1 and L2+1. units of pi. (0.25) (direction angle of branch cuts in QZ plane is twice APB.).
+0.0.le.APB.le.+1.0 branch includes pos imaginary axis of wx- plane. -
0.5.le.APB.le.+0.5 branch includes pos real axis of wx- plane. Default
APB1=0.25, APB2=0.25, not conventional specification. Rather, imag(wx).get
real(wx). bound and leaky mode roots for lossless dielectric structures are all on
same principal branch. Branch cuts in QZ plane are in positive imaginary
direction. (conventional choice of branches, APB=0.5, KBD=2. bound proper
mode roots on principal branch and Riemann sheet of QZ. leaky improper mode
roots on second branch and Riemann sheet. Branch cuts in QZ plane in negative
real direction.)
- F1 - Determines how far the integration range will extend into layer 1 or layer
LN, respectively (see subroutine fldint)
- KBC1 - Control type of boundary conditions at 1-st and last body L1,L2.KBC2
open-body semi-infinite wave admit/impede, or fixed surf admit/impede, also
eigen, non-eigen, conditions, and acceptable solutions.
le.0 open boundary condition, non-eigen condition, no search made. Inward and
outward solution both acceptable see KBD1,KBD2 field solution exits for each of
KBC1=0, or KBC2=0, or both. If both, two independent field solutions exist.
Calculation independent from two body condition same as for KBC=1, and
direction implied by KBD1,KBD2.
=1 open boundary, eigen condition. only a single exponential wave solution
acceptable in outer semi-infinite layer. (default).

=0,1 wave admit/impede for semi-infinite layer is function of $w_x(qz)$, always defined from w_x on principal branch. see KBD1,2 and APB1,2. =2 closed body, a fixed surf admit/impede YB1,YB2. ZB1,ZB2 ignored.

=3 closed body, a fixed surf impede/admit ZB1,ZB2. YB1,YB2 ignored

=2,3 a closed bdy eigen condition. outer semi-infinite layers ignored.

- KBD1 - Controls implied direction of single solution in semi-infinite KBD2 layers inward/outward direction interpretation depends on branch def.

KBD1=1 pos. exponent (inward) complex wave solution in layer L1

KBD1=2 neg. exponent (outward) complex wave solution in layer L1

- KBD2=1 neg. exponent (inward) complex wave solution in layer L2+1

KBD2=2 pos. exponent (outward) complex wave solution in layer L2+1

Default values KBD1=2,KBD2=2. outward solution in semi-infinite layers.

Iff APB= 0.5, then $\text{imag}(w_x)$ is positive, and direction sense in/out is that of exp decay regardless of phase propagation. inward= leaky, improper or incoming lossy wave. outward= bound, proper or out going lossy wave. iff APB= 0.0, $\text{real}(w_x)$ is pos. and direction is that of phase propagation regardless of exp decay or growth. Direction sense also used for non-eigen case (KBC1,KBC2=0) in generating solutions based on each body condition independently. KBD. also used for direction sense for YB,ZB surf admit/impede.

- KPOL - Polarization. transverse to z-propagation, and to x-norm direct. (1)

.le.1 te, transverse electric case. $f_y = e_y$. (default)

> .ge.2 tm, transverse magnetic case. $f_y = h_y$

- L1 - First and last boundary for outer boundary conditions.

- L2 preset to L1=1, L2=LN-1 for each case.

For other values (partial structures), L1,L2 must be input for each successive case.

Note. adjacent layers ($l = L1$ and $L2+1$) are taken to be >semi-infinite for closed body condition. (KBC=2,3). all outer layers ignored.

Chapter 3 MATSYS and WAVEGUIDE INPUT/OUTPUT Parameters

- YB1R, YB1I - Fixed body surface admit(te)/impede(tm) looking.
- YB2R, YB2I outward at L1,L2. Used only if respective KBC1,KBC2 are equal to 2 (1.0,0.0).
- ZB1R, ZB1I - Fixed body surface impede(te)/admit(tm) looking outward ZB2R, • ZB2I at L1,L2. Used only respective if KBC1,KBC2 are equal to 3. (1.0,0.0).
looking outward iff KBD1,2 equal 2 (default).

3.4.1.3 STRUCT Parameters

- BW - Barrier width
- **GRW - Graded layer width**

3.4.1.4 LAYER Parameters

- AIR - Air layer effective index
- GRW - Graded layer width
- NLOSS - Loss in the specified layer
- NREAL – Index of the specified layer
- NSLC - Number of slices for the graded layer

3.4.1.5 GAMOUT Parameters

- COMPGAM - Complex confinement factor (gamma) flag
- GAMALL - Gamma layers to output to output file
- LAYGAM - Gamma layers to output to .db file

The confinement factors (GAMMA) are discussed in chapter 2.

3.4.1.6 LOOPX Parameters

- FINV - Final value of the of the loop variable when looping
- ILX - Loop variable selection flag
 - 0 or 'OFF' = no looping
 - 1 or 'TL' = loop on thickness (TL)
 - 2 or 'NREAL' = loop on effective index (NREAL)
 - 3 or 'NLOSS' = loop on the loss (NLOSS)
- LAYCH - Layer number to loop on
- XINC - Loop increment value

3.4.1.7 LOOPZ Parameters

- FINV - Final value of the of the loop variable when looping
- ILZ - Loop variable selection flag
 - 0 or 'OFF' = no looping
 - 1 or 'WVL' = loop on wavelength (WVL)
 - 2 or 'GRW' =loop on graded width (GRW)

Chapter 3 MATSYS and WAVEGUIDE INPUT/OUTPUT Parameters

- 3 or 'QW' = loop on quantum well width (QW)
- 4 or 'NQW' = loop on quantum well index (NQW)
- 9 or 'GRW2' = loop on graded width 2
- 10 or 'GRW3' = loop on graded width 3
- 11 or 'GRW4' = loop on graded width 4
- 12 or 'NSLC1' = loop on number of slices 1
- 13 or 'NSLC2' = loop on number of slices 2
- 14 or 'BW' = loop on barrier width
- 15 or 'NBAR' = loop on barrier index
- 16 or 'NUMQWS' = loop on number of quantum wells
- 17 or 'QZMR' = loop on initial guess (real part)
- 18 or 'QZMI' = loop on initial guess (imag part)
- ZINC - Loop increment value

3.4.1.8 OUTPUT Flag Parameters

- DBOUT - .db file output flag (1-enabled)
- DPRINT - .db file auto print flag (0-disabled)
- FFOUT - Far field file output flag (1-enabled)
- FPRINT - Far field file auto print flag (0-disabled)
- FWHPNO - Near field full width half power .db output flag
- FWHPFO - Far field full width half power .db output flag
- GAMMAO - Confinement factor (GAMMA) .db output flag
- LPRINT - Layer file auto print flag (0-disabled)

- MODOUT - Output file output flag (1-enabled)
- NFOUT - Near field file output flag (0-disabled)
- NPRINT - Near field file auto print flag (0-disabled)
- OPRINT - Output file auto print flag (0-disabled)
- PHMO - PHM (phase integral) .db output flag (1-enabled)
- QZIO - QZ root search (imag part) .db output flag
- QZRO - QZ root search (real part) .db output flag
- QZMIO - Initial guess (imag part) .db output flag
- QZMRO - Initial guess (real part) .db output flag
- SCROUT - Screen output flag (1-enabled)
- WZIO - WZ (imag part) .db output flag
- WZRO - WZ (real part) .db output flag

3.4.2 Output Parameters

- PHM - Phase integral
- GAMMA - Confinement factor
- WZR - Eigenvalue root (real part)
- WZI - Eigenvalue root (imaginary part)
- QZR - WZR squared
- QZI - WZI squared
- FWHPN - Near field full width half power
- FWHPF - Far field full width half power

3.5 Summary

Examples of using MATSYS and the various input and output parameters are shown throughout this manual. The earlier chapters of this manual are designed to step you through simple examples so you get familiar with using WAVEGUIDE. For many cases, the input parameters can be used with their default values.

References

- (1) Sadao Adachi Musashino Electrical Communication Laboratory, Nippon Telegraph and Telephone Public Corporation, Musashino-shi, Tokyo 180, Japan, "GaAs, AlAs, Al(x)Ga(1-x)As: Material Parameters for use in Research and Device Applications," *Journal of Applied Physics* 58 (3), 1 August 1985, pp. R1-R29.
- (2) David W. Jenkins, "Optical Constants of Al(x)Ga(1-x)As," *Journal of Applied Physics* 68 (4), 15 August 1990, pp. 1848-1853.
- (3) M. Gudent and J. Piprek, "Material parameters of Quaternary III-V Semiconductors for Multilayer Mirrors at 1.55um Wavelength," *Modelling Simul. Mater. Sci. Eng.* 4(1996) 349-357.
- (4) Sado Adachi, "Physical Properties of III-V Semiconductor Compounds," Published by Wiley Interscience.
- (5) "Quantum Well Lasers", edited by Dr. Zory.

(6) M.J. Mondry, D.I. Babic, J.E. Bowers and L.A. Coldren, "Refractive Indexes of (Al,Ga,In)As Epilayer on InP for Optoelectronic Applications," IEEE. PTL. vol.4, no.6, pp.627-630.

(7) H.C. Casey, Jr. and M.B. Panish, "Heterostructure Lasers, " Published by Academic Press.

(8) Sadao Adachi Musashino Electrical Communication Laboratory, Nippon Telegraph and Telephone Public Corporation, Musashino-shi, Tokyo 180, Japan, "Refractive indices of III-V compounds: Key properties of InGaAsP relevant to device design," Journal of Applied Physics, Vol.53, No.8 August 1982

Chapter 4 Dispersion for Glass Slab Waveguides

In this chapter, we use a three-layer slab waveguide to simulate the light dispersion in a glass material system. We introduce the total dispersion, which includes the material dispersion and waveguide dispersion. Two ways of calculation of total dispersion are presented in this chapter. One is to use the WAVEGUIDE to calculate the total dispersion. The other one is to use the WAVEGUIDE to calculate the waveguide dispersion and add up the material dispersion as the total dispersion.

4.1 Introduction

For fiber telecommunication, three types of dispersions cause the broadening and distortion of the signal. Internal modal dispersion exists for the multi-mode fiber. Two orthogonal polarized HE₁₁ waves in a single mode fiber cause polarization-mode dispersion. The third type of dispersion, chromatic dispersion, is the main focus in this chapter.

4.1.1 Chromatic dispersion

Chromatic dispersion includes the waveguide dispersion and material dispersion. The material refractive index varies with wavelengths for each material. This variation makes the material dispersion. The effective refractive index for a waveguide also changes with wavelengths for a fixed layer thickness, even if the layer materials are not dispersive. This is the waveguide dispersion. Both dispersions varies with wavelength. Usually, the material and waveguide dispersion are present simultaneously. The chromatic dispersion is caused by the influence of both of material and waveguide dispersion.

In WAVEGUIDE, the application of “MATSYS” parameter can calculate the chromatic dispersion, which considers the material and waveguide dispersion at the same time. If we use the refractive index for each layer instead of using “MATSYS”, we can only obtain the waveguide dispersion because the program uses the fixed refractive index for each layer for looping with different wavelength. Later in this chapter, we will discuss two methods of calculating the chromatic dispersion. One method is to use

“MATSYS”. The other is the summation of the waveguide and material dispersion as the chromatic dispersion.

4.1.2 Material System

The material used for the three-layer slab waveguide simulation is glass materials from Fleming’s paper[1]. These materials are similar to the fiber composition. In Fleming’s paper, six kinds of glass compositions have been studied for the material dispersion. Table 1 shows the six glass compositions. In WAVEGUIDE, the material system corresponding to these glass compositions is “MATSYS=14”. “XPERC” parameters give the sample letter from “A” to “F” with the number from “1” to “6”. For example, “XPERC=2” means that the sample B is the chosen material. The calculation of the refractive index of each composition as a function of wavelengths is based on the formula provided in section 4.2.

Table 4.1.2.1 Glass compositions and zero material dispersion [1]

Sample	Composition (Moles)	Wavelength of zero material dispersion (um)
A	Quenched SiO ₂	1.284
B	13.5GeO ₂ :86.5SiO ₂	1.383
C	9.1P ₂ O ₅ :90.9SiO ₂	1.274
D	13.3B ₂ O ₃ :86.7SiO ₂	1.231
E	1.0F:99.0SiO ₂	1.284
F	16.9Na ₂ O:32.5B ₂ O ₃ :50.6SiO ₂	1.283

4.2 Calculation of Material Dispersions

This section gives the formulation of the material dispersion and the material dispersion plot for the glass compositions.

4.2.1 Formulation

Based on Fleming's experiments, the refractive index of the glass compositions can be fitted to the following form [1]:

$$n^2 - 1 = \sum_{i=1}^3 \frac{A_i \lambda^2}{\lambda^2 - l_i^2} \quad (4.1)$$

where n is the refractive index

λ is the wavelength

A_i are constants related to material oscillator strengths

l_i are oscillator wavelength

Users can find A_i and l_i values from Fleming's paper. The material dispersion for each glass composition is calculated based on formula (4.1). The refractive index of the material is a function of wavelength. We know that the pulse spreading is related to the second derivative of the material index with respect to wavelength. Equation (4.2) shows this relation [2].

$$\Delta(\tau/L) = -\frac{\lambda}{c} n'' \Delta\lambda = -M\Delta\lambda \quad (4.2)$$

where M is the material dispersion = $\lambda * n'' / c$, usually has unit of ps/(nm*km)

λ is the wavelength (nm)

c is the speed of light (km/ps)

n'' is the second derivative of refractive index with respect to wavelength

$\Delta(\tau/L)$ is the pulse spread per unit length or pulse spreading

By taking second derivative of (1) and plugging in (2), we can get a material dispersion curve with respect to wavelength.

4.2.2 Dispersion plot

Figure 4.2.2.1 shows the refractive index of each glass composition based on equation (1). After we obtain the plot, we can take the second derivative of this curve to get material dispersion. Figure 4.2.2.2 shows the material dispersion curve for each

4.2 Calculation of Material Dispersions

composition. From Figure 4.2.2.2, we can find, between the wavelength 0.9 to 1.5 μm , the sample “D” $13.3\text{B}_2\text{O}_3:86.7\text{SiO}_2$ exhibits lower material dispersion. Therefore, we choose this sample as the cladding for our simulation. The material dispersion for the addition of B_2O_3 to SiO_2 , sample D, goes to zero at a shorter wavelengths than other compositions. On the other hand, GeO_2 composition, sample B, shifts the point of zero material dispersion to longer wavelengths. We can see that a different dopant for silica glass can shift the zero material dispersion to a desired wavelength. Most of the composition has the zero dispersion around $1.2\mu\text{m}$ as also shown in Talbe 4.1.2.1.

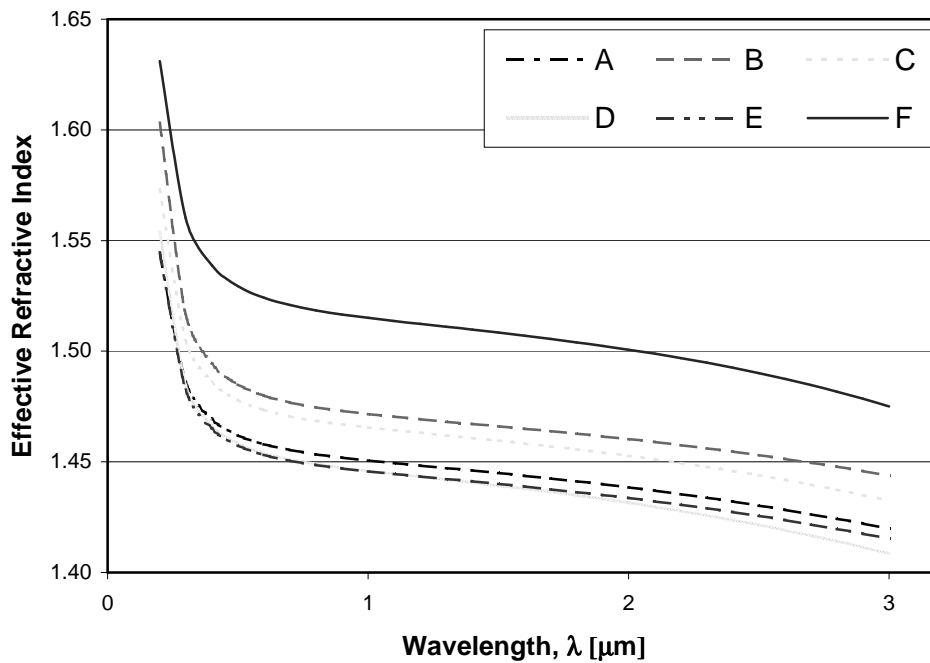


Figure 4.2.2.1 Refractive index verse wavelength

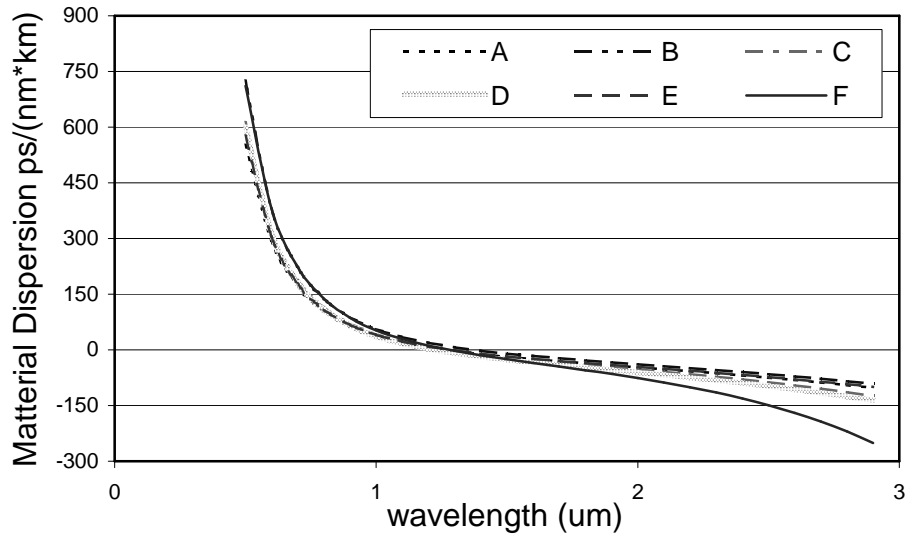


Figure 4.2.2.2 Material dispersion verse wavelength

4.3 Calculation of waveguide dispersion

This section gives the formulation of the waveguide dispersion and the waveguide dispersion plot for the slab waveguide.

4.3.1 Formulation

We use a simple three-layer symmetry slab waveguide for the simulation. Figure 4.3.1.1 shows a dielectric slab waveguide. In the waveguide, the refractive index in the center is larger than both side layers. We can fix the thickness of the center layer and use the fixed refractive index for each layer to get a mode chart for the TE₀ mode. From figure 4.3.1.2, an example of mode chart for a symmetric slab waveguide, we can see the effective refractive index for a mode varies with wavelength for a fixed film thickness. Different mode has a different effective refractive index verse d/λ curve. In this chapter, we will focus on the TE₀ fundamental single mode operation.

In the similar sense of refractive index as a function of wavelength, the effective refractive index of the waveguide is a function of wavelength for each mode. The variation of n_{eff} makes the pulse spreading like refractive index, n , does. This is

4.3 Calculation of Waveguide Dispersions

waveguide dispersion. Base on this sense, we can directly write down the waveguide dispersion equation:

$$\Delta(\tau / L) = -\frac{\lambda}{c} n_{eff}'' \Delta\lambda = -M_g \Delta\lambda \quad (4.3)$$

where n_{eff} is the effective refractive index

M_g is the waveguide dispersion = $\lambda * n_{eff}'' / c$, usually has unit of ps/(nm*km)

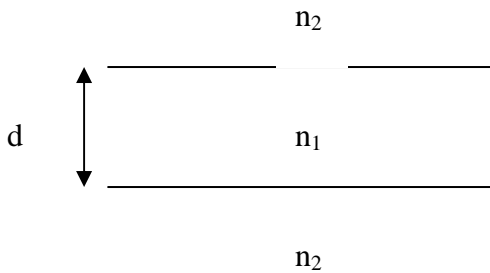


Figure 4.3.1.1 Dielectric symmetry slab waveguide

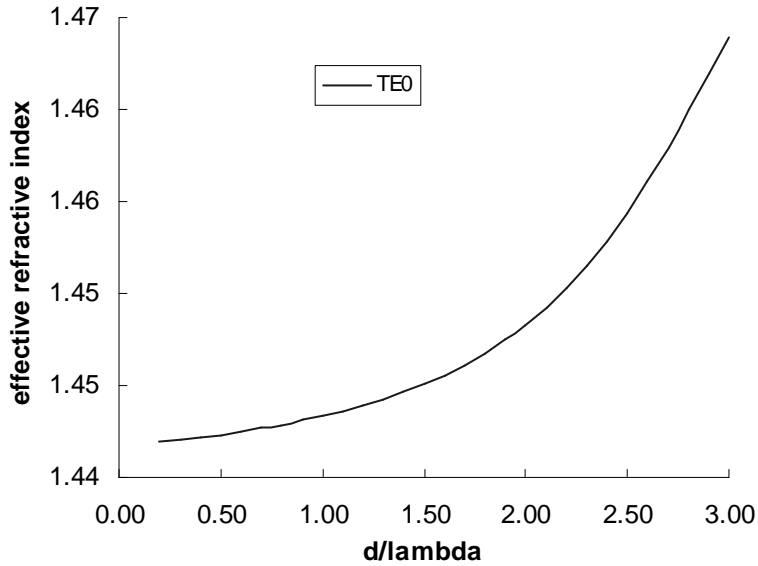


Figure 4.3.1.2 Mode chart for TE₀ mode

4.3.2 Input file

We will have different combinations of waveguide parameters and material for the simulation. The following is one input file example for our simulation. In this example, we use sample D as the core material and sample B as the side layers or cladding layers. n of these two material is 0.0263 under wavelength 1.3 μ m. The core thickness is 1 μ m. We enter the “NREAL” number for each layer. For looping through the wavelength, the “NREAL” number is the same. Generally, for the waveguide dispersion calculation, we can change the “NREAL” number and thickness of center layer to obtain different kinds of waveguide dispersion for the same material. In a later simulation section, we will show the results of different cases.

```
-----  
!CASE Parameter Set  
CASE KASE=TE0 SYM  
CASE EPS1=1E-9 EPS2=1E-9 GAMEPS=1E-3 QZMR=2.15052 QZMI=0.000  
CASE PRINTF=1 INITGS=0 AUTOQW=0 NFPLT=1 FFPLT=1 IL=30  
!MODCON Parameter Set  
MODCON KPOL=1 APB1 =0.25 APB2=0.25  
!STRUCT Parameter Set  
STRUCT WVL=3  
!LAYER Parameter Set  
LAYER NREAL=1.44192 NLOSS=0.0 TL=60  
LAYER NREAL=1.46817 NLOSS=0.0 TL=1  
LAYER NREAL=1.44192 NLOSS=0.0 TL=60  
!OUTPUT Parameter Set  
OUTPUT PHMO=1 GAMMAO=0 WZRO=1 WZIO=1 QZRO=1 QZIO=1  
OUTPUT FWHPNO=0 FWHPFO=0 KMO=1 ITO=1  
OUTPUT SPLTFL=0 MODOUT=0 LYROUT=0  
!GAMOUT Parameter Set  
GAMOUT LAYGAM=10 COMPGAM=0 GAMALL=0  
!LOOPZ Parameter Set  
LOOPZ1 ILZ="WVL" FINV=0.2 ZINC=-0.1  
END  
-----
```

4.3.3 Dispersion plot

From the output ‘*.db’ file of running previous section’s input file, we can plot “WZR” verse wavelength because “WZR” is the resulted effective refractive index for the waveguide. Figure 4.3.3.1 shows this plot. From Figure 4.3.3.1, we can take the second derivative of this graph and equation (3) to get the waveguide dispersion plot as shown in Figure 4.3.3.2.

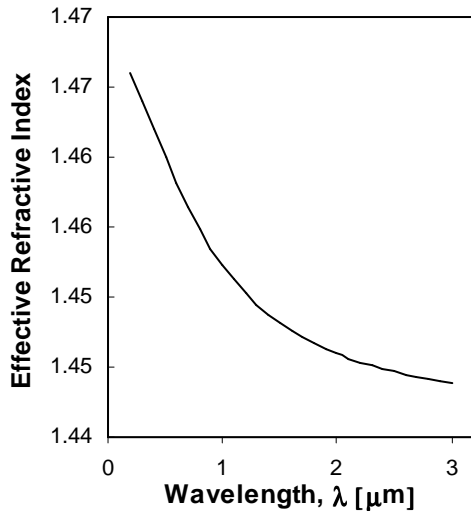
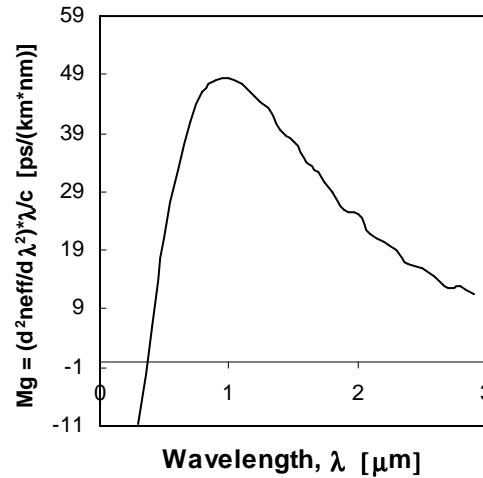
Figure 4.3.3.1 n_{eff} verse wavelength

Figure 4.3.3.2 Mg verse wavelength

4.4 Chromatic dispersion from WAVEGUIDE

In this section, we use WAVEGUIDE to directly calculate the chromatic dispersion. WAVEGUIDE take the refractive index of material changing with wavelengths into account. As a result, it calculates the effective refractive index for a single mode based on a certain wavelength. We can see the chromatic dispersion (M_c) becomes a function of wavelength in this way: $M_c(n_{\text{eff}}(n(\lambda)))$.

4.4.1 Input file

Similar to the waveguide dispersion calculation, we have a very similar input file for the example calculation. This example uses 1um core thickness. Sample D is the core material and sample B is side layers. The only difference is that we use the “MATSYS”

Chapter 4 Dispersion for Slab Glass Waveguide

parameter for refractive index of each layer instead of “NREAL”. The following shows the input file”

```
-----  
!CASE Parameter Set  
CASE KASE=TE0 SYM  
CASE EPS1=1E-9 EPS2=1E-9 GAMEPS=1E-3 QZMR=2.0696 QZMI=0.000  
CASE PRINTF=1 INITGS=0 AUTOQW=0 NFPLT=1 FFPLT=1 IL=30  
!MODCON Parameter Set  
MODCON KPOL=1 APB1 =0.25 APB2=0.25  
!STRUCT Parameter Set  
STRUCT WVL=3  
!LAYER Parameter Set  
LAYER MATSYS=14 XPERC=4 TL=60  
LAYER MATSYS=14 XPERC=2 TL=1  
LAYER MATSYS=14 XPERC=4 TL=60  
!OUTPUT Parameter Set  
OUTPUT PHMO=1 GAMMAO=0 WZRO=1 WZIO=1 QZRO=1 QZIO=1  
OUTPUT FWHPNO=0 FWHPFO=0 KMO=1 ITO=1  
OUTPUT SPLTFL=0 MODOUT=0 LYROUT=0  
!GAMOUT Parameter Set  
GAMOUT LAYGAM=10 COMPGAM=0 GAMALL=0  
!LOOPX Parameter Set  
!LOOPX1 ILX="TL" FINV=0.3 XINC=-0.5 LAYCH=2  
!LOOPZ Parameter Set  
LOOPZ1 ILZ="WVL" FINV=0.4 ZINC=-0.1  
!LOOPZ1 ILZ="QZMR" FINV=1.9853 ZINC=-0.05  
END  
-----
```

4.4.2 Dispersion plot

From the output ‘*.db’ file of running previous section’s input file, we can plot “WZR” verse wavelength because “WZR” is the resulted effective refractive index for the waveguide. Figure 4.4.2.1 shows this plot. From figure 4.4.2.1, we can take second derivative of this graph and equation (3) to get the waveguide dispersion plot as figure 4.4.2.2.

4.4 Chromatic dispersion from WAVEGUIDE

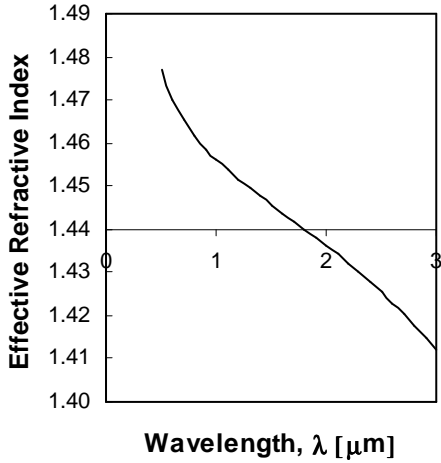


Figure 4.4.2.1 n_{eff} verse wavelength

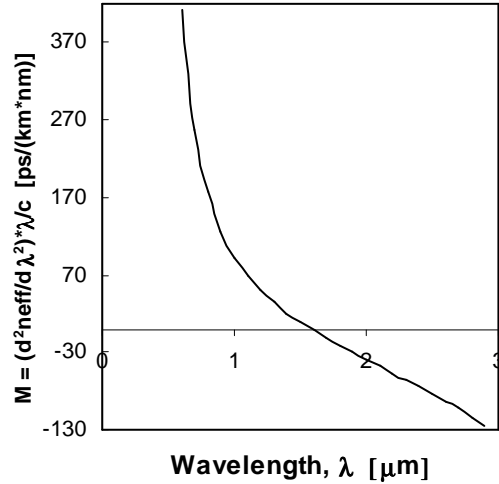


Figure 4.4.2.2 M_c verse wavelength

4.5 Simulation

We do a series of comparison between the chromatic dispersion from the WAVEGUIDE and the total dispersion, which is the summation of the material and waveguide dispersion. These comparisons are based on different Δn , core thickness and different material composition for core and cladding layers. Table 4.5.1 gives the different simulation case conditions.

Table 4.5.1 Simulation cases

Material	Case number	Conditions	
		Core thickness(d) (um)	$\Delta n(n_1-n_2)$
Core: B, Cladding :D	1	1	0.0263 ^a
	2	1	0.0268 ^b
	3	1	0.0353 ^c
	4	5	0.0263
	5	10	0.0263
Core:F, Cladding:D	6	1	0.06911 ^a

a: n_1 and n_2 is calculated under $\lambda=1.3\mu\text{m}$

Chapter 4 Dispersion for Slab Glass Waveguide

b: n_1 and n_2 is calculated under $\lambda=1.5\mu\text{m}$

c: n_1 and n_2 is calculated under $\lambda=3\mu\text{m}$

4.5.1 Results

Figure 4.5.1.1-4.5.1.6 show the results of the simulation cases from Table 4.5.1. The graphs show the waveguide dispersion (M_g), material dispersion for core layer (M_m), summation of waveguide and material dispersion and chromatic dispersion (M_c) from WAVEGUIDE for each simulation case. For case 1, 2 and 3, the difference among these cases is Δn . Δn can affect waveguide dispersion. The difference of Δn is not too big as a result of similar trends for these three cases. However, the summation of M_g and M_m , which will be called M_{total} for the rest of the section, is larger than M_c for the wavelength range larger than $0.8\mu\text{m}$. The wavelength of zero dispersion point for M_{total} is longer than M_c .

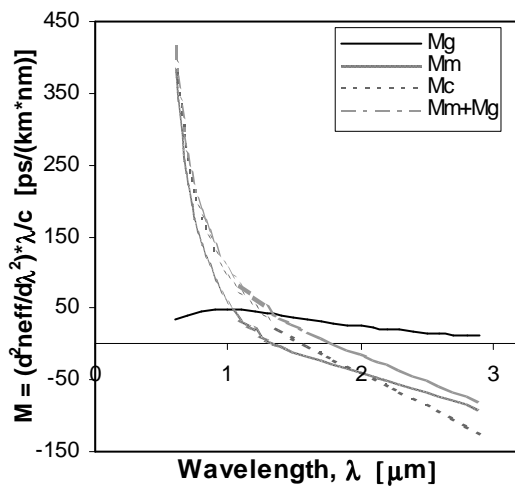


Figure 4.5.1.1 Case 1

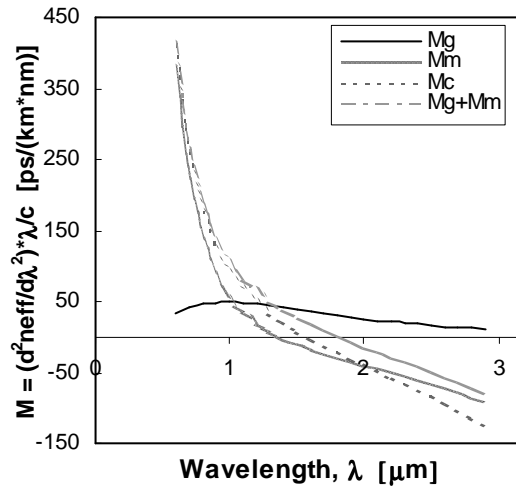


Figure 4.5.1.2 Case 2

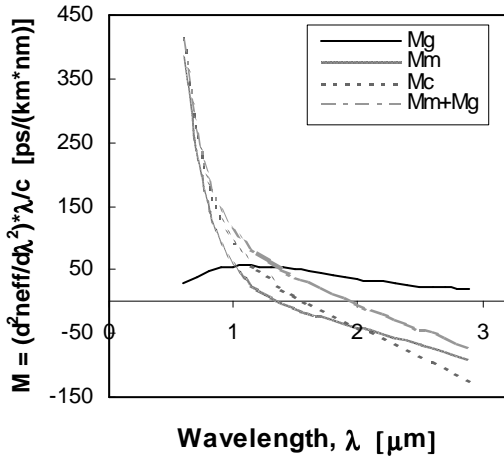


Figure 4.5.1.3 Case 3

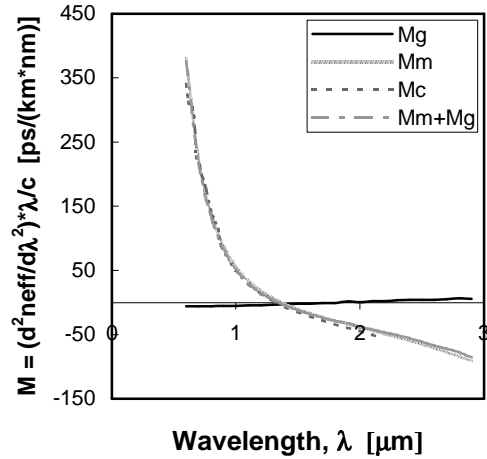


Figure 4.5.1.4 Case 4

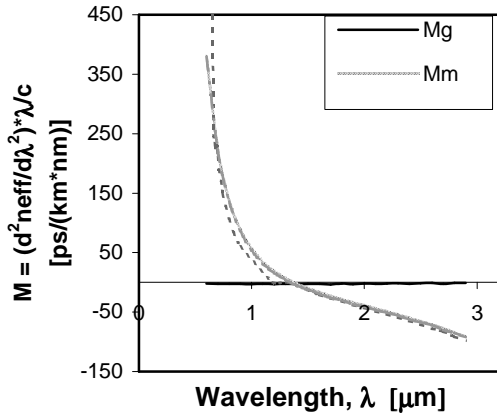


Figure 4.5.1.5 Case 5

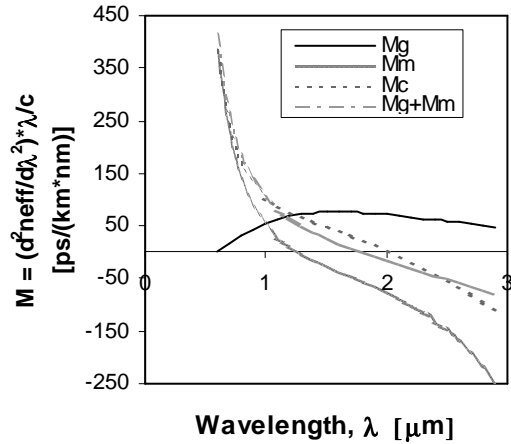


Figure 4.5.1.6 Case 6

Case 4 and case5 have different core thickness comparing with the first three cases. In case 4, M_{total} , M_c and M_m are very close to each other. From Figure 4.5.1.4, we can see M_g has small value. Similar trend happens to case 5. In case 5, the agreement among M_{total} , M_c and M_m is deviated beyond the positive dispersion. But, in case 5, M_c and M_m still have a pretty good agreement. We can say that chromatic dispersion is dominated by material dispersion for a thicker core thickness.

For case 6, we use different material, sample F, as the core material for the core thickness 1um. Under the same waveguide structure, Δn for this case is larger than the case, using sample B as the core material. It is clear that waveguide dispersion for this case play an important role for the chromatic dispersion. M_c has the zero dispersion point on a longer wavelength than M_{total} .

4.6 Conclusion

In summary, we compared two ways of chromatic dispersion calculation. If waveguide dispersion has much smaller value than material dispersion, these two ways of calculation have a good agreement with each other because the material dispersion play a big role. Thus, when we calculate the chromatic dispersion, we should be careful how we calculate the chromatic dispersion when waveguide dispersion is not relatively small to material dispersion. The zero dispersion point can have up to 0.5 μm wavelength different between both methods. However, waveguide dispersion can shift the zero material dispersion point to larger wavelength.

Reference

- [1] J.W. Fleming, "Material Dispersion in Lightguide Glasses", Electronics Letters, Vol.14 No.11, May 1978, pp.326-328
- [2] Joseph C. Palais, "Fiber Optic Communications, 4th Edition", Prentice Hall, 1998

Chapter 5 Symmetric – Waveguide Directional Coupler

A directional coupler is a passive device consisting in two or more close waveguides that are parallel to each other. If two waveguides are set up close to each other, energy passing through one is coupled to the other, so we can see the energy switch back and forth from one waveguide to the other during the light propagation. The power ratio at output ports depends on the waveguides thicknesses, distance between the two waveguides, the length of the interaction area, and indices difference between waveguide's core and cladding layers.

In this chapter, we would like to show readers how to simulate the directional coupler with WAVEGUIDE. For the purpose of simplicity, we take a simple coupler with two identical waveguides as an example.

5.1 Structure of Symmetric-Waveguide Directional Coupler

The symmetric-waveguide directional coupler is shown in Figure 5.1.1. The two core layers are identical and the directional coupler is symmetric in the x direction. Therefore they have the same propagation constants. Either waveguide in the directional coupler only supports one mode and for the whole coupler structure, there are two modes - TE₀ mode and TE₁ mode. As shown in Figure 5.1.1, the initially wave can be decomposed into equal composition of TE₀ mode and TE₁ mode with slightly different propagation constants β_0 and β_1 . The TE₀ mode of the directional coupler corresponds to the case that the modes of two waveguides are in-phase and TE₁ mode corresponds to the case that the modes of two waveguides are out-of-phase. Figure 5.1.1 also shows that with the wave initially set up at sub-waveguide 1 (SW₁), the energy in SW₁ will transmit to sub-waveguide 2 (SW₂) gradually along the wave propagating direction (z direction), and then switch back from SW₂ to SW₁. The distance for one complete energy transfer from one waveguide to the other is called “coupling length”. The coupling length L_c can be expressed in terms of the propagation constant of TE₀ mode β_0 and that of TE₁ mode β_1 as

$$L_c = \pi/(\beta_1 - \beta_0) \quad (5.1)$$

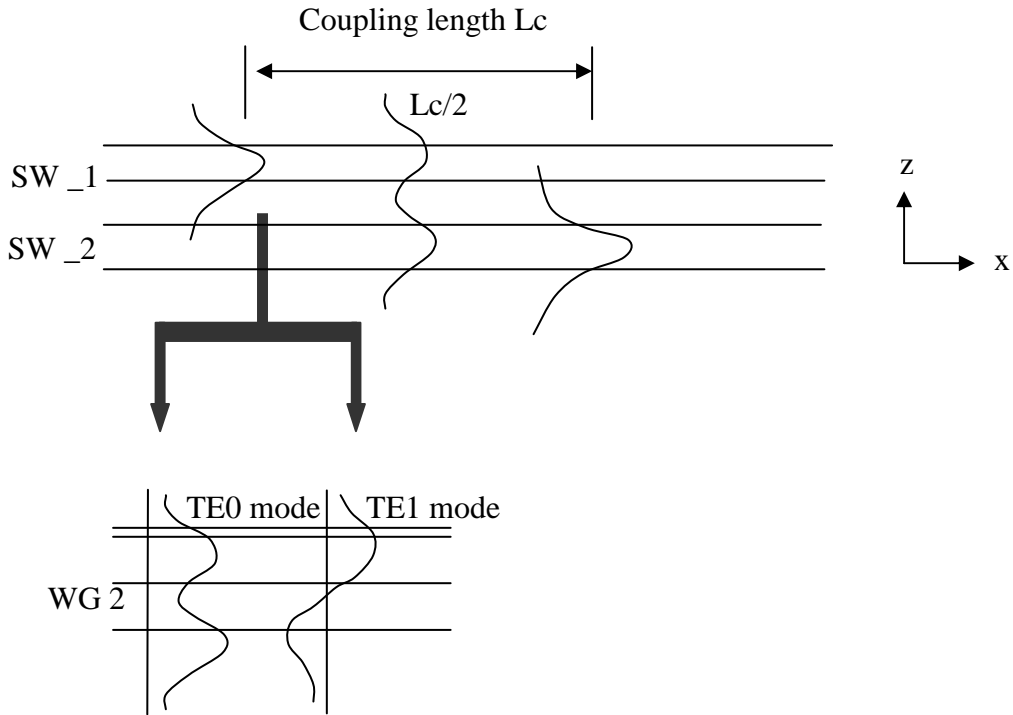


Figure 5.1.1 Structure of symmetric-waveguide directional coupler.

5.2 WAVEGUIDE Simulation of Symmetric-Waveguide Directional Coupler Structure

A 5-layer waveguide structure can be used to simulate the two-guide directional coupler in WAVEGUIDE. The 5-layer waveguide structure is illustrated as in Figure 5.2.1. The “directional coupler” has two “core” regions (SW_1 & SW_2) with an index of refraction of n_1 and three “cladding” regions with an index of refraction of n_2 . In addition, the core regions have a thickness of d and are separated by a distance of D .

5.2 WAVEGUIDE Simulation of Symmetric Waveguide Directional Coupler Structure

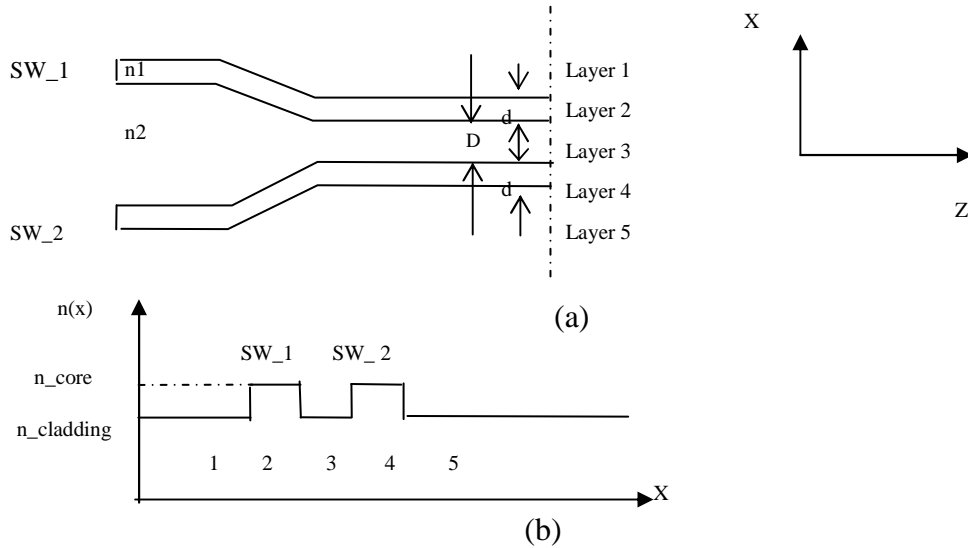


Figure 5.2.1 (a) 5-layer, symmetric-waveguide structure. (b) Layer index profile.

In the subsection below, we are going to show that by using the WAVEGUIDE program and its looping feature, we are able to (1) find the specific mode of a desired directional coupler structure, and calculate the corresponding propagation constants and coupling length; (2) inspect how the field distribution varies along with the sub-waveguide thickness, sub-waveguide separation and the difference of refractive indices of the core and cladding layer; (3) inspect how the propagation constants and coupling length of the directional coupler varies along with the sub-waveguide thickness and sub-waveguide separation.

5.2.1 Mode Finding and Propagation Constant Calculation of Single Mode, Two-guide Directional Coupler

To simulate the two-guide directional coupler, we create a 5-layer waveguide structure with $1 \mu\text{m}$ of wavelength in free space. Layer parameters are listed in table 5.2.1.1. The 2nd layer and the 4th layer are two core regions of the coupler (SW_1 & SW_2) with the same refractive index of 3.4 and thickness of $0.2 \mu\text{m}$. The 1st, 3rd and 5th layers are the “cladding” regions and have the refractive index of 3.4. The 3rd layer has thickness of $0.5 \mu\text{m}$. The thickness of this layer determines how far two sub-waveguides are from each other. We arbitrarily choose the thickness of two outmost

Chapter 5 Symmetric – Waveguide Directional Coupler

layers to be 0.2 μm . However, these two layers are always treated to be infinite thick by WAVEGUIDE. The input and output files are shown in table 5.2.1.2 and 5.2.1.3 respectively.

Table 5.2.1.1 Layer parameters of the directional coupler

LAYER01	NLOSS= 0.00000	NREAL= 3.40000	TL= 0.20000
LAYER02	NLOSS= 0.00000	NREAL= 3.55000	TL= 0.20000
LAYER03	NLOSS= 0.00000	NREAL= 3.40000	TL= 0.50000
LAYER04	NLOSS= 0.00000	NREAL= 3.55000	TL= 0.20000
LAYER05	NLOSS= 0.00000	NREAL= 3.40000	TL= 0.20000

Table 5.2.1.2 WAVEGUIDE input file for directional coupler mode searching

5.2 WAVEGUIDE Simulation of Symmetric Waveguide Directional Coupler Structure

```
!CASE Parameter Set
CASE KASE=Directional coupler (5 layers)
CASE   EPS1=1E-10  EPS2=1E-10  GAMEPS=1E-6
CASE   QZMR=12.60  QZMI=0.0
CASE   PRINTF=0    INITGS=0    AUTOQW=0  NFPLT=1    FFPLT=1

!MODCON Parameter Set
MODCON  KPOL=1    APB1=0.25    APB2=0.25

!STRUCT Parameter Set
STRUCT  WAVL=1

!LAYER Parameter Set
LAYER  NREAL=3.4  NLOSS=0.0    TL=0.2    !n-cladding
LAYER  NREAL=3.55 NLOSS=0.0    TL=0.2    !n-core      SW_1
LAYER  NREAL=3.4  NLOSS=0.00   TL=0.5    !n-cladding
LAYER  NREAL=3.55 NLOSS=0.0    TL=0.2    !n-core      SW_2
LAYER  NREAL=3.4  NLOSS=0.0    TL=0.2    !n-cladding

!OUTPUT Parameter Set
OUTPUT  PHMO=1    GAMMAO=0  WZRO=1  WZIO=0    QZRO=0    QZIO=0
OUTPUT  FWHPNO=0  FWHPFO=1  KMO=1   ITO=1
OUTPUT  MODOUT=1  LYROUT=1  SPLTFL=0
```

```
GAMOUT  LAYGAM=2    COMPGAM=0    GAMALL=0
!LOOPX Parameter Set
LOOPZ1  ILZ='QZMR'  FINV=11.56  ZINC=-0.01
END
```

Table 5.2.1.3 QZMR looping results

Chapter 5 Symmetric – Waveguide Directional Coupler

QZMR	PHM	WZR	FWHPF	KM	IT
		.			
		.			
		.			
1.203000E+01	7.303264E-01	3.430612E+00	2.630991E+01	6	8
1.202000E+01	7.303264E-01	3.430612E+00	2.630991E+01	7	8
1.201000E+01	7.303264E-01	3.430612E+00	2.630991E+01	7	8
1.200000E+01	6.738678E-01	3.448619E+00	3.015387E+01	6	6
1.199000E+01	6.738678E-01	3.448619E+00	3.015387E+01	6	6
1.198000E+01	6.738678E-01	3.448619E+00	3.015387E+01	7	6
		.			
		.			
		.			
1.192000E+01	6.738678E-01	3.448619E+00	3.015387E+01	6	4
1.191000E+01	6.738678E-01	3.448619E+00	3.015387E+01	7	4
1.190000E+01	6.738678E-01	3.448619E+00	3.015387E+01	6	3
1.189000E+01	6.738678E-01	3.448619E+00	3.015387E+01	7	3
1.188000E+01	6.738678E-01	3.448619E+00	3.015387E+01	7	4
1.187000E+01	6.738678E-01	3.448619E+00	3.015387E+01	6	4
		.			
		.			
		.			
1.184000E+01	6.738678E-01	3.448619E+00	3.015387E+01	7	5
1.183000E+01	7.303264E-01	3.430612E+00	2.630991E+01	7	5
1.182000E+01	7.303264E-01	3.430612E+00	2.630991E+01	7	5
		.			
		.			
		.			
1.178000E+01	7.303264E-01	3.430612E+00	2.630991E+01	6	3
1.177000E+01	7.303264E-01	3.430612E+00	2.630991E+01	6	2
1.176000E+01	7.303264E-01	3.430612E+00	2.630991E+01	6	3
1.175000E+01	7.303264E-01	3.430612E+00	2.630991E+01	7	4
		.			
		.			
		.			

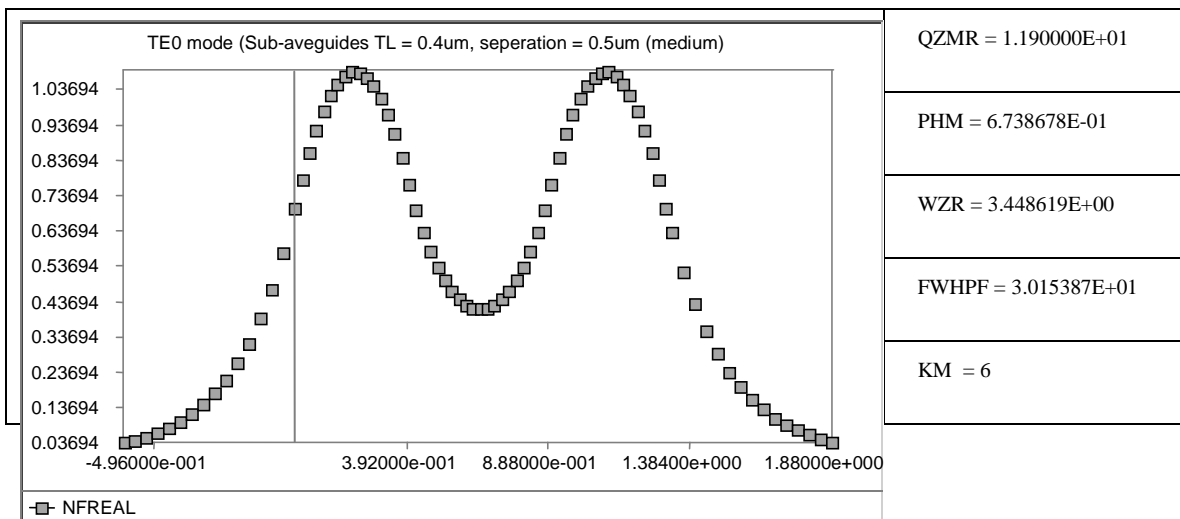
We search for TE0 mode and TE1 mode by looping for parameter QZMR. The up bound of QZMR is usually approximated by the square of the maximum NREAL – WAVEGUIDE parameter that represents real part of the effective index of the structure, and the bottom bound of QZMR is approximated by the square of the minimum NREAL. From the layer information above, we have

$$QZMR_{up} = (3.55)^2 = 12.60$$

$$QZMR_{bottom} = (3.4)^2 = 11.56.$$

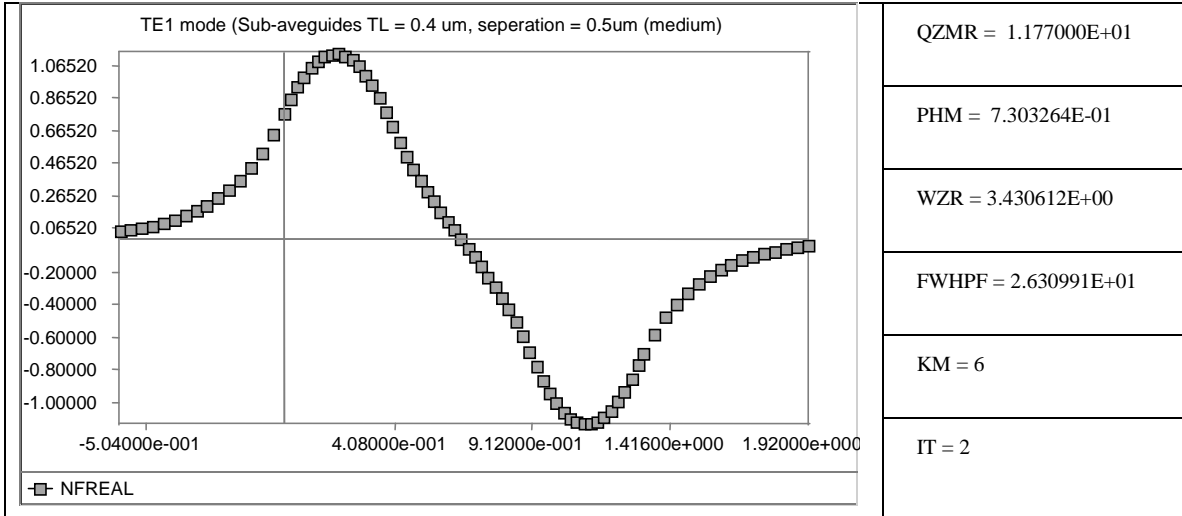
5.2 WAVEGUIDE Simulation of Symmetric Waveguide Directional Coupler Structure

The general criteria to look for a proper QZMR value for the fundamental mode of the waveguide are: (1) $PHM < 1.0$, (2) $KM = 6$ or 7 . The two-guide directional coupler support at least two modes- TE_0 and TE_1 , and it happens when either of the two guides only support fundamental mode. So we can think both TE_0 and TE_1 mode are the fundamental modes of the directional coupler. However, in WAVEGUIDE, the TE_1 mode may or may not meet the first criterion. If we look at the PHM (or WZR) values in table 5.2.1.3, we should see that some QZMR values have the exact same PHM of $7.303264E-01$ (or WZR of 3.448619), and the others have the exact same PHM of $6.738678E-01$ (or WZR of 3.430612). This suggests that these two groups of QZMR values correspond to two different modes of the directional coupler. The TE_0 mode should have smallest PHM (or largest WZR) value, and the TE_1 mode corresponds to the next PHM (WZR) value. For each group, we should pick the QZMR that has the minimum iteration number (IT), which are $QZMR = 11.90$ for TE_0 mode and $QZMR = 11.77$ for TE_1 mode in this case. Then we close the loop and do the WAVEGUIDE evaluation with one QZMR value at a time. For each evaluation, we plot the near field as a function of position along x direction. It'll then be very easy to recognize the TE_0 mode and TE_1 mode from the field profile. The near field plots and the corresponding output parameters are listed in Figure 5.2.1.1.



	IT = 3
--	--------

(a)



(b)

Figure 5.2.1.1 (a) Near field of TE0 mode of the directional coupler. (b) Near field of TE1 mode of the directional coupler.

In WAVEGUIDE, the zero position of x direction, which is indicated by the vertical line in the near field plot, is set at the interface of the 1st layer and 2nd layer (see Figure 5.2.1). From Figure 5.2.1.1, we can see that the peak of the near field occurs at the center of each sub-waveguide (layer 2 & 4) in the directional coupler, and the electric field extends from the “core” layers into the “cladding” layers for both sub-waveguides.

The calculation of the propagation constant and coupling length of the directional coupler is straightforward once we find the effective index of the structure for the specific mode. The formula to calculate the propagation constant is

$$\beta = k * n = (2\pi/\lambda_0) * n \quad (5.2)$$

Where β is the propagation constant, k is the wave number, λ_0 is the wavelength in free space and n is the effective index of the mode which is approximated by the real part of the effective index - WZR. The effective indices and propagation constants for TE0 mode and TE1 mode and the coupling length of the structure are shown in table 5.2.1.4.

5.2 WAVEGUIDE Simulation of Symmetric Waveguide Directional Coupler Structure

Table 5.2.1.4 Effective indices and propagation constants for TE0 mode and TE1 mode of the directional coupler.

	Wavelength (μm)	Effective index	Propagation constant (cm^{-1})	Coupling length (cm)
TE0 mode	1	3.448619	10.83E04	0.01
TE1 mode	1	3.430612	10.78E04	

5.2.2 Field Distribution of Single Mode, Two-guide Directional Coupler

In last section, we introduced how to find the field distribution for specific mode of fixed directional coupler structure. In this section, we want to show readers that by varying the layer parameters of the directional coupler, and comparing the near field plots of those varied structures, we can find out how the sub-waveguide thickness (d), sub-waveguides separation (D) and the difference of refractive indices of the core and cladding layer (Δn) affect the field distribution of symmetric-waveguide directional coupler.

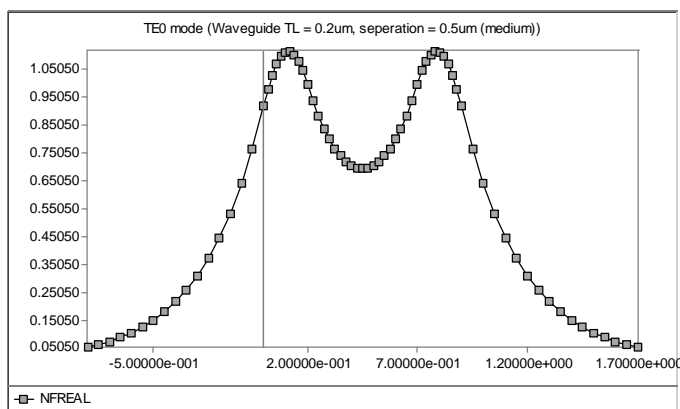
As shown in the table 5.2.2.1, in first group, we fix D to be $0.5 \mu\text{m}$, and Δn to be 0.15 , choose the sub-waveguided thickness d to be $0.2 \mu\text{m}$, $0.4 \mu\text{m}$ and $0.8 \mu\text{m}$, respectively. For each value of the sub-waveguide thickness, we loop the QZMR from the it's up bound to the bottom bound, and find the proper QZMR value for each mode by using the same procedure described in section 5.2.1. With the proper QZMR, the WAVEGUIDE software can generate the near field distribution as a function of position along x direction. Similarly, in second group, we then fix the d and Δn to be $0.4 \mu\text{m}$ and 0.15 , vary the sub-waveguides separation D to be $0.05 \mu\text{m}$, $0.5 \mu\text{m}$ and $4 \mu\text{m}$, and repeat the same steps as those described above. Finally, in last group, we fixed the d and D to be $0.4 \mu\text{m}$ and $0.5 \mu\text{m}$, vary the difference of refractive indices of the core and cladding layer Δn from 0.15 to 0.05 by increase the cladding layer index form 3.4 to 3.5 at a 0.05 space.

Chapter 5 Symmetric – Waveguide Directional Coupler

Table 5.2.2.1 Layer parameters of directional coupler structures

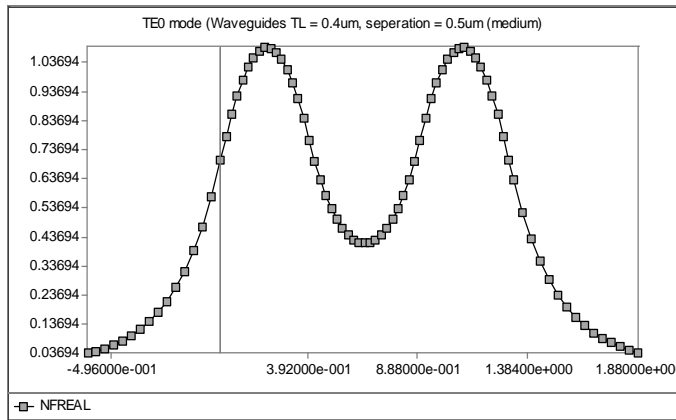
Directional coupler	Sub-waveguide thickness - d (μm)	Sub-waveguide separation - D (μm)	Refractive indices difference of core and cladding - Δn
Group 1	0.2	0.5	0.15
	0.4		
	0.8		
Group 2	0.4	0.05	0.15
		0.5	
		4	
Group 3	0.4	0.5	0.15
			0.10
			0.05

The plots of near field for TE₀ mode of directional coupler group 1, is presented in Figure 5.2.2.1 below. It is obvious that with the other layer parameters fixed, the larger the sub-waveguides thickness d is, the less the fields of two sub-waveguides overlap at the center layer and the weaker the coupling of two sub-waveguides is.

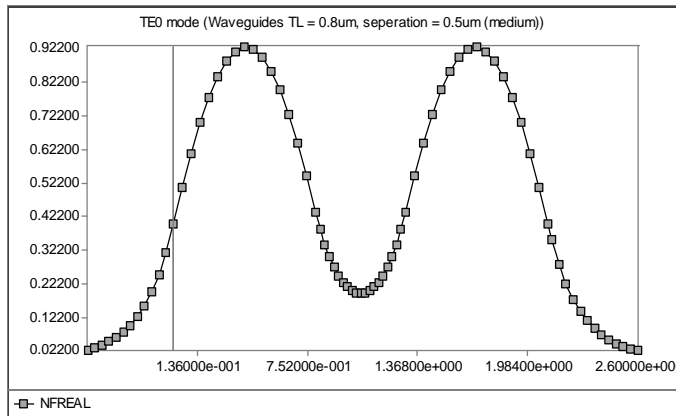


(a)

5.2 WAVEGUIDE Simulation of Symmetric Waveguide Directional Coupler Structure



(b)

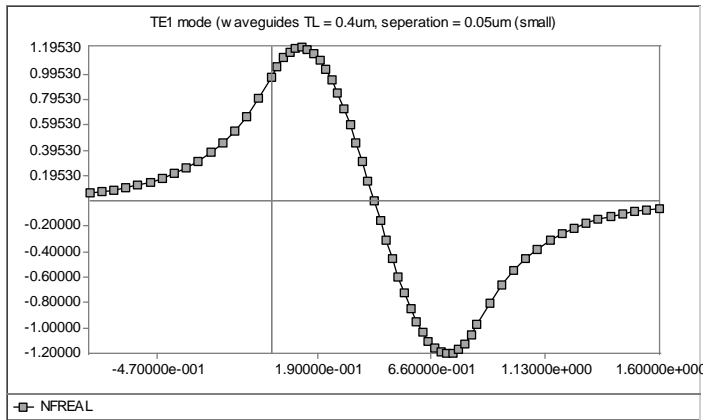


(c)

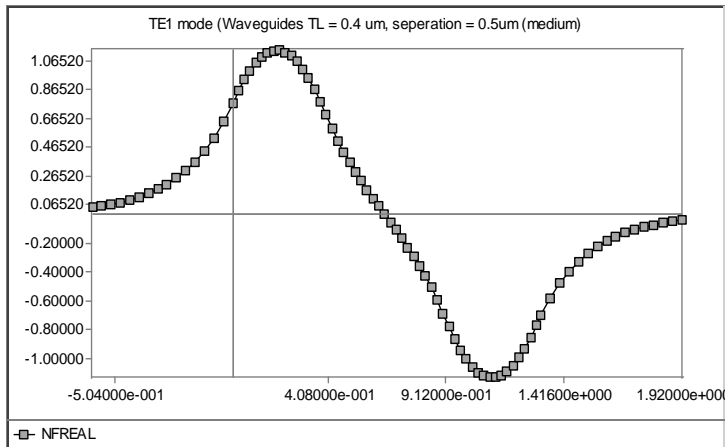
Figure 5.2.2.1 TE₀ field distribution of two-guide directional coupler for (a) sub-waveguide thickness = 0.2 mm and separation = 0.5 mm, (b) sub-waveguide thickness = 0.4 mm and separation = 0.5 mm, (c) sub-waveguide thickness = 0.8 mm and separation = 0.5 mm.

Similarly, the plots of near field for TE₁ mode of directional coupler group 2, which is depicted in Figure 5.2.2.1 below implies that the larger the separation of two sub-waveguides is, the less the electrical fields of two sub-waveguides overlap at the coupler center layer; and therefore the weaker the coupling of two sub-waveguides is.

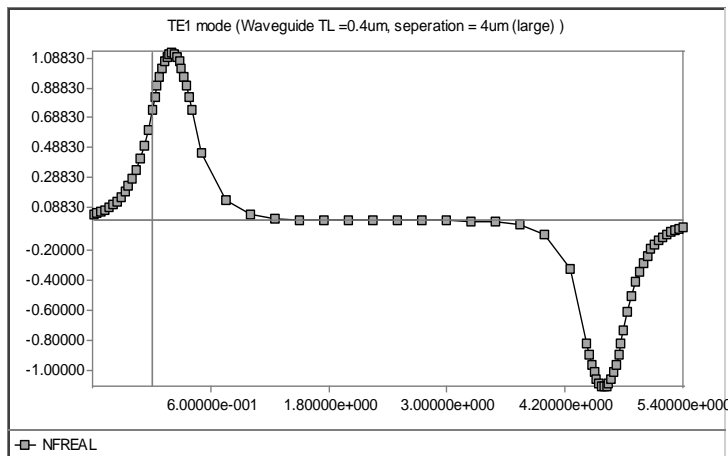
Chapter 5 Symmetric – Waveguide Directional Coupler



(a)



(b)



(c)

Figure 5.2.2.2 TE1 field distribution of two-guide directional coupler for (a) sub-waveguide thickness = 0.4 mm and separation = 0.05 mm, (b) sub-waveguide thickness = 0.4 mm and separation = 0.5 mm, (c) sub-waveguide thickness = 0.4 mm and separation = 4 mm.

5.2 WAVEGUIDE Simulation of Symmetric Waveguide Directional Coupler Structure

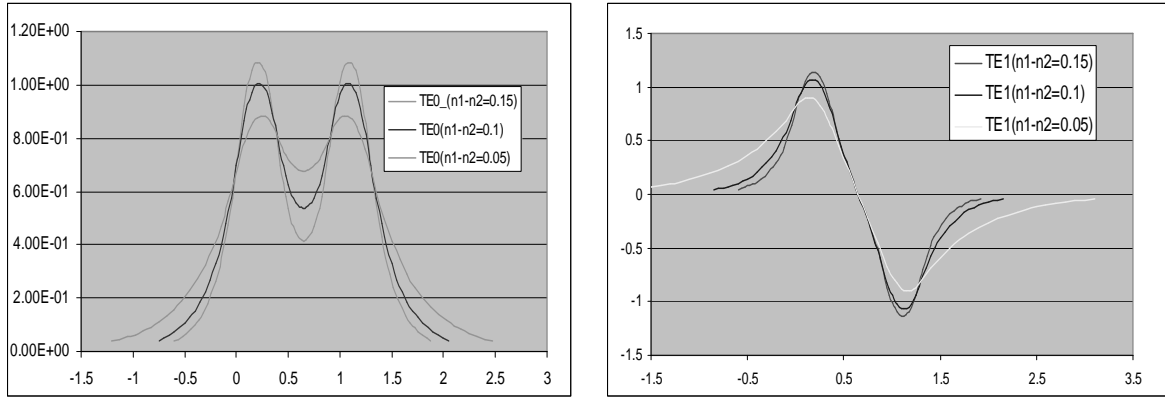


Figure 5.2.2.3 (a) TE0 field distributions of symmetric-waveguide directional coupler with $\Delta n = 0.05$ mm, 0.1 mm and 0.15 mm. (b) TE1 field distributions of symmetric-waveguide directional coupler with $\Delta n = 0.05$ mm, 0.1 mm and 0.15 mm.

Figure 5.2.2.3 plot the near fields for both TE0 mode and TE1 mode of directional coupler group 3. The figure indicates that the smaller the index difference Δn , the larger the electric fields overlap, the stronger the coupling of two sub-waveguides is.

5.2.3 Coupling length of Symmetric-waveguide Directional Coupler

In this section, we would like to show readers how to use the looping feature of the WAVEGUIDE program to calculate propagation constants and coupling length as a function of sub-waveguide separation for 5-layer directional coupler.

Table 5.2.3.1 Input parameters for 5-layer waveguide structures.

Directional coupler	Core index (layer 2 & 4)	Cladding index (layer 1, 3 & 5)	SW.1 & SW.2 thickness (layer 2 & 4) (μm)	Looping waveguide separation (layer 3) (μm)	
				Start value	End value
#1	3.55	3.45	0.2	0.2	3
#2	3.55	3.45	0.4	0.2	3
#3	3.55	3.45	0.8	0.2	3

Chapter 5 Symmetric – Waveguide Directional Coupler

As shown in table 5.2.3.1, we fix the core index of 3.55, cladding index of 3.45 and choose the sub-waveguides separation to be 0.2 μm , 0.4 μm and 0.8 μm for 5-layer directional coupler structure #1, #2 and #3 respectively. Then we evaluate each structure by looping the sub-waveguides separation from 0.2 μm to 3 μm and calculate the corresponding propagation constants and coupling length.

Using structure #1 as an example, the general steps is:

1. Loop the QZMR values, check the “.db” file and find the proper QZMR values for TE0 mode and TE1 mode by using the criteria given in 5.1.1 (See table. 5.2.3.2 and table. 5.2.3.3 for the input and output files).
2. For each mode, plug the selected QZMR into the input file and set the looping parameter –LOOPX1 to be “TL” and layer parameter – LAYCH to be “3” to represent looping for layer 3, which is the sub-waveguides separation layer in 5-layer waveguide. Evaluate the input file (see table 5.2.3.4 for the input file for TE0 mode).
3. The series values of sub-waveguides separations and corresponding refractive indices for TE0 and TE1 modes are given in “TL (3)” column and “WZR” column in the output “.db” file. Copy the two columns into the Excel, calculate and plot the propagation constants and coupling length by using the equation 5.2.1.1 and 5.1.1.1.

Table 5.2.3.2 WAVEGUIDE input file of mode searching for directional coupler structure #1.

```
!CASE Parameter Set
CASE KASE=Directional coupler (5 layers)
CASE   EPS1=1E-6  EPS2=1E-6  GAMEPS=1E-6
CASE   QZMR=12.60  QZMI=0.0
CASE   PRINTF=0   INITGS=0   AUTOQW=0  NFPLT=1   FFPLT=1

!MODCON Parameter Set
MODCON  KPOL=1   APB1=0.25  APB2=0.25
```

5.2 WAVEGUIDE Simulation of Symmetric Waveguide Directional Coupler Structure

```
!STRUCT Parameter Set
STRUCT   WVl=1

!LAYER Parameter Set
LAYER   NREAL=3.4   NLOSS=0.0   TL=0.2   ! cladding
LAYER   NREAL=3.55  NLOSS=0.0   TL=0.4   ! core
LAYER   NREAL=3.4   NLOSS=0.0   TL=0.2   ! cladding
LAYER   NREAL=3.55  NLOSS=0.0   TL=0.4   ! core
LAYER   NREAL=3.4   NLOSS=0.0   TL=0.2   ! cladding

!OUTPUT Parameter Set
OUTPUT  PHMO=1   GAMMAO=0   WZRO=1   WZIO=0   QZRO=0   QZIO=0
OUTPUT  FWHPNO=0   FWHPFO=1   KMO=1   ITO=1
OUTPUT  MODOUT=1   LYROUT=1   SPLTFL=0
GAMOUT  LAYGAM=2   COMPGAM=0   GAMALL=0

!LOOPZ Parameter Set
LOOPZ1  ILZ='QZMR'  FINV=11.56  ZINC=-0.01

END
```

Table 5.2.3.3 QZMR looping result for directional coupler structure #1.

Chapter 5 Symmetric – Waveguide Directional Coupler

QZMR	PHM	WZR	FWHPF	KM	IT
		.			
		.			
		.			
1.226000E+01	9.648328E-01	3.498409E+00	3.635308E+01	6	3
1.225000E+01	9.648327E-01	3.498409E+00	3.635303E+01	6	2
1.224000E+01	9.648328E-01	3.498409E+00	3.635311E+01	6	1
1.223000E+01	9.648328E-01	3.498409E+00	3.635310E+01	6	2
1.222000E+01	9.648328E-01	3.498409E+00	3.635308E+01	6	3
		.			
		.			
		.			
1.207000E+01	1.205002E+00	3.469193E+00	3.161936E+01	6	3
1.206000E+01	1.205002E+00	3.469193E+00	3.161936E+01	6	3
1.205000E+01	1.205002E+00	3.469193E+00	3.161930E+01	6	2
1.204000E+01	1.205002E+00	3.469193E+00	3.161936E+01	6	2
1.203000E+01	1.205002E+00	3.469193E+00	3.161936E+01	6	2
1.202000E+01	1.205002E+00	3.469193E+00	3.161942E+01	6	2
1.201000E+01	1.205002E+00	3.469193E+00	3.161936E+01	6	3
		.			
		.			
		.			

Table 5.2.3.4 Input file to loop the sub-waveguide separation for directional coupler structure #1 with TE0 mode.

```
!CASE Parameter Set
```


5.2 WAVEGUIDE Simulation of Symmetric Waveguide Directional Coupler Structure

```
CASE KASE=Directional coupler (5 layers)
CASE     EPS1=1E-6  EPS2=1E-6  GAMEPS=1E-6
CASE     QZMR= 12.24  QZMI=0.0   ! TE0
CASE     PRINTF=0   INITGS=0   AUTOQW=0  NFPLT=1   FFPLT=1

!MODCON Parameter Set
MODCON   KPOL=1    APB1=0.25   APB2=0.25

!STRUCT Parameter Set
STRUCT   WVL=1

!LAYER Parameter Set
LAYER    NREAL=3.4  NLOSS=0.0   TL=0.2   ! cladding
LAYER    NREAL=3.55 NLOSS=0.0   TL=0.4   ! core
LAYER    NREAL=3.4  NLOSS=0.0   TL=0.2   ! cladding
LAYER    NREAL=3.55 NLOSS=0.0   TL=0.4   ! core
LAYER    NREAL=3.4  NLOSS=0.0   TL=0.2   ! cladding

!OUTPUT Parameter Set
OUTPUT   PHMO=1    GAMMAO=0   WZRO=1   WZIO=0   QZRO=0   QZIO=0
OUTPUT   FWHPNO=0  FWHPFO=1   KMO=1    ITO=1
OUTPUT   MODOUT=1  LYROUT=1   SPLTFL=0
GAMOUT   LAYGAM=2   COMPGAM=0   GAMALL=0

!LOOPX Parameter Set
LOOPX1   ILX='TL'  FINV=3    XINC=0.05  LAYCH=3

END
```

Table 5.2.3.4 Waveguide separation looping result for directional coupler structure #1 with TE0 mode.

Chapter 5 Symmetric – Waveguide Directional Coupler

TL(3)	PHM	WZR	FWHPF	KM	IT
2.000000E-01	9.648328E-01	3.498409E+00	3.635311E+01	6	1
2.500000E-01	9.904514E-01	3.495611E+00	3.459116E+01	6	3
3.000000E-01	1.009986E+00	3.493427E+00	3.289045E+01	6	3
3.500000E-01	1.025066E+00	3.491711E+00	3.133612E+01	6	3
.					
1.200000E+00	1.079220E+00	3.485331E+00	1.710198E+01	6	1
1.250000E+00	1.079425E+00	3.485306E+00	1.664205E+01	6	1
1.300000E+00	1.079586E+00	3.485287E+00	1.618088E+01	6	1
1.350000E+00	1.079712E+00	3.485272E+00	1.576260E+01	6	1
1.400000E+00	1.079812E+00	3.485260E+00	1.536916E+01	6	1
.					
2.800000E+00	1.080178E+00	3.485215E+00	6.235332E+00	6	1
2.850000E+00	1.080178E+00	3.485215E+00	6.245429E+00	6	1
2.900000E+00	1.080178E+00	3.485215E+00	6.261909E+00	6	1
2.950000E+00	1.080178E+00	3.485215E+00	6.260620E+00	6	1
3.000000E+00	1.080178E+00	3.485215E+00	6.237595E+00	6	1

Figure 5.2.3.1 and Figure 5.2.3.2 exhibit the propagation constant in logarithm as a function of sub-waveguides separation and the coupling length in logarithm as a function of sub-waveguides separation for the structures listed in table 5.2.3.1. It is clear that at fixed sub-waveguides thickness, for both TE₀ mode and TE₁ mode, when the distance between two sub-waveguides of the coupler increases, the difference of β_0 and β_1 decrease; therefore the coupling length of the directional coupler increases. These simulation results match the theoretical prediction and the conclusion drawn in section 5.2.2. When increasing the separation of two sub-waveguides, their coupling strength

5.2 WAVEGUIDE Simulation of Symmetric Waveguide Directional Coupler Structure

decreases, so the energy transmitting from one sub-waveguide to the other becomes more slower; therefore we should expect that it'll takes longer distance to transmit all the energy from one sub-waveguide to the other. Figure 5.2.3.1 also predicts that if the two sub-waveguides are separated far enough, they will become two independent (uncoupled) waveguides with same propagation constant.

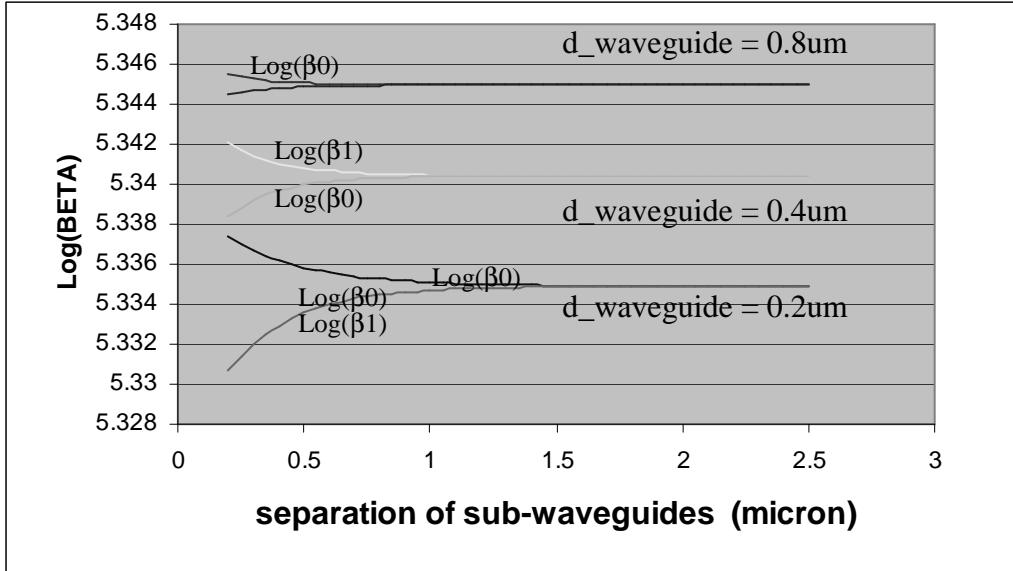


Figure. 5.2.3.1 Propagation constants β_0 and β_1 in logarithm vs. separation of sub-waveguides for sub-waveguide thickness =0.2 μm , 0.4 μm and 0.8 μm (Propagation constant has the unit of cm^{-1}).

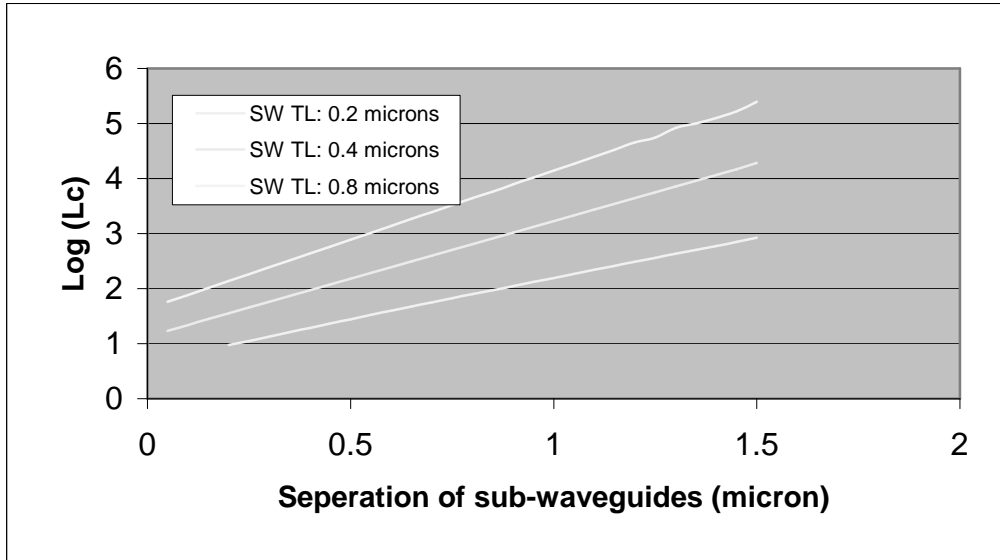


Figure. 5.2.3.2 Coupling length in logarithm vs. separation of sub-waveguides for sub-waveguide thickness =0.2 μm , 0.4 μm and 0.8 μm (coupling length has the unit of μm^{-1}).

Chapter 6 – InGaAs/AlGaAs/GaAs Structure with GRINSCH and AlGaAs/AlGaAs/GaAs Structure with Multiple QW Examples

6.1 Introduction

This chapter uses material system InGaAs/AlGaAs/GaAs for an example of a semiconductor laser structure at 975 nm and material system AlGaAs/AlGaAs/GaAs for an example of a laser at 820 nm. For the 975 nm structure, the quantum well will be InGaAs, the cladding and SCH layers will be AlGaAs, and the substrate and cap will be GaAs. The 820 nm structure also has a GaAs substrate and cap, but the quantum well, SCH, and cladding layers are all AlGaAs.

We will highlight two WAVEGUIDE features including a graded index separate confinement heterostructure (GRINSCH) and a multiple quantum well structure (MQW). We will start with a generic single quantum well structure using InGaAs/AlGaAs/GaAs as the first example and change the structure by making the SCH layer graded for the second example. Then we will move more quickly through a generic single quantum well AlGaAs/AlGaAs/GaAs structure and then change the number of quantum wells for the third example. By the end of this chapter, you should feel more comfortable with modifying the WAVEGUIDE input file to describe a customized laser structure.

6.2 MATSYS Options for AlGaAs/GaAs

There are three possible ways to enter the refractive index for each AlGaAs/GaAs layer in WAVEGUIDE. You can directly assign the refractive index value to NREAL

Chapter 6 InGaAs/AlGaAs/GaAs Structure with GRINSCH and AlGaAs/AlGaAs/GaAs Structure with Multiple QW Examples

parameter in the LAYER definition or you can use one of the two MATSYS options.

MATSYS will calculate the refractive index for you based on the composition you input and has option AlGaAs 1 which is based on a paper by Adachi (see reference 1 in chapter section 3.3) or you can use AlGaAs 2 which is based on a paper by Jenkins (see reference 2 in chapter section 3.3). The examples in this section use the Jenkins model which has MATSYS code 0.1.

6.3 Single Quantum Well Structure with GRINSCH at 980 nm

In this first example, the initial WAVEGUIDE input file (Example 6-1) is based on a structure (Table 6.3.1) analyzed in the GAIN program manual for material system 6. To get started in WAVEGUIDE, the SCH and cladding layer thicknesses are arbitrarily selected. MATSYS is used for the all the layers except the quantum well where the refractive index is entered directly.

Table 6.3.1

Layer	λ (μm)	Strain	Thickness (\AA)
QW ($\text{In}_x\text{Ga}_{1-x}\text{As}$)	1.06	-0.0119285	90
SCH ($\text{Al}_x\text{Ga}_{1-x}\text{As}$)	0.871	-	100
Cladding($\text{Al}_x\text{Ga}_{1-x}\text{As}$)	0.6665	-	100

Example 6-1 Input File

```
!WIF generated by WIFE (Waveguide Input File Editor)
!CASE Parameter Set - 975 nm Structure
```

6.3 Single Quantum Well Structure with GRINSCH at 980 nm

```
CASE KASE=WIFE
CASE EPS1=1E-8 EPS2=1E-8 GAMEPS=1E-6 QZMR=11.60 QZMI=0
CASE PRINTF=1 INITGS=0 AUTOQW=0 NFPLT=1 FFPLT=1 IL=30

!MODCON Parameter Set
MODCON KPOL=0 APB1=0.25 APB2=0.25

!STRUCT Parameter Set
STRUCT WV=0.975

!LAYER Parameter Set
LAYER MATSYS=0.1 XPERC=0.0 NLOSS=0.0 TL=0.0 !L1 Substrate and Buffer
LAYER MATSYS=0.1 XPERC=0.35 NLOSS=0.0 TL=1.5 !L2 AlGaAs n-Cladding at 35% Al
LAYER MATSYS=0.1 XPERC=0.15 NLOSS=0.0 TL=0.3 !L3 AlGaAs n-SCH at 15% Al
LAYER MATSYS=0.1 XPERC=0.0 TL=0.005 !L4 GaAs Shoulder
LAYER NREAL=3.635219 NLOSS=0.00 TL=0.009 !L5 InGaAs QW at 15% In
LAYER MATSYS=0.1 XPERC=0.0 TL=0.005 !L6 GaAs Shoulder
LAYER MATSYS=0.1 XPERC=0.15 NLOSS=0.0 TL=0.3 !L7 AlGaAs p-SCH at 15% Al
LAYER MATSYS=0.1 XPERC=0.35 NLOSS=0.0 TL=1.5 !L8 AlGaAs p-Cladding at 35%
LAYER MATSYS=0.1 XPERC=0.0 NLOSS=0.0 TL=0.2 !L9 GaAs cap

!OUTPUT Parameter Set
OUTPUT PHMO=1 GAMMAO=1 WZRO=1 WZIO=1 QZRO=1 QZIO=1
OUTPUT FWHPNO=0 FWHPFO=0 KMO=1 ITO=1
OUTPUT SPLTFL=0 MODOUT=1 LYROUT=1

!GAMOUT Parameter Set
GAMOUT LAYGAM=5 COMPGAM=0 GAMALL=0

!LOOPX Parameter Set
!LOOPX1 ILX='TL' FINV=0.25 XINC=0.0001 LAYCH=30
```

Chapter 6 InGaAs/AlGaAs/GaAs Structure with GRINSCH and AlGaAs/AlGaAs/GaAs Structure with Multiple QW Examples

```
!LOOPZ Parameter Set
!LOOPZ1 ILZ="QZMR" FINV=11.0 ZINC=-0.01
!LOOPZ1 ILZ="WVL" FINV=1.1 ZINC=.005
END
```

A layer file with the calculated refractive indices listed for each layer can be generated by clicking the center button on the main screen in WAVEGUIDE. It is recommended that you check the layer file (*.ly file) and verify the structure is what you expected. The layer file is shown below and the refractive indices and layer thicknesses are what I expected. The layer file is also useful for finding the layer number of the quantum well which I will assign to the LAYGAM parameter so calculations of confinement in the quantum well will be performed. In this case the quantum well is layer 5.

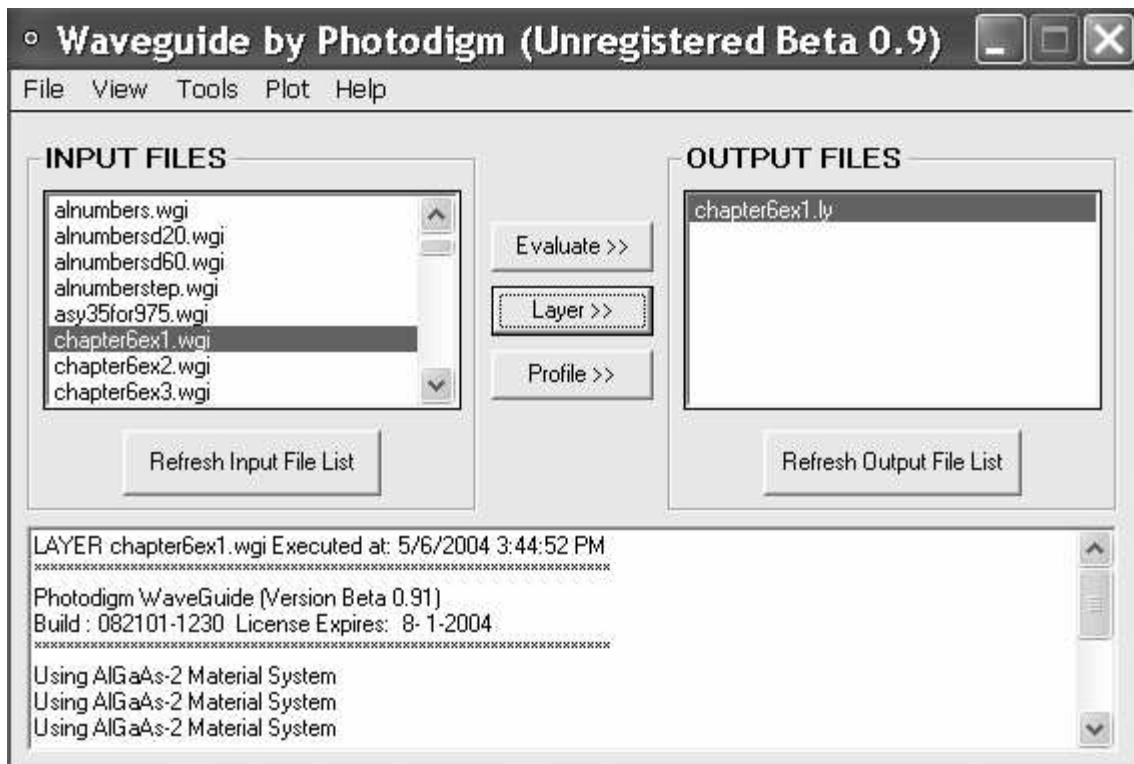


Figure 6.3.1 A layer description file can be generated using the “Layer>>” button.

Example 6-1 Layer File

# of layers =	9		
LAYER01	NLOSS= 0.00000	NREAL= 3.53212	TL= 0.00000
LAYER02	NLOSS= 0.00000	NREAL= 3.32663	TL= 1.50000
LAYER03	NLOSS= 0.00000	NREAL= 3.43305	TL= 0.30000
LAYER04	NLOSS= 0.00000	NREAL= 3.53212	TL= 0.00500
LAYER05	NLOSS= 0.00000	NREAL= 3.63522	TL= 0.00900
LAYER06	NLOSS= 0.00000	NREAL= 3.53212	TL= 0.00500
LAYER07	NLOSS= 0.00000	NREAL= 3.43305	TL= 0.30000
LAYER08	NLOSS= 0.00000	NREAL= 3.32663	TL= 1.50000
LAYER09	NLOSS= 0.00000	NREAL= 3.53212	TL= 0.00000

After verifying the structure is entered properly, the QZMR parameter is found by looping (LOOPZ1) from 12.0 to 11.0. One of the values (11.60) with the convergence parameter (KM) equal to 7 was selected. The db output file below shows the looping.

Example 6-1 dB File

QZMR	PHM	GAMMA(5)	KM
1.200000E+01	5.405490E+00	0.000000E+00	3
1.199000E+01	6.449031E+00	0.000000E+00	3
1.198000E+01	6.450929E+00	0.000000E+00	3
1.197000E+01	6.452955E+00	0.000000E+00	3
1.196000E+01	6.455115E+00	0.000000E+00	3
1.195000E+01	6.457413E+00	0.000000E+00	3

Chapter 6 InGaAs/AlGaAs/GaAs Sturcture with GRINSCH and AlGaAs/AlGaAs/GaAs
Structure with Multiple QW Examples

.
.
1.163000E+01	5.861396E-01	1.852656E-02		7
1.162000E+01	5.861396E-01	1.852656E-02		7
1.161000E+01	5.861396E-01	1.852656E-02		7
1.160000E+01	5.861396E-01	1.852656E-02		7
1.159000E+01	5.861396E-01	1.852656E-02		7
1.158000E+01	5.861396E-01	1.852656E-02		6
1.157000E+01	5.861396E-01	1.852656E-02		7
1.156000E+01	5.861396E-01	1.852656E-02		7
1.155000E+01	5.861396E-01	1.852656E-02		7
1.154000E+01	5.861396E-01	1.852656E-02		7
1.153000E+01	5.861396E-01	1.852656E-02		6
1.152000E+01	5.091807E+00	1.591408E-03		5
1.151000E+01	5.091807E+00	1.591408E-03		5
.
.
.
1.113000E+01	3.083710E+00	6.530596E-04		5
1.112000E+01	3.083710E+00	6.530596E-04		5
1.111000E+01	3.083710E+00	6.530596E-04		5
1.110000E+01	1.283672E+00	1.354180E-06		6
1.109000E+01	1.283672E+00	1.354180E-06		7
1.108000E+01	1.283672E+00	1.354180E-06		7
1.107000E+01	1.283672E+00	1.354180E-06		6
1.106000E+01	1.283672E+00	1.354180E-06		6
1.105000E+01	1.283672E+00	1.354180E-06		7
1.104000E+01	1.283672E+00	1.354180E-06		6
1.103000E+01	3.083710E+00	6.530596E-04		5
1.102000E+01	3.083710E+00	6.530596E-04		5

6.3 Single Quantum Well Structure with GRINSCH at 980 nm

1.101000E+01	3.083710E+00	6.530596E-04	5
1.100000E+01	3.083710E+00	6.530596E-04	5

The near field intensity and magnitude are plotted in Figure 6.1 to verify the QZMR value of 11.60 results in a single mode. Note this plot was made using the plotting feature in WAVEGUIDE.

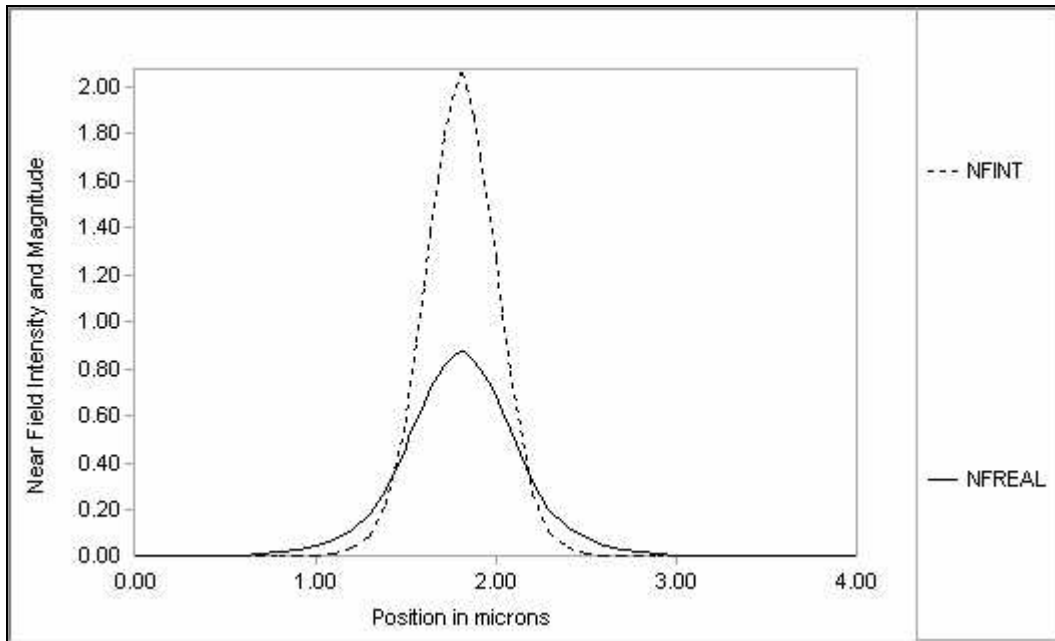


Figure 6.3.2 Near field plots verify single mode.

Now that we have a generic laser structure defined, we will modify the structure to have a graded separate confinement heterostructure (GRINSCH) and then optimize the structure.

We can change the SCH layers to GRINSCH layers by modifying the input file. The n-side SCH layer is replaced with 3 lines. The first line indicates the composition we are starting with and the total thickness of the GRINSCH. The second line indicates the ending composition, the total GRINSCH thickness, and the number of graded layers (NSLC). For this example, we will have ten graded layers. The third line indicates again

Chapter 6 InGaAs/AlGaAs/GaAs Structure with GRINSCH and AlGaAs/AlGaAs/GaAs Structure with Multiple QW Examples
the final composition for the GRINSCH and the total thickness. We do the same process for the p side SCH layer.

Original n-SCH:

```
LAYER MATSYS=0.1 XPERC=0.15 NLOSS=0.0 TL=0.3 !L3 AlGaAs n-SCH at 15% Al
```

is replaced with:

```
LAYER MATSYS=0.1 XPERC=0.35 NLOSS=0.0 TL=0.30 !L3 Base starts at 35% Al
LAYER MATSYS=0.1 XPERC=0.15 NLOSS=0.0 TL=0.30 NSLC=10 !n-Graded
LAYER MATSYS=0.1 XPERC=0.15 NLOSS=0.0 TL=0.30 !L13 Top ends at 15% Al
```

Original p-SCH:

```
LAYER MATSYS=0.1 XPERC=0.15 NLOSS=0.0 TL=0.3 !L7 AlGaAs p-SCH at 15% Al
```

is replaced with:

```
LAYER MATSYS=0.1 XPERC=0.15 NLOSS=0.0 TL=0.30 !L17 Base starts at 15% Al
LAYER MATSYS=0.1 XPERC=0.35 NLOSS=0.0 TL=0.30 NSLC=10 !p-Graded
LAYER MATSYS=0.1 XPERC=0.35 NLOSS=0.0 TL=0.30 !L27 Top ends at 35% Al
```

The modified input file is shown in Example 6-2 below. Note this input file also includes LOOPX1 parameters for each layer in the n and p side GRINSCH. This will enable looping on the GRINSCH layers to optimize the structure.

Example 6-2 Input File

```
!WIF generated by WIFE (Waveguide Input File Editor)
!CASE Parameter Set - 975 nm Structure with GRINSCH
CASE KASE=WIFE
CASE EPS1=1E-8 EPS2=1E-8 GAMEPS=1E-6 QZMR=11.36 QZMI=0
CASE PRINTF=1 INITGS=0 AUTOQW=0 NFPLT=1 FFPLT=1 IL=30
```

6.3 Single Quantum Well Structure with GRINSCH at 980 nm

```
!MODCON Parameter Set
MODCON KPOL=0 APB1=0.25 APB2=0.25

!STRUCT Parameter Set
STRUCT WAVL=0.975

!LAYER Parameter Set
LAYER MATSYS=0.1 XPERC=0.0 NLOSS=0.0 TL=0.0 !L1 Substrate and Buffer
LAYER MATSYS=0.1 XPERC=0.35 NLOSS=0.0 TL=1.5 !L2 AlGaAs at 35% Al
LAYER MATSYS=0.1 XPERC=0.35 NLOSS=0.0 TL=0.30 !L3 Base starts at 35% Al
LAYER MATSYS=0.1 XPERC=0.15 NLOSS=0.0 TL=0.30 NSLC=10 !n-Graded
LAYER MATSYS=0.1 XPERC=0.15 NLOSS=0.0 TL=0.30 !L13 Top ends at 15% Al
LAYER MATSYS=0.1 XPERC=0.0 TL=0.005 !L14 GaAs Shoulder
LAYER NREAL=3.635219 NLOSS=0.00 TL=0.009 !L15 InGaAs QW at 15% In
LAYER MATSYS=0.1 XPERC=0.0 TL=0.005 !L16 GaAs Shoulder
LAYER MATSYS=0.1 XPERC=0.15 NLOSS=0.0 TL=0.30 !L17 Base starts at 15% Al
LAYER MATSYS=0.1 XPERC=0.35 NLOSS=0.0 TL=0.30 NSLC=10 !p-Graded
LAYER MATSYS=0.1 XPERC=0.35 NLOSS=0.0 TL=0.30 !L27 Top ends at 35% Al
LAYER MATSYS=0.1 XPERC=0.35 NLOSS=0.0 TL=1.5 !L28 AlGaAs at 35%
LAYER MATSYS=0.1 XPERC=0.0 NLOSS=0.0 TL=0.2 !L29 GaAs contact

!OUTPUT Parameter Set
OUTPUT PHMO=1 GAMMAO=1 WZRO=1 WZIO=1 QZRO=0 QZIO=0
OUTPUT FWHPNO=0 FWHPFO=0 KMO=1 ITO=1
OUTPUT SPLTFL=0 MODOUT=1 LYROUT=1

!GAMOUT Parameter Set
GAMOUT LAYGAM=15 COMPGAM=0 GAMALL=0

!LOOPX Parameter Set
!LOOPX1 ILX='TL' FINV=0.25 XINC=0.0001 LAYCH=30
```

Chapter 6 InGaAs/AlGaAs/GaAs Structure with GRINSCH and AlGaAs/AlGaAs/GaAs Structure with Multiple QW Examples

```
!LOOPX1 ILX='TL' FINV=0.0 XINC=0.005 LAYCH=32
!LOOPX1 ILX='TL' FINV=0.1 XINC=0.001 LAYCH=5
!GRINSCH 1
!LOOPX1 ILX='TL' FINV=0.00 XINC=-0.00025 LAYCH=3
!LOOPX1 ILX='TL' FINV=0.015 XINC=-0.0005 LAYCH=4
!LOOPX1 ILX='TL' FINV=0.015 XINC=-0.0005 LAYCH=5
!LOOPX1 ILX='TL' FINV=0.015 XINC=-0.0005 LAYCH=6
!LOOPX1 ILX='TL' FINV=0.015 XINC=-0.0005 LAYCH=7
!LOOPX1 ILX='TL' FINV=0.015 XINC=-0.0005 LAYCH=8
!LOOPX1 ILX='TL' FINV=0.015 XINC=-0.0005 LAYCH=9
!LOOPX1 ILX='TL' FINV=0.015 XINC=-0.0005 LAYCH=10
!LOOPX1 ILX='TL' FINV=0.015 XINC=-0.0005 LAYCH=11
!LOOPX1 ILX='TL' FINV=0.015 XINC=-0.0005 LAYCH=12
!LOOPX1 ILX='TL' FINV=0.00 XINC=-0.00025 LAYCH=13
!GRINSCH 2
LOOPX1 ILX='TL' FINV=0.00 XINC=-0.00025 LAYCH=17
!LOOPX1 ILX='TL' FINV=0.015 XINC=-0.0005 LAYCH=18
!LOOPX1 ILX='TL' FINV=0.015 XINC=-0.0005 LAYCH=19
!LOOPX1 ILX='TL' FINV=0.015 XINC=-0.0005 LAYCH=20
!LOOPX1 ILX='TL' FINV=0.015 XINC=-0.0005 LAYCH=21
!LOOPX1 ILX='TL' FINV=0.015 XINC=-0.0005 LAYCH=22
!LOOPX1 ILX='TL' FINV=0.015 XINC=-0.0005 LAYCH=23
!LOOPX1 ILX='TL' FINV=0.015 XINC=-0.0005 LAYCH=24
!LOOPX1 ILX='TL' FINV=0.015 XINC=-0.0005 LAYCH=25
!LOOPX1 ILX='TL' FINV=0.015 XINC=-0.0005 LAYCH=26
!LOOPX1 ILX='TL' FINV=0.00 XINC=-0.00025 LAYCH=27
!LOOPZ Parameter Set
!LOOPZ1 ILZ="QZMR" FINV=11.0 ZINC=-0.01
!LOOPZ1 ILZ="WVL" FINV=1.1 ZINC=.005
END
```

6.3 Single Quantum Well Structure with GRINSCH at 980 nm

The layer output file shows the GRINSCH layers are evenly divided into 9 layers with thickness 0.03 μm and the first and last layers are 0.015 μm thick. The total thickness of the n or p side GRINSCH is 0.3 μm and each has eleven layers. The composition is linearly graded in steps over the total layer.

Example 6-2 Layer File

# of layers =	29		
LAYER01	NLOSS= 0.00000	NREAL= 3.53212	TL= 0.00000
LAYER02	NLOSS= 0.00000	NREAL= 3.32663	TL= 1.50000
LAYER03	NLOSS= 0.00000	NREAL= 3.32663	TL= 0.01500
LAYER04	NLOSS= 0.00000	NREAL= 3.33727	TL= 0.03000
LAYER05	NLOSS= 0.00000	NREAL= 3.34791	TL= 0.03000
LAYER06	NLOSS= 0.00000	NREAL= 3.35855	TL= 0.03000
LAYER07	NLOSS= 0.00000	NREAL= 3.36920	TL= 0.03000
LAYER08	NLOSS= 0.00000	NREAL= 3.37984	TL= 0.03000
LAYER09	NLOSS= 0.00000	NREAL= 3.39048	TL= 0.03000
LAYER10	NLOSS= 0.00000	NREAL= 3.40112	TL= 0.03000
LAYER11	NLOSS= 0.00000	NREAL= 3.41176	TL= 0.03000
LAYER12	NLOSS= 0.00000	NREAL= 3.42241	TL= 0.03000
LAYER13	NLOSS= 0.00000	NREAL= 3.43305	TL= 0.01500
LAYER14	NLOSS= 0.00000	NREAL= 3.53212	TL= 0.00500
LAYER15	NLOSS= 0.00000	NREAL= 3.63522	TL= 0.00900
LAYER16	NLOSS= 0.00000	NREAL= 3.53212	TL= 0.00500
LAYER17	NLOSS= 0.00000	NREAL= 3.43305	TL= 0.01500
LAYER18	NLOSS= 0.00000	NREAL= 3.42241	TL= 0.03000
LAYER19	NLOSS= 0.00000	NREAL= 3.41176	TL= 0.03000
LAYER20	NLOSS= 0.00000	NREAL= 3.40112	TL= 0.03000
LAYER21	NLOSS= 0.00000	NREAL= 3.39048	TL= 0.03000
LAYER22	NLOSS= 0.00000	NREAL= 3.37984	TL= 0.03000

Chapter 6 InGaAs/AlGaAs/GaAs Structure with GRINSCH and AlGaAs/AlGaAs/GaAs Structure with Multiple QW Examples

LAYER23	NLOSS= 0.00000	NREAL= 3.36920	TL= 0.03000
LAYER24	NLOSS= 0.00000	NREAL= 3.35855	TL= 0.03000
LAYER25	NLOSS= 0.00000	NREAL= 3.34791	TL= 0.03000
LAYER26	NLOSS= 0.00000	NREAL= 3.33727	TL= 0.03000
LAYER27	NLOSS= 0.00000	NREAL= 3.32663	TL= 0.01500
LAYER28	NLOSS= 0.00000	NREAL= 3.32663	TL= 1.50000
LAYER29	NLOSS= 0.00000	NREAL= 3.53212	TL= 0.00000

The refractive index profile of this structure is shown in Figure 6.3.3.

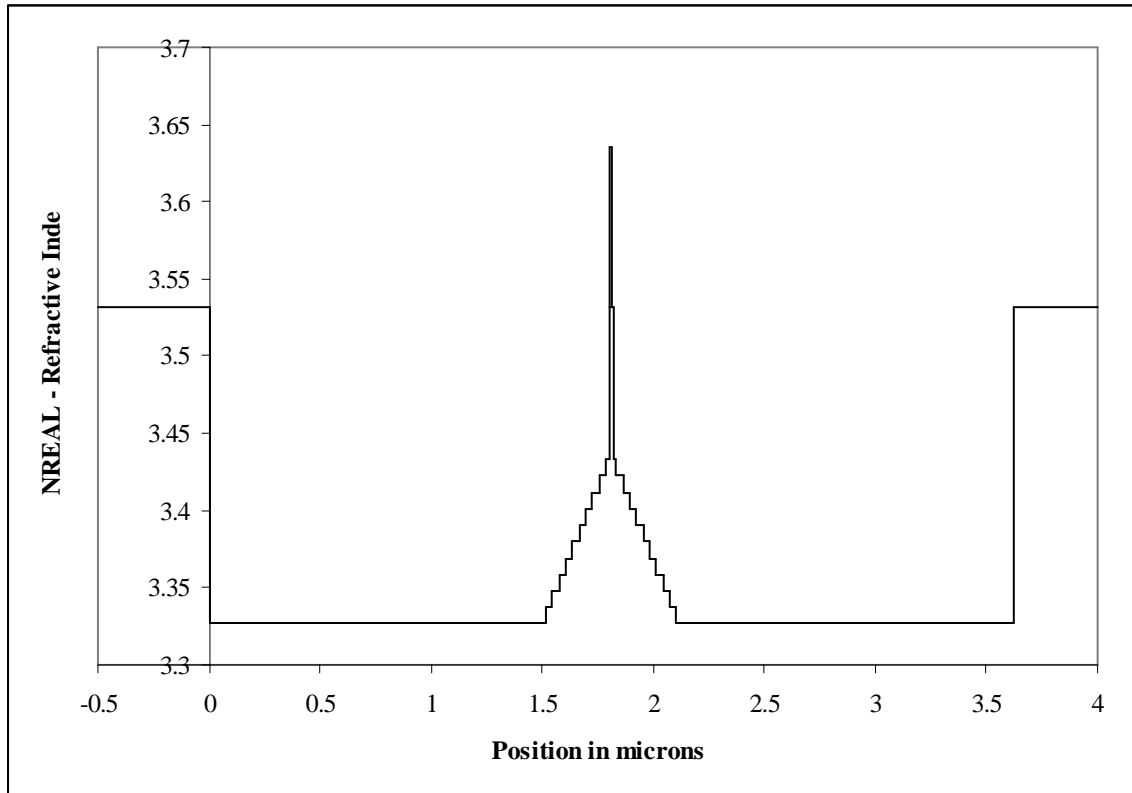


Figure 6.3.3 Refractive index profile for the GRINSCH is plotted with the zero point at the interface of the substrate and first layer of growth.

6.3 Single Quantum Well Structure with GRINSCH at 980 nm

We can optimize the cladding thickness by looping and selecting the thickness which gives a negligible loss term. For wavelength 0.975 μm , I have selected the cladding thickness of 2.1 μm (Figure 6.3.4) which corresponds to loss $\sim 0.00130 \text{ cm}^{-1}$. The loss is calculated using the following formula with WZI taken from the db output file:

$$\alpha = \text{WZI} \cdot (4\pi/\lambda) \cdot 10^4 / \text{cm}$$

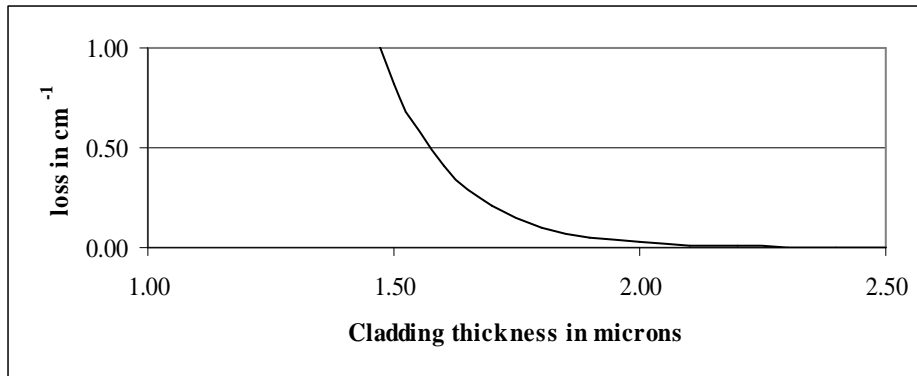


Figure 6.3.4 Loss is negligible for cladding thickness of 2.1 μm .

Next, we can optimize the confinement factor in the quantum well by varying the thickness of the GRINCH layers. In general, we will start with a maximum thickness and loop to a minimum thickness to optimize parameters. (This method is used to minimize the numerical error in the code.) So for the GRINSCH thicknesses, we will start at 0.5 μm thick and loop for QZMR. The new QZMR is 11.46. Then we loop the GRINSCH layers. A plot of the quantum well confinement factor vs. the GRINSCH layer thicknesses is shown in Figure 6.3.5. A maximum confinement factor of 0.02010344 is achieved at GRINSCH thickness 0.27 μm . The effective index of the structure at this maximum confinement factor is 3.366145 (Figure 6.3.6).

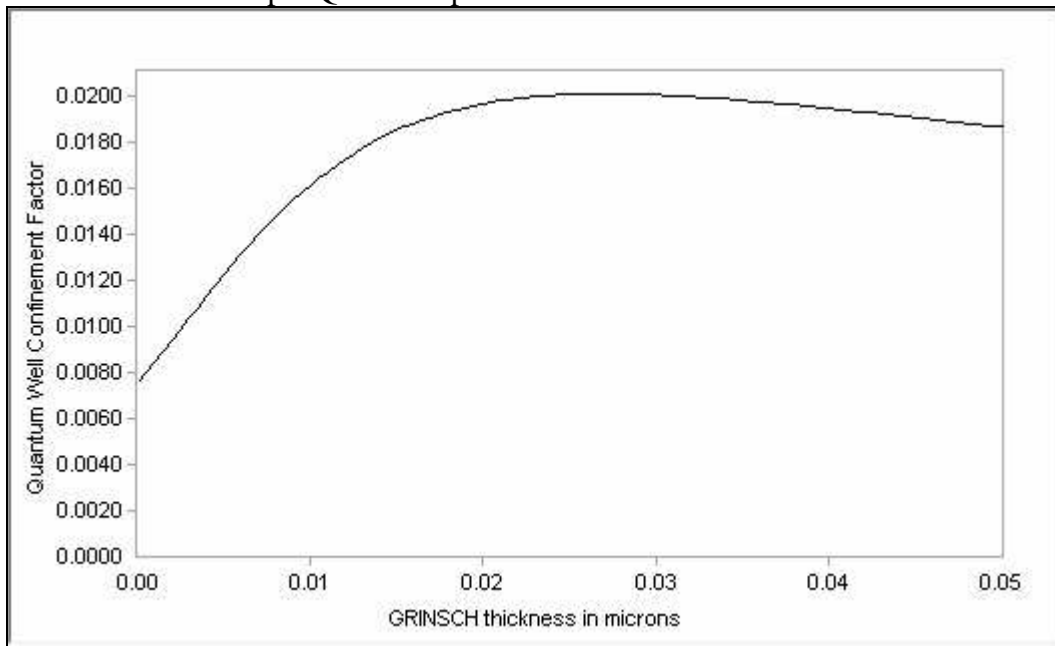


Figure 6.3.5 The maximum confinement in the quantum well (GAMMA) occurs at GRINSCH thickness 0.27 μm .

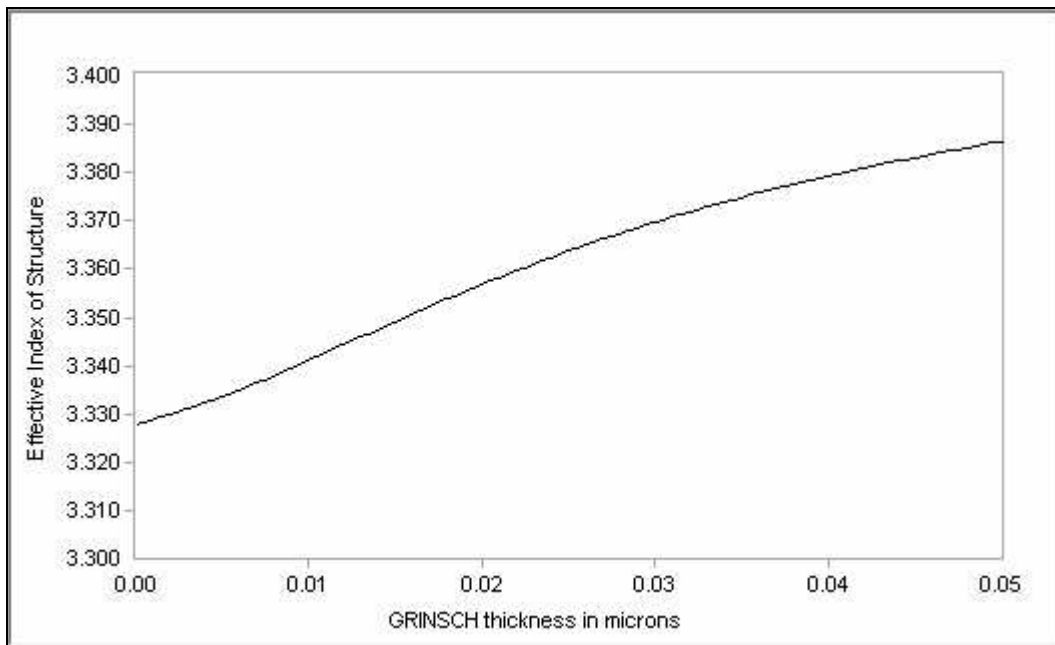


Figure 6.3.6 The effective index of the structure (WZR) varies as the thickness of the GRINSCH layers vary.

6.3 Single Quantum Well Structure with GRINSCH at 980 nm

With our final structure parameters of cladding layer thickness 2.1 μm and GRINSCH layer thickness 0.27 μm , our new QZMR value is 11.33. It is critical that each time you modify the input file, you find the new QZMR value – otherwise you will get garbage out and waste time trying to interpret results that are unexpected!

Our final input file for example 2 is shown below.

Example 2 – Final Input File

```
!WIF generated by WIFE (Waveguide Input File Editor)
!CASE Parameter Set - 975 nm Structure with GRINSCH
CASE KASE=WIFE
CASE EPS1=1E-8 EPS2=1E-8 GAMEPS=1E-6 QZMR=11.33 QZMI=0
CASE PRINTF=1 INITGS=0 AUTOQW=0 NFPLT=1 FFPLT=1 IL=30

!MODCON Parameter Set
MODCON KPOL=0 APB1=0.25 APB2=0.25

!STRUCT Parameter Set
STRUCT WAVL=0.975

!LAYER Parameter Set
LAYER MATSYS=0.1 XPERC=0.0 NLOSS=0.0 TL=0.0      !L1 Substrate and
Buffer
LAYER MATSYS=0.1 XPERC=0.35 NLOSS=0.0 TL=2.1    !L2 AlGaAs at 35% Al
```

Chapter 6 InGaAs/AlGaAs/GaAs Structure with GRINSCH and AlGaAs/AlGaAs/GaAs Structure with Multiple QW Examples

```
LAYER MATSYS=0.1 XPERC=0.35 NLOSS=0.0 TL=0.27 !L3 Base starts at 35%
Al
LAYER MATSYS=0.1 XPERC=0.15 NLOSS=0.0 TL=0.27 NSLC=10 !Graded
LAYER MATSYS=0.1 XPERC=0.15 NLOSS=0.0 TL=0.27 !L13 Top ends at 15% Al
LAYER MATSYS=0.1 XPERC=0.0 TL=0.005 !L14 GaAs Shoulder
LAYER NREAL=3.635219 NLOSS=0.00 TL=0.009 !L15 InGaAs QW at 15% In
LAYER MATSYS=0.1 XPERC=0.0 TL=0.005 !L16 GaAs Shoulder
LAYER MATSYS=0.1 XPERC=0.15 NLOSS=0.0 TL=0.27 !L17 Base starts at 15%
Al
LAYER MATSYS=0.1 XPERC=0.35 NLOSS=0.0 TL=0.27 NSLC=10 !Graded
LAYER MATSYS=0.1 XPERC=0.35 NLOSS=0.0 TL=0.27 !L27 Top ends at 35% Al
LAYER MATSYS=0.1 XPERC=0.35 NLOSS=0.0 TL=2.1 !L28 AlGaAs at 35%
LAYER MATSYS=0.1 XPERC=0.0 NLOSS=0.0 TL=0.2 !L29 GaAs contact

!OUTPUT Parameter Set
OUTPUT PHMO=1 GAMMAO=1 WZRO=1 WZIO=1 QZRO=0 QZIO=0
OUTPUT FWHPNO=1 FWHPFO=1 KMO=1 ITO=1
OUTPUT SPLTFL=0 MODOUT=1 LYROUT=1

!GAMOUT Parameter Set
GAMOUT LAYGAM=15 COMPGAM=0 GAMALL=0

!LOOPX Parameter Set
!LOOPX1 ILX='TL' FINV=.5 XINC=-0.1 LAYCH=2
!LOOPX1 ILX='TL' FINV=.5 XINC=-0.1 LAYCH=28
!LOOPX1 ILX='TL' FINV=0.1 XINC=0.001 LAYCH=5
!GRINSCH 1
!LOOPX1 ILX='TL' FINV=0.00 XINC=-0.00025 LAYCH=3
!LOOPX1 ILX='TL' FINV=0.015 XINC=-0.0005 LAYCH=4
```

6.3 Single Quantum Well Structure with GRINSCH at 980 nm

```
!LOOPX1 ILX='TL' FINV=0.015 XINC=-0.0005 LAYCH=5
!LOOPX1 ILX='TL' FINV=0.015 XINC=-0.0005 LAYCH=6
!LOOPX1 ILX='TL' FINV=0.015 XINC=-0.0005 LAYCH=7
!LOOPX1 ILX='TL' FINV=0.015 XINC=-0.0005 LAYCH=8
!LOOPX1 ILX='TL' FINV=0.015 XINC=-0.0005 LAYCH=9
!LOOPX1 ILX='TL' FINV=0.015 XINC=-0.0005 LAYCH=10
!LOOPX1 ILX='TL' FINV=0.015 XINC=-0.0005 LAYCH=11
!LOOPX1 ILX='TL' FINV=0.015 XINC=-0.0005 LAYCH=12
!LOOPX1 ILX='TL' FINV=0.00 XINC=-0.00025 LAYCH=13
!GRINSCH 2
!LOOPX1 ILX='TL' FINV=0.00 XINC=-0.00025 LAYCH=17
!LOOPX1 ILX='TL' FINV=0.015 XINC=-0.0005 LAYCH=18
!LOOPX1 ILX='TL' FINV=0.015 XINC=-0.0005 LAYCH=19
!LOOPX1 ILX='TL' FINV=0.015 XINC=-0.0005 LAYCH=20
!LOOPX1 ILX='TL' FINV=0.015 XINC=-0.0005 LAYCH=21
!LOOPX1 ILX='TL' FINV=0.015 XINC=-0.0005 LAYCH=22
!LOOPX1 ILX='TL' FINV=0.015 XINC=-0.0005 LAYCH=23
!LOOPX1 ILX='TL' FINV=0.015 XINC=-0.0005 LAYCH=24
!LOOPX1 ILX='TL' FINV=0.015 XINC=-0.0005 LAYCH=25
!LOOPX1 ILX='TL' FINV=0.015 XINC=-0.0005 LAYCH=26
!LOOPX1 ILX='TL' FINV=0.00 XINC=-0.00025 LAYCH=27

!LOOPZ Parameter Set
!LOOPZ1 ILZ="QZMR" FINV=11.0 ZINC=-0.01
!LOOPZ1 ILZ="WVL" FINV=1.1 ZINC=.005

END
```

Chapter 6 InGaAs/AlGaAs/GaAs Structure with GRINSCH and AlGaAs/AlGaAs/GaAs Structure with Multiple QW Examples

The final near field plots of magnitude (NFREAL) and intensity (NFINT) are shown in Figure 6.3.7 and the plot of the far field is shown in Figure 6.3.8. Note we did not optimize the far field for this particular structure. Other chapter examples in the manual discuss optimizing the far field or you can try for yourself.

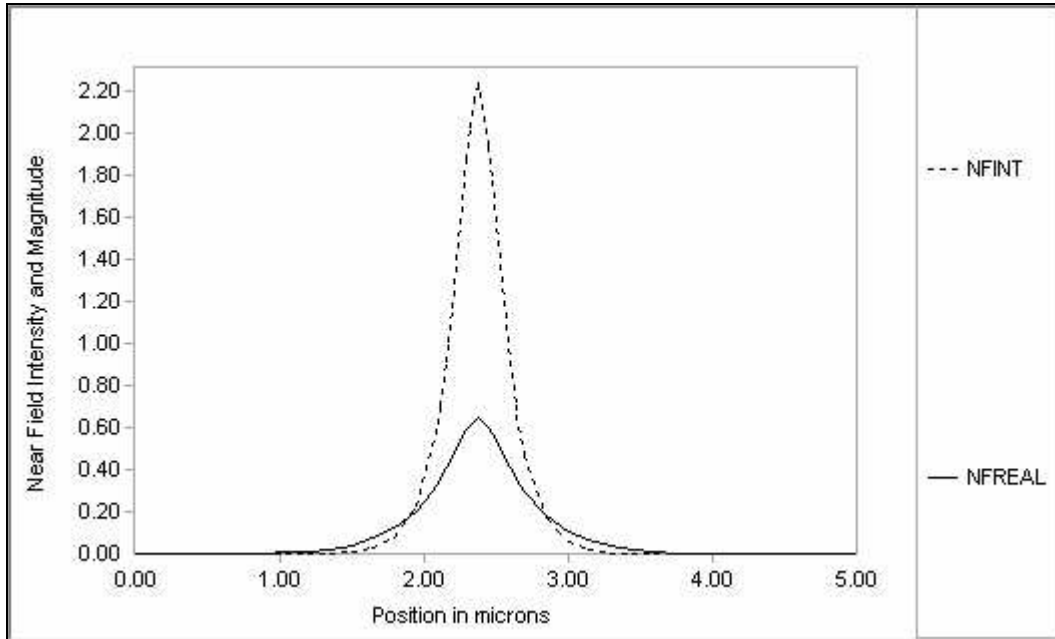
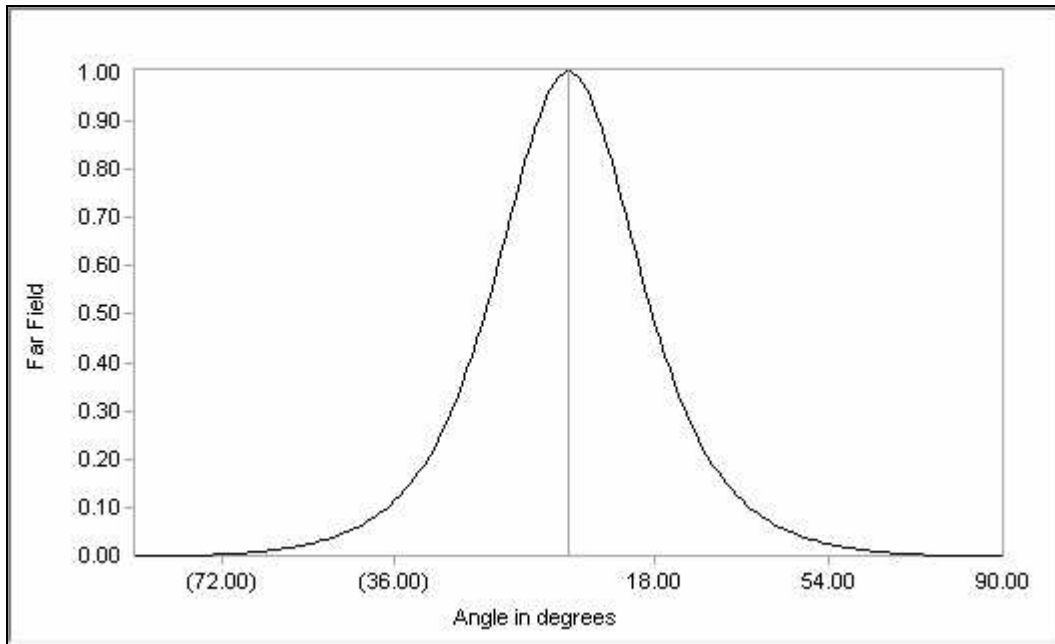


Figure 6.3.7 The near field magnitude (NFREAL) and intensity (NFINT) are plotted.

6.3 Single Quantum Well Structure with GRINSCH at 980 nm



6.3.8 The far field plot has a full width half power max (FWHPF) of 34.8 degrees.

6.4 Multiple Quantum Well AlGaAs/AlGaAs/GaAs Structure at 820 nm

In this example, the initial WAVEGUIDE input file (Example 6-3) is based on a structure (Table 6.4.1) analyzed in the GAIN program manual for material system 1. To get started in WAVEGUIDE, the SCH and cladding layer thicknesses are arbitrarily selected. MATSYS is used for the all the layers and again the Jenkins model for AlGaAs is selected.

Table 6.4.1

Layer	λ (μm)	Strain	Thickness (\AA)
QW ($\text{Al}_x\text{Ga}_{1-x}\text{As}$)	0.87	-	50
SCH ($\text{Al}_x\text{Ga}_{1-x}\text{As}$)	0.74	-	60

Chapter 6 InGaAs/AlGaAs/GaAs Structure with GRINSCH and AlGaAs/AlGaAs/GaAs Structure with Multiple QW Examples

Cladding($\text{Al}_x\text{Ga}_{1-x}\text{As}$)	0.58	-	100
---	------	---	-----

Example 3 – Input File

```

!WIF generated by WIFE (Waveguide Input File Editor)

!CASE Parameter Set - 820 nm Structure

CASE KASE=WIFE

CASE EPS1=1E-8 EPS2=1E-8 GAMEPS=1E-6 QZMR=12.15 QZMI=0

CASE PRINTF=1 INITGS=0 AUTOQW=0 NFPLT=1 FFPLT=1 IL=30

!MODCON Parameter Set

MODCON KPOL=0 APB1=0.25 APB2=0.25

!STRUCT Parameter Set

STRUCT WVL=0.82

!LAYER Parameter Set

LAYER MATSYS=0.1 XPERC=0.0 NLOSS=0.0 TL=0.0 !L1 Substrate and Buffer

LAYER MATSYS=0.1 XPERC=0.56 NLOSS=0.0 TL=2.5 !L2 AlGaAs n-Cladding at 56% Al

LAYER MATSYS=0.1 XPERC=0.20 NLOSS=0.0 TL=0.5 !L3 AlGaAs n-SCH at 20% Al

LAYER MATSYS=0.1 XPERC=0.10 TL=0.005 !L4 AlGaAs QW at 10% Al

LAYER MATSYS=0.1 XPERC=0.20 NLOSS=0.0 TL=0.5 !L5 AlGaAs p-SCH at 20% Al

LAYER MATSYS=0.1 XPERC=0.56 NLOSS=0.0 TL=2.5 !L6 AlGaAs p-Cladding at 56%

LAYER MATSYS=0.1 XPERC=0.0 NLOSS=0.0 TL=0.2 !L7 GaAs cap

!OUTPUT Parameter Set

OUTPUT PHMO=1 GAMMAO=1 WZRO=1 WZIO=1 QZRO=0 QZIO=0

OUTPUT FWHPNO=0 FWHPFO=0 KMO=1 ITO=1

OUTPUT SPLTFL=0 MODOUT=1 LYROUT=1

```


6.4 Multiple Quantum Well AlGaAs/AlGaAs/GaAs Structure at 820 nm

```
!GAMOUT Parameter Set
GAMOUT LAYGAM=4 COMPGAM=0 GAMALL=0

!LOOPX Parameter Set
LOOPX1 ILX='TL' FINV=0.5 XINC=-0.01 LAYCH=2 !n Cladding
LOOPX1 ILX='TL' FINV=0.5 XINC=-0.01 LAYCH=6 !p Cladding

!LOOPZ Parameter Set
!LOOPZ1 ILZ="QZMR" FINV=11.0 ZINC=-0.01
!LOOPZ1 ILZ="WVL" FINV=1.1 ZINC=.005

END
```

The layer file is viewed to verify the structure is entered properly.

```
# of layers =          7
LAYER01  NLOSS= 0.00000      NREAL= 3.67080      TL= 0.00000
LAYER02  NLOSS= 0.00000      NREAL= 3.28629      TL= 2.50000
LAYER03  NLOSS= 0.00000      NREAL= 3.50104      TL= 0.50000
LAYER04  NLOSS= 0.00000      NREAL= 3.58503      TL= 0.00500
LAYER05  NLOSS= 0.00000      NREAL= 3.50104      TL= 0.50000
LAYER06  NLOSS= 0.00000      NREAL= 3.28629      TL= 2.50000
LAYER07  NLOSS= 0.00000      NREAL= 3.67080      TL= 0.00000
```

The cladding is varied from 2.5 μm to 0.5 μm to select a thickness with acceptable loss. A plot of the region with the lowest loss is shown in Figure 6.4.1. In this example, a cladding layer thickness of 1 μm is selected based on the negligible loss at that thickness.

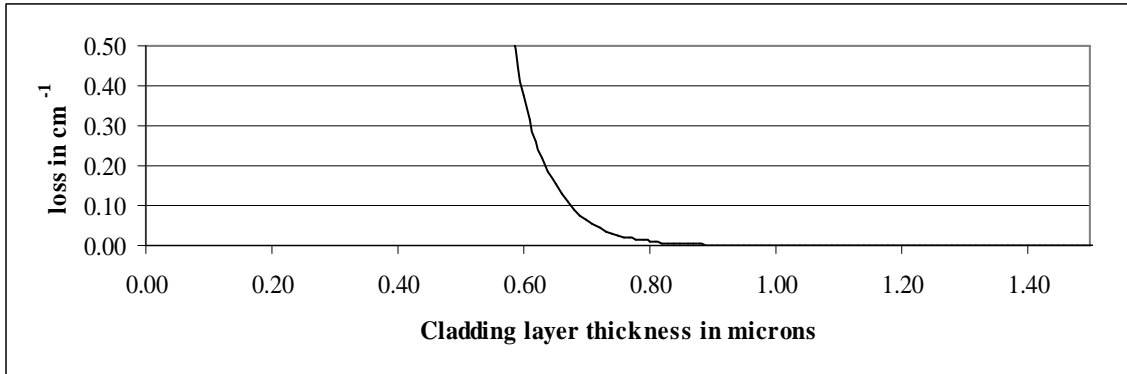


Figure 6.4.1 The cladding layer thickness is selected to be 1 μm and has negligible loss.

Next, we can optimize the quantum well confinement by varying the thickness of the SCH layers. The optimal confinement in the quantum well is 0.01899 and occurs at SCH layer thickness of 0.09 μm . The plot of confinement vs. layer thickness is shown in Figure 6.4.2.

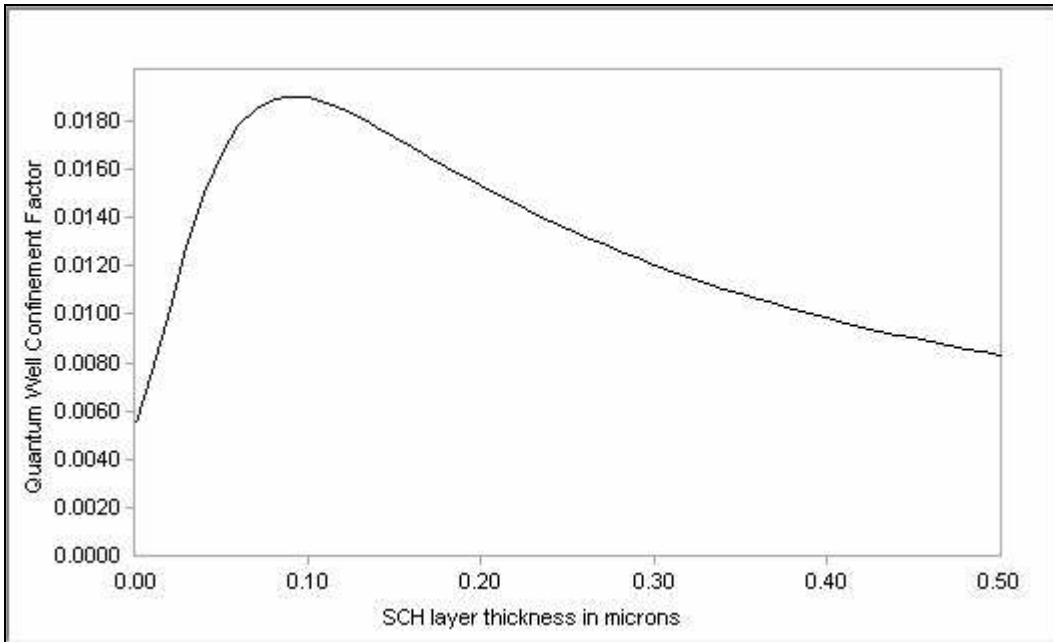


Figure 6.4.2 The maximum quantum well confinement occurs at SCH layer thickness 0.09 μm .

Next we show how to change this single quantum well structure (SQW) into a multiple quantum well structure (MQW). A simple modification to the input file will allow us to incorporate as many quantum wells as desired. For this example, we will add two quantum wells to the SQW structure for a total of 3 quantum wells.

The original structure:

```
LAYER MATSYS=0.1 XPERC=0.0 NLOSS=0.0 TL=0.0      !L1 Substrate and Buffer
LAYER MATSYS=0.1 XPERC=0.56 NLOSS=0.0 TL=1.0     !L2 AlGaAs n-Cladding at 56% Al
LAYER MATSYS=0.1 XPERC=0.20 NLOSS=0.0 TL=0.09    !L3 AlGaAs n-SCH at 20% Al
LAYER MATSYS=0.1 XPERC=0.10 TL=0.005             !L4 AlGaAs QW at 10% Al
LAYER MATSYS=0.1 XPERC=0.20 NLOSS=0.0 TL=0.09    !L5 AlGaAs p-SCH at 20% Al
LAYER MATSYS=0.1 XPERC=0.56 NLOSS=0.0 TL=1.0     !L6 AlGaAs p-Cladding at 56%
LAYER MATSYS=0.1 XPERC=0.0 NLOSS=0.0 TL=0.2      !L7 GaAs cap
```

can be modified by inserting extra lines into the LAYER definition:

```
LAYER MATSYS=0.1 XPERC=0.0 NLOSS=0.0 TL=0.0      !L1 Substrate and Buffer
LAYER MATSYS=0.1 XPERC=0.56 NLOSS=0.0 TL=1.0     !L2 AlGaAs n-Cladding at 56% Al
LAYER MATSYS=0.1 XPERC=0.20 NLOSS=0.0 TL=0.09    !L3 AlGaAs n-SCH at 20% Al
LAYER MATSYS=0.1 XPERC=0.10 TL=0.005             !L4 AlGaAs QW at 10% Al
LAYER MATSYS=0.1 XPERC=0.20 NLOSS=0.0 TL=0.005 !L5 AlGaAs barrier at 20% Al
LAYER MATSYS=0.1 XPERC=0.10 TL=0.005             !L6 AlGaAs QW at 10% Al
LAYER MATSYS=0.1 XPERC=0.20 NLOSS=0.0 TL=0.005 !L7 AlGaAs barrier at 20% Al
LAYER MATSYS=0.1 XPERC=0.10 TL=0.005             !L8 AlGaAs QW at 10% Al
LAYER MATSYS=0.1 XPERC=0.20 NLOSS=0.0 TL=0.09    !L9 AlGaAs p-SCH at 20% Al
```

Chapter 6 InGaAs/AlGaAs/GaAs Structure with GRINSCH and AlGaAs/AlGaAs/GaAs Structure with Multiple QW Examples

```
LAYER MATSYS=0.1 XPERC=0.56 NLOSS=0.0 TL=1.0 !L10 AlGaAs p-Cladding at 56%
LAYER MATSYS=0.1 XPERC=0.0 NLOSS=0.0 TL=0.2 !L11 GaAs cap
```

After inspecting the layer file to verify the structure is what I intended, I plotted the refractive index in Figure 6.4.3. Plotting the refractive index profile can be done by copying the data from the layer file and using your favorite plotting software. A feature of WAVEGUIDE that is planned to be added is plotting the structure profile using the *.ip file generated by clicking on the “Profile” tab on the main screen of WAVEGUIDE.

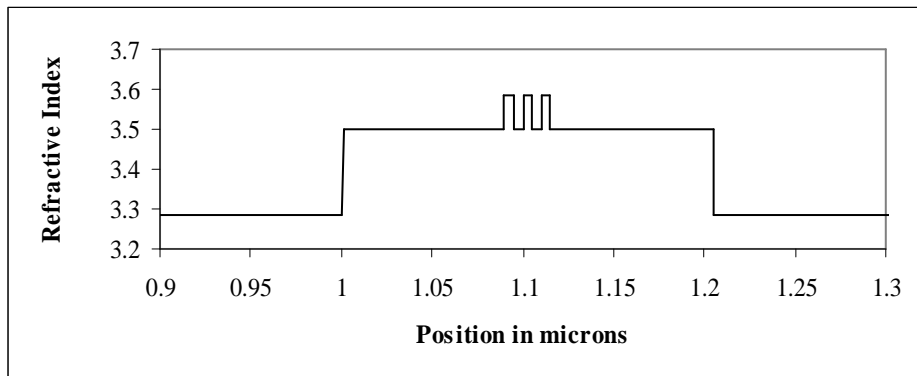


Figure 6.4.3 The refractive index profile is plotted for the cladding, SCH, barriers, and quantum well layers.

We can also modify the input file to output the confinement factor for each of the quantum wells. We can change the parameter LAYGAM=4 from the SQW case to LAYGAM=4,6,8. With this change, the *.db file (shown below) will now include the confinement factor for all three quantum wells. Since this is a symmetric structure, the center quantum well has the highest confinement and the other two quantum wells have slightly lower but equal confinement. The effective index (WZR) of this structure is 3.385398 and the KM=7 indicates the best numerical convergence.

Example 3 – Output file .db

GAMMA(4)	GAMMA(6)	GAMMA(8)	WZR	KM
-----------	-----------	-----------	-----	----

6.4 Mutiple Quantum Well AlGaAs/AlGaAs/GaAs Structure at 820 nm

1.919871E-02	1.932253E-02	1.919871E-02	3.385398E+00	7
--------------	--------------	--------------	--------------	---

The final input file for the 820 nm wavelength AlGaAs/AlGaAs/GaAs example is shown below.

Example 3 – Final Input File

```
!WIF generated by WIFE (Waveguide Input File Editor)
!CASE Parameter Set - 820 nm MQW Structure
CASE KASE=WIFE
CASE EPS1=1E-8 EPS2=1E-8 GAMEPS=1E-6 QZMR=11.46 QZMI=0
CASE PRINTF=1 INITGS=0 AUTOQW=0 NFPLT=1 FFPLT=1 IL=30

!MODCON Parameter Set
MODCON KPOL=0 APB1=0.25 APB2=0.25

!STRUCT Parameter Set
STRUCT WVL=0.82

!LAYER Parameter Set
LAYER MATSYS=0.1 XPERC=0.0 NLOSS=0.0 TL=0.0      !L1 Substrate and
Buffer
LAYER MATSYS=0.1 XPERC=0.56 NLOSS=0.0 TL=1.0     !L2 AlGaAs n-Cladding
at 56% Al
LAYER MATSYS=0.1 XPERC=0.20 NLOSS=0.0 TL=0.09    !L3 AlGaAs n-SCH at 20%
Al
LAYER MATSYS=0.1 XPERC=0.10 TL=0.005             !L4 AlGaAs QW at 10% Al
LAYER MATSYS=0.1 XPERC=0.20 NLOSS=0.0 TL=0.005   !L5 AlGaAs barrier at
20% Al
LAYER MATSYS=0.1 XPERC=0.10 TL=0.005             !L6 AlGaAs QW at 10% Al
```

Chapter 6 InGaAs/AlGaAs/GaAs Structure with GRINSCH and AlGaAs/AlGaAs/GaAs Structure with Multiple QW Examples

```

LAYER MATSYS=0.1 XPERC=0.20 NLOSS=0.0 TL=0.005 !L7 AlGaAs barrier at
20% Al

LAYER MATSYS=0.1 XPERC=0.10 TL=0.005 !L8 AlGaAs QW at 10% Al

LAYER MATSYS=0.1 XPERC=0.20 NLOSS=0.0 TL=0.09 !L9 AlGaAs p-SCH at 20%
Al

LAYER MATSYS=0.1 XPERC=0.56 NLOSS=0.0 TL=1.0 !L10 AlGaAs p-Cladding
at 56%

LAYER MATSYS=0.1 XPERC=0.0 NLOSS=0.0 TL=0.2 !L11 GaAs cap

!OUTPUT Parameter Set

OUTPUT PHMO=0 GAMMAO=1 WZRO=1 WZIO=0 QZRO=0 QZIO=0

OUTPUT FWHPNO=0 FWHPFO=0 KMO=1 ITO=0

OUTPUT SPLTFL=0 MODOUT=1 LYROUT=1

!GAMOUT Parameter Set

GAMOUT LAYGAM=4,6,8 COMPGAM=0 GAMALL=0

!LOOPX Parameter Set

!LOOPX1 ILX='TL' FINV=0.5 XINC=-0.01 LAYCH=2 !n Cladding
!LOOPX1 ILX='TL' FINV=0.5 XINC=-0.01 LAYCH=6 !p Cladding
!LOOPX1 ILX='TL' FINV=0.0 XINC=-0.01 LAYCH=3 !n SCH
!LOOPX1 ILX='TL' FINV=0.0 XINC=-0.01 LAYCH=5 !p SCH

!LOOPZ Parameter Set

!LOOPZ1 ILZ="QZMR" FINV=11.0 ZINC=-0.01
!LOOPZ1 ILZ="WVL" FINV=1.1 ZINC=.005

END

```

6.4 Multiple Quantum Well AlGaAs/AlGaAs/GaAs Structure at 820 nm

The near field magnitude and intensity are plotted in Figure 6.4.4 and the far field is plotted in Figure 6.4.5. Similar to example 2 in this chapter, the far field has not been optimized. Other chapters in this manual highlight optimizing the far field as well as the many additional features of WAVEGUIDE.

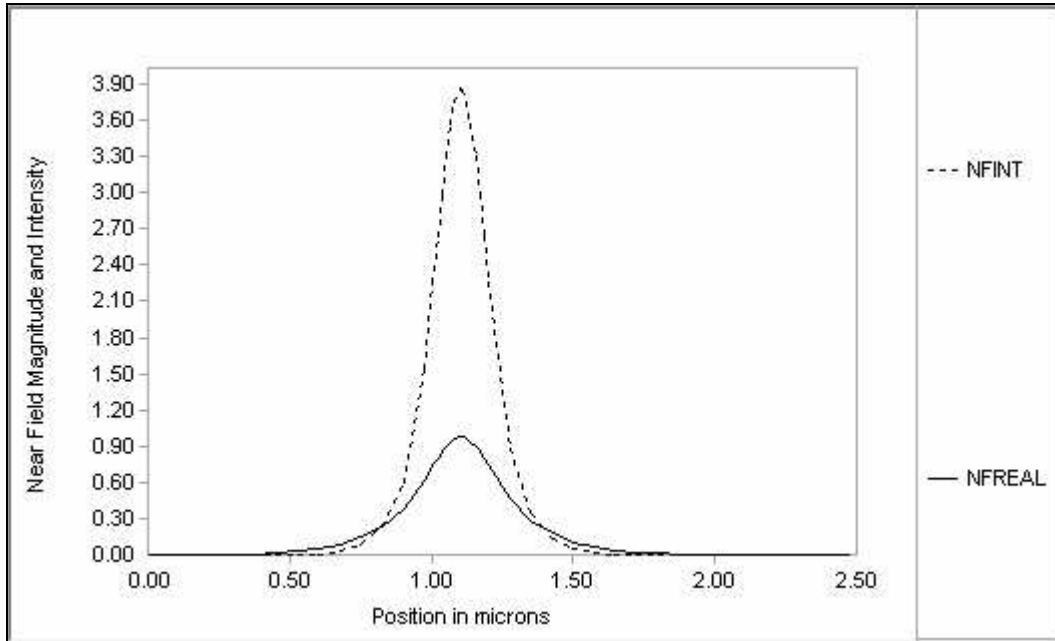


Figure 6.4.4 Near field magnitude and intensity are plotted for the MQW structure.

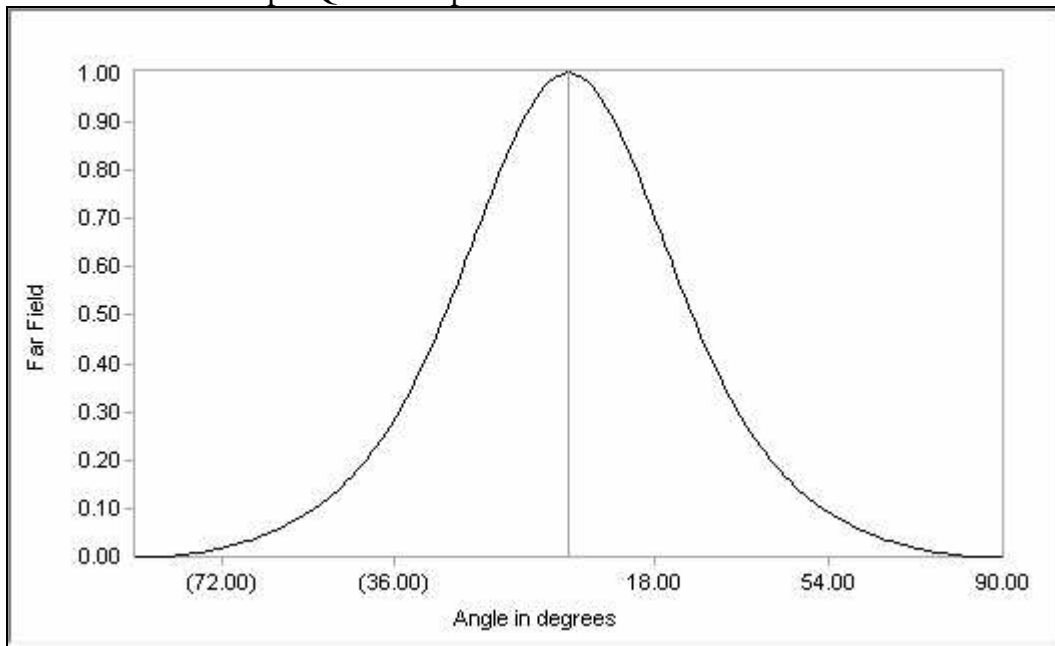


Figure 6.4.5 The far field is plotted for the MQW structure and the HWFPH parameter output in the *.db file indicates the divergence is 51.5 degrees.

6.5 Summary

This chapter has introduced two features of WAVEGUIDE that are useful in the design and modeling of semiconductor lasers. The first feature discussed was the graded index separate confinement heterostructure (GRINSCH) which assumes a linear grade over the number of layers in the GRINSCH defined by the user. The second feature discussed was a multiple quantum well structure (MQW). Both of these features are used by directly modifying the WAVEGUIDE input file. The examples in this chapter demonstrated how to change a simple laser structure to include the more complicated GRINSCH or MQW structures in your modeling efforts.

Chapter 7 InGaAsP/InGaAsP/InP Lasers

7.1 InGaAsP/InGaAsP/InP (1310nm)

7.1.1 Introduction

InGaAsP/InP Multiple Quantum Well (MQW) lasers are of great interests in telecommunication systems. Using WAVEGUIDE software, we present procedures for designing a broad area InGaAsP/InP 5-QW laser operating at 1310nm with fundamental TE mode. Three main steps are involved, and criterions for determining parameters in each step are also discussed. Firstly, we loop for QZMR to determine the effective refractive index of the fundamental TE mode. Second, thickness of the Separated Confinement Heterostrucutre (SCH) is looped and determined. Finally, loss in a highly doped layer is taken into account, and the thickness of the p-cladding layer is looped and determined. After using these determined parameters, we simulate optical confinement factor, near filed/ far field, and loss. The simulation results indicate that the laser structure is acceptable, and good performances are obtained.

7.1.2 Initial input file

The waveguide structure of a laser shown in Table 7.1.1 consists of a p-cap layer, a p-cladding layer, an etch-stop layer, a p-spacer layer, a p-separate confinement heterostrucutre (p-SCH) layer, five quantum wells, four barriers, a n-SCH layer, a n-cladding layer, and a InP substrate. The composition and thickness of the quantum well, barrier, p-SCH, and n-SCH layers are determined by the GAIN software, and the initial input file is given in Table 7.1.2.

Table 7.1.1 Initial Laser structure (5-QW InGaAsP) for the 1310nm InGaAsP/InP laser structure.

Layer	Thickness (μm)	Refractive	Loss

Chapter 7 InGaAsP/InGaAsP/InP Laser

		Index	
n-substrate	0	3.20081	0
n-cladding	1.0	3.20081	0
n-SCH	0.08	3.33097	0
Quantum well	0.006	3.49722	0
Barrier	0.02	3.33097	0
Quantum well	0.006	3.49722	0
Barrier	0.02	3.33097	0
Quantum well	0.006	3.49722	0
Barrier	0.02	3.33097	0
Quantum well	0.006	3.49722	0
Barrier	0.02	3.33097	0
Quantum well	0.006	3.49722	0
Barrier	0.02	3.33097	0
Quantum well	0.006	3.49722	0
Barrier	0.02	3.33097	0
Quantum well	0.006	3.49722	0
p-spacer	0.08	3.33097	0
p-SCH	0.2	3.20081	0
Etch-stop	0.001	3.33097	0
p-cladding	1.0	3.20081	0
p-cap	0.2	3.20081	0

Table 7.1.2 Initial input file

7.1 InGaAsP/InGaAsP/InP (1310nm)

!DESCRIPTION: lattice matched 5-QW InGaAsP/InP laser operating at 1310nm.

!CASE Parameter Set

CASE KASE=InGaAsP (5 wells)

CASE EPS1=1E-8 EPS2=1E-8 GAMEPS=1E-6

CASE QZMR=12.3 QZMI=0.0

CASE PRINTF=0 INITGS=0 AUTOQW=0 NFPLT=0 FFPLT=1

!MODCON Parameter Set

MODCON KPOL=1 APB1=0.25 APB2=0.25

!STRUCT Parameter Set

STRUCT WVL=1.3

!LAYER Parameter Set

!----- beginning of structure -----

LAYER MATSYS=1 XPERC=0 YPERC=0 TL=0.0 !n-substrate

LAYER MATSYS=1 XPERC=0 YPERC=0 TL=2.0 !n-cladding

LAYER MATSYS=12 XPERC=1.10 TL=0.09 !n- InGaAsP waveguide (SCH)

LAYER MATSYS=12 XPERC=1.28 TL=0.006 !QW

LAYER MATSYS=12 XPERC=1.10 TL=0.02 !barrier

LAYER MATSYS=12 XPERC=1.28 TL=0.006 !QW

LAYER MATSYS=12 XPERC=1.10 TL=0.02 !barrier

LAYER MATSYS=12 XPERC=1.28 TL=0.006 !QW

LAYER MATSYS=12 XPERC=1.10 TL=0.02 !barrier

LAYER MATSYS=12 XPERC=1.28 TL=0.006 !QW

LAYER MATSYS=12 XPERC=1.10 TL=0.02 !barrier

LAYER MATSYS=12 XPERC=1.28 TL=0.006 !QW

LAYER MATSYS=12 XPERC=1.10 TL=0.09 !p-InGaAsP waveguide (SCH)

LAYER MATSYS=1 XPERC=0 YPERC=0 TL=0.2 !P-spacer

LAYER MATSYS=12 XPERC=1.10 TL=0.008 !etch stop

LAYER MATSYS=1 XPERC=0.0 YPERC=0 TL=1.0 !P-cladding

Chapter 7 InGaAsP/InGaAsP/InP Laser

```
LAYER  MATSYS=1 XPERC=0.53 YPERC=0 TL=0.2    !P-cap
!----- end of structure -----
!OUTPUT Parameter Set
OUTPUT  PHMO=1      GAMMAO=1    WZRO=1    WZIO=1    QZRO=1    QZIO=1
OUTPUT  FWHPNO=1   FWHPFO=1   KMO=1     ITO=1
OUTPUT  MODOUT=1   LYROUT=1   SPLTFL=0
!GAMOUT Parameter Set
GAMOUT  LAYGAM=4    COMPGAM=0  GAMALL=0
GAMOUT  LAYGAM=6    COMPGAM=0  GAMALL=0
GAMOUT  LAYGAM=8    COMPGAM=0  GAMALL=0
GAMOUT  LAYGAM=10   COMPGAM=0  GAMALL=0
GAMOUT  LAYGAM=12   COMPGAM=0  GAMALL=0
LOOPZ1  ILZ='QZMR'  FINV=10.24  ZINC=-0.01
!LOOPZ1  ILZ='WVL'  FINV=1.32   ZINC=0.001
!LOOPX1  ILX='TL'   FINV=2      XINC=0.05   LAYCH=16
!LOOPX1  ILX='TL'   FINV=0.35   XINC=0.005  LAYCH=3
!LOOPX1  ILX='TL'   FINV=0.35   XINC=0.005  LAYCH=13
!LOOPX1  ILX='TL'   FINV=2      XINC=0.05   LAYCH=2
END
```

7.1.3 QZMR looping and modes searching

The fundamental TE mode is searched by looping the QZMR defined as the square of the effective refractive index n_{eff}^2 . The value of QZMR should be in the range of square of the minimum refractive index n_{min}^2 and maximum refractive index n_{max}^2 ; therefore, the QZMR is looped from the 10.245 (n_{min}^2) to 12.23 (n_{max}^2), and the input file is given in Table 7.1.3. After looping the QZMR, we obtain results shown in Table 7.1.4. To pick up the QZMR for the fundamental TE mode, several criteria including PHM < 1.0, KM=6 or 7, and IT < 10 are applied. Based on these criteria, the QZMR for the

fundamental TE mode is 10.53, which is highlighted in this table. The near field and far fields are shown in Fig. 7.1.1 and Fig. 7.1.2.

Table 7.1.3 Input file

```

CASE KASE=InGaAsP (5 wells)

CASE     EPS1=1E-8  EPS2=1E-8  GAMEPS=1E-6

CASE     QZMR=12.23  QZMI=0.0

CASE     PRINTF=0    INITGS=0    AUTOQW=0  NFPLT=0    FFPLT=1

MODCON   KPOL=1     APB1=0.25  APB2=0.25

STRUCT   WVL=1.3

LAYER    MATSYS=1   XPERC=0   YPERC=0   TL=0.0    !InP N-substrate
LAYER    MATSYS=1   XPERC=0   YPERC=0   TL=2.0    !InP N-cladding
LAYER    MATSYS=12  XPERC=1.10  TL=0.06    !InGaAsP waveguide
LAYER    MATSYS=12  XPERC=1.28  TL=0.006   !QW
LAYER    MATSYS=12  XPERC=1.10  TL=0.02    !barrier
LAYER    MATSYS=12  XPERC=1.28  TL=0.006   !QW
LAYER    MATSYS=12  XPERC=1.10  TL=0.02    !barrier
LAYER    MATSYS=12  XPERC=1.28  TL=0.006   !QW
LAYER    MATSYS=12  XPERC=1.10  TL=0.02    !barrier
LAYER    MATSYS=12  XPERC=1.28  TL=0.006   !QW
LAYER    MATSYS=12  XPERC=1.10  TL=0.02    !barrier
LAYER    MATSYS=12  XPERC=1.28  TL=0.006   !QW
LAYER    MATSYS=12  XPERC=1.10  TL=0.02    !barrier
LAYER    MATSYS=12  XPERC=1.28  TL=0.006   !QW
LAYER    MATSYS=12  XPERC=1.10  TL=0.06    !InGaAsP waveguide
LAYER    MATSYS=1   XPERC=0   YPERC=0   TL=0.2    !P-spacer
LAYER    MATSYS=12  XPERC=1.10  TL=0.008    !etch stop
LAYER    MATSYS=1   XPERC=0.0  YPERC=0   TL=1.0    !P-cladding
LAYER    MATSYS=1   XPERC=0.53  YPERC=0   TL=0.2    !P-cap

OUTPUT   PHMO=1     GAMMAO=1   WZRO=1    WZIO=1    QZRO=1    QZIO=1

```

Chapter 7 InGaAsP/InGaAsP/InP Laser

```

OUTPUT  FWHPNO=1    FWHPFO=1    KMO=1    ITO=1

OUTPUT  MODOUT=1    LYROUT=1    SPLTFL=0

GAMOUT  LAYGAM=4    COMPGAM=0    GAMALL=0

GAMOUT  LAYGAM=6    COMPGAM=0    GAMALL=0

GAMOUT  LAYGAM=8    COMPGAM=0    GAMALL=0

GAMOUT  LAYGAM=10   COMPGAM=0    GAMALL=0

GAMOUT  LAYGAM=12   COMPGAM=0    GAMALL=0

LOOPZ1  ILZ= 'QZMR'  FINV=10.24   ZINC=-0.01

!LOOPZ1 ILZ= 'WVL'   FINV=1.32    ZINC=0.001

!LOOPX1 ILX= 'TL'    FINV=2       XINC=0.05    LAYCH=16

!LOOPX1 ILX= 'TL'    FINV=0.35    XINC=0.005   LAYCH=3

!LOOPX1 ILX= 'TL'    FINV=0.35    XINC=0.005   LAYCH=13

!LOOPX1 ILX= 'TL'    FINV=2       XINC=0.05    LAYCH=2

END

```

Table 7.1.4 QZMR looping results

QZMR	PHM	GAMMA(8)		WZR	WZI		QZR			
QZI	FWHPN	FWHPF		KM	IT	...				
1.057000E+01	1.268803E+00	0.000000E+00	3.203805E+00	1.335073E-02	1.026419E+01	8.554627E-02	0.000000E+00	0.000000E+00	4	30
1.056000E+01	1.304147E+00	0.000000E+00	3.202628E+00	1.319513E-02	1.025665E+01	8.451819E-02	0.000000E+00	0.000000E+00	4	30
1.055000E+01	1.342505E+00	0.000000E+00	3.201541E+00	1.313573E-02	1.024969E+01	8.410913E-02	0.000000E+00	0.000000E+00	4	30
1.054000E+01	1.160656E+00	0.000000E+00	3.199640E+00	6.956230E-03	1.023765E+01	4.451486E-02	0.000000E+00	0.000000E+00	4	30
1.053000E+01	3.135298E-01	1.100744E-02	3.236279E+00	1.039882E-16	1.047350E+01	6.730699E-16	4.271949E-01	3.344259E+01	6	7
1.052000E+01	3.135298E-01	1.100744E-02	3.236279E+00	2.187776E-18	1.047350E+01	1.416050E-17	4.271949E-01	3.344259E+01	6	7
1.051000E+01	3.135298E-01	1.100744E-02	3.236279E+00	-1.688206E-18	1.047350E+01	-1.092701E-17	4.271949E-01	3.344259E+01	6	6
1.050000E+01	3.135298E-01	1.100744E-02	3.236279E+00	2.911808E-19	1.047350E+01	1.884685E-18	4.271949E-01	3.344259E+01	6	5
1.049000E+01	3.135298E-01	1.100744E-02	3.236279E+00	-2.458654E-18	1.047350E+01	-1.591378E-17	4.271949E-01	3.344259E+01	6	4

7.1 InGaAsP/InGaAsP/InP (1310nm)

1.048000E+01	3.135298E-01	1.100744E-02	3.236279E+00	-2.096278E-25	1.047350E+01	-1.356828E-24	4.271949E-01	3.344259E+01	7	4
1.047000E+01	3.135298E-01	1.100744E-02	3.236279E+00	7.590129E-19	1.047350E+01	4.912755E-18	4.271949E-01	3.344259E+01	6	3
1.046000E+01	3.135298E-01	1.100744E-02	3.236279E+00	-2.634251E-20	1.047350E+01	-1.705034E-19	4.271949E-01	3.344259E+01	6	4
1.045000E+01	3.135298E-01	1.100744E-02	3.236279E+00	4.536042E-25	1.047350E+01	2.935980E-24	4.271949E-01	3.344259E+01	7	5
1.044000E+01	3.135298E-01	1.100744E-02	3.236279E+00	-1.035368E-21	1.047350E+01	-6.701481E-21	4.271949E-01	3.344259E+01	6	5
1.043000E+01	3.135298E-01	1.100744E-02	3.236279E+00	4.555056E-17	1.047350E+01	2.948286E-16	4.271949E-01	3.344259E+01	6	5
1.042000E+01	3.135298E-01	1.100744E-02	3.236279E+00	-1.255406E-18	1.047350E+01	-8.125687E-18	4.271949E-01	3.344259E+01	6	6
1.041000E+01	8.796903E-01	0.000000E+00	3.200812E+00	3.480292E-03	1.024518E+01	2.227952E-02	0.000000E+00	0.000000E+00	4	30

1.040000E+01 **6.020**

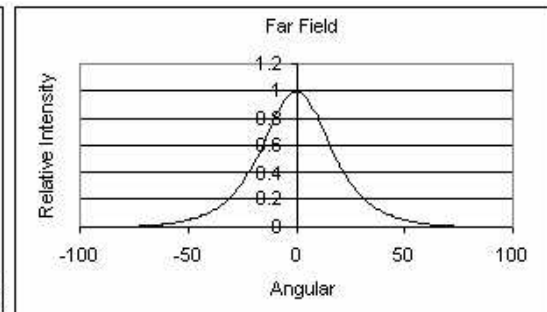
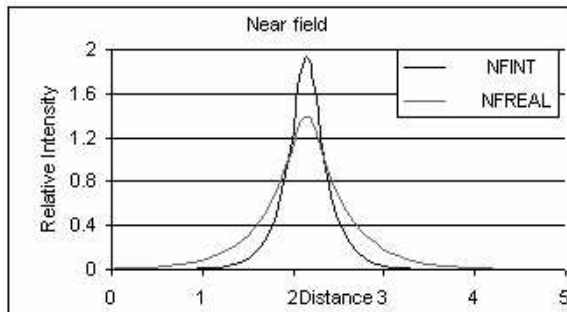


Figure 7.1.1. Fundamental mode near field plot for initial waveguide parameters.

Figure 7.1.2. Fundamental mode far field plot for initial waveguide parameters.

The output parameters are:

PHM = 3.135298E-01
 GAMMA(4) = 1.037769E-02
 GAMMA(6) = 1.084085E-02
 GAMMA(8) = 1.100744E-02
 GAMMA(10) = 1.086821E-02
 GAMMA(12) = 1.043089E-02
 WZR = 3.236279E+00
 WZI = 1.039882E-16
 FWHPF = 3.344259E+01

KM = 6

IT = 7

7.1.4. Thickness of SCH layer (SCH-TL) looping

The p-SCH and n-SCH layers have strong effects on optical confinement factor (Γ) and far field divergence (FWHPF). In this subsection, the thickness of the p-SCH and n-SCH (the 3th and the 13th layers) are looped and determined. The range of the thickness is from 0.06 μm to 0.35 μm , and the input file and looping results are shown in Table 7.1.5 and 7.1.6, respectively. The criterion for determining the SCH-TL is to obtain a large confinement factor and small far field divergence, but a higher optical confinement factor always leads to a larger far field divergence, and vice versa. Therefore, the SCH-TL is determined by optimizing the optical confinement factor and far field divergence. Fig. 7.1.3 shows the optical confinement factor and far field divergence versus SCH-TL. As can be seen, the far field divergence monotonously increases with SCH-TL. However, a peak value of optical confinement factor exists at 0.13 μm , and the optical confinement factor decreases with either increasing or decreasing SCH-TL. The SCH-TL is taken as 0.09 μm after comprising the optical confinement factor and far field divergence.

Table 7.1.5 Input file

```

CASE KASE=InGaAsP (5 wells)

CASE     EPS1=1E-8   EPS2=1E-8   GAMEPS=1E-6

CASE     QZMR=10.53  QZMI=0.0

CASE     PRINTF=0    INITGS=0    AUTOQW=0   NFPLT=0    FFPLT=1

MODCON   KPOL=1     APB1=0.25  APB2=0.25

STRUCT   WVL=1.3

LAYER    MATSYS=1   XPERC=0    YPERC=0    TL=0.0    !InP N-substrate

LAYER    MATSYS=1   XPERC=0    YPERC=0    TL=2.0    !InP N-cladding

```


7.1 InGaAsP/InGaAsP/InP (1310nm)

```

LAYER  MATSYS=12 XPERC=1.10  TL=0.06    !InGaAsP waveguide
LAYER  MATSYS=12 XPERC=1.28  TL=0.006 !QW
LAYER  MATSYS=12 XPERC=1.10  TL=0.02    !barrier
LAYER  MATSYS=12 XPERC=1.28  TL=0.006 !QW
LAYER  MATSYS=12 XPERC=1.10  TL=0.02    !barrier
LAYER  MATSYS=12 XPERC=1.28  TL=0.006 !QW
LAYER  MATSYS=12 XPERC=1.10  TL=0.02    !barrier
LAYER  MATSYS=12 XPERC=1.28  TL=0.006 !QW
LAYER  MATSYS=12 XPERC=1.10  TL=0.02    !barrier
LAYER  MATSYS=12 XPERC=1.28  TL=0.006 !QW
LAYER  MATSYS=12 XPERC=1.10  TL=0.06    !InGaAsP waveguide
LAYER  MATSYS=1  XPERC=0  YPERC=0  TL=0.2    !P-spacer
LAYER  MATSYS=12 XPERC=1.10  TL=0.008    !etch stop
LAYER  MATSYS=1  XPERC=0.0  YPERC=0  TL=1.0    !P-cladding
LAYER  MATSYS=1  XPERC=0.53 YPERC=0  TL=0.2    !P-cap

OUTPUT PHMO=1      GAMMAO=1    WZRO=1    WZIO=1    QZRO=1    QZIO=1

OUTPUT FWHPNO=1    FWHPFO=1    KMO=1     ITO=1

OUTPUT MODOUT=1    LYROUT=1    SPLTFL=0

GAMOUT LAYGAM=4      COMPGAM=0    GAMALL=0
GAMOUT LAYGAM=6      COMPGAM=0    GAMALL=0
GAMOUT LAYGAM=8      COMPGAM=0    GAMALL=0
GAMOUT LAYGAM=10     COMPGAM=0    GAMALL=0
GAMOUT LAYGAM=12     COMPGAM=0    GAMALL=0

!LOOPZ1  ILZ='QZMR'  FINV=10.24  ZINC=-0.1
!LOOPZ1  ILZ='WVL'   FINV=1.32   ZINC=0.001
!LOOPX1  ILX='TL'   FINV=2      XINC=0.05  LAYCH=16
LOOPX1   ILX='TL'   FINV=0.35  XINC=0.005 LAYCH=3
LOOPX1   ILX='TL'   FINV=0.35  XINC=0.005 LAYCH=13
!LOOPX1  ILX='TL'   FINV=2      XINC=0.05  LAYCH=2

```

Chapter 7 InGaAsP/InGaAsP/InP Laser

END

Table 7.1.6 SCH-TL looping results

TL (3)	TL(13)	PHM	GAMMA(8)	WZR	WZI	QZR	QZI	FWHPF	KM	IT
6.00000E-02	6.00000E-02	3.135298E-01	1.100744E-02	3.236279E+00	1.583542E-16	1.047350E+01	1.024956E-15	3.344259E+01	6	7
6.50000E-02	6.50000E-02	3.229414E-01	1.114423E-02	3.238097E+00	-2.368270E-21	1.048527E+01	-1.533738E-20	3.418434E+01	6	4
7.00000E-02	7.00000E-02	3.321173E-01	1.126589E-02	3.239901E+00	-1.617249E-21	1.049696E+01	-1.047945E-20	3.487698E+01	6	4
7.50000E-02	7.50000E-02	3.410613E-01	1.137331E-02	3.241688E+00	-1.084038E-21	1.050854E+01	-7.028224E-21	3.553005E+01	6	4
8.00000E-02	8.00000E-02	3.497774E-01	1.146734E-02	3.243455E+00	-7.272668E-22	1.052000E+01	-4.717714E-21	3.615444E+01	6	4
8.50000E-02	8.50000E-02	3.582700E-01	1.154883E-02	3.245200E+00	-4.805193E-22	1.053132E+01	-3.118762E-21	3.678144E+01	6	4
9.00000E-02	9.00000E-02	3.665436E-01	1.161886E-02	3.246921E+00	-3.201700E-22	1.054250E+01	-2.079133E-21	3.735181E+01	6	4
9.50000E-02	9.50000E-02	3.746030E-01	1.167736E-02	3.248617E+00	-2.117109E-22	1.055351E+01	-1.375535E-21	3.788866E+01	6	4
1.00000E-01	1.00000E-01	3.824529E-01	1.172595E-02	3.250286E+00	-1.378439E-22	1.056436E+01	-8.960641E-22	3.841106E+01	7	4
1.05000E-01	1.05000E-01	3.900983E-01	1.176505E-02	3.251928E+00	2.111198E-23	1.057503E+01	1.373093E-22	3.890644E+01	7	4
1.10000E-01	1.10000E-01	3.975440E-01	1.179535E-02	3.253541E+00	1.484773E-22	1.058553E+01	9.661538E-22	3.937338E+01	7	4
1.15000E-01	1.15000E-01	4.047950E-01	1.181750E-02	3.255124E+00	7.583282E-23	1.059583E+01	4.936905E-22	3.981403E+01	7	4
1.20000E-01	1.20000E-01	4.118563E-01	1.183211E-02	3.256678E+00	-4.275982E-24	1.060595E+01	-2.785099E-23	4.023261E+01	7	4
1.25000E-01	1.25000E-01	4.187329E-01	1.183970E-02	3.258201E+00	-1.468280E-23	1.061587E+01	-9.567902E-23	4.064002E+01	7	4
1.30000E-01	1.30000E-01	4.254295E-01	1.184098E-02	3.259693E+00	5.611551E-27	1.062560E+01	3.658387E-26	4.101890E+01	7	4
1.35000E-01	1.35000E-01	4.319510E-01	1.183629E-02	3.261155E+00	-6.765800E-24	1.063513E+01	-4.412865E-23	4.137542E+01	7	4
1.40000E-01	1.40000E-01	4.383023E-01	1.182616E-02	3.262586E+00	-9.616109E-24	1.064447E+01	-6.274676E-23	4.171113E+01	7	4
1.45000E-01	1.45000E-01	4.444879E-01	1.181105E-02	3.263986E+00	1.209900E-24	1.065361E+01	7.898193E-24	4.202610E+01	7	4
1.50000E-01	1.50000E-01	4.505125E-01	1.179137E-02	3.265356E+00	2.489512E-24	1.066255E+01	1.625828E-23	4.233540E+01	7	4
1.55000E-01	1.55000E-01	4.563805E-01	1.176750E-02	3.266695E+00	-2.160847E-24	1.067130E+01	-1.411766E-23	4.262063E+01	7	4
1.60000E-01	1.60000E-01	4.620964E-01	1.173981E-02	3.268005E+00	-6.315428E-25	1.067985E+01	-4.127770E-24	4.288808E+01	7	4
1.65000E-01	1.65000E-01	4.676644E-01	1.170863E-02	3.269284E+00	2.076899E-25	1.068822E+01	1.357995E-24	4.313849E+01	7	4
1.70000E-01	1.70000E-01	4.730887E-01	1.167411E-02	3.270535E+00	4.965797E-25	1.069640E+01	3.248162E-24	4.337115E+01	7	4
1.75000E-01	1.75000E-01	4.783734E-01	1.163704E-02	3.271756E+00	5.012743E-25	1.070439E+01	3.280095E-24	4.359009E+01	7	4
1.80000E-01	1.80000E-01	4.835225E-01	1.159718E-02	3.272949E+00	1.115703E-26	1.071220E+01	7.303278E-26	4.379253E+01	7	4

7.1 InGaAsP/InGaAsP/InP (1310nm)

1.850000E-01	1.850000E-01	4.885397E-01	1.155496E-02	3.274114E+00	-7.063129E-26	1.071982E+01	-4.625098E-25	4.398171E+01	7	4
1.900000E-01	1.900000E-01	4.934289E-01	1.151060E-02	3.275252E+00	2.199018E-26	1.072728E+01	1.440468E-25	4.416227E+01	7	4
1.950000E-01	1.950000E-01	4.981937E-01	1.146432E-02	3.276363E+00	-4.394031E-26	1.073455E+01	-2.879288E-25	4.432859E+01	7	4
2.000000E-01	2.000000E-01	5.028376E-01	1.141632E-02	3.277447E+00	-1.739460E-26	1.074166E+01	-1.140197E-25	4.448476E+01	7	4
2.050000E-01	2.050000E-01	5.073639E-01	1.136677E-02	3.278506E+00	-2.421000E-25	1.074860E+01	-1.587453E-24	4.462305E+01	7	4
2.100000E-01	2.100000E-01	5.117761E-01	1.131586E-02	3.279539E+00	5.534428E-26	1.075538E+01	3.630075E-25	4.475387E+01	7	4
2.150000E-01	2.150000E-01	5.160772E-01	1.126372E-02	3.280548E+00	-1.388722E-27	1.076199E+01	-9.111541E-27	4.487420E+01	7	4
2.200000E-01	2.200000E-01	5.202705E-01	1.121051E-02	3.281532E+00	-2.287986E-27	1.076845E+01	-1.501620E-26	4.498346E+01	7	4
2.250000E-01	2.250000E-01	5.243589E-01	1.115636E-02	3.282493E+00	-4.649419E-26	1.077476E+01	-3.052338E-25	4.508195E+01	7	4
2.300000E-01	2.300000E-01	5.283453E-01	1.110139E-02	3.283431E+00	9.936085E-28	1.078092E+01	6.524890E-27	4.517266E+01	7	4
2.350000E-01	2.350000E-01	5.322326E-01	1.104572E-02	3.284347E+00	-9.941077E-29	1.078693E+01	-6.529989E-28	4.525296E+01	7	4
2.400000E-01	2.400000E-01	5.360234E-01	1.098944E-02	3.285240E+00	4.237763E-27	1.079280E+01	2.784414E-26	4.532424E+01	7	4
2.450000E-01	2.450000E-01	5.397203E-01	1.093266E-02	3.286113E+00	5.292082E-28	1.079854E+01	3.478075E-27	4.538764E+01	7	4
2.500000E-01	2.500000E-01	5.433260E-01	1.087546E-02	3.286964E+00	-1.310371E-26	1.080413E+01	-8.614288E-26	4.544274E+01	7	4
2.550000E-01	2.550000E-01	5.468429E-01	1.081793E-02	3.287795E+00	1.075372E-26	1.080960E+01	7.071207E-26	4.548559E+01	7	4
2.600000E-01	2.600000E-01	5.502734E-01	1.076013E-02	3.288607E+00	-3.656380E-27	1.081494E+01	-2.404879E-26	4.552701E+01	7	4
2.650000E-01	2.650000E-01	5.536197E-01	1.070214E-02	3.289399E+00	6.437741E-27	1.082015E+01	4.235260E-26	4.555926E+01	7	4
2.700000E-01	2.700000E-01	5.568841E-01	1.064402E-02	3.290173E+00	-1.873556E-26	1.082524E+01	-1.232864E-25	4.558578E+01	7	4
2.750000E-01	2.750000E-01	5.600687E-01	1.058582E-02	3.290928E+00	4.488132E-27	1.083021E+01	2.954023E-26	4.560529E+01	7	4
2.800000E-01	2.800000E-01	5.631757E-01	1.052760E-02	3.291665E+00	8.202291E-27	1.083506E+01	5.399839E-26	4.561867E+01	7	4
2.850000E-01	2.850000E-01	5.662070E-01	1.046941E-02	3.292386E+00	5.361304E-27	1.083980E+01	3.530296E-26	4.562548E+01	7	4
2.900000E-01	2.900000E-01	5.691647E-01	1.041129E-02	3.293089E+00	5.568379E-27	1.084443E+01	3.667433E-26	4.562697E+01	7	4
2.950000E-01	2.950000E-01	5.720505E-01	1.035329E-02	3.293776E+00	7.837625E-27	1.084896E+01	5.163076E-26	4.562060E+01	7	4
3.000000E-01	3.000000E-01	5.748663E-01	1.029543E-02	3.294447E+00	-7.816185E-27	1.085338E+01	-5.150002E-26	4.561057E+01	7	4
...										

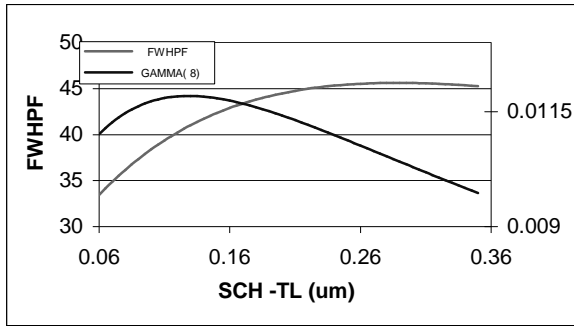


Figure 7.1.3. QW confinement factor and FWHPF vs. SCH thickness.

The output parameters are:

```

PHM           = 3.665436E-01
GAMMA(4)     = 1.100883E-02
GAMMA(6)     = 1.145845E-02
GAMMA(8)     = 1.161856E-02
GAMMA(10)    = 1.148095E-02
GAMMA(12)    = 1.105268E-02
WZR          = 3.246921E+00
WZI          = -1.773925E-20
FWHPF        = 3.735181E+01
KM           = 6
IT           = 4

```

7.1.5 Thickness of the p-cladding layer (p-cladding-TL) looping

In order to design a semiconductor laser with low threshold current density, total loss within cavity should be carefully analyzed and reduced. Some physical originations, such as free carrier absorption and nonradiative Auger recombination, contribute to the loss, which have been widely investigated. In addition, laser waveguide structure also affects the loss, especially the thickness of p-cladding layer.

In this subsection, the effect of the thickness of p-cladding layer on the loss is studied. After setting the QZMR and the thickness of SCH found in the previous subsections, we loop the thickness of p-cladding layer from 0 to 2.0 μm . The input file and the looping results are shown in Table 7.1.7 and 7.1.8, respectively. It should be

indicated that the loss of each layer should be included in the input file, especially in a high doping layer such as the p-cap layer. In order to make it brief, only the loss in the p-cap layer is considered in this demonstration, and users can include losses in all layers obtain a better results. Fig. 7.1.4 shows the relationship between loss, FWHPF and the thickness of the p-cladding layer. As can be seen, the loss decreases with the thickness of the p-cladding layer. The loss reduces significantly at small thickness of the p-cladding layer, and keeps almost constant when the thickness of the p-cladding layer is larger than $1.0\mu\text{m}$. The reason may be the field penetration of the p-cap layer or even radiation from the transverse direction. Since the field decreases exponentially in transverse direction of the p-cladding layer, a significant amount of field penetrates and propagates in the lossy p-cap layer when the p-cladding layer is thin enough, which results in a high loss and threshold current density. However, when the p-cladding layer is thick enough, the field almost dies out in the p-cladding layer and the field in the p-cap layer can be neglected; therefore, the loss keeps constant in a thick p-cladding layer.

Table 7.1.7 Input file

```

CASE KASE=InGaAsP (5 wells)

CASE     EPS1=1E-8   EPS2=1E-8   GAMEPS=1E-6

CASE     QZMR=10.53  QZMI=0.0

CASE     PRINTF=0    INITGS=0    AUTOQW=0    NFPLT=0     FFPLT=1

MODCON   KPOL=1     APB1=0.25   APB2=0.25

STRUCT   WVL=1.3

LAYER    MATSYS=1   XPERC=0    YPERC=0    NLOSS=0.0  TL=0.0    !InP N-substrate
LAYER    MATSYS=1   XPERC=0    YPERC=0    NLOSS=0.0  TL=2.0    !InP N-cladding
LAYER    MATSYS=12  XPERC=1.10  NLOSS=0.0  TL=0.09    !InGaAsP waveguide
LAYER    MATSYS=12  XPERC=1.28  NLOSS=0.000  TL=0.006  !QW
LAYER    MATSYS=12  XPERC=1.10  NLOSS=0.000  TL=0.02    !barrier
LAYER    MATSYS=12  XPERC=1.28  NLOSS=0.000  TL=0.006  !QW
LAYER    MATSYS=12  XPERC=1.10  NLOSS=0.000  TL=0.02    !barrier
LAYER    MATSYS=12  XPERC=1.28  NLOSS=0.000  TL=0.006  !QW

```

Chapter 7 InGaAsP/InGaAsP/InP Laser

```

LAYER  MATSYS=12 XPERC=1.10  NLOSS=0.000 TL=0.02  !barrier
LAYER  MATSYS=12 XPERC=1.28  NLOSS=0.000 TL=0.006 !QW
LAYER  MATSYS=12 XPERC=1.10  NLOSS=0.000 TL=0.02  !barrier
LAYER  MATSYS=12 XPERC=1.28  NLOSS=0.000 TL=0.006 !QW
LAYER  MATSYS=12 XPERC=1.10  NLOSS=0.000 TL=0.09  !InGaAsP waveguide
LAYER  MATSYS=1  XPERC=0 YPERC=0  NLOSS=0.000 TL=0.2  !P-spacer
LAYER  MATSYS=12 XPERC=1.10  NLOSS=0.000 TL=0.008  !etch stop
LAYER  MATSYS=1  XPERC=0.0 YPERC=0  NLOSS=0.005 TL=0.0  !P-cladding
LAYER  MATSYS=1  XPERC=0.53 YPERC=0  NLOSS=0.01 TL=0.2 !P-cap
OUTPUT PHMO=1      GAMMAO=1  WZRO=1  WZIO=1  QZRO=1  QZIO=1
OUTPUT FWHPNO=0    FWHPFO=1  KMO=1   ITO=1
OUTPUT MODOUT=1    LYROUT=1  SPLTFL=0
!GAMOUT LAYGAM=4    COMPGAM=0  GAMALL=0
!GAMOUT LAYGAM=6    COMPGAM=0  GAMALL=0
GAMOUT  LAYGAM=8    COMPGAM=0  GAMALL=0
!GAMOUT LAYGAM=10   COMPGAM=0  GAMALL=0
!GAMOUT LAYGAM=12   COMPGAM=0  GAMALL=0
!LOOPZ1 ILZ='QZMR'  FINV=10.24  ZINC=-0.1
!LOOPZ1 ILZ='WVL'   FINV=1.32  ZINC=0.001
LOOPX1  ILX='TL'    FINV=2      XINC=0.05  LAYCH=16
!LOOPX1 ILX='TL'    FINV=0.35  XINC=0.005 LAYCH=3
!LOOPX1 ILX='TL'    FINV=0.35  XINC=0.005 LAYCH=13
!LOOPX1 ILX='TL'    FINV=2      XINC=0.05  LAYCH=2
END

```

Table 7.1.8 p-cladding-TL looping results

TL(16)	PHM	GAMMA(8)	WZR	WZI	QZR	QZI	FWHPF	KM	IT
0.000000E+00	3.773318E-01	1.162245E-02	3.246895E+00	5.325267E-04	1.054232E+01	3.458116E-03	3.879116E+01	7	4
5.000000E-02	3.750182E-01	1.162235E-02	3.246899E+00	4.089916E-04	1.054236E+01	2.655909E-03	3.854882E+01	6	2

7.1 InGaAsP/InGaAsP/InP (1310nm)

1.000000E-01	3.731975E-01	1.162212E-02	3.246904E+00	3.141278E-04	1.054238E+01	2.039885E-03	3.855318E+01	6	2
1.500000E-01	3.717657E-01	1.162181E-02	3.246907E+00	2.412780E-04	1.054241E+01	1.566814E-03	3.834371E+01	6	2
2.000000E-01	3.706402E-01	1.162147E-02	3.246910E+00	1.853309E-04	1.054242E+01	1.203505E-03	3.816291E+01	6	2
2.500000E-01	3.697559E-01	1.162112E-02	3.246912E+00	1.423624E-04	1.054244E+01	9.244766E-04	3.815898E+01	6	2
3.000000E-01	3.690615E-01	1.162078E-02	3.246914E+00	1.093600E-04	1.054245E+01	7.101653E-04	3.800487E+01	6	2
3.500000E-01	3.685165E-01	1.162046E-02	3.246916E+00	8.401094E-05	1.054246E+01	5.455529E-04	3.787452E+01	6	2
4.000000E-01	3.680889E-01	1.162017E-02	3.246917E+00	6.453941E-05	1.054247E+01	4.191082E-04	3.786986E+01	6	2
4.500000E-01	3.677535E-01	1.161991E-02	3.246918E+00	4.958204E-05	1.054248E+01	3.219776E-04	3.776004E+01	7	2
5.000000E-01	3.674906E-01	1.161969E-02	3.246919E+00	3.809187E-05	1.054248E+01	2.473624E-04	3.766814E+01	7	2
5.500000E-01	3.672846E-01	1.161950E-02	3.246919E+00	2.926494E-05	1.054248E+01	1.900418E-04	3.766349E+01	7	2
6.000000E-01	3.671232E-01	1.161934E-02	3.246920E+00	2.248375E-05	1.054249E+01	1.460058E-04	3.758920E+01	7	2
6.500000E-01	3.669968E-01	1.161919E-02	3.246920E+00	1.727407E-05	1.054249E+01	1.121751E-04	3.752802E+01	7	2
7.000000E-01	3.668979E-01	1.161908E-02	3.246920E+00	1.327165E-05	1.054249E+01	8.618396E-05	3.752465E+01	7	2
7.500000E-01	3.668205E-01	1.161899E-02	3.246920E+00	1.019666E-05	1.054249E+01	6.621552E-05	3.747467E+01	6	1
8.000000E-01	3.667599E-01	1.161891E-02	3.246921E+00	7.834191E-06	1.054249E+01	5.087399E-05	3.743381E+01	6	1
8.500000E-01	3.667126E-01	1.161884E-02	3.246921E+00	6.019111E-06	1.054249E+01	3.908715E-05	3.743089E+01	6	1
9.000000E-01	3.666756E-01	1.161879E-02	3.246921E+00	4.624578E-06	1.054249E+01	3.003127E-05	3.739788E+01	6	1
9.500000E-01	3.666466E-01	1.161874E-02	3.246921E+00	3.553147E-06	1.054249E+01	2.307358E-05	3.737132E+01	6	1
1.000000E+00	3.666240E-01	1.161871E-02	3.246921E+00	2.729955E-06	1.054250E+01	1.772790E-05	3.736888E+01	6	1
1.050000E+00	3.666063E-01	1.161868E-02	3.246921E+00	2.097484E-06	1.054250E+01	1.362073E-05	3.734778E+01	6	1
1.100000E+00	3.665926E-01	1.161866E-02	3.246921E+00	1.611546E-06	1.054250E+01	1.046512E-05	3.733101E+01	6	1
1.150000E+00	3.665818E-01	1.161864E-02	3.246921E+00	1.238189E-06	1.054250E+01	8.040606E-06	3.732920E+01	6	1
1.200000E+00	3.665734E-01	1.161862E-02	3.246921E+00	9.513316E-07	1.054250E+01	6.177797E-06	3.731613E+01	6	1
1.250000E+00	3.665668E-01	1.161862E-02	3.246921E+00	7.309322E-07	1.054250E+01	4.746558E-06	3.730590E+01	6	1
1.300000E+00	3.665617E-01	1.161861E-02	3.246921E+00	5.615942E-07	1.054250E+01	3.646904E-06	3.730457E+01	6	1
1.350000E+00	3.665577E-01	1.161859E-02	3.246921E+00	4.314878E-07	1.054250E+01	2.802014E-06	3.729676E+01	6	1
1.400000E+00	3.665546E-01	1.161859E-02	3.246921E+00	3.315235E-07	1.054250E+01	2.152862E-06	3.729123E+01	6	1
1.450000E+00	3.665522E-01	1.161859E-02	3.246921E+00	2.547184E-07	1.054250E+01	1.654101E-06	3.729029E+01	6	1
1.500000E+00	3.665503E-01	1.161858E-02	3.246921E+00	1.957071E-07	1.054250E+01	1.270891E-06	3.728580E+01	6	1
1.550000E+00	3.665488E-01	1.161858E-02	3.246921E+00	1.503671E-07	1.054250E+01	9.764600E-07	3.728245E+01	6	1
1.600000E+00	3.665477E-01	1.161858E-02	3.246921E+00	1.155312E-07	1.054250E+01	7.502413E-07	3.728180E+01	6	1
1.650000E+00	3.665468E-01	1.161858E-02	3.246921E+00	8.876578E-08	1.054250E+01	5.764310E-07	3.727938E+01	6	1
1.700000E+00	3.665461E-01	1.161857E-02	3.246921E+00	6.820123E-08	1.054250E+01	4.428880E-07	3.727760E+01	6	1
1.750000E+00	3.665455E-01	1.161857E-02	3.246921E+00	5.240088E-08	1.054250E+01	3.402830E-07	3.727717E+01	6	1
1.800000E+00	3.665451E-01	1.161857E-02	3.246921E+00	4.026104E-08	1.054250E+01	2.614489E-07	3.727593E+01	6	1
1.850000E+00	3.665448E-01	1.161872E-02	3.246921E+00	3.093367E-08	1.054250E+01	2.008784E-07	3.727506E+01	6	1
1.900000E+00	3.665445E-01	1.161857E-02	3.246921E+00	2.376720E-08	1.054250E+01	1.543404E-07	3.727479E+01	6	1
1.950000E+00	3.665443E-01	1.161857E-02	3.246921E+00	1.826100E-08	1.054250E+01	1.185840E-07	3.727298E+01	6	1
2.000000E+00	3.665442E-01	1.161863E-02	3.246921E+00	1.403043E-08	1.054250E+01	9.111139E-08	3.727260E+01	6	1
...									

In the looping results, the loss is represented by the WZI. The corresponding loss (/cm) is given by $\alpha = (WZI \cdot (4\pi/\lambda) \cdot 10^4) / \text{cm}$. The loss is small (0.265/cm) when the

thickness of p-cladding layer is larger than $1.0\mu\text{m}$; therefore, the thickness of p-cladding layer is taken as $1.0\mu\text{m}$.

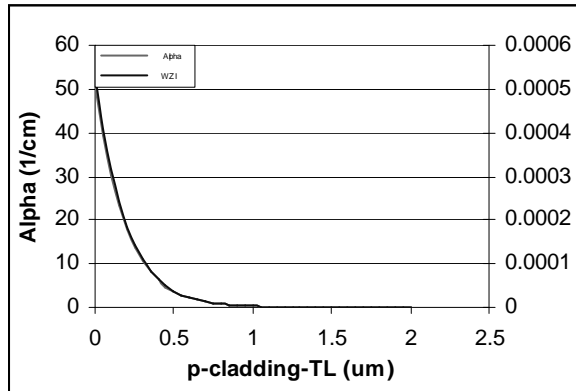


Figure 7.1.4 Loss and WZI vs. p-cladding thickness.

The output results are:

```

PHM           = 3.665990E-01
GAMMA(4)      = 1.100898E-02
GAMMA(6)      = 1.145860E-02
GAMMA(8)      = 1.161871E-02
GAMMA(10)     = 1.148110E-02
GAMMA(12)     = 1.105281E-02
WZR           = 3.246921E+00
WZI           = 2.729955E-06
FWHPF        = 3.749374E+01
KM            = 7
IT            = 4
    
```

7.1.6 Simulation results

After determining the values of the QZMR, thickness of p-SCH, n-SCH layers, and p-cladding layer, we set these values in the input files shown in Table 7.1.9. The near and far fields are shown in Fig. 7.1.5 and Fig. 7.1.6.

Table 7.1.9 Input file

7.1 InGaAsP/InGaAsP/InP (1310nm)

```

CASE KASE=InGaAsP (5 wells)

CASE     EPS1=1E-8  EPS2=1E-8  GAMEPS=1E-6

CASE     QZMR=10.53  QZMI=0.0

CASE     PRINTF=0    INITGS=0    AUTOQW=0  NFPLT=0    FFPLT=1

MODCON   KPOL=1     APB1=0.25  APB2=0.25

STRUCT   WVl=1.3

LAYER    MATSYS=1   XPERC=0   YPERC=0   NLOSS=0.0  TL=0.0    !InP N-substrate
LAYER    MATSYS=1   XPERC=0   YPERC=0   NLOSS=0.0  TL=1.0    !InP N-cladding
LAYER    MATSYS=12  XPERC=1.10  NLOSS=0.0  TL=0.09    !InGaAsP SCH
LAYER    MATSYS=12  XPERC=1.28  NLOSS=0.000  TL=0.006   !QW
LAYER    MATSYS=12  XPERC=1.10  NLOSS=0.000  TL=0.02    !barrier
LAYER    MATSYS=12  XPERC=1.28  NLOSS=0.000  TL=0.006   !QW
LAYER    MATSYS=12  XPERC=1.10  NLOSS=0.000  TL=0.02    !barrier
LAYER    MATSYS=12  XPERC=1.28  NLOSS=0.000  TL=0.006   !QW
LAYER    MATSYS=12  XPERC=1.10  NLOSS=0.000  TL=0.02    !barrier
LAYER    MATSYS=12  XPERC=1.28  NLOSS=0.000  TL=0.006   !QW
LAYER    MATSYS=12  XPERC=1.10  NLOSS=0.000  TL=0.02    !barrier
LAYER    MATSYS=12  XPERC=1.28  NLOSS=0.000  TL=0.006   !QW
LAYER    MATSYS=12  XPERC=1.10  NLOSS=0.000  TL=0.09    !InGaAsP SCH
LAYER    MATSYS=1   XPERC=0   YPERC=0   NLOSS=0.000  TL=0.2    !P-spacer
LAYER    MATSYS=12  XPERC=1.10  NLOSS=0.000  TL=0.008    !etch stop
LAYER    MATSYS=1   XPERC=0.0  YPERC=0   NLOSS=0.000  TL=1.0    !P-cladding
LAYER    MATSYS=1   XPERC=0.53  YPERC=0   NLOSS=0.03  TL=0.2    !P-cap

OUTPUT   PHMO=1     GAMMAO=1   WZRO=1    WZIO=1    QZRO=1    QZIO=1

OUTPUT   FWHPNO=0   FWHPFO=1   KMO=1     ITO=1

OUTPUT   MODOUT=1   LYROUT=1   SPLTFL=0

GAMOUT   LAYGAM=4   COMPGAM=0  GAMALL=0

GAMOUT   LAYGAM=6   COMPGAM=0  GAMALL=0

GAMOUT   LAYGAM=8   COMPGAM=0  GAMALL=0

```

Chapter 7 InGaAsP/InGaAsP/InP Laser

```

GAMOUT LAYGAM=10  COMPGAM=0  GAMALL=0
GAMOUT LAYGAM=12  COMPGAM=0  GAMALL=0
!LOOPZ1  ILZ='QZMR'  FINV=10.24  ZINC=-0.1
!LOOPZ1  ILZ='WVL'  FINV=1.32  ZINC=0.001
!LOOPX1  ILX='TL'  FINV=2  XINC=0.05  LAYCH=16
!LOOPX1  ILX='TL'  FINV=0.35  XINC=0.005  LAYCH=3
!LOOPX1  ILX='TL'  FINV=0.35  XINC=0.005  LAYCH=13
!LOOPX1  ILX='TL'  FINV=2  XINC=0.05  LAYCH=2
END

```

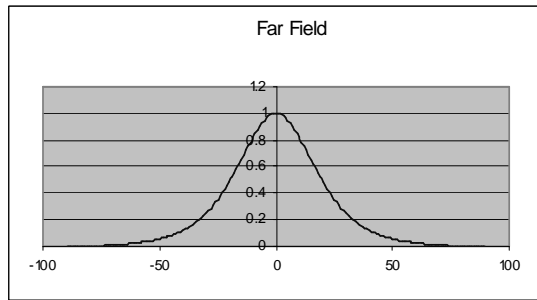
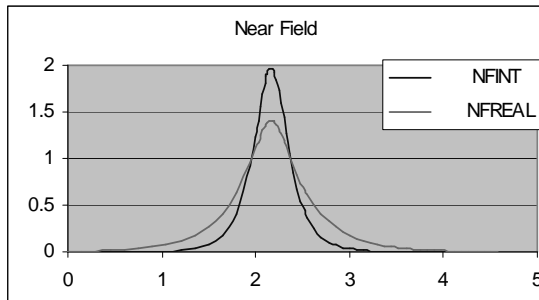


Figure 7.1.5. Fundamental mode near field plot for full structure.

Figure 7.1.6. Fundamental mode far field plot for full structure.

The Final laser structure for this 1310nm InGaAsP laser design can be found in the table 7.1.2 as follows:

Table 7.1.2 Final Laser structure (5-QW InGaAsP) for the 1310nm InGaAsP/InP laser structure.

7.1 InGaAsP/InGaAsP/InP (1310nm)

Layer	Thickness (μm)	Refractive Index	Loss
n-substrate	0	3.20081	0
n-cladding	1.0	3.20081	0
n-SCH	0.08	3.33097	0
Quantum well	0.006	3.49722	0
Barrier	0.02	3.33097	0
Quantum well	0.006	3.49722	0
Barrier	0.02	3.33097	0
Quantum well	0.006	3.49722	0
Barrier	0.02	3.33097	0
Quantum well	0.006	3.49722	0
Barrier	0.02	3.33097	0
Quantum well	0.006	3.49722	0
Barrier	0.02	3.33097	0
Quantum well	0.006	3.49722	0
Barrier	0.02	3.33097	0
Quantum well	0.006	3.49722	0
p-spacer	0.08	3.33097	0
p-SCH	0.2	3.20081	0
Etch-stop	0.001	3.33097	0
p-cladding	1.0	3.20081	0
p-cap	0.2	3.20081	0.03

7.1.7. The Refractive Index Profile

According to the final structure, we can plot the refractive index profile according to the distance of the layers for the laser structure as following:

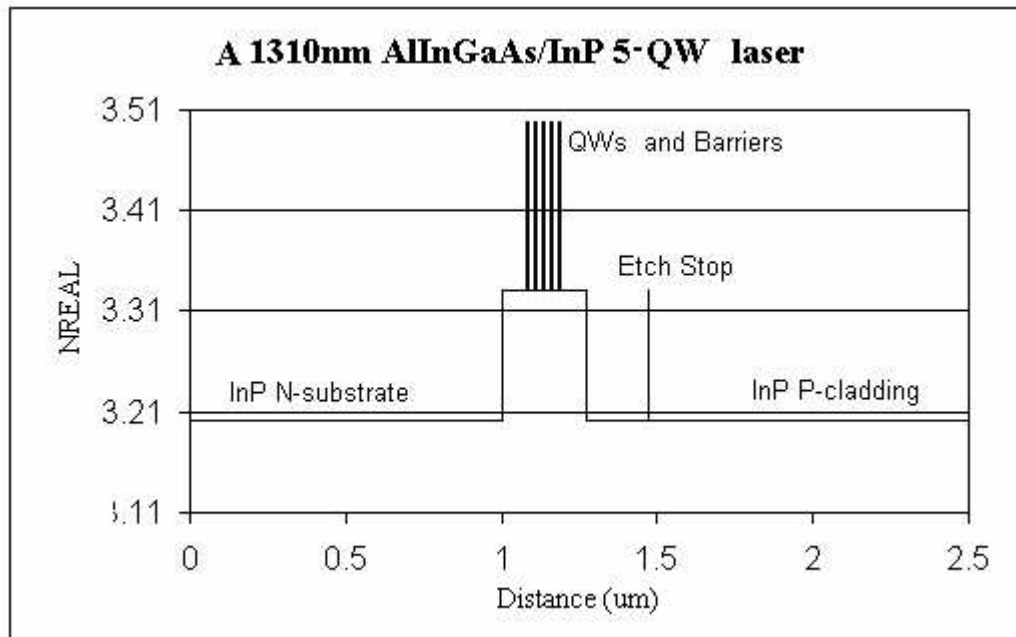


Figure 7.1.7 The laser structure of a 1310nm InGaAsP 5-QW Laser.

The output results are:

```

PHM           = 3.665990E-01
GAMMA(4)      = 1.100898E-02
GAMMA(6)      = 1.145860E-02
GAMMA(8)      = 1.161871E-02
GAMMA(10)     = 1.148110E-02
GAMMA(12)     = 1.105281E-02
WZR           = 3.246921E+00
WZI           = 2.729955E-06
FWHPF        = 3.749374E+01
KM            = 7
IT            = 4
    
```

7.2 InGaAsP/InGaAsP/InP (1550nm)

7.2.1 Introduction

In this section, the InGaAsP/InGaAsP/InP 1550 nm laser structure design will be introduced by using WAVEGUIDE. The design procedures, input files and output will be

explained in detail. The basic layers, the material compositions, layer thicknesses, QW numbers are designed in GAIN. The initial structure for the layers, the material compositions and layer thicknesses are shown in Table 7.2.1.

Table 7.2.1 Initial Laser structure (2-QW InGaAsP) for the 1.55um InGaAsP/InP laser structure.

Layer	Composition	Thickness (um)
n-substrate	InP	1.00
n-cladding	InP	0.50
n-SCH	$\text{In}_{0.0.748}\text{Ga}_{0.252}\text{As}_{0.547}\text{P}_{0.453}$	0.1
QW-1	$\text{In}_{0.49}\text{Ga}_{0.51}\text{As}_{0.939}\text{P}_{0.061}$	0.01
Barrier	$\text{In}_{0.0.748}\text{Ga}_{0.252}\text{As}_{0.547}\text{P}_{0.453}$	0.01
QW-2	$\text{In}_{0.49}\text{Ga}_{0.51}\text{As}_{0.939}\text{P}_{0.061}$	0.01
p-SCH	$\text{In}_{0.0.748}\text{Ga}_{0.252}\text{As}_{0.547}\text{P}_{0.453}$	0.1
p-spacer	InP	0.05
Etch stop layer	$\text{In}_{0.0.748}\text{Ga}_{0.252}\text{As}_{0.547}\text{P}_{0.453}$	0.01
p-cladding	InP	2.00
P cap	InP	1.00

7.2.2 The Initial Input File

The initial input file is based on the Table 7.2.1. The parameters for QW and barrier layers are fixed. The other layer thicknesses will be determined for the optimized laser operation. The initial input file is as follows:

```

CASE      KASE=WIFE
CASE      EPS1=1E-8  EPS2=1E-8  GAMEPS=1E-6
CASE      QZMR=13.223  QZMI=0.0  !QZMR=13.223

```

Chapter 7 InGaAsP/InGaAsP/InP Laser

```
CASE      PRINTF=0    INITGS=0    AUTOQW=0    NFPLT=1      FFPLT=1
!CASE     DXIN=0.2    QZMR=10.932
!CASE     IL=100     KGSS=1

MODCON    KPOL=1     APB1=0.25   APB2=0.25

STRUCT    WV=1.55

LAYER     NREAL=3.165  NLOSS=0.0012  TL=1.00    !N-sub, InP (layer 1)
LAYER     NREAL=3.165  NLOSS=0.00    TL=0.5     !n-cladding InP (layer 2)
LAYER     NREAL=3.370  NLOSS=0.0     TL=0.1     !n-SCH (layer 3)
LAYER     NREAL=3.6363 NLOSS=0.00    TL=0.01    !QW, InGaAsP (layer 4)
LAYER     NREAL=3.370  NLOSS=0.00    TL=0.01    !barrier InGaAsP (layer 5)
LAYER     NREAL=3.6363 NLOSS=0.00    TL=0.01    !QW, InGaAsP (layer 6)
LAYER     NREAL=3.370  NLOSS=0.0     TL=0.1     !p-SCH (layer 7)
LAYER     NREAL=3.165  NLOSS=0.0     TL=0.05    !p-Spacer (layer 8)
LAYER     NREAL=3.370  NLOSS=0.0     TL=0.01    !Etch stop layer (layer 9)
LAYER     NREAL=3.165  NLOSS=0.00    TL=2       !p-cladding InP (layer 10)
LAYER     NREAL=3.165  NLOSS=0.0012  TL=1.00    !p+cap, InP (layer 11)
!LAYER    NREAL=3.066696 NLOSS=0.00    TL=0.5     !p+cap, In0.53Ga0.47As

OUTPUT    PHMO=1     GAMMAO=1     WZRO=1     WZIO=1     QZRO=1     QZIO=0
OUTPUT    FWHPNO=1   FWHPFO=1    KMO=1     ITO=1
OUTPUT    MODOUT=1   LYROUT=1    SPLTFL=0
GAMOUT    LAYGAM=4   COMPGAM=0   GAMALL=0

!LOOPX1   ILX='TL'  FINV=0.00  XINC=-0.001  LAYCH=2
!LOOPX1   ILX='TL'  FINV=0.00  XINC=-0.001  LAYCH=10
!LOOPX1   ILX='TL'  FINV=0.50  XINC=0.001   LAYCH=3
!LOOPX1   ILX='TL'  FINV=0.50  XINC=0.001   LAYCH=7
LOOPZ1    ILZ='QZMR'  FINV=10.05  ZINC=-0.005  ! This loops to find
initial guess

END
```

7.2.3. Searching the Fundamental Mode, Looping for QZMR

Now first to search for TE₀ mode by Looping for QZMR from $N_{\max}^2 = 3.6363^2 = 13.22267769$ to $N_{\min}^2 = 3.165^2 = 10.017225$.

Use the same criterion as already introduced in previous section, we loop the QZMR and find: QZMR = 10.288 gives KM=6 and IT=2. So change QZMR to 10.288 and close looping.

The far field (real part and intensity) and near field (real part and intensity) plots are:

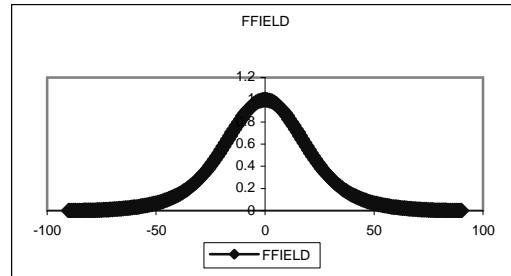
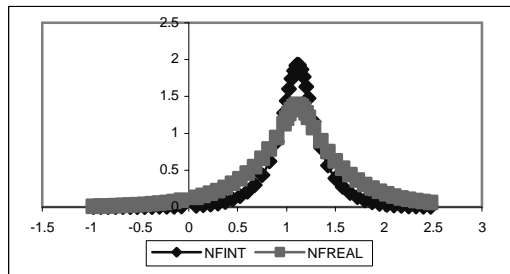


Figure 7.2.1. Fundamental mode near field plot for initial waveguide parameters. **Figure 7.2.2. Fundamental mode far field plot for initial waveguide parameters.**

The output parameters are calculated and listed below:

```
PHM           = 2.712949E-01
GAMMA(4)     = 1.733469E-02
WZR          = 3.207423E+00
WZI          = 1.235363E-05
KM           = 6
IT           = 2
```

The layer structure is:

```
# of layers =          11
LAYER01  NLOSS= 0.00120    NREAL= 3.16500    TL= 1.00000
LAYER02  NLOSS= 0.00000    NREAL= 3.16500    TL= 0.50000
LAYER03  NLOSS= 0.00000    NREAL= 3.37000    TL= 0.10000
LAYER04  NLOSS= 0.00000    NREAL= 3.63630    TL= 0.01000
LAYER05  NLOSS= 0.00000    NREAL= 3.37000    TL= 0.01000
```

Chapter 7 InGaAsP/InGaAsP/InP Laser

LAYER06	NLOSS= 0.00000	NREAL= 3.63630	TL= 0.01000
LAYER07	NLOSS= 0.00000	NREAL= 3.37000	TL= 0.10000
LAYER08	NLOSS= 0.00000	NREAL= 3.16500	TL= 0.05000
LAYER09	NLOSS= 0.00000	NREAL= 3.37000	TL= 0.01000
LAYER10	NLOSS= 0.00000	NREAL= 3.16500	TL= 2.00000
LAYER11	NLOSS= 0.00120	NREAL= 3.16500	TL= 0.00000

7.2.4. Looping the SCH layers to find the proper thickness for fundamental mode confinement.

We Loop both the n-SCH and p-SCH layers from 0.1um to 0 um to find the proper thickness to get max confinement in-QW. Note that we check for QW confinement and full-width at half-maximum power for far field (FWHPF) and make a proper choice. We cannot get high confinement and low FWHPF at the same time so it is a compromise. Generally the values are chosen according to design specifications.

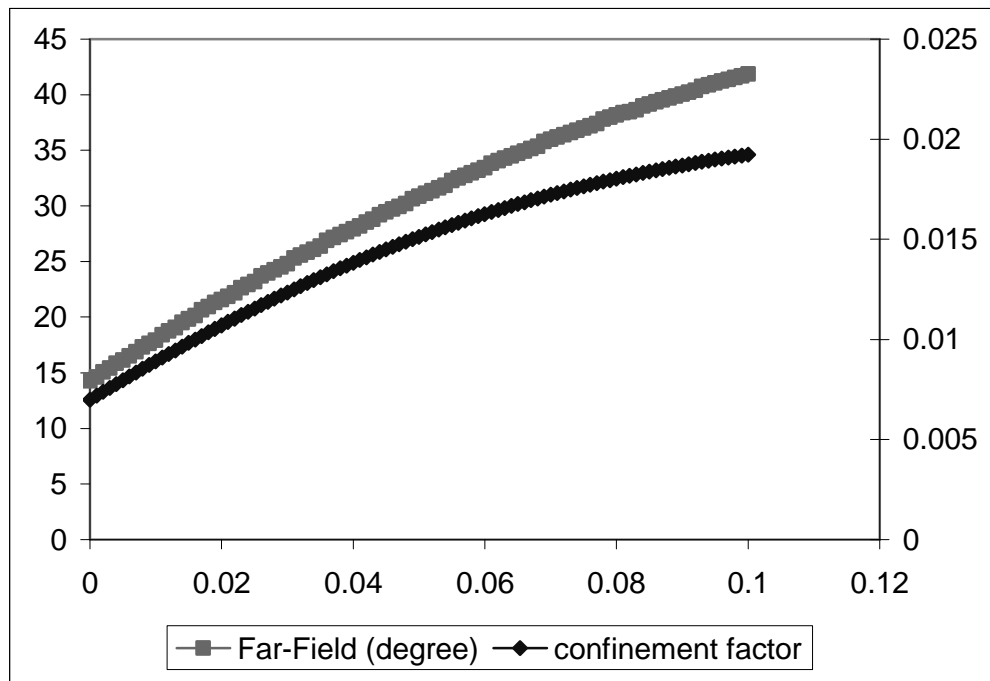


Figure 7.2.3. QW confinement factor and FWHPF vs. SCH thickness.

So From the figure 7.2.3, we can choose the proper thickness of the SCH layer as 0.09 um to keep high confinement factor and also keep the far field in an acceptable range.

The .db out file as below:

7.2 InGaAsP/InGaAsP/InP (1550nm)

TL(3)	TL(7)	PHM	GAMMA(4)	WZR	WZI	QZR	FWHPN	FWHPF	KM	IT
1.000000E-01	1.000000E-01	3.239530E-01	1.922807E-02	3.222069E+00	7.325493E-06	1.038173E+01	4.067586E-01	4.185234E+01	6	6
9.900000E-02	9.900000E-02	3.219795E-01	1.918006E-02	3.221477E+00	7.471165E-06	1.037792E+01	4.080715E-01	4.169669E+01	6	3
.										
.										
.										
9.000000E-02	9.000000E-02	3.037583E-01	1.869350E-02	3.216117E+00	8.948819E-06	1.034341E+01	4.109323E-01	4.004294E+01	6	3
.										
.										
.										
4.000000E-03	4.000000E-03	9.066865E-02	7.774586E-03	3.171312E+00	6.703739E-05	1.005722E+01	9.082471E-01	1.587498E+01	6	3
3.000000E-03	3.000000E-03	8.796983E-02	7.580945E-03	3.170992E+00	6.895929E-05	1.005519E+01	9.310005E-01	1.542500E+01	6	3
2.000000E-03	2.000000E-03	8.528067E-02	7.386240E-03	3.170680E+00	7.095729E-05	1.005321E+01	9.567164E-01	1.508054E+01	6	3
1.000000E-03	1.000000E-03	8.260290E-02	7.190504E-03	3.170375E+00	7.303616E-05	1.005128E+01	9.807017E-01	1.463627E+01	6	3
7.632783E-17	7.632783E-17	7.993848E-02	6.993770E-03	3.170078E+00	7.520100E-05	1.004939E+01	1.005827E+00	1.428214E+01	6	2

the output parameters are calculated and listed below:

PHM = 3.037583E-01
 GAMMA(4) = 1.869350E-02
 WZR = 3.216117E+00
 WZI = 8.948819E-06
 FWHPF = 4.004294E+01
 KM = 6
 IT = 3

The layer structure is:

of layers = 11

LAYER	NLOSS	NREAL	TL
LAYER01	0.00120	3.16500	1.00000
LAYER02	0.00000	3.16500	0.50000
LAYER03	0.00000	3.37000	0.09000
LAYER04	0.00000	3.63630	0.01000
LAYER05	0.00000	3.37000	0.01000
LAYER06	0.00000	3.63630	0.01000
LAYER07	0.00000	3.37000	0.09000
LAYER08	0.00000	3.16500	0.10000
LAYER09	0.00000	3.37000	0.01000
LAYER10	0.00000	3.16500	2.00000
LAYER11	0.00120	3.16500	0.00000

The far field (real part and intensity) and near field (real part and intensity) plots are:

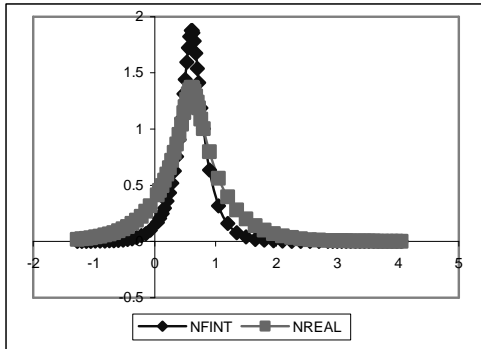


Figure 7.2.4. Fundamental mode near field plot with 0.16um SCH.

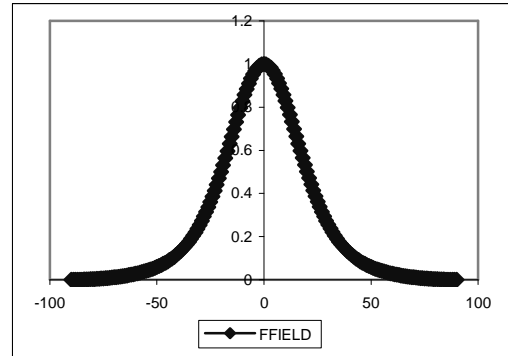


Figure 7.2.5. Fundamental mode far field plot with 0.16um SCH.

7.2.5. Making the Full Structure and Including Loss parameters

From the previous steps, the QZMR and the thickness of the SCH layer are decided, now we need to make the full structure and include the loss layers. Since we add the etch stop layer in the p-cladding layer and the original p-cladding layer is divided into first p-cladding (p-spacer) layer and second p-cladding layer. First we need to re-find the QZMR at the giving start thickness of the p-spacer and second p-cladding, then loop this two layers to find the proper thickness at the QZMR value. The input file for this structure is show in the text box as follows:

```

CASE      KASE=WIFE
CASE      EPS1=1E-8  EPS2=1E-8  GAMEPS=1E-6
CASE      QZMR=16    QZMI=0.0
CASE      PRINTF=0   INITGS=0   AUTOQW=0  NFPLT=1    FFPLT=1
!CASE     DXIN=0.2  QZMR=10.932
!CASE     IL=100   KGSS=1

MODCON    KPOL=1    APB1=0.25   APB2=0.25

STRUCT    WVL=1.55

LAYER     NREAL=3.165  NLOSS=0.00012  TL=1.00  !N-sub, InP
LAYER     NREAL=3.165  NLOSS=0.00    TL=0.5   !n-cladding InP

```

7.2 InGaAsP/InGaAsP/InP (1550nm)

```

LAYER  NREAL=3.370  NLOSS=0.0  TL=0.09  !n-SCH
LAYER  NREAL=3.6363 NLOSS=0.00 TL=0.01  !QW, InGaAsP
LAYER  NREAL=3.370  NLOSS=0.00 TL=0.01  !barrier InGaAsP
LAYER  NREAL=3.6363 NLOSS=0.00 TL=0.01  !QW, InGaAsP
LAYER  NREAL=3.370  NLOSS=0.0  TL=0.09  !p-SCH
LAYER  NREAL=3.165  NLOSS=0.0  TL=0.00  !p-Spacer
LAYER  NREAL=3.370  NLOSS=0.0  TL=0.01  !Etch stop layer
LAYER  NREAL=3.165  NLOSS=0.00 TL=1.00  !p-cladding InP
LAYER  NREAL=3.165  NLOSS=0.0012 TL=1.00  !p+cap, InP
LAYER  NREAL=3.7      NLOSS=18.2415 TL=0.05  !Ti
LAYER  NREAL=4.64     NLOSS=26.6731 TL=0.12  !Pt
LAYER  NREAL=0.18     NLOSS=41.3474 TL=0.20  !Au

OUTPUT PHMO=1  GAMMAO=1  WZRO=1  WZIO=1  QZRO=1  QZIO=0
OUTPUT FWHPNO=1  FWHPFO=1  KMO=1  ITO=1
OUTPUT MODOUT=1  LYROUT=1  SPLTFL=0
GAMOUT LAYGAM=4  COMPGAM=0  GAMALL=0

!LOOPX1  ILX='TL'  FINV=0.00  XINC=-0.001  LAYCH=2
!LOOPX1  ILX='TL'  FINV=0.00  XINC=-0.001  LAYCH=10
!LOOPX1  ILX='TL'  FINV=0.00  XINC=-0.001  LAYCH=8
!LOOPX1  ILX='TL'  FINV=0.00  XINC=-0.001  LAYCH=9
!LOOPX1  ILX='TL'  FINV=0.0  XINC=-0.001  LAYCH=3
!LOOPX1  ILX='TL'  FINV=0.0  XINC=-0.001  LAYCH=7
LOOPZ1  ILZ='QZMR'  FINV=10.05  ZINC=-0.005
END

```

Same as section 7.2.3, we loop the QZMR and find:

QZMR = 10.35 gives KM=6 and IT=2.

So change QZMR to 10.35 and close looping QZMR .

The far field (real part and intensity) and near field (real part and intensity) plots are as follows:

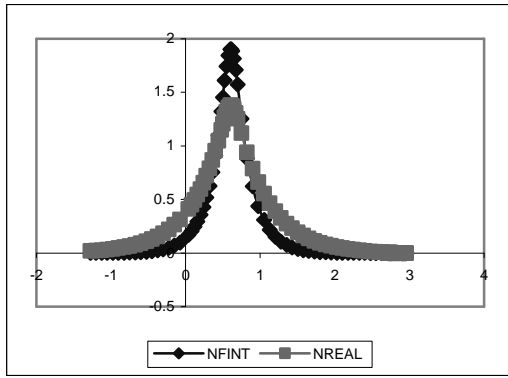


Figure 7.2.6. Fundamental mode near field plot for full structure.

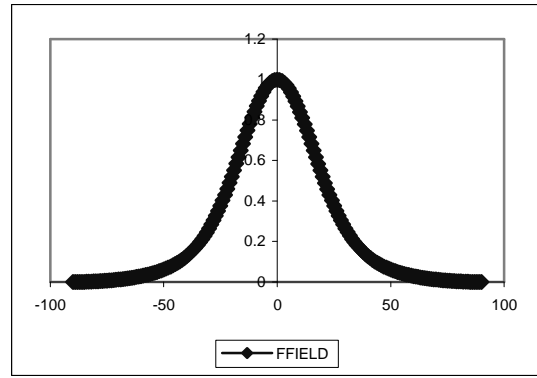


Figure 7.2.7. Fundamental mode far field plot for full structure.

We have to increase the p-cladding thickness so that the modal loss drops falls into acceptable limits. Looping the second p-clad thickness from 1.0 μm to 0.0 μm , we obtain the modal intensity loss as function of the p-cladding thickness as following figure:

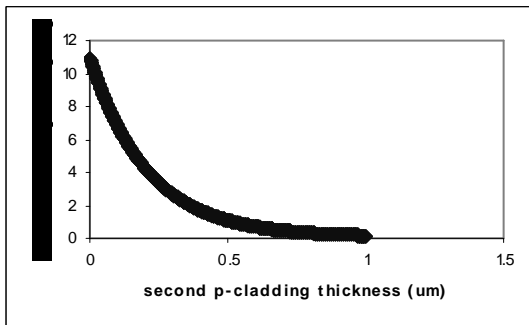


Figure 7.2.8. Modal intensity loss vs. p-clad thickness.

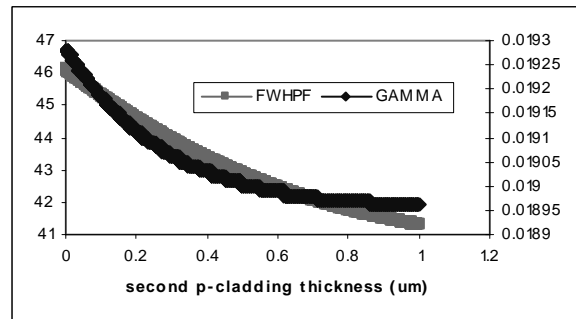


Figure 7.2.9. QW confinement factor and FWHPF vs. p-clad thickness.

Based on the plots shown in Figures 7.2.8 and 7.2.9, we can choose the thickness value of 1 μm for the second p-cladding since the loss curve drops to minimum and higher thickness will cause lower confinement factor. The intensity modal loss is calculated from WZI values (amplitude loss in μm^{-1}) as the formula:

$$\alpha = WZI \cdot (4\pi/\lambda) \cdot 10^4 \text{ /cm}$$

Since we choose the second p-cladding thickness as 1 μm , we need to re-find the QZMR according to the new second-p cladding thickness as previous section. QZMR can be set at 10.35. Then we can start to find the proper p-spacer thickness: Loop the p-spacer thickness from 0 to 1 μm to check the modal loss and confinement factor.

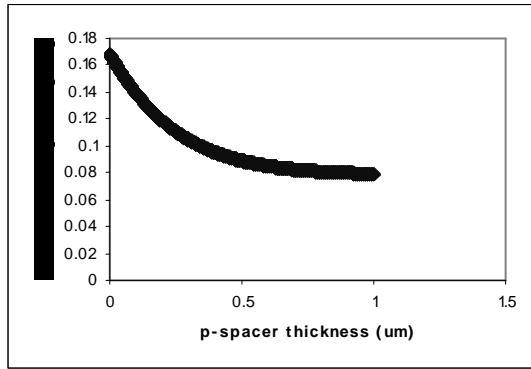


Figure 7.2.10. Modal intensity loss vs. p-spacer thickness.

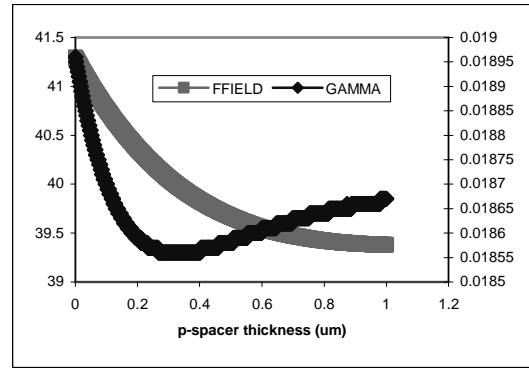


Figure 7.2.11. QW confinement factor and FWHPF vs. p-spacer thickness.

Based on the plots shown in Figures 7.2.10 and 7.2.11, we can choose the thickness value of 1 μm for the p-spacer layer since the loss curve drops to minimum the confinement factor can also get high value at this point. The design will stop here!

7.2.6. Output Parameters and Plots

From the previous design to optimize the laser structure, we can get the final output values as listed below:

```

PHM           = 1.178654E+00
GAMMA( 8 )   = 1.866676E-02
WZR          = 3.214231E+00
WZI          = 9.756738E-07
FWHHPF      = 3.937932E+01
KM           = 6
IT           = 4

```

The layer structure is:

```

# of layers =          14
LAYER01  NLOSS= 0.00012   NREAL= 3.16500   TL= 1.00000
LAYER02  NLOSS= 0.00000   NREAL= 3.16500   TL= 0.50000
LAYER03  NLOSS= 0.00000   NREAL= 3.37000   TL= 0.09000
LAYER04  NLOSS= 0.00000   NREAL= 3.63630   TL= 0.01000
LAYER05  NLOSS= 0.00000   NREAL= 3.37000   TL= 0.01000
LAYER06  NLOSS= 0.00000   NREAL= 3.63630   TL= 0.01000
LAYER07  NLOSS= 0.00000   NREAL= 3.37000   TL= 0.09000
LAYER08  NLOSS= 0.00000   NREAL= 3.16500   TL= 1.00000
LAYER09  NLOSS= 0.00000   NREAL= 3.37000   TL= 0.01000

```

Chapter 7 InGaAsP/InGaAsP/InP Laser

LAYER10	NLOSS= 0.00000	NREAL= 3.16500	TL= 1.00000
LAYER11	NLOSS= 0.00120	NREAL= 3.16500	TL= 1.00000
LAYER12	NLOSS=18.24150	NREAL= 3.70000	TL= 0.05000
LAYER13	NLOSS=26.67310	NREAL= 4.64000	TL= 0.12000
LAYER14	NLOSS=41.34740	NREAL= 0.18000	TL= 0.00000

Near field and far field plots are shown as following for the final structure:

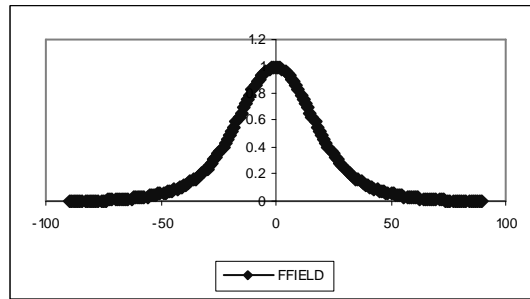
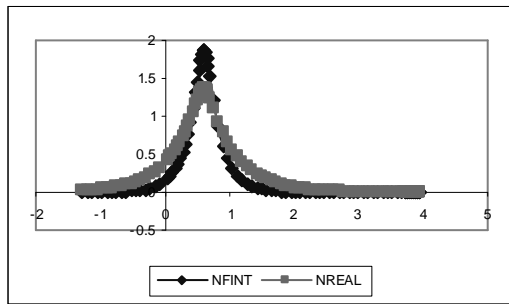


Figure 7.2.12. Fundamental mode near field plot for final structure.

Figure 7.2.13. Fundamental mode far field plot for final structure.

The Final laser structure for this 1.55 μm InGaAsP laser design can be found in the table 7.2.2 as follows:

Table 7.2.2 Final Laser structure (2-QW InGaAsP) for the 1.55 μm InGaAsP/InP laser structure.

Layer	Composition	Thickness (μm)
n-substrate	InP	1.00

7.2 InGaAsP/InGaAsP/InP (1550nm)

n-cladding	InP	0.50
n-SCH	In _{0.0.748} Ga _{0.252} As _{0.547} P _{0.453}	0.09
QW-1	In _{0.49} Ga _{0.51} As _{0.939} P _{0.061}	0.01
barrier	In _{0.0.748} Ga _{0.252} As _{0.547} P _{0.453}	0.01
QW-2	In _{0.49} Ga _{0.51} As _{0.939} P _{0.061}	0.01
p-SCH	In _{0.0.748} Ga _{0.252} As _{0.547} P _{0.453}	0.09
p-spacer	InP	1.00
Etch stop layer	In _{0.0.748} Ga _{0.252} As _{0.547} P _{0.453}	0.01
p-cladding	InP	1.00
P cap	InP	1.00

The final input file for WAVEGUIDE is also shown as follows:

```

CASE      KASE=WIFE
CASE      EPS1=1E-8  EPS2=1E-8  GAMEPS=1E-6
CASE      QZMR=10.35  QZMI=0.0
CASE      PRINTF=0   INITGS=0   AUTOQW=0  NFPLT=1   FFPLT=1
!CASE     DXIN=0.2  QZMR=10.932
!CASE     IL=100   KGSS=1

MODCON    KPOL=1    APB1=0.25   APB2=0.25

STRUCT    WVL=1.55

LAYER     NREAL=3.165  NLOSS=0.00012  TL=1.00   !N-sub, InP
LAYER     NREAL=3.165  NLOSS=0.00     TL=0.5    !n-cladding InP
LAYER     NREAL=3.370  NLOSS=0.0      TL=0.09   !n-SCH
LAYER     NREAL=3.6363 NLOSS=0.00     TL=0.01   !QW, InGaAsP
LAYER     NREAL=3.370  NLOSS=0.00     TL=0.01   !barrier InGaAsP

```

Chapter 7 InGaAsP/InGaAsP/InP Laser

```
LAYER  NREAL=3.6363  NLOSS=0.00  TL=0.01  !QW, InGaAsP
LAYER  NREAL=3.370   NLOSS=0.0   TL=0.09  !p-SCH
LAYER  NREAL=3.165   NLOSS=0.0   TL=1.00  !p-Spacer
LAYER  NREAL=3.370   NLOSS=0.0   TL=0.01  !Etch stop layer
LAYER  NREAL=3.165   NLOSS=0.00  TL=1.00  !p-cladding InP
LAYER  NREAL=3.165   NLOSS=0.0012  TL=1.00  !p+cap, InP
LAYER  NREAL=3.7      NLOSS=18.2415  TL=0.05  !Ti
LAYER  NREAL=4.64     NLOSS=26.6731  TL=0.12  !Pt
LAYER  NREAL=0.18     NLOSS=41.3474  TL=0.20  !Au
```

```
OUTPUT  PHMO=1  GAMMAO=1  WZRO=1  WZIO=1  QZRO=1  QZIO=0
OUTPUT  FWHPNO=1  FWHPFO=1  KMO=1  ITO=1
OUTPUT  MODOUT=1  LYROUT=1  SPLTFL=0
GAMOUT  LAYGAM=4  COMPGAM=0  GAMALL=0
```

```
!LOOPX1  ILX='TL'  FINV=0.00  XINC=-0.001  LAYCH=2
!LOOPX1  ILX='TL'  FINV=0.00  XINC=-0.001  LAYCH=10
!LOOPX1  ILX='TL'  FINV=1.00  XINC=0.001  LAYCH=8
!LOOPX1  ILX='TL'  FINV=0.00  XINC=-0.001  LAYCH=9
!LOOPX1  ILX='TL'  FINV=0.0  XINC=-0.001  LAYCH=3
!LOOPX1  ILX='TL'  FINV=0.0  XINC=-0.001  LAYCH=7
!LOOPZ1  ILZ='QZMR'  FINV=10.05  ZINC=-0.005
END
```

7.2.7. The Refractive Index Profile

According to the final structure, we can plot the refractive index profile according to the distance of the layers for the laser structure as following:

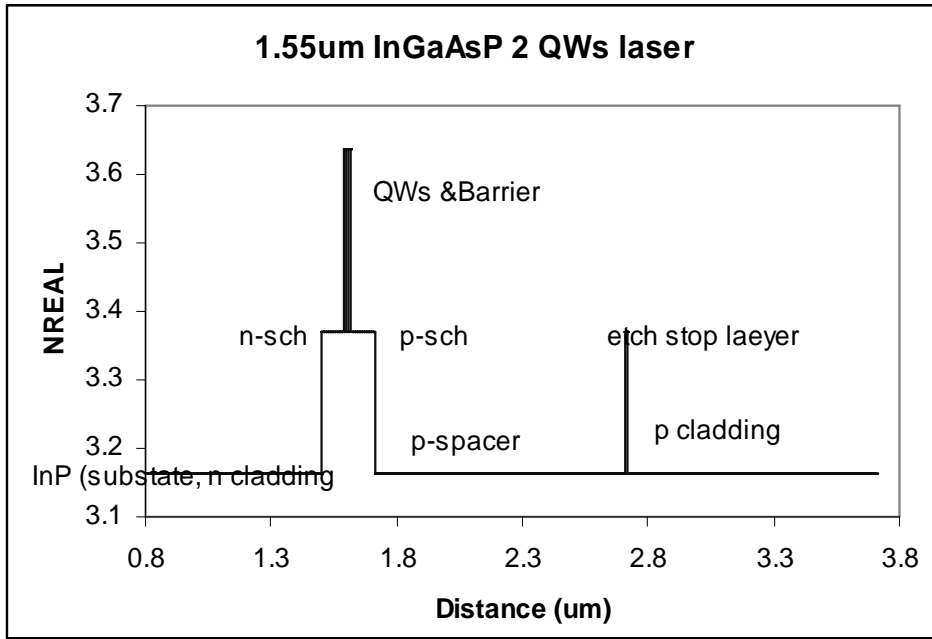


Figure 7.2.14 The laser structure of a 1.55 um InGaAsP 2-QW Laser.

Chapter 8 AlInGaAs / InP Lasers

Compared with the InGaAsP/InP system, which is introduced in Chapter 7, the AlInGaAs/InP system has some superior features, such as single element III, larger conduction band offset, and higher Schottky barriers. This material system is better for the device applications which requires high temperature operation. It has also been shown that this system is a good challenger to InGaAsP for optoelectronic applications. Integration with microelectronic devices might make it even more attractive. It might turn out to be the best candidate for future OEICs.

This chapter includes two examples of using the AlInGaAs/InP material system. Section 8.1 introduces a 1550-nm laser structure design with TM mode, and Section 8.2 introduces a 1310-nm laser structure design with TE mode. **TE mode** is the transverse electric mode whose electric field vector is normal to the direction of propagation, while **TM mode** is the transverse magnetic mode whose magnetic field vector is normal to the direction of propagation.

8.1 TM-mode 1550-nm Semiconductor Laser Design

8.1.1 Introduction

TM polarization in semiconductor lasers can be achieved by having tensile strain in quantum wells. The active layers of the TM-mode laser operating at a wavelength of 1550 nm was designed earlier by SMU Photonics group [1, *Material System # 9 in Gain program*] using the GAIN program [2]. The input parameters to the GAIN program for this design are shown in Table 8.1.1 [1, *Table C.9.1*].

Table 8.1.1 Active Waveguide Layers (QWs, barrier and inner clads) for the Laser

Layer	λ (μm)	Strain	Thickness (\AA)
QW ($\text{In}_x\text{Ga}_{1-x}\text{As}$)	1.51	5.1231E-003	150
SCH ($\text{Al}_x\text{Ga}_y\text{In}_{1-x-y}\text{As}$)	1.28	-	1500
Cladding ($\text{Al}_x\text{Ga}_y\text{In}_{1-x-y}\text{As}$)	0.83	-	380

The theoretical study for this laser, the energy levels, L-I curve of the laser, optical gain- λ curve of the laser, and mode gain as a function of current density (J) can be found in details in [1]. Below is the final structure for the active layers, and the material compositions and layer thicknesses of the active layers are shown in Table 8.1.2.

Table 8.1.2 Active Layer Composition and Thickness Specification for the Laser.

Layer	Composition	Thickness (μm)
inner n-cladding	$\text{Al}_{0.48}\text{In}_{0.52}\text{As}$	0.0375
n-GRIN	$\text{Al}_{0.48}\text{In}_{0.52}\text{As} - \text{Al}_{0.1392}\text{Ga}_{0.3408}\text{In}_{0.52}\text{As}$	0.15
QW	$\text{Ga}_{0.55}\text{InAs}$	0.015
barrier	$\text{Al}_{0.1392}\text{Ga}_{0.3408}\text{InAs}$	0.01
QW	$\text{Ga}_{0.55}\text{InAs}$	0.015
p-GRIN	$\text{Al}_{0.1392}\text{Ga}_{0.3408}\text{In}_{0.52}\text{As} - \text{Al}_{0.48}\text{In}_{0.52}\text{As}$	0.15
inner p-cladding	$\text{Al}_{0.48}\text{In}_{0.52}\text{As}$	0.0375

8.1.2 The Initial Input File

The active layers are obtained from Table 8.1.2. The parameters for QW and barrier layers are fixed. The other layer thicknesses will be determined for the optimized laser operation. The initial input file is as follows:

Chapter 8 TM-mode 1550-nm semiconductor laser design

```

!DESCRIPTION: -0.51 Tensile 2-QW InGaAs/AlGaInAs/InP laser operating at 1.55 μm.
!Material System is the Mondry's refractive index modeling which is MATSYS=13.0.

!CASE Parameter Set
CASE KASE=WIFE
CASE EPS1=1E-9 EPS2=1E-9 GAMEPS=1E-3 QZMR=12.0 QZMI=0.001
CASE PRINTF=1 INITGS=0 AUTOQW=0 NFPLT=1 FFPLT=1 IL=30

!MODCON Parameter Set
MODCON KPOL=2 APB1=0.25 APB2=0.25

!STRUCT Parameter Set
STRUCT WV=1.55

!LAYER Parameter Set
!----- beginning of structure -----
!n-sub InP LAYS: 1
LAYER MATSYS=1.0 XPERC=0.0 YPERC=0.0 NLOSS=0.0 TL=0.0

!n-GRIN LAYS: 2-12
STRUCT GRW = 0.0 ! graded width (microns)
! effective index of first slice (implicit):
LAYER MATSYS=13.0 XPERC=0.48 YPERC=0.0 NLOSS=0.0
LAYER NSLC = 10 ! number of slices
! effective index of last slice (implicit):
LAYER MATSYS=13.0 XPERC=0.1392 YPERC=0.0 NLOSS=0.0

!Active region 1 Barrier and 2 QWs InGaAs/AlGaInAs LAYS: 13-15
LAYER MATSYS=9.0 XPERC=0.55 YPERC=0.0 NLOSS=0.0 TL=0.015
LAYER MATSYS=13.0 XPERC=0.1392 YPERC=0.3408 NLOSS=0.0 TL=0.01
LAYER MATSYS=9.0 XPERC=0.55 YPERC=0.0 NLOSS=0.0 TL=0.015

!p-GRIN LAYS: 16-26
STRUCT GRW = 0.0 ! graded width (microns)
! effective index of first slice(implicit)
LAYER MATSYS=13.0 XPERC=0.1392 YPERC=0.0 NLOSS=0.0
LAYER NSLC = 10 ! number of slices
! effective index of last slice (implicit)
LAYER MATSYS=13.0 XPERC=0.48 YPERC=0.0 NLOSS=0.0

!p-clad LAYS: 27
LAYER MATSYS=1.0 XPERC=0.0 YPERC=0.0 NLOSS=0.0 TL=0.0
!----- end of structure -----

!OUTPUT Parameter Set
OUTPUT PHMO=1 GAMMAO=1 WZRO=1 WZIO=1 QZRO=0 QZIO=0
OUTPUT FWHPNO=0 FWHPFO=1 KMO=1 ITO=1
OUTPUT SPLTF=0 MODOUT=0 LYROUT=0

!GAMOUT Parameter Set
GAMOUT LAYGAM=13 LAYGAM=15 COMPGAM=0 GAMALL=0

!LOOPX Parameter Set
!LOOPZ1 ILZ='QZMR' FINV=10.0 ZINC=-0.01
!LOOPZ1 ILZ='WVL' FINV=1.6 ZINC=0.001
!LOOPZ1 ILZ='GRW' FINV=0.0 ZINC=-0.01
!LOOPX1 ILX='TL' FINV=0.1 XINC=0.001 LAYCH=01

END

```

In the input file KPOL=2 is to set TM polarization (KPOL=1 corresponds to TE mode). The material system is InGaAs/AlGaInAs/AlGaInAs (substrate InP). WAVEGUIDE has two models for the material system Al(x)Ga(y)In(1-x-y)As, the Adachi's (Material System 2) and Mondry's models (Material System 13). In our calculations we preferred the Mondry's model since the calculated refractive indices look closer to the values in the literature. One should check both models, compare the results

to some measured (experimental) values and decide which to use. For detailed description of material systems in WAVEGUIDE, refer to Chapter 3.

Furthermore, the GRIN layers can be represented in a compact form as seen in the input file. Detailed explanations about the usage of GRIN can be found in Chapter 3. In the representation GRW is the total grin thickness, NSLC is the number of steps in the grin. One also should input the initial (first slice) and final (last slice) material compositions for the grin structure.

The refractive indices, the real and imaginary part loss terms, for the waveguide layers were initially calculated as follows. The number of layers is ten for both n-GRIN and p-GRIN sections, therefore there are 27 layers in the structure initially, which is shown below. The top layer is the n-substrate.

```
# of layers = 27
LAYER01 NLOSS= 0.00000    NREAL= 3.16492    TL= 0.00000
LAYER02 NLOSS= 0.00000    NREAL= 3.19969    TL= 0.00000
LAYER03 NLOSS= 0.00000    NREAL= 3.22246    TL= 0.00000
LAYER04 NLOSS= 0.00000    NREAL= 3.24523    TL= 0.00000
LAYER05 NLOSS= 0.00000    NREAL= 3.26800    TL= 0.00000
LAYER06 NLOSS= 0.00000    NREAL= 3.29077    TL= 0.00000
LAYER07 NLOSS= 0.00000    NREAL= 3.31354    TL= 0.00000
LAYER08 NLOSS= 0.00000    NREAL= 3.33631    TL= 0.00000
LAYER09 NLOSS= 0.00000    NREAL= 3.35907    TL= 0.00000
LAYER10 NLOSS= 0.00000    NREAL= 3.38184    TL= 0.00000
LAYER11 NLOSS= 0.00000    NREAL= 3.40461    TL= 0.00000
LAYER12 NLOSS= 0.00000    NREAL= 3.42738    TL= 0.00000
LAYER13 NLOSS= 0.00000    NREAL= 3.57493    TL= 0.01500
LAYER14 NLOSS= 0.00000    NREAL= 3.42738    TL= 0.01000
LAYER15 NLOSS= 0.00000    NREAL= 3.57493    TL= 0.01500
LAYER16 NLOSS= 0.00000    NREAL= 3.42738    TL= 0.00000
LAYER17 NLOSS= 0.00000    NREAL= 3.40461    TL= 0.00000
LAYER18 NLOSS= 0.00000    NREAL= 3.38184    TL= 0.00000
LAYER19 NLOSS= 0.00000    NREAL= 3.35907    TL= 0.00000
LAYER20 NLOSS= 0.00000    NREAL= 3.33631    TL= 0.00000
LAYER21 NLOSS= 0.00000    NREAL= 3.31354    TL= 0.00000
LAYER22 NLOSS= 0.00000    NREAL= 3.29077    TL= 0.00000
LAYER23 NLOSS= 0.00000    NREAL= 3.26800    TL= 0.00000
LAYER24 NLOSS= 0.00000    NREAL= 3.24523    TL= 0.00000
LAYER25 NLOSS= 0.00000    NREAL= 3.22246    TL= 0.00000
LAYER26 NLOSS= 0.00000    NREAL= 3.19969    TL= 0.00000
LAYER27 NLOSS= 0.00000    NREAL= 3.16492    TL= 0.00000
```

8.1.3 Searching the Fundamental Mode, Looping for QZMR

We started with GRIN thickness of 0.0 μm but we could start with a small value like 0.05 μm . We searched for TM_0 mode by looping for QZMR from $n_{\text{max}}^2 = (3.57493)^2 \approx 12.0$ to $n_{\text{min}}^2 = (3.16492)^2 \approx 10.0$, where n_{max} is the highest refractive index and is n_{min} the lowest refractive index in the structure.

Chapter 8 TM-mode 1550-nm semiconductor laser design

A criterion is to look for a value where PHM becomes < 1.0 . Here all the QZMR values looks OK, but this is not the usual case, that is PHM becomes < 1.0 for certain QZMR values. Generally PHM criterion works for symmetric lossless structures. Other criteria are IT and KM. IT is the iteration number to find the root and usually a number less than 10 is good. We normally look for even lower values. KM is a qualitative indication and mostly it must be 6 or 7 (7 indicates the best case for the solution). Another parameter that might be helpful is WZR. It is the real part of the effective index and any guided mode must have an effective index value which is between the refractive indices of the core and the cladding. Therefore, if there is a block of values for WZR, which is between the refractive indices of the core and the cladding, there is a great chance that the mode is located there. In order to make sure that we get the desired mode (usually fundamental mode), we should check the near field plots, especially the real part of it.

The looping results are calculated as follows:

QZMR	PHM	GAMMA(13)	GAMMA(15)	WZR	WZI	FWHPF	KM	IT
1.200000E+01	8.089334E-02	9.608850E-03	9.608850E-03	3.168996E+00	2.935066E-17	1.409274E+01	6	15
1.199000E+01	8.089334E-02	9.608850E-03	9.608850E-03	3.168996E+00	-1.849002E-17	1.409274E+01	6	15
1.198000E+01	8.089334E-02	9.608850E-03	9.608850E-03	3.168996E+00	-4.384558E-17	1.409274E+01	6	15
1.197000E+01	8.089334E-02	9.608848E-03	9.608848E-03	3.168996E+00	-1.780146E-11	1.409274E+01	6	15
...
1.008000E+01	8.089334E-02	9.608850E-03	9.608850E-03	3.168996E+00	3.340669E-12	1.409274E+01	6	4
1.007000E+01	8.089334E-02	9.608850E-03	9.608850E-03	3.168996E+00	1.274324E-13	1.409274E+01	6	4
1.006000E+01	8.089334E-02	9.608850E-03	9.608850E-03	3.168996E+00	7.214575E-16	1.409274E+01	6	4
1.005000E+01	8.089334E-02	9.608850E-03	9.608850E-03	3.168996E+00	2.574181E-12	1.409274E+01	6	3
1.004000E+01	8.089334E-02	9.608850E-03	9.608850E-03	3.168996E+00	-1.070434E-15	1.409274E+01	6	3
1.003000E+01	8.089334E-02	9.608850E-03	9.608850E-03	3.168996E+00	1.266772E-12	1.409274E+01	6	4
1.002000E+01	8.089334E-02	9.608852E-03	9.608852E-03	3.168996E+00	5.704662E-11	1.409275E+01	6	6
1.001000E+01	8.089334E-02	9.608850E-03	9.608850E-03	3.168996E+00	-1.134112E-15	1.409274E+01	6	7
1.000000E+01	8.089334E-02	9.608849E-03	9.608849E-03	3.168996E+00	4.161345E-11	1.409274E+01	6	6

QZMR=10.05 gives KM=6 and IT=3. Also the WZR values repeated over this range. Then we end the looping and set the QZMR value to 10.05. For this fixed value we run the program and obtain the output parameters db file, near field and far field plots. For the TM_0 mode, near field (real part and intensity) and far field plots are in Figures 8.1.1 and 8.1.2 below.

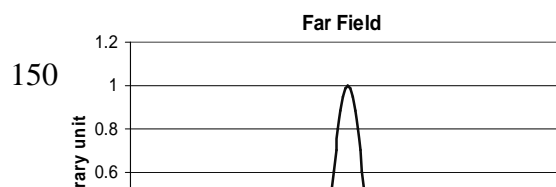
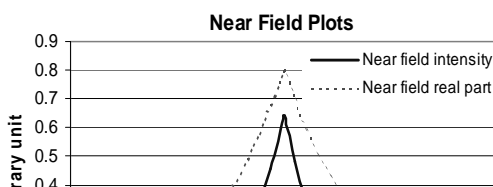


Figure 8.1.1 Fundamental mode near field plots for initial waveguide parameters. GRIN thickness=0.0 μm .

Figure 8.1.2 Fundamental mode far field plot for initial waveguide parameters. GRIN thickness=0.0 μm .

The calculated output parameters in the db file are listed below:

```

PHM                = 8.089334E-02
GAMMA(13)          = 9.608850E-03
GAMMA(15)          = 9.608850E-03
WZR                = 3.168996
WZI                = 2.538510E-12
FWHPF              = 1.409274E+01
KM                 = 6
IT                 = 3
    
```

8.1.4 Fundamental Mode Confinement and GRIN Looping

We loop for GRIN thickness (GRW) from 0.0 to 1.0 μm to get max confinement in QWs. Note that we check for QW confinement and full-width at half-maximum power for far field (FWHPF) and make a proper choice. We cannot get high confinement and low FWHPF at the same time so it is a compromise. Generally the values are chosen according to design specifications.

GRW1	PHM	GAMMA(13)	GAMMA(15)	WZR	WZI	FWHPF	KM	IT
0.000000E+00	8.089334E-02	9.608850E-03	9.608850E-03	3.168996E+00	2.538510E-12	1.409274E+01	6	3
1.000000E-02	1.047463E-01	1.160557E-02	1.160557E-02	3.170928E+00	-5.036174E-20	1.698126E+01	6	4
2.000000E-02	1.281249E-01	1.352827E-02	1.352827E-02	3.173196E+00	-1.879758E-14	1.981909E+01	6	3
2.400000E-01	4.090194E-01	3.116812E-02	3.116812E-02	3.253860E+00	1.180554E-14	5.288010E+01	6	2
2.500000E-01	4.140660E-01	3.119973E-02	3.119973E-02	3.257180E+00	2.472019E-15	5.298805E+01	6	2
2.600000E-01	4.181026E-01	3.121183E-02	3.121183E-02	3.260406E+00	-4.163405E-14	5.360970E+01	6	2
2.700000E-01	4.208223E-01	3.120034E-02	3.120034E-02	3.263540E+00	-1.905086E-14	5.393142E+01	6	2
2.800000E-01	4.211745E-01	3.116917E-02	3.116917E-02	3.266581E+00	-3.143539E-14	5.422922E+01	6	2
9.800000E-01	4.282952E-01	2.340898E-02	2.340898E-02	3.356311E+00	7.132523E-22	5.012366E+01	7	3
9.900000E-01	4.265284E-01	2.333671E-02	2.333671E-02	3.356817E+00	-8.471022E-22	4.999298E+01	7	3
1.000000E+00	4.243346E-01	2.326544E-02	2.326544E-02	3.357315E+00	-1.742098E-22	4.989145E+01	7	3

The plots for QW confinement factor and FWHPF vs. GRIN thickness are shown in Figure 8.1.3. In this case we picked up a value that gives the maximum confinement factor in QWs so GRIN thickness=0.26 μm . This value should be determined according to design specifications.

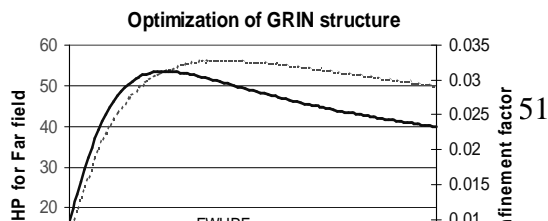


Figure 8.1.3 QW confinement factor and FWHPF vs. GRIN thickness.

Then we set QZMR to 10.63 and GRIN thickness to 0.26 μm . For this value the effective index for the fundamental mode is WZR=3.260406 and the output parameters in db file are as follows:

```

PHM      = 4.181026E-01
GAMMA(13) = 3.121183E-02
GAMMA(15) = 3.121183E-02
WZR      = 3.260406
WZI      = 2.862518E-11
FWHPF    = 5.360991E+01
KM       = 6
IT       = 1
    
```

The near field and far field plots for the GRIN thickness of 0.26 μm are shown in Figures 8.1.4 and 8.1.5, respectively.

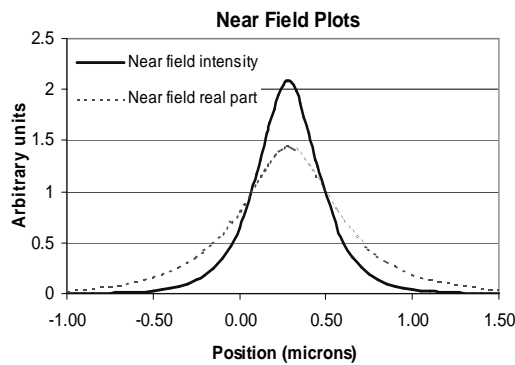


Figure 8.1.4 Fundamental mode near field plots for GRIN thickness=0.26 μm .

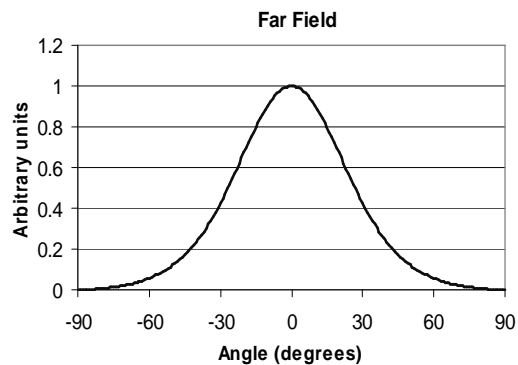


Figure 8.1.5 Fundamental mode far field plot for GRIN thickness=0.26 μm .

Now the layer parameters are calculated and listed below:

8.1 TM-mode 1550-nm Semiconductor Laser Design

```
# of layers = 27
LAYER01 NLOSS= 0.00000 NREAL= 3.16492 TL= 0.00000
LAYER02 NLOSS= 0.00000 NREAL= 3.19969 TL= 0.01300
LAYER03 NLOSS= 0.00000 NREAL= 3.22246 TL= 0.02600
LAYER04 NLOSS= 0.00000 NREAL= 3.24523 TL= 0.02600
LAYER05 NLOSS= 0.00000 NREAL= 3.26800 TL= 0.02600
LAYER06 NLOSS= 0.00000 NREAL= 3.29077 TL= 0.02600
LAYER07 NLOSS= 0.00000 NREAL= 3.31354 TL= 0.02600
LAYER08 NLOSS= 0.00000 NREAL= 3.33631 TL= 0.02600
LAYER09 NLOSS= 0.00000 NREAL= 3.35907 TL= 0.02600
LAYER10 NLOSS= 0.00000 NREAL= 3.38184 TL= 0.02600
LAYER11 NLOSS= 0.00000 NREAL= 3.40461 TL= 0.02600
LAYER12 NLOSS= 0.00000 NREAL= 3.42738 TL= 0.01300
LAYER13 NLOSS= 0.00000 NREAL= 3.57493 TL= 0.01500
LAYER14 NLOSS= 0.00000 NREAL= 3.42738 TL= 0.01000
LAYER15 NLOSS= 0.00000 NREAL= 3.57493 TL= 0.01500
LAYER16 NLOSS= 0.00000 NREAL= 3.42738 TL= 0.01300
LAYER17 NLOSS= 0.00000 NREAL= 3.40461 TL= 0.02600
LAYER18 NLOSS= 0.00000 NREAL= 3.38184 TL= 0.02600
LAYER19 NLOSS= 0.00000 NREAL= 3.35907 TL= 0.02600
LAYER20 NLOSS= 0.00000 NREAL= 3.33631 TL= 0.02600
LAYER21 NLOSS= 0.00000 NREAL= 3.31354 TL= 0.02600
LAYER22 NLOSS= 0.00000 NREAL= 3.29077 TL= 0.02600
LAYER23 NLOSS= 0.00000 NREAL= 3.26800 TL= 0.02600
LAYER24 NLOSS= 0.00000 NREAL= 3.24523 TL= 0.02600
LAYER25 NLOSS= 0.00000 NREAL= 3.22246 TL= 0.02600
LAYER26 NLOSS= 0.00000 NREAL= 3.19969 TL= 0.01300
LAYER27 NLOSS= 0.00000 NREAL= 3.16492 TL= 0.00000
```

8.1.5 Building the Full Structure with Loss Parameters

The full structure includes cladding, transition, inner cladding and GRIN layers on both n and p sides, as well as active layers in between. The doping concentration is higher for the outmost layers and decreases as it gets closer to active layers. Therefore, the absorption losses for the outer layers are higher compared to inner layers. The loss figures for the layers were obtained from the work done by Babic and others [3], [4] on the absorption loss in GaAs and InP at different wavelengths of interest. The loss values for different doping levels were calculated and the updated input file is shown below. Here only the loss values in GRIN structure were not taken into account for simplicity of the calculations. Since the doping level is low the effect will be low, yet the field confinement is relatively high. Therefore, one should take into account all these considerations.

```
!The optimized structure for laser at 1.55 um.
!Material System based, Mondry's refractive index modeling is used.
!DESCRIPTION: -0.51 Tensile 2-QW InGaAs/AlGaInAs/InP.

!CASE Parameter Set
CASE KASE=WIFE
CASE EPS1=1E-9 EPS2=1E-9 GAMEPS=1E-3 QZMR=10.63 QZMI=0.001
CASE PRINTF=1 INITGS=0 AUTOQW=0 NFPLT=1 FFPLT=1 IL=30

!MODCON Parameter Set
MODCON KPOL=2 APB1=0.25 APB2=0.25

!STRUCT Parameter Set
```

Chapter 8 TM-mode 1550-nm semiconductor laser design

```

STRUCT WVL=1.55

!LAYER Parameter Set
!----- beginning of structure -----
!n-sub / n-clad are InP LAYS: 1/2
LAYER MATSYS=1.0  XPERC=0.0  YPERC=0.0  NLOSS=0.00025  TL=0.0
LAYER MATSYS=1.0  XPERC=0.0  YPERC=0.0  NLOSS=0.00025  TL=2.0

!n-transition LAYS: 3-5
LAYER MATSYS=13.0 XPERC=0.4128 YPERC=0.0672      NLOSS=0.00075  TL=0.0025
LAYER MATSYS=13.0 XPERC=0.44592 YPERC=0.03408     NLOSS=0.00075  TL=0.005
LAYER MATSYS=13.0 XPERC=0.48    YPERC=0.0         NLOSS=0.00075  TL=0.0025

!inner n-clad LAYS: 6
LAYER MATSYS=13.0 XPERC=0.48    YPERC=0.0         NLOSS=0.000125 TL=0.0

!n-GRIN LAYS: 7-17 Optimized =0.26
STRUCT GRW = 0.26                ! graded width (microns)
! effective index of first slice(implicit)
LAYER MATSYS=13.0 XPERC=0.48    YPERC=0.0         NLOSS=0.0000125
LAYER NSLC = 10                  ! number of slices
! effective index of last slice (implicit)
LAYER MATSYS=13.0 XPERC=0.1392 YPERC=0.0         NLOSS=0.0000125

!Active region 1 Barrier and 2 QWs InGaAs/AlGaInAs LAYS: 18-20
LAYER MATSYS=9.0   XPERC=0.55    YPERC=0.0         NLOSS=0.0        TL=0.015
LAYER MATSYS=13.0 XPERC=0.1392 YPERC=0.3408     NLOSS=0.0        TL=0.01
LAYER MATSYS=9.0   XPERC=0.55    YPERC=0.0         NLOSS=0.0        TL=0.015

!p-GRIN LAYS: 21-31
STRUCT GRW = 0.26                ! graded width (microns)
! effective index of first slice(implicit)
LAYER MATSYS=13.0 XPERC=0.1392 YPERC=0.0         NLOSS=0.00005
LAYER NSLC = 10                  ! number of slices
! effective index of last slice (implicit)
LAYER MATSYS=13.0 XPERC=0.48    YPERC=0.0         NLOSS=0.00005

!inner p-clad LAYS: 32
LAYER MATSYS=13.0 XPERC=0.48    YPERC=0.0         NLOSS=0.0005    TL=0.0

!p-transition LAYS: 33-35
LAYER MATSYS=13.0 XPERC=0.48    YPERC=0.0         NLOSS=0.0005    TL=0.0025
LAYER MATSYS=13.0 XPERC=0.44592 YPERC=0.03408     NLOSS=0.0005    TL=0.005
LAYER MATSYS=13.0 XPERC=0.4128 YPERC=0.0672      NLOSS=0.0005    TL=0.0025

!p-clad LAYS: 36
LAYER MATSYS=1.0  XPERC=0.0  YPERC=0.0  NLOSS=0.00075  TL=2.0

!p-cap LAYS: 37
LAYER NREAL=3.52                NLOSS=0.0125    TL=0.2

!AIR on top LAYS: 38
LAYER AIR=1.0                    TL=0.0
!----- end of structure -----

!OUTPUT Parameter Set
OUTPUT PHMO=1 GAMMAO=1 WZRO=1 WZIO=1 QZRO=0 QZIO=0
OUTPUT FWHPNO=0 FWHPFO=1 KMO=1 ITO=1
OUTPUT SPLTFL=0 MODOUT=0 LYROUT=0

!GAMOUT Parameter Set
GAMOUT LAYGAM=18 LAYGAM=20 COMPGAM=0 GAMALL=0

!LOOPX Parameter Set
!LOOPZ1 ILZ='QZMR'  FINV=10.0    ZINC=-0.01
!LOOPZ1 ILZ='WVL'   FINV=1.6     ZINC=0.001
!LOOPZ1 ILZ='GRW'   FINV=1.0     ZINC=0.01
!LOOPX1 ILX='TL'    FINV=0.1     XINC=0.001  LAYCH=06
!LOOPX1 ILX='TL'    FINV=0.1     XINC=0.001  LAYCH=32
!LOOPX1 ILX='TL'    FINV=0.1     XINC=0.001  LAYCH=02
!LOOPX1 ILX='TL'    FINV=0.1     XINC=0.001  LAYCH=36

```

END

8.1.6 Inner Cladding Optimization to Minimize Loss

First, the fundamental mode (TM₀) was sought by looping for QZMR for the updated structure. The initial values for the n and p inner-clads=0.0 μm, and clads=2.0 μm. The looping results are depicted below.

QZMR	PHM	GAMMA(18)	GAMMA(20)	WZR	WZI	FWHPF	KM	IT
1.100000E+01	5.985674E+00	4.447605E-04	4.025810E-04	3.041720E+00	2.208746E-02	4.982005E+00	5	29
1.099000E+01	5.985674E+00	4.447605E-04	4.025810E-04	3.041720E+00	2.208746E-02	4.982005E+00	5	29
1.098000E+01	5.985674E+00	4.447605E-04	4.025810E-04	3.041720E+00	2.208746E-02	4.982005E+00	5	29
.								
1.065000E+01	7.595679E-01	3.113686E-02	3.113686E-02	3.261166E+00	3.083322E-05	4.982645E+01	6	4
1.064000E+01	7.595679E-01	3.113686E-02	3.113686E-02	3.261166E+00	3.083322E-05	4.982645E+01	7	4
1.063000E+01	7.595679E-01	3.113686E-02	3.113686E-02	3.261166E+00	3.083322E-05	4.982645E+01	7	4
1.062000E+01	7.595679E-01	3.113686E-02	3.113686E-02	3.261166E+00	3.083322E-05	4.982645E+01	6	4
1.061000E+01	7.595679E-01	3.113686E-02	3.113686E-02	3.261166E+00	3.083322E-05	4.982645E+01	7	5
.								
1.002000E+01	2.584146E+00	2.008284E-04	1.404630E-04	3.153059E+00	9.454015E-04	4.880579E+00	5	15
1.001000E+01	2.584146E+00	2.008284E-04	1.404630E-04	3.153059E+00	9.454015E-04	4.880579E+00	5	16
1.000000E+01	2.584146E+00	2.008284E-04	1.404630E-04	3.153059E+00	9.454015E-04	4.880579E+00	5	13

For QZMR=10.63, WZR makes sense and KM=7 and IT=4 look reasonable. To verify that this corresponds to TM₀ mode near field and far field plots should be checked. These plots are shown in Figures 8.1.6 and 8.1.7 and the output parameters in db file are listed below:

```

PHM           = 7.595679E-01
GAMMA(18)    = 3.113686E-02
GAMMA(20)    = 3.113686E-02
WZR          = 3.261166
WZI          = 3.083322E-05
FWHPF       = 4.982645E+01
KM           = 7
IT           = 4
    
```

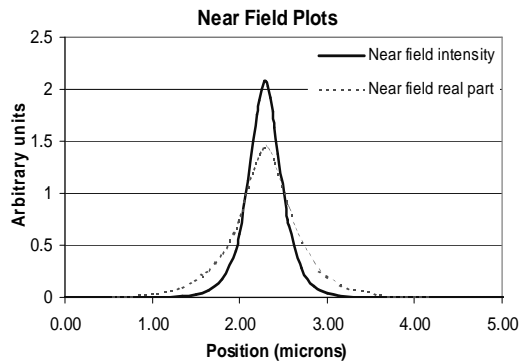


Figure 8.1.6 Fundamental mode near field plots for the updated structure including all the layers and loss figures.

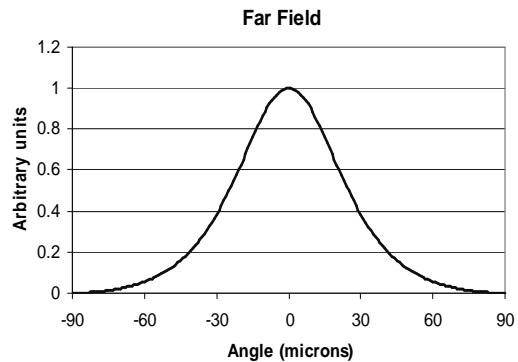


Figure 8.1.7 Fundamental mode far field plot for the updated structure including all the layers and loss figures.

We have to increase the inner-clad thickness so that the modal loss drops falls into acceptable limits. Looping for the inner-clad thickness from 0.0 μm to 1.0 μm, we obtain:

Chapter 8 TM-mode 1550-nm semiconductor laser design

TL (6)	TL (32)	PHM	GAMMA(18)	GAMMA(20)	WZR	WZI	FWHPF	KM	IT
0.000000E+00	0.000000E+00	7.595679E-01	3.113686E-02	3.113686E-02	3.261166E+00	3.083322E-05	4.982645E+01	7	4
1.000000E-03	1.000000E-03	7.593857E-01	3.113179E-02	3.113179E-02	3.261214E+00	3.076259E-05	4.983146E+01	7	3
2.000000E-03	2.000000E-03	7.592044E-01	3.112673E-02	3.112673E-02	3.261262E+00	3.069250E-05	4.983434E+01	7	3
4.980000E-01	4.980000E-01	7.235864E-01	2.933575E-02	2.933575E-02	3.268938E+00	2.201114E-05	4.815140E+01	7	2
4.990000E-01	4.990000E-01	7.235789E-01	2.933421E-02	2.933421E-02	3.268941E+00	2.201018E-05	4.814455E+01	7	2
5.000000E-01	5.000000E-01	7.235714E-01	2.933264E-02	2.933264E-02	3.268943E+00	2.200922E-05	4.813846E+01	7	2
5.010000E-01	5.010000E-01	7.235640E-01	2.933107E-02	2.933107E-02	3.268946E+00	2.200827E-05	4.813254E+01	7	2
5.020000E-01	5.020000E-01	7.235566E-01	2.932951E-02	2.932951E-02	3.268949E+00	2.200734E-05	4.812778E+01	7	2
9.980000E-01	9.980000E-01	7.225282E-01	2.896721E-02	2.896721E-02	3.269402E+00	2.198895E-05	4.582991E+01	7	2
9.990000E-01	9.990000E-01	7.225284E-01	2.896702E-02	2.896702E-02	3.269402E+00	2.198907E-05	4.582669E+01	7	2
1.000000E+00	1.000000E+00	7.225285E-01	2.896683E-02	2.896683E-02	3.269402E+00	2.198919E-05	4.582347E+01	7	2

Based on the plots shown in Figures 8.1.8 and 8.1.9, we pick up the thickness value of 0.5 μm for the inner-clads. In Figure 8.1.8, α is the intensity modal loss in cm^{-1} and it is calculated from WZI values (amplitude loss in μm^{-1}) as follows:

$$\alpha = WZI \cdot (4\pi/\lambda) \cdot 10^4 \text{ /cm} \quad (8.1)$$

Modal intensity loss vs. inner-clad thickness, and FWHPF and Gamma for QW vs. inner-clad thickness plots are shown below and as we see from Figure 8.1.8, for the inner-clad thickness of 0.5 μm and higher, the loss curve does not change considerably. Therefore, 0.5 μm is a good choice since for this value the loss is minimum and a higher value for inner cladding will result in the drop of QW confinement factor as seen from Figure 8.1.9.

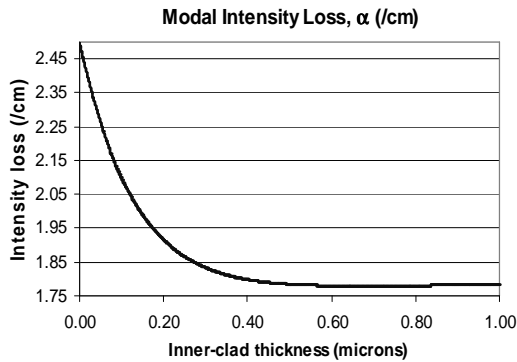


Figure 8.1.8 Modal intensity loss vs. inner-clad thickness.

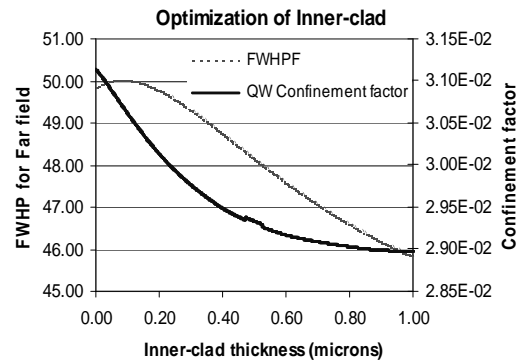


Figure 8.1.9 QW confinement factor and FWHPF vs. inner-clad thickness.

8.1.7 Cladding Optimization to Minimize Loss

The following is the calculated output parameters for inner-clad value of 0.5 μm in the output db file:

```

PHM      = 7.235714E-01
GAMMA(18) = 2.933264E-02
GAMMA(20) = 2.933264E-02
WZR      = 3.268943
WZI      = 2.200922E-05
FWHPF    = 4.813846E+01
    
```

8.1 TM-mode 1550-nm Semiconductor Laser Design

KM = 7
IT = 6

Next the p-clad thickness will be optimized to obtain the minimum desired loss. Current loss is calculated as $\alpha=1.78$ /cm, which corresponds to $WZI=2.200922E-05$.

TL (36)	PHM	GAMMA(18)	GAMMA(20)	WZR	WZI	FWHPF	KM	IT
2.000000E+00	7.235714E-01	2.933264E-02	2.933264E-02	3.268943E+00	2.200922E-05	4.813846E+01	7	6
1.990000E+00	7.235633E-01	2.929703E-02	2.929703E-02	3.268943E+00	2.200922E-05	4.813845E+01	7	2
1.980000E+00	7.235552E-01	2.929591E-02	2.929591E-02	3.268943E+00	2.200922E-05	4.813846E+01	7	2
1.020000E+00	7.227757E-01	2.932320E-02	2.932322E-02	3.268944E+00	2.202715E-05	4.822136E+01	7	2
1.010000E+00	7.227674E-01	2.929339E-02	2.929341E-02	3.268944E+00	2.202835E-05	4.822470E+01	7	2
1.000000E+00	7.227592E-01	2.929591E-02	2.929594E-02	3.268944E+00	2.202963E-05	4.822881E+01	7	2
9.900000E-01	7.227509E-01	2.929930E-02	2.929933E-02	3.268944E+00	2.203100E-05	4.823252E+01	7	2
9.800000E-01	7.227427E-01	2.929901E-02	2.929904E-02	3.268944E+00	2.203246E-05	4.823651E+01	7	2
2.000000E-02	7.206226E-01	2.912019E-02	2.913829E-02	3.269347E+00	3.383818E-05	5.102692E+01	6	2
1.000000E-02	7.205250E-01	2.912834E-02	2.914771E-02	3.269375E+00	3.464711E-05	5.111527E+01	6	2
1.641048E-15	7.204211E-01	2.911967E-02	2.914038E-02	3.269405E+00	3.551305E-05	5.120447E+01	6	2

Looping for p-cladding thickness from 0.0 μm to 2.0 μm , it looks that the optimum value is 1.0 μm considering QW confinement factor, FWHPF, and WZI plots shown in Figures 8.1.10 and 8.1.11 below:

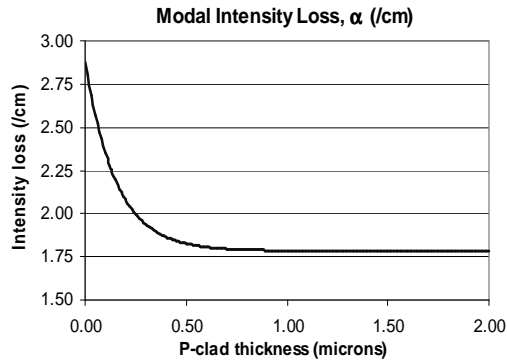


Figure 8.1.10 Modal intensity loss vs. p-clad thickness.

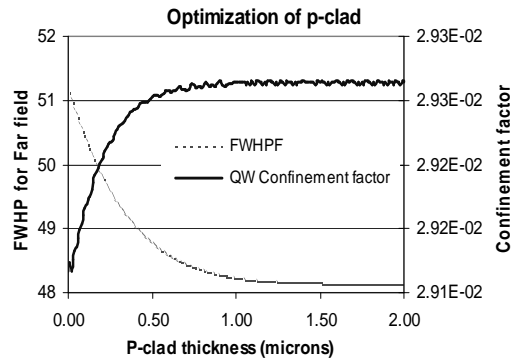


Figure 8.1.11 QW confinement factor and FWHPF vs. p-clad thickness.

8.1.8 Output Parameters and Plots

The optimized value for p-clad thickness is 1.0 μm and the modal loss is 1.78 /cm again. The output values are listed below:

PHM = 7.227592E-01
 GAMMA(18) = 2.929591E-02
 GAMMA(20) = 2.929594E-02
 WZR = 3.268944
 WZI = 2.202963E-05
 FWHPF = 4.822881E+01
 KM = 7
 IT = 6

Near field and far field plots are shown in Figures 8.1.12 and 8.1.13 for the final structure:

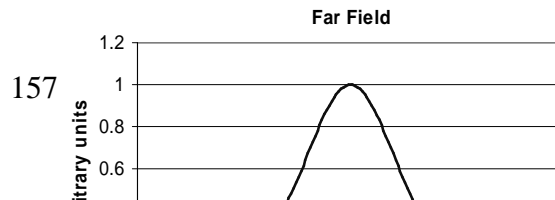
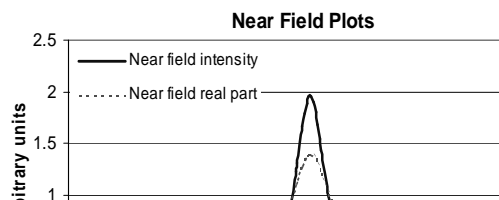


Figure 8.1.12 Fundamental mode near field plots for the final optimized structure. **Figure 8.1.13** Fundamental mode far field plot for the final optimized structure.

The layer parameters for the final structure are listed below:

# of layers = 38				
LAYER01	NLOSS=	0.00025	NREAL= 3.16492	TL= 0.00000
LAYER02	NLOSS=	0.00025	NREAL= 3.16492	TL= 2.00000
LAYER03	NLOSS=	0.00075	NREAL= 3.23470	TL= 0.00250
LAYER04	NLOSS=	0.00075	NREAL= 3.21713	TL= 0.00500
LAYER05	NLOSS=	0.00075	NREAL= 3.19969	TL= 0.00250
LAYER06	NLOSS=	0.00013	NREAL= 3.19969	TL= 0.50000
LAYER07	NLOSS=	0.00001	NREAL= 3.19969	TL= 0.01300
LAYER08	NLOSS=	0.00000	NREAL= 3.22246	TL= 0.02600
LAYER09	NLOSS=	0.00000	NREAL= 3.24523	TL= 0.02600
LAYER10	NLOSS=	0.00000	NREAL= 3.26800	TL= 0.02600
LAYER11	NLOSS=	0.00000	NREAL= 3.29077	TL= 0.02600
LAYER12	NLOSS=	0.00000	NREAL= 3.31354	TL= 0.02600
LAYER13	NLOSS=	0.00000	NREAL= 3.33631	TL= 0.02600
LAYER14	NLOSS=	0.00000	NREAL= 3.35907	TL= 0.02600
LAYER15	NLOSS=	0.00000	NREAL= 3.38184	TL= 0.02600
LAYER16	NLOSS=	0.00000	NREAL= 3.40461	TL= 0.02600
LAYER17	NLOSS=	0.00001	NREAL= 3.42738	TL= 0.01300
LAYER18	NLOSS=	0.00000	NREAL= 3.57493	TL= 0.01500
LAYER19	NLOSS=	0.00000	NREAL= 3.42738	TL= 0.01000
LAYER20	NLOSS=	0.00000	NREAL= 3.57493	TL= 0.01500
LAYER21	NLOSS=	0.00005	NREAL= 3.42738	TL= 0.01300
LAYER22	NLOSS=	0.00000	NREAL= 3.40461	TL= 0.02600
LAYER23	NLOSS=	0.00000	NREAL= 3.38184	TL= 0.02600
LAYER24	NLOSS=	0.00000	NREAL= 3.35907	TL= 0.02600
LAYER25	NLOSS=	0.00000	NREAL= 3.33631	TL= 0.02600
LAYER26	NLOSS=	0.00000	NREAL= 3.31354	TL= 0.02600
LAYER27	NLOSS=	0.00000	NREAL= 3.29077	TL= 0.02600
LAYER28	NLOSS=	0.00000	NREAL= 3.26800	TL= 0.02600
LAYER29	NLOSS=	0.00000	NREAL= 3.24523	TL= 0.02600
LAYER30	NLOSS=	0.00000	NREAL= 3.22246	TL= 0.02600
LAYER31	NLOSS=	0.00005	NREAL= 3.19969	TL= 0.01300
LAYER32	NLOSS=	0.00050	NREAL= 3.19969	TL= 0.50000
LAYER33	NLOSS=	0.00050	NREAL= 3.19969	TL= 0.00250
LAYER34	NLOSS=	0.00050	NREAL= 3.21713	TL= 0.00500
LAYER35	NLOSS=	0.00050	NREAL= 3.23470	TL= 0.00250
LAYER36	NLOSS=	0.00075	NREAL= 3.16492	TL= 1.00000
LAYER37	NLOSS=	0.01250	NREAL= 3.52000	TL= 0.20000
LAYER38	NLOSS=	0.00000	NREAL= 1.00000	TL= 0.00000

8.2 TE-mode 1310-nm Semiconductor Laser Design

8.2.1 Introduction

In this section the 1310-nm laser structure design will be introduced by using WAVEGUIDE. The design procedures, input files and output will be explained in detail.

TE polarization in semiconductor lasers can be achieved by having compressive strain in quantum wells. The TE-mode laser operating at a wavelength of 1310 nm was designed according to Sandra R. Selmic's paper [5]. The initial structure for the layers, the material compositions and layer thicknesses are shown in Table 8.2.1.

Table 8.2.1 Initial laser structure (5-QW AlInGaAs) for the 1.3- μm AlInGaAs/InP.

Layer	Composition	Thickness (μm)
n-substrate	InP	---
Inner n-cladding	$\text{Al}_{0.48}\text{In}_{0.52}\text{As}$	0.30
n-SCH	$\text{Al}_{0.267}\text{Ga}_{0.203}\text{In}_{0.53}\text{As}$	0.50
QW-1	$\text{Al}_{0.161}\text{Ga}_{0.102}\text{In}_{0.737}\text{As}$	0.005
barrier	$\text{Al}_{0.267}\text{Ga}_{0.203}\text{In}_{0.53}\text{As}$	0.010
QW-2	$\text{Al}_{0.161}\text{Ga}_{0.102}\text{In}_{0.737}\text{As}$	0.005
barrier	$\text{Al}_{0.267}\text{Ga}_{0.203}\text{In}_{0.53}\text{As}$	0.010
QW-3	$\text{Al}_{0.161}\text{Ga}_{0.102}\text{In}_{0.737}\text{As}$	0.005
barrier	$\text{Al}_{0.267}\text{Ga}_{0.203}\text{In}_{0.53}\text{As}$	0.010
QW-4	$\text{Al}_{0.161}\text{Ga}_{0.102}\text{In}_{0.737}\text{As}$	0.005
barrier	$\text{Al}_{0.267}\text{Ga}_{0.203}\text{In}_{0.53}\text{As}$	0.010
QW-5	$\text{Al}_{0.161}\text{Ga}_{0.102}\text{In}_{0.737}\text{As}$	0.005
n-SCH	$\text{Al}_{0.267}\text{Ga}_{0.203}\text{In}_{0.53}\text{As}$	0.50
Inner n-cladding	$\text{Al}_{0.48}\text{In}_{0.52}\text{As}$	0.30

8.2.2. The Initial Input File

The initial input file is based on the parameters shown in Table 8.2.1. The parameters for QW and barrier layers are kept fixed. The other layer thicknesses will be determined for the optimized laser operation. The initial input file is as follows:

```

CASE      KASE=mcqw-s-1
CASE      EPS1=1E-8  EPS2=1E-8  GAMEPS=1E-6
CASE      QZMR=12.145  QZMI=0.0
CASE      PRINTF=0    INITGS=0    AUTOQW=0  NFPLT=1    FFPLT=1
!CASE     DXIN=0.2  QZMR=10.932
!CASE     IL=100   KGSS=1

MODCON    KPOL=1    APB1=0.25    APB2=0.25

STRUCT    WVl=1.3

LAYER     NREAL=3.1987  NLOSS=0.00  TL=0.00    !N-sub, InP
LAYER     NREAL=3.2310  NLOSS=0.00  TL=0.30    !inner n-cladding AlInAs
LAYER     NREAL=3.3728  NLOSS=0.0   TL=0.50    !n-SCH,AlInGaAs
LAYER     NREAL=3.4850  NLOSS=0.00  TL=0.005   !QW, AlInGaAs
LAYER     NREAL=3.3728  NLOSS=0.00  TL=0.010   !barrier,AlInGaAs
LAYER     NREAL=3.4850  NLOSS=0.00  TL=0.005   !QW, AlInGaAs
LAYER     NREAL=3.3728  NLOSS=0.00  TL=0.010   !barrier,AlInGaAs
LAYER     NREAL=3.4850  NLOSS=0.00  TL=0.005   !QW, AlInGaAs
LAYER     NREAL=3.3728  NLOSS=0.00  TL=0.010   !barrier,AlInGaAs
LAYER     NREAL=3.4850  NLOSS=0.00  TL=0.005   !QW, AlInGaAs
LAYER     NREAL=3.3728  NLOSS=0.0   TL=0.50    !p-SCH,AlInGaAs
LAYER     NREAL=3.2310  NLOSS=0.00  TL=0.30    !inner p-cladding AlInAs
OUTPUT    PHMO=1      GAMMAO=1    WZRO=1     WZIO=1     QZRO=1     QZIO=0
OUTPUT    FWHPNO=1   FWHPFO=1   KMO=1      ITO=1
OUTPUT    MODOUT=1   LYROUT=1   SPLTFL=0
GAMOUT    LAYGAM=8   COMPGAM=0  GAMALL=0

!LOOPX1   ILX='NREAL'  FINV=3.6837  XINC=0.01   LAYCH=39
!LOOPX1   ILX='TL'    FINV=0.00   XINC=-0.02  LAYCH=2
!LOOPX1   ILX='TL'    FINV=0.00   XINC=-0.005 LAYCH=14
LOOPZ1    ILZ='QZMR'  FINV=10.230  ZINC=-0.025 ! This loops to find
!initial guess
END

```

In the input file $KPOL=1$ is to set TE polarization. The material system is AlInAs/AlGaInAs/AlGaInAs (substrate InP).

8.2.3. Searching the Fundamental Mode, Looping for QZMR

First, we start with searching for TE_0 mode by looping for QZMR from $n_{\max}^2 = (3.4850)^2 \cong 12.145$ to $n_{\min}^2 = (3.1987)^2 \cong 10.232$.

Using the same criterion as already introduced in the previous section, we loop the QZMR and find the following:

QZMR = 11.22 gives KM=6 and IT=3.

So we change QZMR to 11.22 and close looping. The near field (real part and intensity) and far field plots are shown in Figures 8.2.1 and 8.2.2.

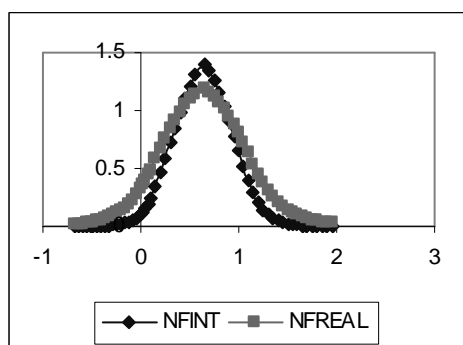


Figure 8.2.1 Fundamental mode near field plot for initial waveguide parameters.

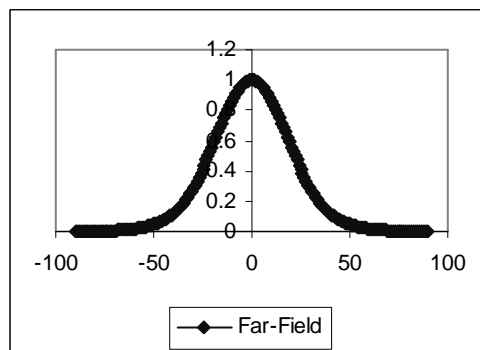


Figure 8.2.2 Fundamental mode far field plot for initial waveguide parameters.

The output parameters are calculated and listed below:

```
PHM           = 6.780389E-01
GAMMA(8)     = 6.923083E-03
WZR          = 3.348926E+00
WZI          = 1.717388E-20
FWHPF       = 4.526491E+01
KM           = 6
IT           = 3
```

The layer structure is:

```
# of layers = 14
LAYER01 NLOSS= 0.00000 NREAL= 3.19870 TL= 0.00000
LAYER02 NLOSS= 0.00000 NREAL= 3.23100 TL= 0.30000
LAYER03 NLOSS= 0.00000 NREAL= 3.37280 TL= 0.50000
LAYER04 NLOSS= 0.00000 NREAL= 3.48500 TL= 0.00500
LAYER05 NLOSS= 0.00000 NREAL= 3.37280 TL= 0.01000
LAYER06 NLOSS= 0.00000 NREAL= 3.48500 TL= 0.00500
LAYER07 NLOSS= 0.00000 NREAL= 3.37280 TL= 0.01000
LAYER08 NLOSS= 0.00000 NREAL= 3.48500 TL= 0.00500
LAYER09 NLOSS= 0.00000 NREAL= 3.37280 TL= 0.01000
LAYER10 NLOSS= 0.00000 NREAL= 3.48500 TL= 0.00500
LAYER11 NLOSS= 0.00000 NREAL= 3.37280 TL= 0.01000
LAYER12 NLOSS= 0.00000 NREAL= 3.48500 TL= 0.00500
LAYER13 NLOSS= 0.00000 NREAL= 3.37280 TL= 0.50000
LAYER14 NLOSS= 0.00000 NREAL= 3.23100 TL= 0.00000
```

8.2.4. Looping the SCH layers to find the proper thickness for the fundamental mode confinement.

We loop both the n-SCH and p-SCH layers from 0.5 μm to 0 μm to find the proper thickness to get maximum confinement in QWs. Note that we check for QW confinement and angle at full-width at half-maximum power for far field (FWHPF) and then make a proper choice. We cannot get high confinement and low FWHPF angle at the same time so it is a compromise. Generally, the values are chosen according to design specifications.

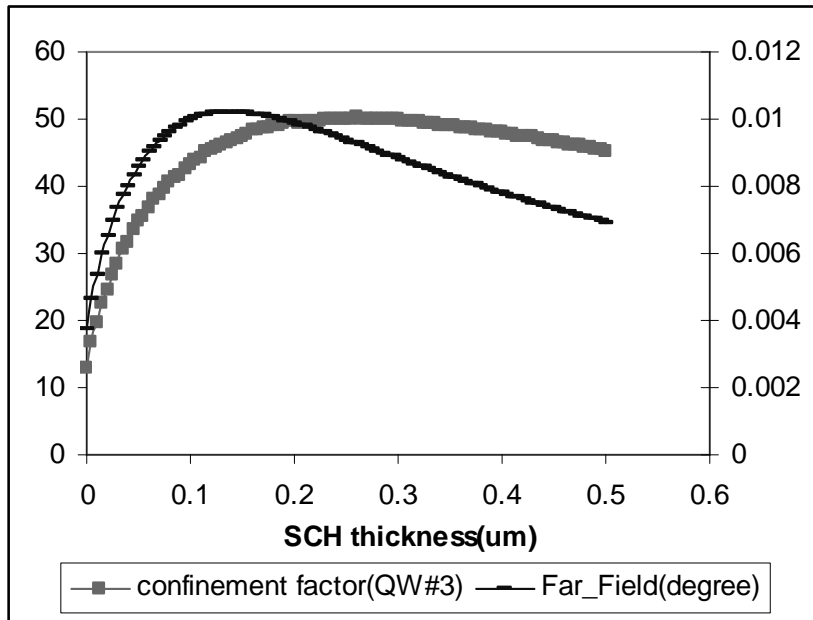


Figure 8.2.3 QW confinement factor and FWHPF vs. SCH thickness

From figures 8.2.3, we can decide the proper thickness of the SCH layer as 0.140 μm since the confinement factor has the maximum value and the far-field angle is satisfactorily low at this thickness.

The .db output file is as shown below:

TL(3)	TL(13)	PHM	GAMMA(8)	WZR	WZI	QZR	FWHPN	FWHPF	KM	IT
5.000000E-01	5.000000E-01	6.780389E-01	6.923083E-03	3.348926E+00	1.629364E-21	1.121530E+01	7.045997E-01	4.526491E+01	6	3
4.950000E-01	4.950000E-01	6.764395E-01	6.962301E-03	3.348584E+00	-5.397067E-16	1.121301E+01	7.002861E-01	4.538071E+01	6	2
1.400000E-01	1.400000E-01	4.151027E-01	1.021052E-02	3.287700E+00	-4.496412E-15					
1.080897E+01	4.094267E-01	4.677912E+01	6	2						

8.2 AlInGaAs/AlInGaAs/InP(1310nm, TE mode)

```

2.000000E-02  2.000000E-02  1.593417E-01  4.911944E-03  5.085040E-03  5.198442E-03  5.249395E-03  5.236662E-03  3.236628E+00 -2.272725E-17  1.047576E+01  7.033353E-01
1.893432E+01      6      4

1.734723E-16  1.734723E-16  1.081582E-01  1.539442E-03  1.606108E-03  1.653928E-03  1.681719E-03  1.688793E-03  3.233169E+00 -4.636668E-15  1.045338E+01  2.080428E+00
5.249361E+00      6      9

```

The output parameters are calculated and listed below:

```

GAMMA(8)      = 1.021052E-02
WZR           = 3.287700E+00
WZI           = -4.496412E-15
FWHPF        = 4.677912E+01
KM            = 6
IT            = 2

```

The layer structure is:

```

# of layers = 14
LAYER01  NLOSS= 0.00000  NREAL= 3.19870  TL= 0.00000
LAYER02  NLOSS= 0.00000  NREAL= 3.23100  TL= 0.30000
LAYER03  NLOSS= 0.00000  NREAL= 3.37280  TL= 0.14000
LAYER04  NLOSS= 0.00000  NREAL= 3.48500  TL= 0.00500
LAYER05  NLOSS= 0.00000  NREAL= 3.37280  TL= 0.01000
LAYER06  NLOSS= 0.00000  NREAL= 3.48500  TL= 0.00500
LAYER07  NLOSS= 0.00000  NREAL= 3.37280  TL= 0.01000
LAYER08  NLOSS= 0.00000  NREAL= 3.48500  TL= 0.00500
LAYER09  NLOSS= 0.00000  NREAL= 3.37280  TL= 0.01000
LAYER10  NLOSS= 0.00000  NREAL= 3.48500  TL= 0.00500
LAYER11  NLOSS= 0.00000  NREAL= 3.37280  TL= 0.01000
LAYER12  NLOSS= 0.00000  NREAL= 3.48500  TL= 0.00500
LAYER13  NLOSS= 0.00000  NREAL= 3.37280  TL= 0.14000
LAYER14  NLOSS= 0.00000  NREAL= 3.23100  TL= 0.00000

```

The near field (real part and intensity) and far field plots are shown in Figures 8.2.4 and 8.2.5:

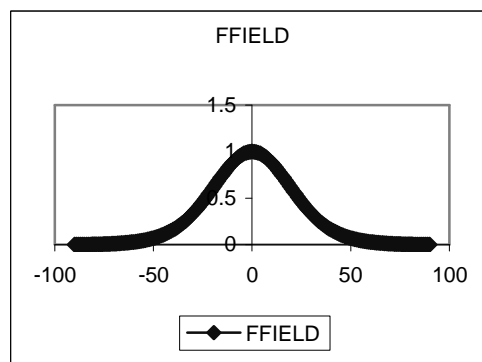
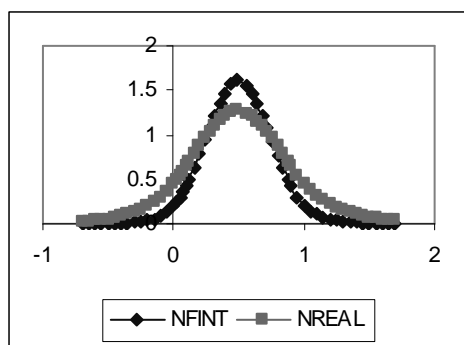


Figure 8.2.4 Fundamental mode near field plot with 0.16 μm SCH.

Figure 8.2.5 Fundamental mode far field plot with 0.16 μm SCH.

8.2.5. Making the Full Structure and Including Loss parameters

From the previous steps, the QZMR and the thickness of the SCH layer are decided. Now we need to form the full structure and include the loss layers. Add the outer p-cladding layer and the p-cap layer. For the new structure we need to find the QZMR value again at the given start thicknesses of the outer p-cladding layer and the p-cap layer. Then we loop the inner n, p-cladding layers simultaneously to find the proper thickness at the QZMR value. The input file for this structure is shown below:

```

CASE      KASE=mqw-s-1
CASE      EPS1=1E-8  EPS2=1E-8  GAMEPS=1E-6
CASE      QZMR=12.145  QZMI=0.0  !max is 12.145
CASE      PRINTF=0    INITGS=0    AUTOQW=0  NFPLT=1    FFPLT=1
!CASE     DXIN=0.2  QZMR=10.932
!CASE     IL=100   KGSS=1

MODCON    KPOL=1    APB1=0.25    APB2=0.25
STRUCT    WVL=1.3

LAYER     NREAL=3.1987  NLOSS=0.0025  TL=0.00    !N-sub, InP
LAYER     NREAL=3.2310  NLOSS=0.00    TL=0.50    !inner n-cladding AlInAs
LAYER     NREAL=3.3728  NLOSS=0.00    TL=0.14    !n-SCH, AlInGaAs
LAYER     NREAL=3.4850  NLOSS=0.00    TL=0.005   !QW, AlInGaAs
LAYER     NREAL=3.3728  NLOSS=0.00    TL=0.010   !barrier, AlInGaAs
LAYER     NREAL=3.4850  NLOSS=0.00    TL=0.005   !QW, AlInGaAs
LAYER     NREAL=3.3728  NLOSS=0.00    TL=0.010   !barrier, AlInGaAs
LAYER     NREAL=3.4850  NLOSS=0.00    TL=0.005   !QW, AlInGaAs
LAYER     NREAL=3.3728  NLOSS=0.00    TL=0.010   !barrier, AlInGaAs
LAYER     NREAL=3.4850  NLOSS=0.00    TL=0.005   !QW, AlInGaAs
LAYER     NREAL=3.3728  NLOSS=0.00    TL=0.010   !barrier, AlInGaAs
LAYER     NREAL=3.4850  NLOSS=0.00    TL=0.005   !QW, AlInGaAs
LAYER     NREAL=3.3728  NLOSS=0.00    TL=0.010   !barrier, AlInGaAs
LAYER     NREAL=3.4850  NLOSS=0.00    TL=0.005   !QW, AlInGaAs
LAYER     NREAL=3.3728  NLOSS=0.00    TL=0.014   !p-SCH, AlInGaAs
LAYER     NREAL=3.2310  NLOSS=0.00    TL=0.50    !inner p-cladding AlInAs
LAYER     NREAL=3.1987  NLOSS=0.0025  TL=1.25    ! outer p-cladding InP
LAYER     NREAL=3.0667  NLOSS=0.0025  TL=0.2     !p+cap, InGaAs
!LAYER    NREAL=1.8     NLOSS=0.00    TL=0.03    !Si3N4
LAYER     NREAL=3.7     NLOSS=18.2415  TL=0.05    !Ti
LAYER     NREAL=4.64    NLOSS=26.6731  TL=0.12    !Pt
LAYER     NREAL=0.18    NLOSS=41.3474  TL=0.20    !Au

OUTPUT    PHMO=1    GAMMAO=1    WZRO=1    WZIO=1    QZRO=1    QZIO=0
OUTPUT    FWHPNO=1    FWHPFO=1    KMO=1    ITO=1
OUTPUT    MODOUT=1    LYROUT=1    SPLTFL=0
GAMOUT    LAYGAM=8    COMPGAM=0    GAMALL=0

!LOOPX1   ILX='TL'  FINV=2.00  XINC=0.005  LAYCH=2
!LOOPX1   ILX='TL'  FINV=2.00  XINC=0.005  LAYCH=14
!LOOPX1   ILX='TL'  FINV=0.00  XINC=-0.005  LAYCH=3
!LOOPX1   ILX='TL'  FINV=0.00  XINC=-0.005  LAYCH=13
LOOPZ1    ILZ='QZMR'  FINV=9.405  ZINC=-0.025  ! This loops to find
!initial guess
END

```

As we did in section 8.2.3, we loop the QZMR and find:

QZMR = 10.77 gives KM=6 and IT=4.

So change QZMR to 10.77 and close looping QZMR.

The near field (real part and intensity) and far field plots are shown in Figures 8.2.6 and 8.2.7:

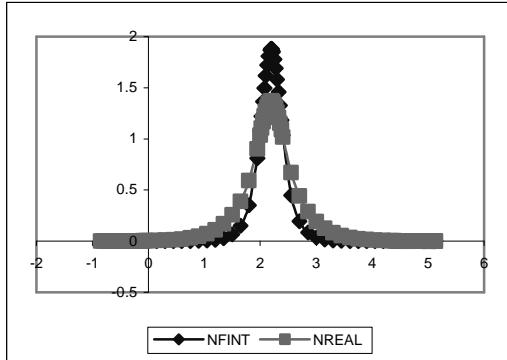


Figure 8.2.6 Fundamental mode near field plot for full structure.

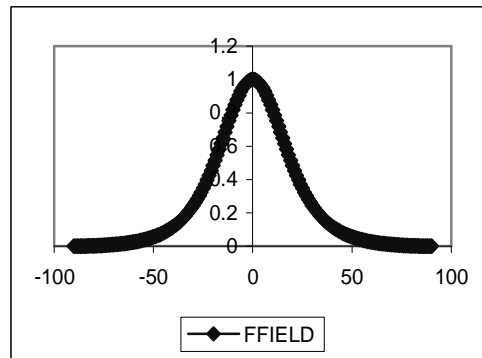


Figure 8.2.7 Fundamental mode far field plot for full structure.

We have to increase the p-cladding thickness so that the modal loss drops into acceptable limits. Looping the second p-clad thickness from $0.30\mu\text{m}$ to $2.00\mu\text{m}$, we obtain the modal intensity loss as function of the p-cladding thickness as shown in Figure 8.2.8. The QW confinement factor and FWHPF as a function of p-clad thickness for the updated structure is shown in Figure 8.2.9.

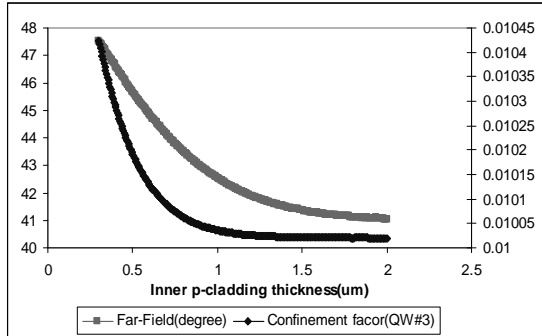
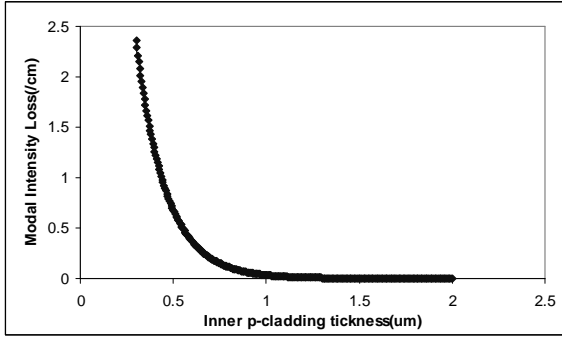


Figure 8.2.8 Modal intensity loss vs. Inner p-clad thickness.

Figure 8.2.9 QW confinement factor and FWHPF vs. Inner p-clad thickness.

Based on the plots shown in Figures 8.2.8 and 8.2.9, we can choose the thickness value of 0.5 μm for the inner p-cladding since the loss curve drops to 0.5 and higher thickness will cause lower confinement factor. The intensity modal loss is calculated from WZI values (amplitude loss in μm⁻¹) using the formula:

$$\alpha = WZI \cdot (4\pi/\lambda) \cdot 10^4 \text{ /cm}$$

Since we choose the inner p-cladding thickness as 0.5 μm, we need to calculate the QZMR for the new inner p-cladding thickness as done in the previous section. QZMR can be set to 10.820.

8.2.6. Output Parameters and Plots

Now we can get the final output values as listed below:

```

PHM           = 1.428585E+00
GAMMA ( 8 )  = 1.019220E-02
WZR           = 3.288050E+00
WZI           = 7.078846E-06
FWHPF        = 4.568929E+01
KM            = 7
IT            = 4
    
```

The layer structure is:

# of layers = 19			
LAYER01	NLOSS= 0.00250	NREAL= 3.19870	TL= 0.00000
LAYER02	NLOSS= 0.00000	NREAL= 3.23100	TL= 0.50000
LAYER03	NLOSS= 0.00000	NREAL= 3.37280	TL= 0.14000
LAYER04	NLOSS= 0.00000	NREAL= 3.48500	TL= 0.00500
LAYER05	NLOSS= 0.00000	NREAL= 3.37280	TL= 0.01000
LAYER06	NLOSS= 0.00000	NREAL= 3.48500	TL= 0.00500
LAYER07	NLOSS= 0.00000	NREAL= 3.37280	TL= 0.01000
LAYER08	NLOSS= 0.00000	NREAL= 3.48500	TL= 0.00500
LAYER09	NLOSS= 0.00000	NREAL= 3.37280	TL= 0.01000
LAYER10	NLOSS= 0.00000	NREAL= 3.48500	TL= 0.00500
LAYER11	NLOSS= 0.00000	NREAL= 3.37280	TL= 0.01000
LAYER12	NLOSS= 0.00000	NREAL= 3.48500	TL= 0.00500
LAYER13	NLOSS= 0.00000	NREAL= 3.37280	TL= 0.14000
LAYER14	NLOSS= 0.00000	NREAL= 3.23100	TL= 0.50000
LAYER15	NLOSS= 0.00250	NREAL= 3.19870	TL= 1.25000
LAYER16	NLOSS= 0.00250	NREAL= 3.06670	TL= 0.20000
LAYER17	NLOSS=18.24150	NREAL= 3.70000	TL= 0.05000
LAYER18	NLOSS=26.67310	NREAL= 4.64000	TL= 0.12000
LAYER19	NLOSS=41.34740	NREAL= 0.18000	TL= 0.00000

Near field and far field plots for the final structure are shown in Figures 8.2.12 and 8.2.13 below:

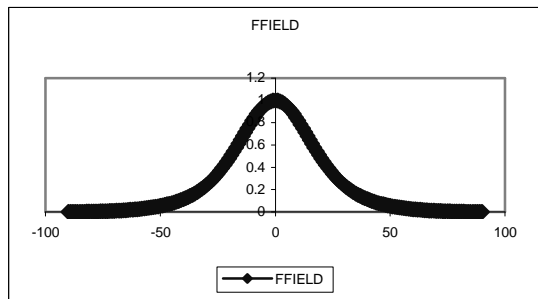
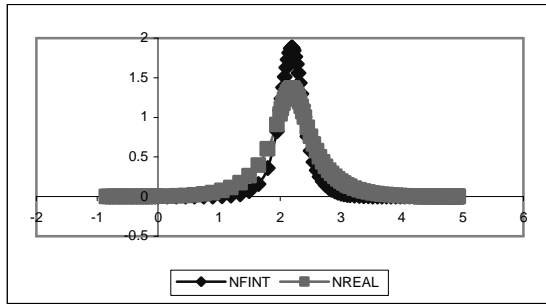


Figure 8.2.12 Fundamental mode near field plot for final structure.

Figure 8.2.13 Fundamental mode far field plot for final structure.

The Final laser structure for this 1.3 μm AlInGaAs laser design can be found in Table 8.2.2 as follows:

Table 8.2.2 Final laser structure (5-QW AlInGaAs) for the 1.3 μm AlInGaAs/InP.

Layer	Composition	Thickness (μm)
n-substrate	InP	---
Inner n-cladding	$\text{Al}_{0.48}\text{In}_{0.52}\text{As}$	0.50
n-SCH	$\text{Al}_{0.267}\text{Ga}_{0.203}\text{In}_{0.53}\text{As}$	0.14
QW-1	$\text{Al}_{0.161}\text{Ga}_{0.102}\text{In}_{0.737}\text{As}$	0.005
barrier	$\text{Al}_{0.267}\text{Ga}_{0.203}\text{In}_{0.53}\text{As}$	0.010
QW-2	$\text{Al}_{0.161}\text{Ga}_{0.102}\text{In}_{0.737}\text{As}$	0.005
barrier	$\text{Al}_{0.267}\text{Ga}_{0.203}\text{In}_{0.53}\text{As}$	0.010
QW-3	$\text{Al}_{0.161}\text{Ga}_{0.102}\text{In}_{0.737}\text{As}$	0.005
barrier	$\text{Al}_{0.267}\text{Ga}_{0.203}\text{In}_{0.53}\text{As}$	0.010
QW-4	$\text{Al}_{0.161}\text{Ga}_{0.102}\text{In}_{0.737}\text{As}$	0.005
barrier	$\text{Al}_{0.267}\text{Ga}_{0.203}\text{In}_{0.53}\text{As}$	0.010
QW-5	$\text{Al}_{0.161}\text{Ga}_{0.102}\text{In}_{0.737}\text{As}$	0.005
n-SCH	$\text{Al}_{0.267}\text{Ga}_{0.203}\text{In}_{0.53}\text{As}$	0.14
Inner n-cladding	$\text{Al}_{0.48}\text{In}_{0.52}\text{As}$	0.50
Outer n-cladding	InP	1.25
P-cap	InGaAs	0.2

The final input file for WAVEGUIDE is also shown as follows:

```

CASE      KASE=mqw-s-1
CASE      EPS1=1E-8  EPS2=1E-8  GAMEPS=1E-6
CASE      QZMR=10.820  QZMI=0.0  !max is 12.145
CASE      PRINTF=0    INITGS=0    AUTOQW=0  NFPLT=1    FFPLT=1
!CASE     DXIN=0.2  QZMR=10.932
!CASE     IL=100  KGSS=1

MODCON    KPOL=1    APB1=0.25    APB2=0.25

STRUCT    WVL=1.3

LAYER     NREAL=3.1987  NLOSS=0.0025  TL=0.00    !N-sub, InP
LAYER     NREAL=3.2310  NLOSS=0.00    TL=0.50    !inner n-cladding AlInAs
LAYER     NREAL=3.3728  NLOSS=0.00    TL=0.14    !n-SCH, AlInGaAs
LAYER     NREAL=3.4850  NLOSS=0.00    TL=0.005   !QW, AlInGaAs
LAYER     NREAL=3.3728  NLOSS=0.00    TL=0.010   !barrier, AlInGaAs
LAYER     NREAL=3.4850  NLOSS=0.00    TL=0.005   !QW, AlInGaAs
LAYER     NREAL=3.3728  NLOSS=0.00    TL=0.010   !barrier, AlInGaAs
LAYER     NREAL=3.4850  NLOSS=0.00    TL=0.005   !QW, AlInGaAs

```


8.2 AlInGaAs/AlInGaAs/InP(1310nm, TE mode)

```

LAYER  NREAL=3.3728  NLOSS=0.00  TL=0.010  !barrier,AlInGaAs
LAYER  NREAL=3.4850  NLOSS=0.00  TL=0.005  !QW, AlInGaAs
LAYER  NREAL=3.3728  NLOSS=0.00  TL=0.010  !barrier,AlInGaAs
LAYER  NREAL=3.4850  NLOSS=0.00  TL=0.005  !QW, AlInGaAs
LAYER  NREAL=3.3728  NLOSS=0.00  TL=0.14   !p-SCH,AlInGaAs
LAYER  NREAL=3.2310  NLOSS=0.00  TL=0.50   !inner p-cladding AlInAs
LAYER  NREAL=3.1987  NLOSS=0.0025 TL=1.25  ! outer p-cladding InP
LAYER  NREAL=3.0667  NLOSS=0.0025 TL=0.2    !p+cap, InGaAs
!LAYER  NREAL=1.8    NLOSS=0.00  TL=0.03  !Si3N4
LAYER  NREAL=3.7    NLOSS=18.2415 TL=0.05 !Ti
LAYER  NREAL=4.64   NLOSS=26.6731 TL=0.12 !Pt
LAYER  NREAL=0.18   NLOSS=41.3474 TL=0.20 !Au

OUTPUT  PHMO=1      GAMMAO=1      WZRO=1      WZIO=1      QZRO=1      QZIO=0
OUTPUT  FWHPNO=1    FWHPFO=1    KMO=1      ITO=1
OUTPUT  MODOUT=1    LYROUT=1    SPLTFL=0
GAMOUT  LAYGAM=8    COMPGAM=0   GAMALL=0

!LOOPX1  ILX='TL'    FINV=2.00   XINC=0.005  LAYCH=2
!LOOPX1  ILX='TL'    FINV=2.00   XINC=0.005  LAYCH=14
!LOOPX1  ILX='TL'    FINV=0.00   XINC=-0.005 LAYCH=3
!LOOPX1  ILX='TL'    FINV=0.00   XINC=-0.005 LAYCH=13
!LOOPZ1  ILZ='QZMR'  FINV=9.405  ZINC=-0.025 ! This loops to find
!initial guess
END

```

8.2.7. The Refractive Index Profile

Now we can plot the refractive index profile according to the distance of the layers for the laser structure as following:

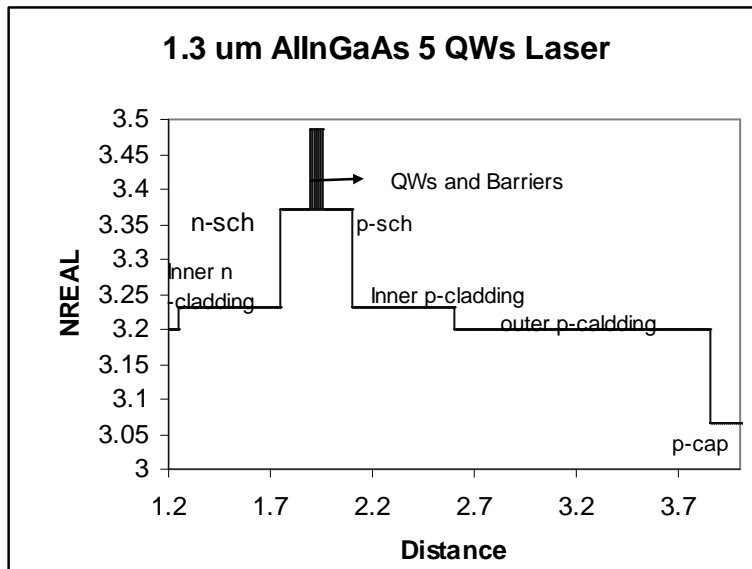


Figure 8.2.14 The structure of 1.3-um AlInGaAs 5-QW Laser.

REFERENCES:

- [1]. <http://engr.smu.edu/ee/smuphotonics/GainManualAppendixC/AppendixC.htm>
- [2]. <http://engr.smu.edu/ee/smuphotonics/Gain.htm>
- [3]. Z.-L. Liao and J. N. Walpole, “Mass-transported GaInAsP/InP lasers”, *Lincoln Laboratory Journal*, vol.2, 77, 1989.
- [4]. E. R. Hegblom, D. I. Babic, B. J. Thibeault, and L. A. Coldren, “Scattering losses from dielectric apertures in vertical-cavity lasers”, *IEEE Journal of Selected Topics in Quantum Electronics*, vol.3, 379, 1997.
- [5]. Sandra R. Selmic, Tso-Min Chou, JiehPing Sih, Jay B.Kirk, Art Mantie, Jerome K. Bulter, David Bour, and Gary A. Evans, “Design and Characterization of 1.3- μm AlGaInAs-InP Multiple-Quantum-Well Lasers”, *IEEE Journal of Selected Topics in Quantum Electronics*, vol. 7, no. 2, March/April 2001.

Chapter 9 TE-mode, 635-nm Red Laser Optimization

This chapter gives an example on how to design a 635-nm, GaInP/AlGaInP/GaAs broad-area red laser structure with the WAVEGUIDE software to achieve optimized key laser parameters such as quantum well confinement factor and far field.

9.1 The Initial Input File and Layer Parameters

Before simulation, we need to construct a WAVEGUIDE input file with desired lasing wavelength, material system and compositions for each layer. For each layer, we have to set up an initial layer thickness in the input file. Using WAVEGUIDE to find out the optimized layer thickness to achieve the desired design is our ultimate target. The structure and the index profile of the TE-mode, 635nm GaInP/AlGaInP/GaAs broad-area red laser is shown below in Table 9.1.1 and Figure 9.1.1. The material compositions for each layer and the quantum well thickness can be calculated with our GAIN software. The initial input file is provided in Table 9.1.2. And the layer parameters are listed in Table 9.1.3. Readers can refer to chapter 2.4 for the method on how to create and evaluate an input file from WAVEGUIDE.

Table 9.1.1 The structure of the TE-mode, 635nm GaInP/AlGaInP/GaAs red laser.

#	Layer name	Material compositions	Refractive index	Energy bandgap
1	Substrate	GaAs	3.82357	1.424
2	n-cladding	Al _{0.5} In _{0.5} P	3.27693	1.897
3	SCH	(Al _{0.6} Ga _{0.4}) _{0.5} In _{0.5} P	3.40423	1.862
4	Quantum well	Ga _{0.6} In _{0.4} P	3.49147	1.896
5	SCH	(Al _{0.6} Ga _{0.4}) _{0.5} In _{0.5} P	3.40423	1.862
6	p-cladding	Al _{0.5} In _{0.5} P	3.27693	1.897
7	p-cap	GaAs	3.82357	1.424

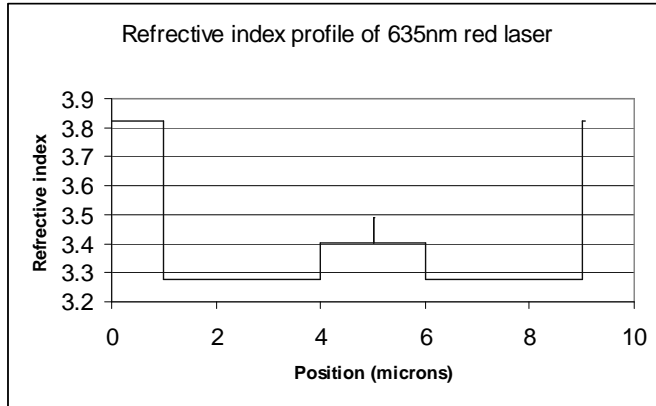


Figure 9.1.1 Index profile of TE mode, 635nm red laser.

Table 9.1.2 Initial input file of TE-mode, 635-nm red laser structure.

```

!CASE Parameter Set
CASE KASE=WIFE
CASE EPS1=1E-9 EPS2=1E-9 GAMEPS=1E-3 QZMR=14.62QZMI=0.001
CASE PRINTF=1 INITGS=0 AUTOQW=0 NFPLT=1 FFPLT=1 IL=30

!MODCON Parameter Set
MODCON KPOL=2 APB1=0.25 APB2=0.25

!STRUCT Parameter Set
STRUCT WVL=0.635
STRUCT XPERC1=0.0 XPERC2=0.0 XPERC3=0.0 XPERC4=0.0
STRUCT YPERC1=0.0 YPERC2=0.0 YPERC3=0.0 YPERC4=0.0

!LAYER Parameter Set
LAYER MATSYS=0.1 XPERC=0 YPERC=0 TL=1.0 !GaAs substrate
LAYER MATSYS=8.0 XPERC=1 YPERC=0 TL=3.0 !Al.5In.5P n-cladding
LAYER MATSYS=8.0 XPERC=0.6 YPERC=0 TL=1 ! (Al.6Ga.4).5In.5P SCH
LAYER MATSYS=11.0 XPERC=0.6 YPERC=0 TL=0.008 !Ga.6In.4P QW
LAYER MATSYS=8.0 XPERC=0.6 YPERC=0 TL=1 ! (Al.6Ga.4).5In.5P SCH
LAYER MATSYS=8.0 XPERC=1 YPERC=0 TL=3.0 !Al.5In.5P p-cladding
LAYER MATSYS=0.1 XPERC=0 YPERC=0 TL=0.05 !GaAs P cap
    
```

```

!OUTPUT Parameter Set
OUTPUT PHMO=1 GAMMAO=1 WZRO=1 WZIO=1 QZRO=0 QZIO=0
OUTPUT FWHPNO=0 FWHPFO=1 KMO=1 ITO=1
OUTPUT SPLTFL=0 MODOUT=0 LYROUT=0

!GAMOUT Parameter Set
GAMOUT LAYGAM=4 COMPGAM=0 GAMALL=0

!LOOPZ Parameter Set
LOOPZ1 ILZ='QZMR' FINV=10.74 ZINC=-0.01
END

```

Table 9.1.2 Layer parameters for TE-mode, 635-nm red laser structure

# of layers =	07		
LAYER01	NLOSS= 0.00000	NREAL= 3.82357	TL= 1.00000
LAYER02	NLOSS= 0.00000	NREAL= 3.27693	TL= 3.00000
LAYER03	NLOSS= 0.00000	NREAL= 3.40423	TL= 1.00000
LAYER04	NLOSS= 0.00000	NREAL= 3.49147	TL= 0.00800
LAYER05	NLOSS= 0.00000	NREAL= 3.40423	TL= 1.00000
LAYER06	NLOSS= 0.00000	NREAL= 3.27693	TL= 3.00000
LAYER07	NLOSS= 0.00000	NREAL= 3.82357	TL= 0.05000

For the purpose of simplicity, in this WAVEGUIDE simulation, we don't include the doping loss for the claddings and the substrate. The main loss for the structures arises from the substrate photon absorption due to the large bandgap of GaAs as relative to that of the active material (see Table 9.1.1).

9.2 Modes Searching, Looping for QZMR

After creating the input file, we search for TE₀ mode by looping for QZMR. The up bound of QZMR is normally approximated by the square of the maximum NREAL of the

Chapter 9 TE-mode 635nm Red Laser Optimization

structure, and the bottom bound of QZMR is approximated by the square of the minimum NREAL of the structure. From the layer information above, we have

$$QZMR_{up} = (3.82357)^2 = 14.62$$

$$QZMR_{bottom} = (3.27693)^2 = 10.74.$$

The looping results calculated by WAVEGUIDE can be find in the WAVEGUIDE “.db” data file. Part of the results is also listed in Table 9.2.1.

Table 9.2.1 QZMR looping results.

QZMR	PHM	GAMMA(4)	WZR	WZI	FWHPF	KM	IT
					.		
					.		
1.159500E+01	5.442224E+00	0.000000E+00	3.344826E+00	1.490495E-02	0.000000E+00	3	30
1.159000E+01	8.230724E-01	7.980746E-03	3.401844E+00	5.520731E-20	1.907207E+01	7	8
1.158500E+01	8.230724E-01	7.980746E-03	3.401844E+00	1.219511E-20	1.907207E+01	7	8
1.158000E+01	8.230724E-01	7.980746E-03	3.401844E+00	-3.208647E-20	1.907209E+01	7	6
1.157500E+01	8.230724E-01	7.980747E-03	3.401844E+00	1.155920E-19	1.907210E+01	7	4
1.157000E+01	8.230724E-01	7.980746E-03	3.401844E+00	2.080785E-21	1.907207E+01	7	4
1.156500E+01	8.230724E-01	7.980744E-03	3.401844E+00	3.931486E-19	1.907203E+01	7	5
1.156000E+01	8.230724E-01	7.980748E-03	3.401844E+00	-1.879757E-19	1.907216E+01	7	6
1.155500E+01	1.825985E+00	3.417337E-07	3.392150E+00	6.345844E-20	1.459100E+01	6	9
					.		
					.		
					.		

The general criteria to look for a proper QZMR value are: (1) PHM < 1.0, (2) KM = 6 or 7. Four QZMR values in above Table meet the criteria. And we can choose the first one that reaches the minimum iteration number, which is IT = 4 in this case.

QZMR = 11.575 gives PHM = 8.230724E-01, KM=7 and IT=4. After we change QZMR to 11.575, we close the looping and run the input file again, plot the near field and far field (Figure 9.2.1) to check that we do get TE0 mode at QZMR = 11.575.

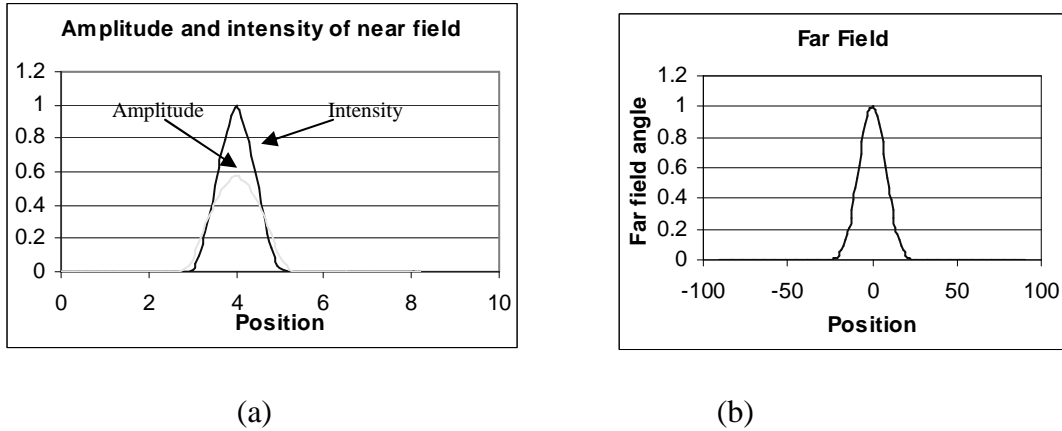


Figure 9.2.1 (a) Near field and field intensity of TE₀ mode (b) Far field of TE₀ mode for the red laser structure.

9.3 SCH Thickness Determination to Achieve Desired Quantum Well Confinement Factor (GAMMA) and Full-Width-Half-Power Far Field (FWHPF)

First of all, we'll optimize the thickness of SCH layers to obtain the desired GAMMA and FWHPF in transverse plane. As shown in the Table 9.3.1, we loop the thickness of n-SCH layer and p-SCH layers by decreasing it from 1 μm to 0.09 μm . Then we plot the quantum well confinement factor GAMMA (4) and FWHPF as a function of the thickness of SCH layers, and find the SCH thickness corresponds to the desired GAMMA and FWHPF. The output file is shown in Table 9.3.2. The quantum well confinement and far field are depicted in Figure 9.3.1.

Chapter 9 TE-mode 635nm Red Laser Optimization

Table 9.3.1 Input file for looping the SCH layer thickness

```
!DESCRIPTION: 635nm red laser design

!CASE Parameter Set
CASE KASE=WIFE
CASE EPS1=1E-9 EPS2=1E-9 GAMEPS=1E-3 QZMR=11.575 QZMI=0.001
CASE PRINTF=1 INITGS=0 AUTOQW=0 NFPLT=1 FFPLT=1 IL=30

!MODCON Parameter Set
MODCON KPOL=2 APB1=0.25 APB2=0.25

!STRUCT Parameter Set
STRUCT WVL=0.635
STRUCT XPERC1=0.0 XPERC2=0.0 XPERC3=0.0 XPERC4=0.0
STRUCT YPERC1=0.0 YPERC2=0.0 YPERC3=0.0 YPERC4=0.0

!LAYER Parameter Set
LAYER MATSYS=0.1 XPERC=0 YPERC=0 TL=1.0 !GaAs substrate
LAYER MATSYS=8.0 XPERC=1 YPERC=0 TL=3.0 !Al.5In.5P n-cladding
LAYER MATSYS=8.0 XPERC=0.6 YPERC=0 TL=1.0 !(Al.6Ga.4).5In.5P SCH
LAYER MATSYS=11.0 XPERC=0.6 YPERC=0 TL=0.008 !Ga.6In.4P QW
LAYER MATSYS=8.0 XPERC=0.6 YPERC=0 TL=1.0 !(Al.6Ga.4).5In.5P SCH
LAYER MATSYS=8.0 XPERC=1 YPERC=0 TL=3.0 !Al.5In.5P p-cladding
LAYER MATSYS=0.1 XPERC=0 YPERC=0 TL=0.05 !GaAs P cap

!OUTPUT Parameter Set
OUTPUT PHMO=1 GAMMAO=1 WZRO=1 WZIO=1 QZRO=0 QZIO=0
OUTPUT FWHPNO=0 FWHPFO=1 KMO=1 ITO=1
OUTPUT SPLTFL=0 MODOUT=0 LYROUT=0

!GAMOUT Parameter Set
GAMOUT LAYGAM=4 COMPGAM=0 GAMALL=0

!LOOPX Parameter Set
LOOPX1 ILX='TL' FINV=0.09 XINC=-0.005 LAYCH=3
LOOPX1 ILX='TL' FINV=0.09 XINC=-0.005 LAYCH=5

END
```


9.3 SCH Thickness Determination to Achieve Desired Quantum Well Confinement

Table 9.3.2 Quantum well confinement factor and far field for varied SCH thickness.

SCH thickness	QW confinement	Far field angle
	.	
	.	
	.	
0.165	0.02731788	43.90352
0.16	0.02621566	44.5087
0.155	0.02796427	43.73485
0.15	0.02811921	43.61582
0.145	0.02855324	43.48656
0.14	0.02941425	43.30508
0.135	0.02914721	43.06164
0.13	0.02942897	42.82628
0.125	0.02975292	42.42262
0.12	0.02992374	42.70239
0.115	0.02997094	41.83623
0.11	0.03024719	41.18996
0.105	0.03036309	40.73937
0.1	0.03057365	40.16159
0.095	0.03055825	39.19299
0.09	0.03043829	38.46472

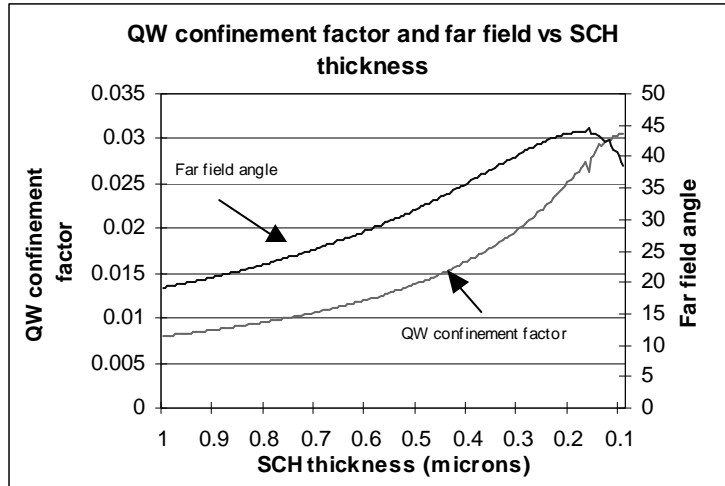


Figure 9.3.1 The quantum well confinement factor and far field as a function of SCH layer thickness.

From the Figure 9.3.1, we can see that the far field angle decreases and the quantum confinement increases as the SCH layers' thickness decreases from 0.16 μm to 0.1 μm . Normally, what specific values we should choose for the quantum well GAMMA and FWHPF is case by case and it may rely on the purpose of your structure. For example, if it's a broad area red laser, it won't be too critical on the far field, and we may want the quantum well confinement factor to be as larger as possible. On the other hand, if it is an edge emitter, we usually want to confine the far field angle not to be too large. In this case, we choose the SCH layer thickness to be of 0.1 μm , which is the case of largest QW confinement factor.

After we find the proper SCH layer thickness, we need to loop the QZMR values again and find the proper QZMR for the TE0 mode of the new structure. The looping results are calculated as in Table 9.3.3. By using the criteria described in section 9.1, we get $QZMR = 11.10$.

9.3 SCH Thickness Determination to Achieve Desired Quantum Well Confinement

Table 9.3.3 QZMR looping results.

QZMR	PHM	GAMMA(4)	WZR	WZI	FWHPF	KM	IT
					.		
					.		
1.113000E+01	5.574488E+00	0.000000E+00	3.279984E+00	2.384832E-02	0.000000E+00	3	30
1.112500E+01	5.586477E+00	0.000000E+00	3.279346E+00	2.337634E-02	0.000000E+00	3	30
1.112000E+01	4.661907E-01	3.057365E-02	3.331836E+00	1.795568E-17	4.016027E+01	7	8
1.111500E+01	4.661907E-01	3.051897E-02	3.331836E+00	1.277176E-17	4.018092E+01	7	7
1.111000E+01	4.661907E-01	3.018867E-02	3.331836E+00	1.729765E-17	4.032949E+01	7	6
1.110500E+01	4.661907E-01	3.057365E-02	3.331836E+00	1.795569E-17	4.016027E+01	7	5
1.110000E+01	4.661907E-01	3.018908E-02	3.331836E+00	1.966636E-17	4.032256E+01	7	4
1.109500E+01	4.661907E-01	3.050136E-02	3.331836E+00	1.565674E-17	4.018570E+01	7	5
1.109000E+01	4.661907E-01	3.057365E-02	3.331836E+00	1.795568E-17	4.016027E+01	7	6
1.108500E+01	4.661907E-01	3.052803E-02	3.331836E+00	1.560890E-17	4.018645E+01	7	6
1.108000E+01	5.904074E+00	0.000000E+00	3.272905E+00	-1.935700E-02	0.000000E+00	3	30
					.		
					.		
					.		

9.4 Cladding Thickness Determination to Minimize the Loss

After we find the proper QZMR for the TE₀ mode, we'll optimize the cladding thickness to minimize the loss under certain value. As mentioned in last section, the loss is mainly caused by the transparency of the substrate to the photons generated at the active layer. The input file is shown in Table 9.4.1. We loop the n cladding and p cladding from 3 to 0.5 um simultaneously. Then from the imaginary part of the effective refractive index (WZI) in the output file, we can calculate the loss as a function of cladding layer thickness. The loss is calculated in terms of the WZI as follows:

$$\alpha = WZI * 2\pi / \lambda * 10^4 \quad (9.4.1)$$

Where α is the amplitude loss and has the unit of cm^{-1} , λ is the wavelength in free space and has the unit of micron. Power loss is 2α . Figure 9.4.1 shows the plot of the loss as a function of the cladding thickness, and the corresponding data are given in Table 9.4.2.

Table 9.4.1 Input file for looping the thickness of cladding layers.

```

!CASE Parameter Set
CASE KASE=WIFE
CASE EPS1=1E-9 EPS2=1E-9 GAMEPS=1E-3 QZMR=11.11 QZMI=0.001
CASE PRINTF=1 INITGS=0 AUTOQW=0 NFPLT=1 FFPLT=1 IL=30

!MODCON Parameter Set
MODCON KPOL=2 APB1=0.25 APB2=0.25

!STRUCT Parameter Set
STRUCT WVL=0.635
STRUCT XPERC1=0.0 XPERC2=0.0 XPERC3=0.0 XPERC4=0.0
STRUCT YPERC1=0.0 YPERC2=0.0 YPERC3=0.0 YPERC4=0.0

!LAYER Parameter Set
LAYER MATSYS=0.1 XPERC=0 YPERC=0 TL=1.0 !GaAs substrate
LAYER MATSYS=8.0 XPERC=1 YPERC=0 TL=3.0 !Al.5In.5P n-cladding
LAYER MATSYS=8.0 XPERC=0.6 YPERC=0 TL=0.1 !(Al.6Ga.4).5In.5P SCH
LAYER MATSYS=11.0 XPERC=0.6 YPERC=0 TL=0.008 !Ga.6In.4P QW
LAYER MATSYS=8.0 XPERC=0.6 YPERC=0 TL=0.1 !(Al.6Ga.4).5In.5P SCH
LAYER MATSYS=8.0 XPERC=1 YPERC=0 TL=3.0 !Al.5In.5P p-cladding
LAYER MATSYS=0.1 XPERC=0 YPERC=0 TL=0.05 !GaAs P cap

!OUTPUT Parameter Set
OUTPUT PHMO=1 GAMMAO=1 WZRO=1 WZIO=1 QZRO=0 QZIO=0
OUTPUT FWHPNO=0 FWHPFO=1 KMO=1 ITO=1
OUTPUT SPLTFL=0 MODOUT=0 LYROUT=0

!GAMOUT Parameter Set
GAMOUT LAYGAM=4 COMPGAM=0 GAMALL=0

!LOOPX Parameter Set
LOOPX1 ILX='TL' FINV=0.5 XINC=-0.05 LAYCH=2
LOOPX1 ILX='TL' FINV=0.5 XINC=-0.05 LAYCH=6

END

```

9.4 Cladding Thickness Determination to Minimize the Loss

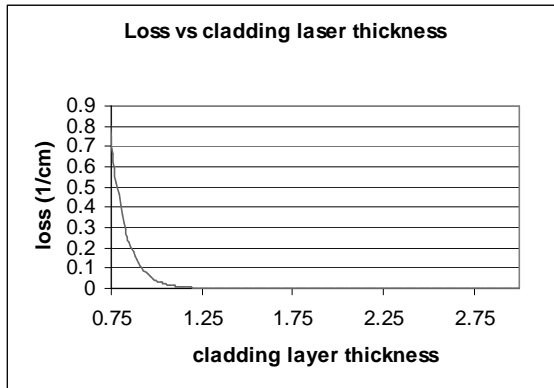


Figure 9.4.1 Loss as a function of $n(p)$ cladding layer thickness for red laser structure.

Table 9.4.2 WZI and loss values for different cladding layer thickness.

TL(2) (microns)	WZI	Loss (1/cm)
3	2.01787E-17	1.99663E-12
2.95	2.20334E-17	2.18016E-12
2.9	2.19546E-17	2.17236E-12
2.85	2.31587E-17	2.2915E-12
	.	
	.	
	.	
1.13	8.16284E-08	0.008076954
1.12	9.19632E-08	0.009099557
1.11	1.03606E-07	0.010251625
1.1	1.16724E-07	0.011549553
1.09	1.31502E-07	0.013011824
1.08	1.48151E-07	0.014659216
1.07	1.66908E-07	0.016515199

.
.
.

Normally, it is sufficient to confine the loss to be less than 10^{-2} . Based on the plot and the data above, we pick 1.12 μm as the cladding thickness. We should recalculate the QZMR value every time we change the structure. Once we fix the p-cladding and n-cladding layer thickness, we loop the QZMR values again, and the looping results are calculated as in Table 9.4.3. And we find that the QZMR value for TE0 mode is still 11.10.

Table 9.4.3 QZMR looping results.

QZMR	PHM	GAMMA(4)	WZR	WZI	FWHPF	KM	IT
.							
.							
.							
1.118000E+01	4.870494E+00	2.213765E-03	3.223972E+00	6.727938E-03	1.615454E+01	5	29
1.117000E+01	4.661945E-01	3.048141E-02	3.331836E+00	9.196321E-08	4.022698E+01	7	9
1.116000E+01	4.661945E-01	3.048141E-02	3.331836E+00	9.196321E-08	4.022698E+01	7	8
1.115000E+01	4.661945E-01	3.048141E-02	3.331836E+00	9.196321E-08	4.022698E+01	6	7
1.114000E+01	4.661945E-01	3.048141E-02	3.331836E+00	9.196321E-08	4.022698E+01	7	7
1.113000E+01	4.661945E-01	3.048141E-02	3.331836E+00	9.196321E-08	4.022698E+01	7	6
1.112000E+01	4.661945E-01	3.048141E-02	3.331836E+00	9.196321E-08	4.022698E+01	7	5
1.111000E+01	4.661945E-01	3.048141E-02	3.331836E+00	9.196321E-08	4.022698E+01	6	4
1.110000E+01	4.661945E-01	3.048141E-02	3.331836E+00	9.196321E-08	4.022698E+01	6	3
1.109000E+01	4.661945E-01	3.048141E-02	3.331836E+00	9.196321E-08	4.022698E+01	6	4
1.108000E+01	4.661945E-01	3.048141E-02	3.331836E+00	9.196321E-08	4.022698E+01	7	5
1.107000E+01	4.661945E-01	3.048141E-02	3.331836E+00	9.196321E-08	4.022698E+01	6	5
.							
.							
.							

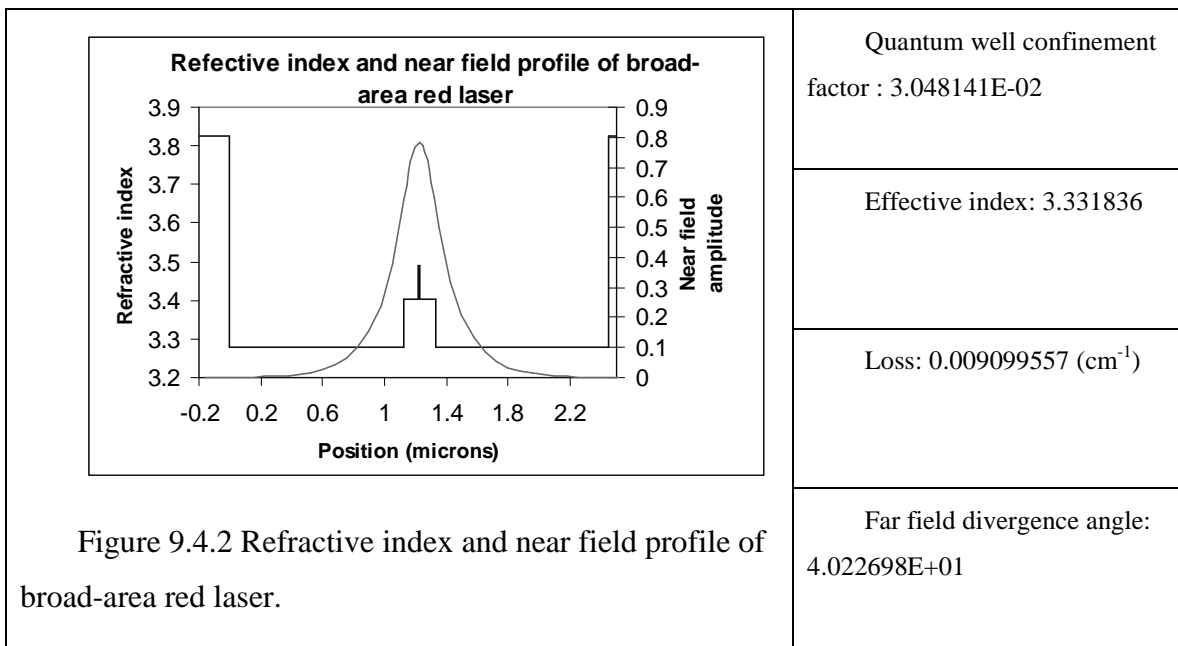
The layer parameter for the final optimized structure of 635nm broad-area red laser is listed in Table 9.4.4. The refractive and near field index profile are given in Figure 9.4.2. This optimization is based on achieving the largest quantum confinement factor for

9.4 Cladding Thickness Determination to Minimize the Loss

the broad-area lasers. However, for edge emitters, we need to consider far field and lateral confinement of the structure as well. Readers can refer to chapter 11 for the edge emitter lasers design with WAVEGUIDE.

Table 9.4.4 Layer parameters for optimized 635-nm broad-area red laser structure

# of layers =	07		
LAYER01	NLOSS= 0.00000	NREAL= 3.82357	TL= 1.00000
LAYER02	NLOSS= 0.00000	NREAL= 3.27693	TL= 1.12000
LAYER03	NLOSS= 0.00000	NREAL= 3.40423	TL= 0.10000
LAYER04	NLOSS= 0.00000	NREAL= 3.49147	TL= 0.00800
LAYER05	NLOSS= 0.00000	NREAL= 3.40423	TL= 0.10000
LAYER06	NLOSS= 0.00000	NREAL= 3.27693	TL= 1.12000
LAYER07	NLOSS= 0.00000	NREAL= 3.82357	TL= 0.05000



Chapter 10 Asymmetric Waveguide Nitride Lasers

A design of asymmetric waveguide structure for nitride laser diodes is introduced here. This chapter is based on a journal paper authored by Dr. Bour [1]. We reproduce the computation results of the optical mode in the paper for the asymmetric waveguide by using the WAVEGUIDE, which is the windows version of MODEIG. The consideration of finite n-cladding layer for the asymmetric structure is also discussed in this chapter. For infinite n-cladding layer, the total optical confinement factors are almost identical with the semi-infinite n-cladding layer.

Section 10.1 gives the introduction about the reference journal paper and the asymmetric waveguide structure. Section 10.2 describes the input file and the material system we use for the calculation of the optical mode for different cladding layer consideration. Section 10.3 demonstrates the plots of the near field and confinement factors for the asymmetric waveguide. Section 10.4 gives the conclusion of this chapter.

10.1 Introduction

The leakage current for the nitride inplane laser is one of the major concerns for the high threshold current and the sensitivity of the temperature. A good design of the waveguide structure can confine the electrons from diffusion from the active region and reduce leakage current. The shorter minority carrier diffusion length makes the nitride material laser have a different waveguide design consideration than other arsenide and phosphide laser materials.

Conventionally, a high bandgap AlGa_N is used as the tunnel barrier layer, which is placed over the active region for the confinement of the injected electrons. In reality, the decrease of hole concentrations with the increase in AlN alloy content makes the AlGa_N difficult to be an ideal tunnel barrier layer. The asymmetric waveguide structure is introduced for the confinement of electrons. In the asymmetric structure, the p-cladding layer is placed immediately next to the multiple quantum wells for the purpose of confining the electrons. From the paper [1], we can see the total confinement factor for the asymmetric structure is higher than the conventional structure. However, this chapter

will give the transverse optical mode analysis for the asymmetric waveguide structure, especially for the confinement factors.

For simplification of analysis, we assume the n-cladding layer has semi-infinite thickness as the ideal case because the number of mode solutions is more than the full epitaxial structure case. The full epitaxial structure case considers the finite n-cladding layer. This approximation of n-cladding layer is calculated for 1 μ m-thick or semi-infinite n-cladding layers.

Another assumption of this analysis is that we don't consider the QW gain and the mode loss associated with the metal contact. The optical confinement factor is not significantly affected by the absorbing of metal contact because of the low real part of refractive index with the metal.

10.1.1 Asymmetric Waveguide Structure

Table 10.1 shows the asymmetric waveguide layer structure used in this chapter. There are five quantum well layers; in addition, the p-cladding layer is located adjacent to the quantum well barrier layer. The thickness of the waveguide layer is undecided here. For the semi-infinite n-cladding layer case, there are 14 layers for the WAVEGUIDE input file. On the other hand, for the finite n-cladding layer, additional two layers will be added to the structure. From Table 10.1.1.1, we notice that the refractive index difference (Δn) between the GaN waveguide and AlGaIn cladding is about 0.05. Such a small Δn makes the laser to be insensitive to QW's asymmetry property in the structure because of the weak transverse waveguiding.

In the simulation of the asymmetric structure, we use the semi-infinite n-cladding layer as the ideal case to calculate the transverse optical field distribution. Then, we also calculate the total optical confinement for the finite n-cladding layer to compare with the semi-finite case. The total optical confinement factor values for finite cladding layer are nearly close to those computed for semi-infinite n-cladding layer.

Table 10.1.1.1 List of refractive index for the layers in the waveguide structure [1]

Layer	N	Thickness	
		Semi- ∞ case	Finite case
Sapphire	1.78	--	Semi- ∞
GaN:Si	2.51	--	4 μ m
Al _{0.07} Ga _{0.93} N:Si cladding	2.46	Semi- ∞	1 μ m
GaN:Si waveguide	2.51	t_n	t_n
In _{0.02} Ga _{0.98} N:Si barrier	2.52	6 nm	6 nm
In _{0.1} Ga _{0.9} N QW	2.56	3.5 nm	3.5 nm
In _{0.02} Ga _{0.98} N:Si barrier	2.52	6 nm	6 nm
In _{0.1} Ga _{0.9} N QW	2.56	3.5 nm	3.5 nm
In _{0.02} Ga _{0.98} N:Si barrier	2.52	6 nm	6 nm
In _{0.1} Ga _{0.9} N QW	2.56	3.5 nm	3.5 nm
In _{0.02} Ga _{0.98} N:Si barrier	2.52	6 nm	6 nm
In _{0.1} Ga _{0.9} N QW	2.56	3.5 nm	3.5 nm
In _{0.02} Ga _{0.98} N:Si barrier	2.52	6 nm	6 nm
In _{0.1} Ga _{0.9} N QW	2.56	3.5 nm	3.5 nm
In _{0.02} Ga _{0.98} N:Si barrier	2.52	6 nm	6 nm
Al _{0.07} Ga _{0.93} N:Mg Cladding	2.46	Semi- ∞	Semi- ∞

10.2 Structure Analysis

In the optical mode analysis, we use a conventional way of finding the best n-waveguide thickness for a good confinement factor of five quantum wells for the semi-infinite case. We also give the procedure of calculation of the optical confinement factor

for the finite n-cladding layer. In this section, we describe the needed parameters and procedure for the calculation of semi- ∞ and finite cladding layer.

10.2.1 Material System

Currently, the WAVEGUIDE does not have InGaN material system for the choice. Therefore, we directly use the refractive index for each layer instead of using the MATSYS function in the input file.

10.2.2 Semi-infinite cladding layer

- a. Searching for a good QZMR value

We can loop QZMR for an assumption of 0.4 μ m thickness, which might be the maximum thickness, of n-cladding layer. In the output “*.db” file, we can look for a certain block where the PHM value is less than one and the resulted QZMR converges to a certain value. The following is the sample input file.

Input:

```

-----
!CASE Parameter Set
CASE EPS1=1E-9 EPS2=1E-9 GAMEPS=1E-3 QZMR=6.5536 QZMI=0.00
CASE PRINTF=1 INITGS=0 AUTOQW=0 NFPLT=1 FFPLT=1 IL=30
!MODCON Parameter Set
MODCON KPOL=1 APB1 =0.25 APB2=0.25
!STRUCT Parameter Set
STRUCT WVL=0.4
!LAYER Parameter Set
LAYER NREAL=2.46 NLOSS=0.0 TL=20
LAYER NREAL=2.51 NLOSS=0.0 TL=0.4
LAYER NREAL=2.52 NLOSS=0.0 TL=0.006
LAYER NREAL=2.56 NLOSS=0.0 TL=0.0035
LAYER NREAL=2.52 NLOSS=0.0 TL=0.006
LAYER NREAL=2.56 NLOSS=0.0 TL=0.0035
LAYER NREAL=2.52 NLOSS=0.0 TL=0.006
LAYER NREAL=2.56 NLOSS=0.0 TL=0.0035

```

Chapter 10 Asymmetric Waveguide Nitride Lasers

```

LAYER NREAL=2.52 NLOSS=0.0 TL=0.006
LAYER NREAL=2.56 NLOSS=0.0 TL=0.0035
LAYER NREAL=2.52 NLOSS=0.0 TL=0.006
LAYER NREAL=2.56 NLOSS=0.0 TL=0.0035
LAYER NREAL=2.52 NLOSS=0.0 TL=0.006
LAYER NREAL=2.46 NLOSS=0.0 TL=20
!OUTPUT Parameter Set
OUTPUT PHMO=1 GAMMAO=1 WZRO=1 WZIO=1 QZRO=1 QZIO=1
OUTPUT FWHPNO=0 FWHPFO=0 KMO=1 ITO=1
OUTPUT SPLTFL=0 MODOUT=1 LYROUT=1
!GAMOUT Parameter Set
GAMOUT LAYGAM=4 LAYGAM=6 LAYGAM=8 LAYGAM=10
GAMOUT LAYGAM=12 LAYGAM=2 COMPGAM=0 GAMALL=1
!LOOPZ Parameter Set
LOOPZ1 ILZ='QZMR' FINV=6.0516 ZINC=-0.001
END

```

Figure 10.2.2.1 Input file of finding QZMR for semi-infinite

Output

```

-----
      QZMR          PHM          WZR          WZI
      QZR          QZI          KM          IT
6.325600E+00      6.355566E-01      2.496297E+00      5.398004E-
      17      6.231501E+00      2.695004E-16      6
6.324600E+00      6.355566E-01      2.496297E+00      -2.182691E-17
      6.231501E+00 -1.089729E-16      6      6
6.323600E+00      6.355566E-01      2.496297E+00      -5.444048E-17
      6.231501E+00 -2.717993E-16      6      6
6.322600E+00      6.355566E-01      2.496297E+00      -6.303027E-17
      6.231501E+00 -3.146846E-16      6      6
.....
6.162600E+00      6.355566E-01      2.496297E+00      1.844258E-20
      6.231501E+00 9.207635E-20      6      5
6.161600E+00      6.355566E-01      2.96297E+00      2.871621E-20
      6.231501E+00 1.433684E-19      6      5
6.160600E+00      6.355566E-01      2.496297E+00      4.381670E-20
      6.231501E+00 2.187590E-19      6      5
-----

```

Figure 10.2.2.2 “*.db” output file

b. Total confinement factors within the quantum well regions

From Figure 10.2.2.2, the converged QZMR is 6.2315. We can then use this value to find the confinement factors in the quantum well region for different n-cladding thickness. The following input file shows the looping through the n-cladding waveguide thickness to find the optimal n-cladding waveguide layer with the highest total confinement factor values.

```

-----
!CASE Parameter Set
CASE EPS1=1E-9 EPS2=1E-9 GAMEPS=1E-3 QZMR=6.2315 QZMI=0.00
CASE PRINTF=1 INITGS=0 AUTOQW=0 NFPLT=1 FFPLT=1 IL=30
!MODCON Parameter Set
MODCON KPOL=1 APB1 =0.25 APB2=0.25
!STRUCT Parameter Set
STRUCT WAVL=0.4
!LAYER Parameter Set
LAYER NREAL=2.46 NLOSS=0.0 TL=20
LAYER NREAL=2.51 NLOSS=0.0 TL=0.4
LAYER NREAL=2.52 NLOSS=0.0 TL=0.006
LAYER NREAL=2.56 NLOSS=0.0 TL=0.0035
LAYER NREAL=2.52 NLOSS=0.0 TL=0.006
LAYER NREAL=2.56 NLOSS=0.0 TL=0.0035
LAYER NREAL=2.52 NLOSS=0.0 TL=0.006
LAYER NREAL=2.56 NLOSS=0.0 TL=0.0035
LAYER NREAL=2.52 NLOSS=0.0 TL=0.006
LAYER NREAL=2.56 NLOSS=0.0 TL=0.0035
LAYER NREAL=2.52 NLOSS=0.0 TL=0.006
LAYER NREAL=2.56 NLOSS=0.0 TL=0.0035
LAYER NREAL=2.52 NLOSS=0.0 TL=0.006
LAYER NREAL=2.56 NLOSS=0.0 TL=0.0035
LAYER NREAL=2.52 NLOSS=0.0 TL=0.006
LAYER NREAL=2.46 NLOSS=0.0 TL=20
!OUTPUT Parameter Set
OUTPUT PHMO=1 GAMMAO=1 WZRO=1 WZIO=1 QZRO=1 QZIO=1
OUTPUT FWHPNO=0 FWHPFO=0 KMO=1 ITO=1
OUTPUT SPLTFL=0 MODOUT=1 LYROUT=1

```

Chapter 10 Asymmetric Waveguide Nitride Lasers

```
!GAMOUT Parameter Set
GAMOUT LAYGAM=4 LAYGAM=6 LAYGAM=8 LAYGAM=10
GAMOUT LAYGAM=12 LAYGAM=2 COMPGAM=0 GAMALL=1
!LOOPX Parameter Set
LOOPX1 ILX='TL' FINV=0.4 XINC=0.01 LAYCH=2
END
```

Figure 10.2.2.3 Input file of varied thickness for semi-infinite layer

From the generated “*.db” file, we can find the confinement factors (GAMMA(#)) for different thickness. The summation of GAMMA(4), GAMMA(6), GAMMA(8), GAMMA(10) and GAMMA(12) is the total confinement factors for the quantum well region. Figure 10.3.2.1 shows the relation of the total confinement factors with the waveguide layer thickness.

c. The input file for getting the near field plot

From Figure 10.3.2.1, we found the maximum confinement factor is at 0.09 μ m n-waveguide layer thickness. We can then fix the n-waveguide thickness to 90nm and the QZMR value to get one set of results and produce the near field data for this structure. Figure 10.2.2.4 is the input file to get the near field plot.

```
!CASE Parameter Set
CASE EPS1=1E-9 EPS2=1E-9 GAMEPS=1E-3 QZMR=6.2315 QZMI=0.00
CASE PRINTF=1 INITGS=0 AUTOQW=0 NFPLT=1 FFPLT=1 IL=30
!MODCON Parameter Set
MODCON KPOL=1 APB1 =0.25 APB2=0.25
!STRUCT Parameter Set
STRUCT WVL=0.4
!LAYER Parameter Set
LAYER NREAL=2.46 NLOSS=0.0 TL=20
LAYER NREAL=2.51 NLOSS=0.0 TL=0.09
LAYER NREAL=2.52 NLOSS=0.0 TL=0.006
LAYER NREAL=2.56 NLOSS=0.0 TL=0.0035
LAYER NREAL=2.52 NLOSS=0.0 TL=0.006
LAYER NREAL=2.56 NLOSS=0.0 TL=0.0035
LAYER NREAL=2.52 NLOSS=0.0 TL=0.006
```

```

LAYER NREAL=2.56 NLOSS=0.0 TL=0.0035
LAYER NREAL=2.52 NLOSS=0.0 TL=0.006
LAYER NREAL=2.56 NLOSS=0.0 TL=0.0035
LAYER NREAL=2.52 NLOSS=0.0 TL=0.006
LAYER NREAL=2.56 NLOSS=0.0 TL=0.0035
LAYER NREAL=2.52 NLOSS=0.0 TL=0.006
LAYER NREAL=2.46 NLOSS=0.0 TL=20
!OUTPUT Parameter Set
OUTPUT PHMO=1 GAMMAO=1 WZRO=1 WZIO=1 QZRO=1 QZIO=1
OUTPUT FWHPNO=0 FWHPFO=0 KMO=1 ITO=1
OUTPUT SPLTFL=0 MODOUT=1 LYROUT=1
!GAMOUT Parameter Set
GAMOUT LAYGAM=4 LAYGAM=6 LAYGAM=8 LAYGAM=10
GAMOUT LAYGAM=12 LAYGAM=2 COMPGAM=0 GAMALL=1
-----

```

Figure 10.2.2.4 Input file at thickness of 0.09 μ m

No looping in this input file. The output file, “*.nf”, gives the near field intensity (NFINT) and the position (XXFT) information. Figure 10.3.1.1 shows this plot. The above method of finding the relation of confinement factor and n-waveguide thickness is good for the structure without leakage wave into the outside of active region. As an alternative, users can try to loop the n-waveguide layer and QZMR at the same time. In this method, if smaller steps are used in the looping, the computation will consume more time and memory. User should be careful about using this method. We do not recommend users to use this method for a bounded mode waveguide structure. An example of QZMR value for the semi-infinite cladding layer, 6.3186, can be obtained by looping the thickness and QZMR at the same time. Next section, we will apply this method for finite n-cladding layer which contain standing wave in the structure.

10.2.3 Finite n-cladding layer

For the comparison to the semi-infinite n-cladding layer, we use a finite n-cladding layer of thickness 1 μ m, add a GaN:Si layer of thickness 4 μ m and make the sapphire layer to be semi-infinite for the finite n-cladding layer structure. In this structure, the total layer becomes 14 layers. This finite n-cladding layer is more close to a full epi-structure.

a. Finding QZMR

The addition of the thick GaN layer makes this structure a leakage structure which causes the difficulty of finding an initial QZMR guess if we follow the previous procedure of semi-finite structure. By using the previous method, the PHM value is difficult to be less than one for all different thickness. Even though some QZMR has a KM value of 7, we found that light is confined mostly in the GaN layer not in waveguide or active layers in this case. Light leaks out into the GaN layer. From the above observations, which cannot satisfy our laser design, we need to find some quasi-leaky modes that can confine most of the light in the waveguide and active layer. From looping the QZMR value from lowest to highest at the maximum n-waveguide thickness, we found that at some range of QZMR the structure has a high loss value. However, since we know that the structure should not be very lossy, we choose the QZMR range with very low loss as the start point. The QZMR ranges from 6.07 to 6.3, which is the similar QZMR range for the semi-finite structure with different n-waveguide layer thickness. Figure 10.2.3.1 and 10.2.3.2 is the input file and partial output values.

```

-----
!CASE Parameter Set
CASE EPS1=1E-9 EPS2=1E-9 GAMEPS=1E-3 QZMR=6.5536 QZMI=0.00
CASE PRINTF=1 INITGS=0 AUTOQW=0 NFPLT=1 FFPLT=1 IL=30
!MODCON Parameter Set
MODCON KPOL=1 APB1 =0.25 APB2=0.25
!STRUCT Parameter Set
STRUCT WVL=0.4
!LAYER Parameter Set
LAYER NREAL=1.78 NLOSS=0.0 TL=20
LAYER NREAL=2.51 NLOSS=0.0 TL=4
LAYER NREAL=2.46 NLOSS=0.0 TL=1
LAYER NREAL=2.51 NLOSS=0.0 TL=0.4
LAYER NREAL=2.52 NLOSS=0.0 TL=0.006
LAYER NREAL=2.56 NLOSS=0.0 TL=0.0035
LAYER NREAL=2.52 NLOSS=0.0 TL=0.006
LAYER NREAL=2.56 NLOSS=0.0 TL=0.0035
LAYER NREAL=2.52 NLOSS=0.0 TL=0.006

```



```

LAYER NREAL=2.56 NLOSS=0.0 TL=0.0035
LAYER NREAL=2.52 NLOSS=0.0 TL=0.006
LAYER NREAL=2.56 NLOSS=0.0 TL=0.0035
LAYER NREAL=2.52 NLOSS=0.0 TL=0.006
LAYER NREAL=2.56 NLOSS=0.0 TL=0.0035
LAYER NREAL=2.52 NLOSS=0.0 TL=0.006
LAYER NREAL=2.46 NLOSS=0.0 TL=20
!OUTPUT Parameter Set
OUTPUT PHMO=1 GAMMAO=1 WZRO=1 WZIO=1 QZRO=1 QZIO=1
OUTPUT FWHPNO=0 FWHPFO=0 KMO=1 ITO=1
OUTPUT SPLTFL=0 MODOUT=1 LYROUT=1
!GAMOUT Parameter Set
GAMOUT LAYGAM=4 LAYGAM=6 LAYGAM=8 LAYGAM=10
GAMOUT LAYGAM=12 LAYGAM=14 COMPGAM=0 GAMALL=1
!LOOPZ Parameter Set
LOOPZ1 ILZ='QZMR' FINV=3.1684 ZINC=-0.01
END

```

Figure 10.2.3.1 Input file

```

-----
          QZMR              PHM              WZR              WZI
QZR              QZI              KM              IT
          6.323600E+00    5.384547E+00  2.498514E+00    -1.250029E-21
6.242573E+00      -6.246430E-21              6              30
          6.313600E+00    4.323808E+00  2.502647E+00    -3.539787E-20
6.263244E+00      -1.771768E-19              6              23
          6.303600E+00    2.201863E+00  2.508162E+00    -1.053702E-20
6.290874E+00      -5.285709E-20              6              13
          .....
          6.073600E+00    1.061256E+01  2.464580E+00    -1.661331E-18
6.074157E+00      -8.188970E-18              5              3
          6.063600E+00    1.080366E+01  2.462906E+00    -1.502795E-18
6.065908E+00      -7.402486E-18              5              4

```

```

        6.053600E+00  1.061256E+01  2.464580E+00  -1.892112E-16
6.074157E+00      -9.326526E-16                5                6

```

Figure 10.2.3.2 Output data

For the convenience purpose, we will not put the input file for the rest of input and output file description. The major part of input file is similar to Figure 10.2.3.1 except for the different value of QZMR, initial TL value for waveguide layer and LOOP parameters. We will address the corresponding values of the above variables for running the rest of the simulation.

If we check the range of QZMR values with the resulted QZMR value from the semi- ∞ case for different n-waveguide thickness, we find that the QZMR value for semi- ∞ case is from 6.23 to 6.07, which is in the range from the result of figure 10.2.3.2. We assume that the modal effective index value might be close to the semi- ∞ case. Therefore, we can use the range 6.23 to 6.07 be our initial guess range. After choosing the QZMR range, we need to have some initial guess points of QZMR value to start with. Here, we introduce a method of looping the QZMR and n-waveguide layer thickness at the same time to find a converged QZMR values as our starting point. As mentioned before, this method is not recommended by regular usage of non-leaky waveguide structure. If the computer speed and memory is not quick or large enough, users can loop through a smaller interval of thickness and QZMR.

Table 10.2.3.1 Input file parameters

	Parameters
Initial guess QZMR	QZMR=6.23
n-waveguide (4 th) layer parameter LAYER	TL=0.4
LOOPX1	ILX='TL' FINV=0.01 XINC=-.01 LAYCH=4
LOOPZ1	FINV=6.06 ZINC=-0.01

From the “*.db” file, we can find about 9 converged QZMR points. We use the QZMR of semi-infinite structure as the range reference and then chose 6.116, 6.154, 6.188, 6.217 and 6.242 as our QZMR guess value for looping through the n-waveguide layer. From latter analysis, we can see these QZMRs are related to the resonant outcoupling occurrences at a certain n-waveguide thickness.

b. Looping of n-waveguide layer

In this step, we only loop through the n-waveguide layer with the initial QZMR values from part a. For the first point, 6.116, we use “**QZMR=6.12**” and looping through the n-waveguide thickness from 0.4um to 0.001um. The “*.db” file gives a result of confinement factor for each layer. From this “*.db” file, we find that at certain range of thickness, from 0.001um to 0.076um, the total confinement has some significant values and the resulted QZMR value changes with the thickness in this range. On the other hand, for the section of the small, almost zero, total confinement value, the QZMR values, which has the value of 6.1155, are almost the same for different thickness. At this point, we know that the relation of the total confinement factors with the waveguide thickness might not be a smooth line.

We loop the thickness from 0.001um to 0.4um for the same “**QZMR=6.12**”. The total confinement factor that is larger than $4.5E-4$ occurs at different section of thickness range, about from 0.067um to 0.144um. From these two runs of same QZMR but different thickness looping order, we get the total confinement factor in the thickness range from 0.001um to around 0.144um. We then repeated the same operations with the other four points. For the point, “**QZMR=6.23**”, we found the total confinement factors with significant values in the range of 0.4um to 0.33um. For the other three initial QZMR values, most of the total confinement values are about $10E-7$ except for one thickness point which is the resonant point with $>4.5E-4$ confinement factor. These resonant points happen at 0.26 um and 0.33um. From these results, the confinement vs. thickness curve exists four resonant point at around 0.076um, 0.144um, 0.26um and 0.33um.

c. Searching for a new QZMR value

Till this point, we have found three segments for the confinement factor verse n-waveguide thickness curve. For finding the other two segments, we need to find a new initial QZMR values. We repeat the procedure of a. to loop through the QZMR and thickness at the same time with small looping step. The looping steps, XINC and ZINC, change from 0.01 to 0.001. We run this operation for different segments, which are from 0.144um to 0.26um and 0.26um to 0.33um. Table 10.2.3.2 shows the QZMR and thickness parameters we use for these two operations. The rest of the input file is the same with Figure 10.2.2.1.

Table 10.2.3.2 QZMR and layer thickness

	0.144~0.26 um	0.26~0.33um
Initial guess QZMR	QZMR=6.11	QZMR=6.19
n-waveguide (4 th) layer parameter LAYER	TL=0.2	TL=0.328
LOOPX1	ILX='TL' FINV=0.14 XINC=-.001 LAYCH=4	ILX='TL' FINV=0.2 XINC=-.001 LAYCH=4
LOOPZ1	FINV=6.17 ZINC=0.001	FINV=6.22 ZINC=0.001

After the simulation, we get the desired total confinement factor varied with the thickness for some good initial QZMR guess values. All information now can be combined to plot the total confinement factors vary with n-waveguide thickness as Figure 10.3.2.1.

The basic idea of finding the quasi-leaky mode with the total confinement of mode profile within the active region is the choice of initial QZMR value for looping the n-waveguide thickness. Figure 10.2.3.3 shows the process flow. This figure gives a schematic view of the previous description of finding the quasi-leaky mode that has zero loss and field is mostly confined in the active region.

Users can also try to pick some QZMR values from the semi-finite layer case to run for the looping of the n-waveguide thickness to get the similar result because we expect the finite case has the similar modal effective index. With good luck, Users might be able to get the answer within a few guess of QZMR value. A good initial QZMR value

might need to have three digits precision after the decimal point. This means that the users can end up with 1000 times QZMR guess, if in bad luck. However, the above operations, from step a to step c, can give users more systematic procedure to find quasi-leaky mode solutions from WAVEGUIDE.

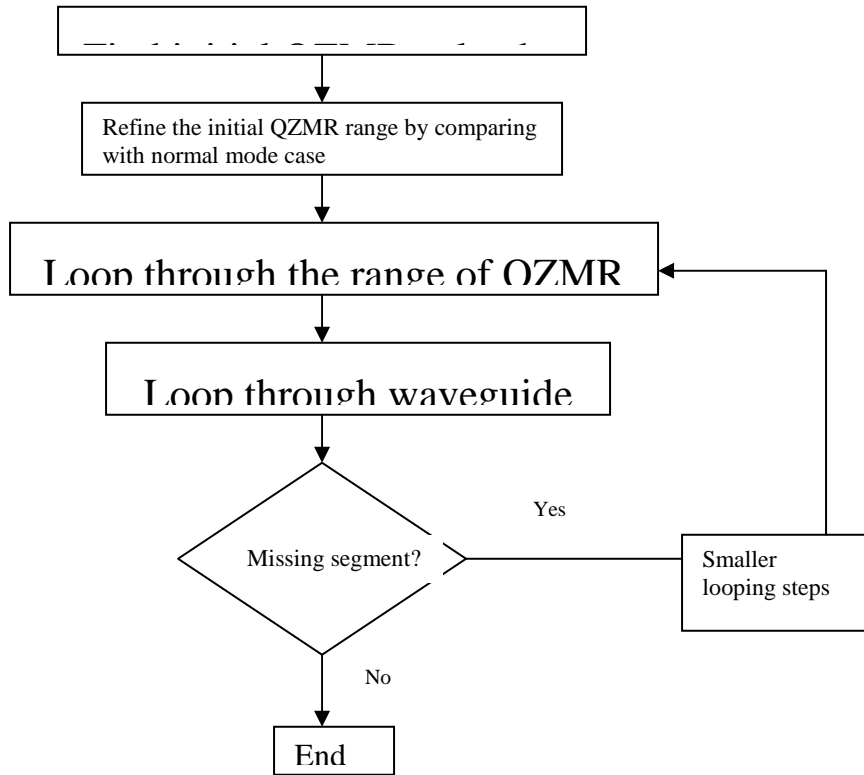


Figure 10.2.3.3 Process flow for the finite n-cladding case.

10.3 Output Plots

A near field plot for the optimized structure is provided in this section. We also analyze the effect of n-waveguide thickness on confinement factor.

10.3.1 Near field

Figure 10.3.1.1 shows the near field intensity plot verse the layer structure distance and the layer refractive index structure for the semi-infinite n-cladding layer and the waveguide thickness is 90nm. The total confinement factor for five quantum wells is

5.3%. Even though the QWs are displaced from the peak of the mode, the total confinement factor is not degraded much. The total confinement factor still exceeds the confinement factor for the conventional structure with AlGaIn layer[1].

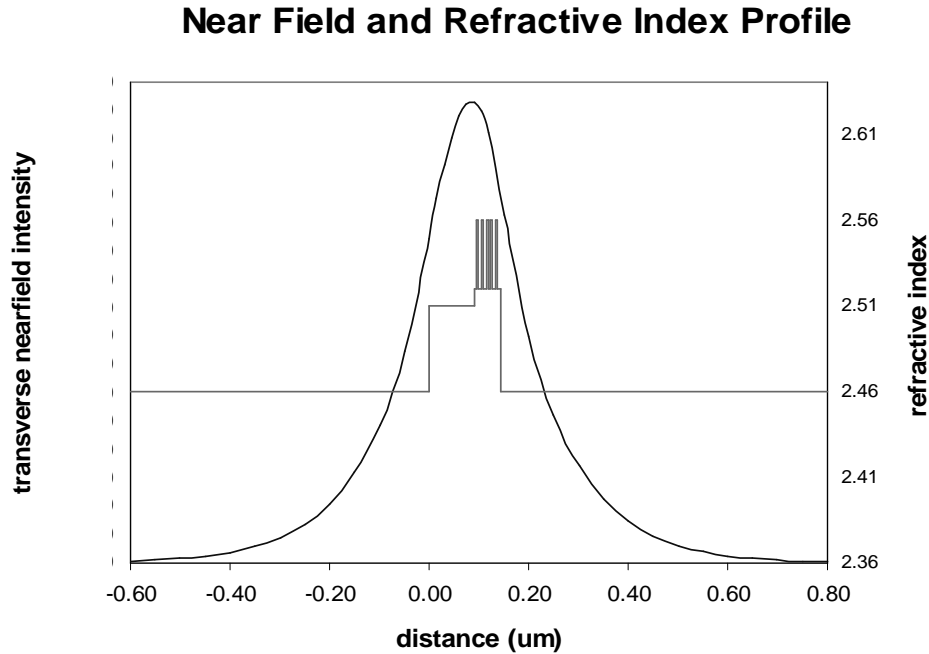


Figure 10.3.1.1 Optical mode intensity profile and refractive index for semi- ∞ at 0.09um. After [1]

10.3.2 Confinement factor for semi- ∞ and finite cladding layer

. By looping the waveguide thickness, we find that the highest confinement factor happens at waveguide thickness=90nm. From Figure 10.3.2.1, we also compare the confinement factor for the finite n-cladding layer case. Both cases have the almost identical confinement factor except for several resonant points where the confinement factor has the lowest value. From Figure 10.3.2.2, we can find the field profile for both cases. The finite case has some light leaks out from the waveguide cladding layer at the resonance point where the waveguide thickness is 0.144um. When we plot Figure 10.3.2.2, we can use “DXIN=0.01” to refine the field solution and get a better resonant field.

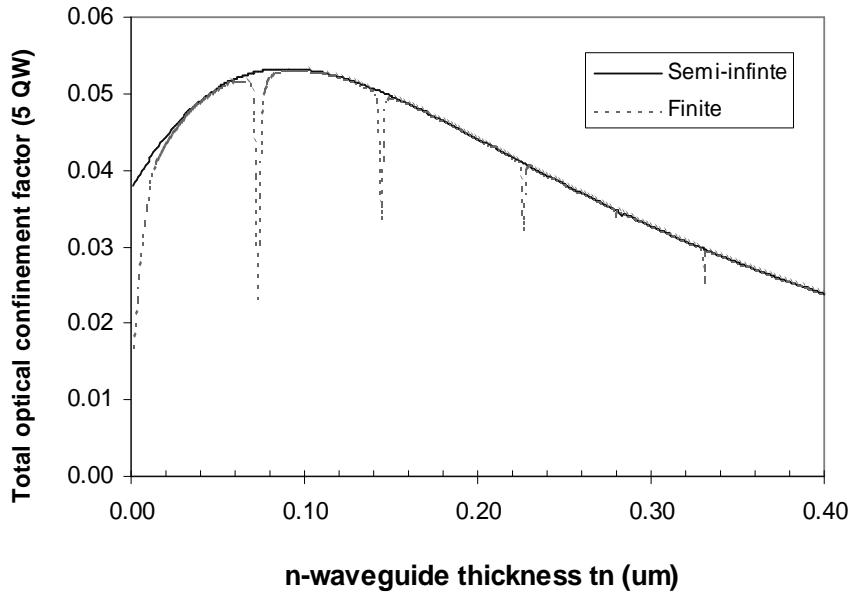


Figure 10.3.2.1 Total confinement factor for finite and semi- ∞ n-cladding layer. After [1]

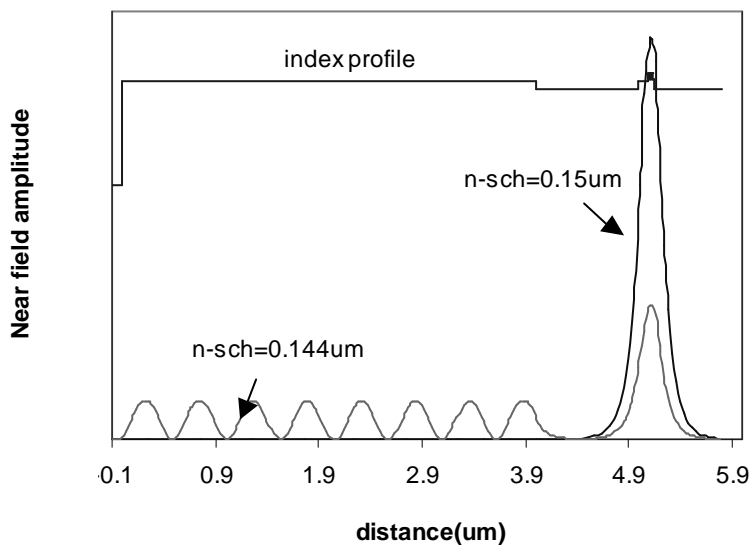


Figure 10.3.2.2 Near field plot for finite n-cladding layer structure at different n-sch thickness. After [1]

10.4 Conclusion

We give the analysis of asymmetry waveguide structure for nitride laser by using WAVEGUIDE. In the analysis of the structure, the assumption of the semi-infinite n-cladding layer obtains almost the same confinement factor result for the more realistic finite n-cladding layer except for some resonance points in the finite cladding layer case. The resonance points reproduced here give the agreement of the resonance points in the paper. These resonance points can be eliminated by using thick AlGa_N:Si instead of GaN:Si.

Reference

[1] D.P.Bour, M.Kneissl, C.G. Van de Walle, G.A. Evans, L.T.Romano, J.Northrup, M.Teepe, R.Wood, T.Schmidt, S.Schoffberger, and N.M.Johnson, "Design and performance of asymmetric waveguide nitride laser diodes", IEEE Journal of Quantum Electronics, vol 36, no. 2, pp184-191, 2000.

Chapter 11 Design a Ridge Waveguide Laser Using WAVEGUIDE Program

Chapter 11 mainly focuses on how to design a ridge waveguide laser using WAVEGUIDE Program. As index-guided lasers, ridge waveguide lasers have the advantages of high confinement factor, high quantum efficiency, low threshold current density, single-mode- operation, and good temperature performance [1].

Figure 11.1.1 illustrates a ridge waveguide laser with cleaved facets. Wave propagates in the z direction, and the laser is a Fabry-Perot laser formed by the resonance cavity and the two cleaved facets as reflective mirrors. In the transverse plane (xy plane), the material compositions in ridge region and channel regions are different, and accordingly the effective refractive indices of the fundamental mode in the regions are different, which is equivalent to a three-layer-dielectric waveguide. By careful design, single-lateral-mode operation of a ridge waveguide laser can be achieved.

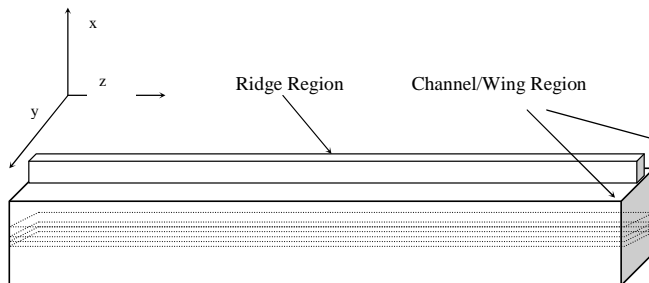


Figure 11.1.1 A ridge waveguide laser

In this chapter, an outline and explanations of how to design a ridge waveguide laser using WAVEGUIDE program are presented first in Section 11.1, including the design of a basic waveguide laser, optimization of the position of an etch stop layer, and considerations in determining ridge width and channel width.

Then an example to design a ridge waveguide multi-quantum-well laser using WAVEGUIDE program is provided in the section 11.2. The design steps outlined and

explained in Section 11.1 are demonstrated by the example with simulation details. And in the end, a summary of the chapter is provided.

11.1 Outline and explanations of the design

In this chapter, an example is provided to illustrate how to design a ridge waveguide laser using WAVEGUIDE program. In the example, the quantum well structure of AlGaInAs material systems with peak lasing wavelength at 1.52 μ m on InP substrate is used, which is designed in the Appendix C.4 of GAIN Program User's Manual [2]. The quantum well structure is shown in Table 11.1.1. In simulations of the GAIN program, the cladding layers are equivalent to the inner cladding layers in the WAVEGUIDE program, which have infinite thicknesses in the GAIN program as outermost layers.

Table 11.1.1 the quantum well structure designed in the Appendix C.4 of GAIN program User's Manual.

Layer	Material Composition	Strain	Thickness (Å)
QW (Ga _x Al _y In _{1-x-y} As)	x = 0.22, y = 0.08	-0.011705	60
Barrier (Ga _x Al _y In _{1-x-y} As)	x = 0.35, y = 0.25	0.0087769	50
Cladding (Ga _x Al _y In _{1-x-y} As)	x = 0, y = 0.48		100

The design of a ridge waveguide laser is summarized into several steps. The first step is to design a basic waveguide, which is explained in section 11.1.1, and the design details corresponding to this step is provided in section 11.2.1. Second, the position of a etch stop layer is optimized to achieve the required lateral effective refractive index difference, as is explained in section 11.1.2 and 11.2.2. Third, the channel width and ridge width are designed to maintain single-lateral-mode and low loss, which is discussed in section 11.1.3 and 11.2.3.

11.1.1 Design a basic waveguide laser

A typical basic waveguide laser is composed of active layers, including quantum wells and barriers, and passive layers, including SCH layers, inner cladding layers, outer cladding layers, n- substrate, and p- cap. As we already have a designed quantum well structure, we can start with a design of a basic waveguide laser. The active region of the

designed ridge waveguide laser in our example is made of six quantum wells using the quantum well laser design in the GAIN program [2], shown in Table 11.1.1. Besides the quantum wells, the waveguide structure of a basic waveguide laser is composed of two SCH layers, two inner cladding layers, two outer cladding layers, n- substrate, and p- cap. Figure 11.1.2 shows the refractive index profile of a basic waveguide laser in x direction defined in Figure 11.1.1, illustrating the layers of the waveguide laser structure mentioned above.

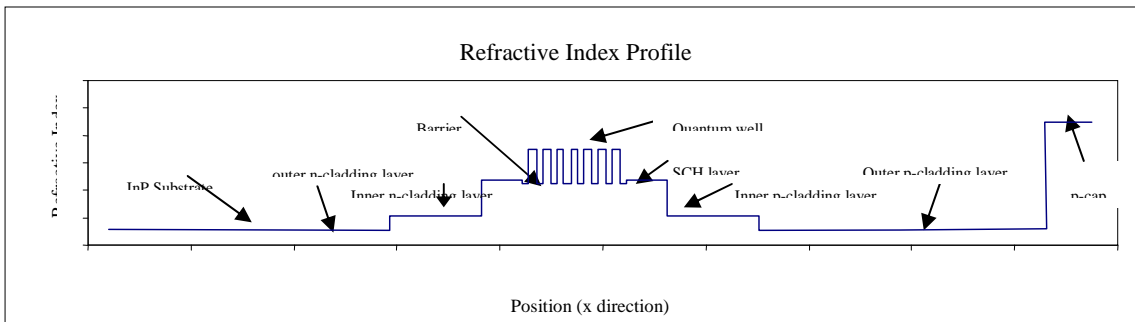


Figure 11.1.2 Refractive index profile of a waveguide laser

The material compositions and thicknesses of quantum wells and barriers have already been designed in the GAIN program, so we can use them in WAVEGUIDE program. The inner n-cladding layer and inner p-cladding layer are n and p doped $\text{Al}_{0.48}\text{In}_{0.52}\text{As}$ as designed in the GAIN program. The outer n- and p- cladding layers are made of n- and p- doped InP respectively. In the WAVEGUIDE program, we can optimize the thicknesses of SCH layers, inner cladding layers, and outer cladding layers to achieve high confinement factor, low loss, and narrow far-field divergence.

From Figure 11.1.2, we can find that p-cap is the top layer of the ridge of the laser. Usually, for AlGaInAs material system on InP substrate, highly doped InGaAs is used as p-cap to reduce sheet resistance of the laser and the thickness is usually 0.1-0.2 μm . As explained in the previous chapters, the two outermost layers, n-substrate and p-cap in our case, are deemed infinite thick in WAVEGUIDE program. Usually, the substrate thickness is not critical to the waveguide structure of a laser, so it is not simulated in this example. If users want to simulate the thicknesses of p-cap and n-substrate, it is advised that p- and n- metal material be added beyond them as outermost layers, and sometimes, to be simple, air can be used for simulations instead of p- and n- metal.

After description of a basic waveguide laser structure, it is clear that the thicknesses of SCH layers, inner cladding layers, and outer cladding layers need to be simulated in the WAVEGUIDE program. In our example, we simulate SCH layer thickness first, and then inner cladding layer thickness, and outer cladding layer thickness. The details will be provided in Section 11.2.1

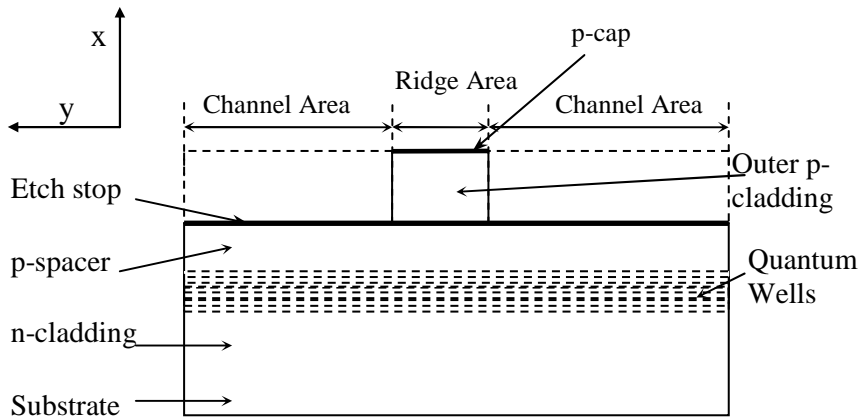


Figure 11.1.3 Diagram of the cross section of a ridge waveguide laser

11.1.2 Position of an etch stop layer: Δn_{eff} vs. p-spacer thickness

Figure 11.1.3 shows the side view (transverse view) of a ridge waveguide laser. In order to fabricate the ridge, an etch stop layer is added in the p-cladding layer of the basic waveguide laser. As shown in Figure 11.1.3, by addition of the etch stop layer, the p-cladding layer is divided into two parts called p-spacer layer and outer p-cladding layer respectively. The layer compositions in the ridge area and channel area are different, resulting in different effective refractive indices in the two regions, n_{eff} and n_{eff}^* .

The refractive index profiles in the channel region (also called wing region) and in the ridge region are illustrated in Figure 11.1.4 and 11.1.5. In the wing region, a thin dielectric layer such as Si_3N_4 is deposited on top of the p-spacer layer for insulation.

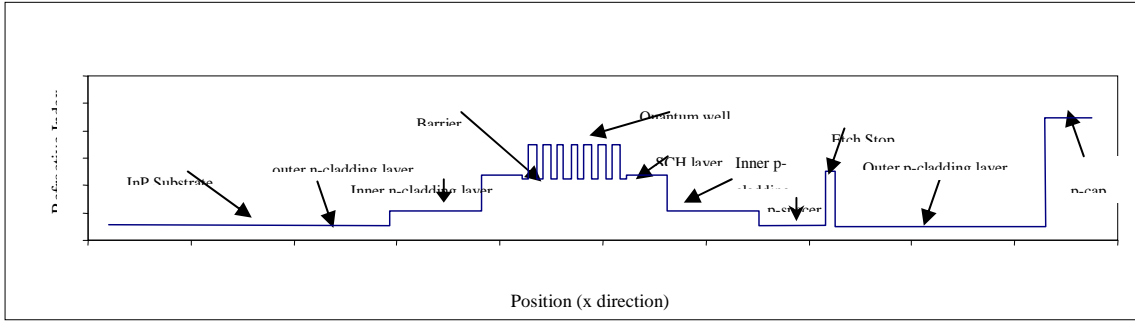


Figure 11.1.4 Refractive index profiles in the channel region

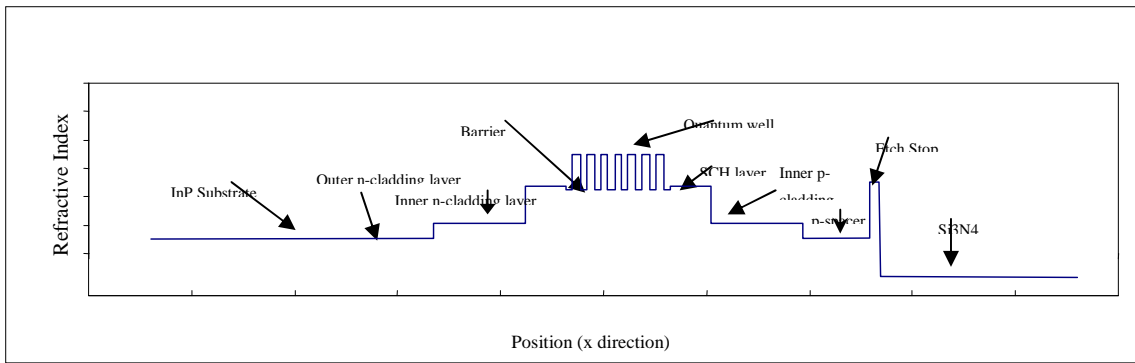


Figure 11.1.5 Refractive index profiles in the ridge region

The layer thickness of the p-spacer, indicating the position of etch stop, influence the effective refractive indices and therefore the difference between them, Δn_{eff} . In addition, the position of an etch stop layer affects the far-field divergence of the ridge waveguide laser. Consequently, knowing the desired or acceptable Δn_{eff} and far-field divergence, the position of the etch stop layer can be determined. The details of simulations will be provided in Section 11.2.2.

11.1.3 Determine ridge width and channel width.

In addition to the design of a ridge waveguide laser discussed in section 11.1.1 and 11.1.2, the ridge width and channel width need to be designed. As shown in Figure 11.1.3, 11.1.4, and 11.1.5, the effective refractive indices in the ridge region and channel regions are different. Therefore, in y direction of the transverse plane shown in Figure 11.1.3, the ridge waveguide laser is equivalent to a three-layer dielectric slab waveguide

with the refractive indices of the core layer (center layer) and the cladding layers (outer layers) equal to the effective refractive indices of the ridge and channel regions respectively, n_{eff} and n_{eff}' , as illustrated in Figure 11.1.6.

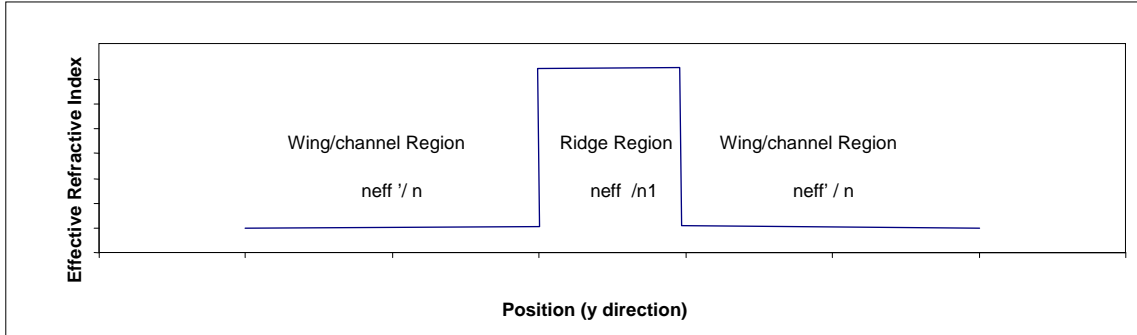


Figure 11.1.6 Refractive index profile of the equivalent three-layer dielectric slab waveguide

Ridge Width

As we know, by solving Maxwell equations and matching boundary conditions of the three-layer dielectric slab waveguide, the graphical solutions can be found for Equation 11.1, 11.2, and 11.3 for TE polarization [1].

$$\alpha \frac{d}{2} = \frac{\mu}{\mu_1} \left(k_x \frac{d}{2} \right) \tan \left(k_x \frac{d}{2} \right) \text{ for even modes (Equation 11.1)}$$

$$\alpha \frac{d}{2} = -\frac{\mu}{\mu_1} \left(k_x \frac{d}{2} \right) \cot \left(k_x \frac{d}{2} \right) \text{ for odd modes (Equation 11.2)}$$

$$\left(\alpha \frac{d}{2} \right)^2 + \left(k_x \frac{d}{2} \right)^2 = \omega^2 (\mu_1 \epsilon_1 - \mu \epsilon) \left(\frac{d}{2} \right)^2 \text{ (Equation 11.3)}$$

where α is the decay constant in the cladding layer I and III as shown in Figure 11.1.7, k_x is the x component of k in the core layer II, d is the thickness of the core layer II, μ and ϵ are the permeability and permittivity of layer I and III, and μ_1 and ϵ_1 are the permeability and permittivity of layer II, ω is the angular momentum of the modes in layer II.

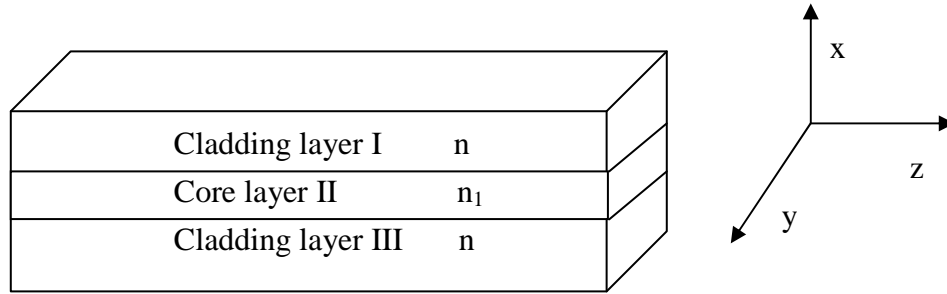


Figure 11.1.7 Diagram of a three-layer dielectric slab waveguide

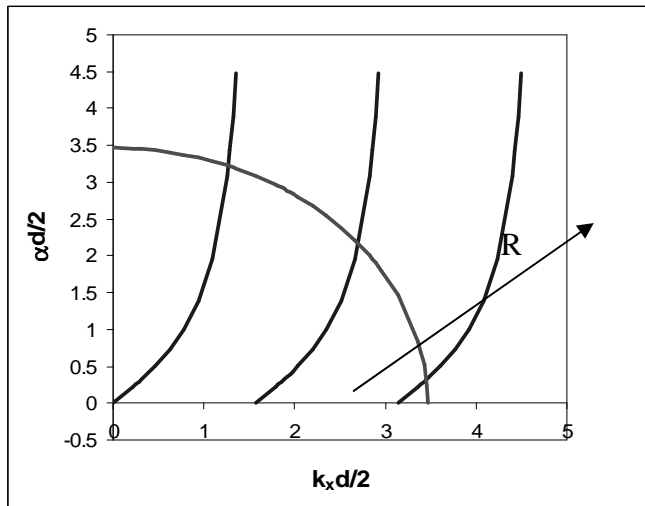


Figure 11.1.8 A graphical solution to the Equations 11.1.1-11.1.3

for a three-layer dielectric slab waveguide

As shown Figure 11.1.8, the number of modes allowed to propagate in the three-layer dielectric slab waveguide is determined by the radius of the quarter circle R, which

is $R = \left(k_x \frac{d}{2}\right) \sqrt{n_1^2 - n^2} < \frac{\pi}{2}$. Therefore, the cutoff condition for the 1st TE mode TE₁ is

derived as $d < \frac{\lambda}{2\sqrt{n_1^2 - n^2}}$ (Equation 11.4). In other words, only one mode, TE₀ mode,

can propagate for the 3-layer dielectric waveguide with the core thickness (ridge width) that meets the condition set by Equation 11.4.

Accordingly, the maximum ridge width for the designed ridge waveguide laser to maintain single-TE-mode operation can be calculated by Equation 11.4. The details of how to determine the ridge width is provided in section 11.2.3.1.

Wing/Channel Width

In order to determine the wing/channel width, we simulate a five-layer dielectric waveguide as shown in Figure 11.1.8. In this way, minimum separation between ridges can be simulated in the WAVEGUIDE program by observing the loss variation as a function of channel width. If the ridges are too close to one another, the effects of neighboring ridges are not negligible, and accordingly the loss of the fundamental mode is huge. On the other hand, if the ridges are far enough, their effects to one another are negligible so that it is equivalent to a three-layer dielectric slab waveguide. Hence, in this step, the channel width is chosen by looping channel width to observe loss variation as a function of channel width. The details of simulations are discussed in section 11.2.3.2.

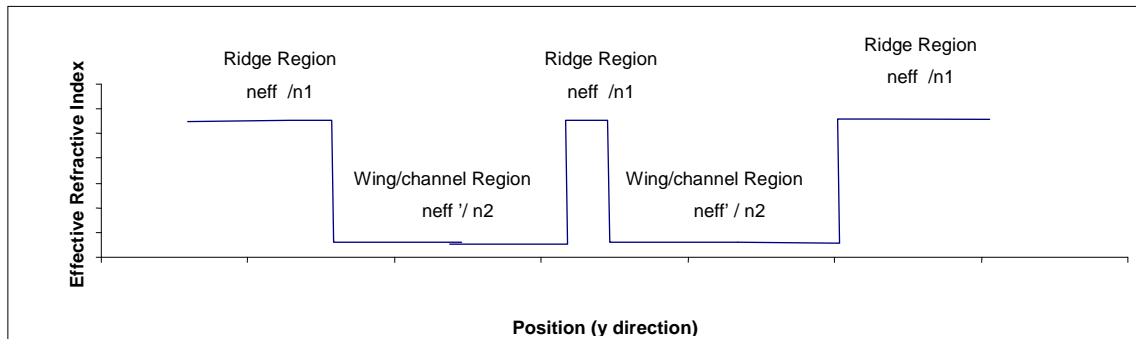


Figure 11.1.8 Refractive index profile of the equivalent five-layer dielectric waveguide

11.2 Simulations details for the design of a ridge waveguide laser using WAVEGUIDE program

After discussion and overview of the ridge waveguide laser design in section 11.1, the details of simulations using WAVEGUIDE program will be provided in this section. Input and output files will be discussed to demonstrate how to optimize layer thicknesses. As discussed in 11.1, we begin with the design of a basic waveguide laser structure.

11.2.1 Design of a basic waveguide laser

11.2.1.1 Optimization of SCH layer thickness

First, we need to optimize the thicknesses of the two SCH layers. Usually, we choose the same thickness for the two SCH layers. As illustrated in Figure 11.1.2, the layer structure of the designed laser includes quantum well and barrier layers, SCH layers, n- and p-cladding layers, n- substrate, and p- cap.

Quantum well and barrier layer thicknesses have been designed using GAIN program, which is shown in Table 11.1.1. As a start, we first give guess thicknesses to the other layers according to experience and find the effective refractive index of the fundamental mode. The initial laser structure is listed in Table 11.2.1. And after that, we loop the thicknesses of the two SCH layers simultaneously to study the variation of confinement factor and far-field divergence with the variation of the SCH layer thickness.

Table 11.2.1 Layer composition and thickness table for the initial structure of the designed basic waveguide laser

Layer	Material Composition	Layer Thickness (TL) (um)
n-substrate	InP	200
Outer n-cladding	InP	2
Inner n-cladding layer	Al _{0.48} In _{0.54} As	0.5
SCH layer	Al _{0.24} In _{0.24} As	0.5
Barrier	Al _{0.25} Ga _{0.35} In _{0.4} As	0.005
Quantum well	Al _{0.08} Ga _{0.22} In _{0.7} As	0.006
Barrier	Al _{0.25} Ga _{0.35} In _{0.4} As	0.005
Quantum well	Al _{0.08} Ga _{0.22} In _{0.7} As	0.006
Barrier	Al _{0.25} Ga _{0.35} In _{0.4} As	0.005
Quantum well	Al _{0.08} Ga _{0.22} In _{0.7} As	0.006
Barrier	Al _{0.25} Ga _{0.35} In _{0.4} As	0.005
Quantum well	Al _{0.08} Ga _{0.22} In _{0.7} As	0.006
Barrier	Al _{0.25} Ga _{0.35} In _{0.4} As	0.005
Quantum well	Al _{0.08} Ga _{0.22} In _{0.7} As	0.006
Barrier	Al _{0.25} Ga _{0.35} In _{0.4} As	0.005
Quantum well	Al _{0.08} Ga _{0.22} In _{0.7} As	0.006

Chapter 11 Design a Ridge Waveguide Laser Using WAVEGUIDE Program

barrier	Al _{0.25} Ga _{0.35} In _{0.4} As	0.005
SCH layer	Al _{0.24} In _{0.24} As	0.5
Inner p-cladding layer	Al _{0.48} In _{0.54} As	0.5
Outer p-cladding	InP	2
p-cap	InP	0.

As instructed in Chapter 2, we can generate input file using WIFE or modifying existing input file and then loop for QZMR to find the effective refractive index of the fundamental mode. After finding good QZMR, which is 10.95964, we loop the thicknesses of SCH layers (layer 4 and layer 18) from 0.5 um to 0.01 um at an increment of -0.01 um simultaneously. The input file is listed in Table 11.2.2. After evaluation of the input file, we can plot total confinement factor of six quantum wells and far-field divergence (FWHM) contained in .db file as a function of SCH layer thickness, as shown in Figure 11.2.1.

Table 11.2.2 Input file to optimize SCH layer thicknesses

```

CASE KASE=AlGaInAs (6 wells)
CASE  EPS1=1E-8 EPS2=1E-8 GAMEPS=1E-6
CASE  QZMR= 10.95964 QZMI=0.0
CASE  PRINTF=0 INITGS=0 AUTOQW=0 NFPLT=1  FFPLT=1

!CASE  DXIN=0.2
!CASE  IL=100 KGSS=1
MODCON KPOL=1  APB1=0.25  APB2=0.25

STRUCT  WV=1.55

LAYER  MATSYS=1 XPERC=0.0 YPERC=0.0 TL=200.0 !n-substrate
LAYER  MATSYS=1 XPERC=0.0 YPERC=0.0 TL=2.0 !n-cladding

LAYER  MATSYS=13 XPERC=0.48 YPERC=0.0 TL=0.5 !n-inner-cladding
LAYER  MATSYS=13 XPERC=0.24 YPERC=0.24 TL=0.5 !sch

LAYER  MATSYS=13 XPERC=0.25 YPERC=0.35 TL=0.005 !barrier
LAYER  MATSYS=13 XPERC=0.08 YPERC=0.22 TL=0.006 !Q-well
LAYER  MATSYS=13 XPERC=0.25 YPERC=0.35 TL=0.005 !barrier
LAYER  MATSYS=13 XPERC=0.08 YPERC=0.22 TL=0.006 !Q-well
LAYER  MATSYS=13 XPERC=0.25 YPERC=0.35 TL=0.005 !barrier
LAYER  MATSYS=13 XPERC=0.08 YPERC=0.22 TL=0.006 !Q-well
LAYER  MATSYS=13 XPERC=0.25 YPERC=0.35 TL=0.005 !barrier
LAYER  MATSYS=13 XPERC=0.08 YPERC=0.22 TL=0.006 !Q-well
LAYER  MATSYS=13 XPERC=0.25 YPERC=0.35 TL=0.005 !barrier
LAYER  MATSYS=13 XPERC=0.08 YPERC=0.22 TL=0.006 !Q-well
LAYER  MATSYS=13 XPERC=0.25 YPERC=0.35 TL=0.005 !barrier
LAYER  MATSYS=13 XPERC=0.08 YPERC=0.22 TL=0.006 !Q-well
LAYER  MATSYS=13 XPERC=0.25 YPERC=0.35 TL=0.005 !barrier

LAYER  MATSYS=13 XPERC=0.24 YPERC=0.24 TL=0.5 !sch
LAYER  MATSYS=13 XPERC=0.48 YPERC=0.0 TL=0.5 !p-inner-cladding

LAYER  MATSYS=1 XPERC=0.0 YPERC=0.0 TL=2.0 !p-cladding

```

11.2 Simulation details for the design of a ridge waveguide laser using WAVEGUIDE

```
LAYER NREAL=3.65 NLOSS=0.0 TL=0.2 !P-cap. InGaAs n from website Adachi's model

OUTPUT PHMO=1 GAMMAO=1 WZRO=1 WZIO=1 QZRO=1 QZIO=0
OUTPUT FWHPNO=0 FWHPFO=1 KMO=1 ITO=1
OUTPUT MODOUT=1 LYROUT=1 SPLTFL=0
GAMOUT LAYGAM=5,7,9,11,13,15 COMPGAM=0 GAMALL=0

!LOOPZ1 ILZ='WVL' FINV=1.33 ZINC=0.005
!LOOPZ1 ILZ='QZMR' FINV=10.0 ZINC=-0.01
LOOPX1 ILX='TL' FINV=0.0 XINC= -0.01 LAYCH=4
LOOPX1 ILX='TL' FINV=0.0 XINC= -0.01 LAYCH=18
!LOOPX1 ILX='TL' FINV=0.3 XINC=-0.01 LAYCH=40

END
```

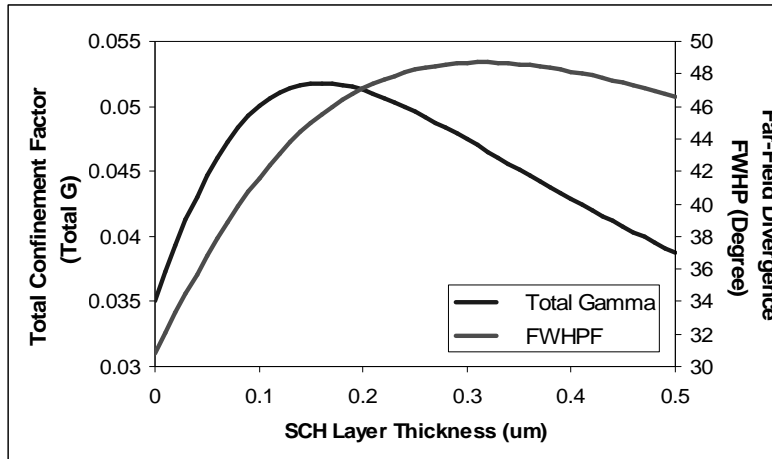


Figure 11.2.1 Plots of the total confinement factor (total Γ) and Far-Field Divergence FWHP (Degree) vs. SCH layer thickness

From Figure 11.2.1, we can see that the maximum total confinement factor, $\Gamma = 0.0518$, happens at SCH layer thickness equal to 0.16 μm , where FWHM of far field intensity equals 45.5 degree. As revealed in Figure 11.2.1, both confinement factor and far-field beam divergence increase with the increase of the SCH layer thickness in the range of 0 to 0.16 μm . Therefore, a balance between confinement factor and far-field beam divergence is required to determine the SCH layer thickness. In this example we choose SCH layer thickness to be 0.16 μm to maximize the confinement factor.

Optimization of inner cladding layer thickness

After the SCH layer thickness is determined, we need to optimize the inner p- and n-cladding layer thicknesses by plotting of loss vs. the inner cladding layer thickness. Usually, we choose the same thickness for inner p- and n-cladding layers.

Chapter 11 Design a Ridge Waveguide Laser Using WAVEGUIDE Program

To be simple, we can generate a new input file by modifying the previous input file. We can first find the QZR of the fundamental mode for SCH layer thickness of 0.16 μm from the previous .db file as an initial guess for QZMR in the new input file, and then loop the thicknesses of inner cladding layers (layer 3 and layer 19) from 1.0 μm to 0.0 μm with an increment of -0.01 μm simultaneously. The new input file is listed in Table 11.2.3 with modified parts highlighted.

After evaluation of the input file, the .db file is plotted, and the plots of loss, the total confinement factor and Far-Field Divergence FWHP as a function of cladding layer thickness are shown in Figure 11.2.2 (a) and (b) respectively.

Table 11.2.3 Input file to optimize inner cladding layer thicknesses.

```
CASE KASE=AlGaInAs (6 wells)
CASE EPS1=1E-8 EPS2=1E-8 GAMEPS=1E-6
CASE QZMR= 10.58612 QZMI=0.0
CASE PRINTF=0 INITGS=0 AUTOQW=0 NFPLT=1 FFPLT=1

!CASE DXIN=0.2
!CASE IL=100 KGSS=1
MODCON KPOL=1 APB1=0.25 APB2=0.25

STRUCT WVWL=1.55

LAYER MATSYS=1 XPERC=0.0 YPERC=0.0 TL=200.0 !n-substrate
LAYER MATSYS=1 XPERC=0.0 YPERC=0.0 TL=2.0 !n-cladding

LAYER MATSYS=13 XPERC=0.48 YPERC=0.0 TL=1 !n-inner-cladding
LAYER MATSYS=13 XPERC=0.24 YPERC=0.24 TL=0.16 !sch

LAYER MATSYS=13 XPERC=0.25 YPERC=0.35 TL=0.005 !barrier
LAYER MATSYS=13 XPERC=0.08 YPERC=0.22 TL=0.006 !Q-well
LAYER MATSYS=13 XPERC=0.25 YPERC=0.35 TL=0.005 !barrier
LAYER MATSYS=13 XPERC=0.08 YPERC=0.22 TL=0.006 !Q-well
LAYER MATSYS=13 XPERC=0.25 YPERC=0.35 TL=0.005 !barrier
LAYER MATSYS=13 XPERC=0.08 YPERC=0.22 TL=0.006 !Q-well
LAYER MATSYS=13 XPERC=0.25 YPERC=0.35 TL=0.005 !barrier
LAYER MATSYS=13 XPERC=0.08 YPERC=0.22 TL=0.006 !Q-well
LAYER MATSYS=13 XPERC=0.25 YPERC=0.35 TL=0.005 !barrier
LAYER MATSYS=13 XPERC=0.08 YPERC=0.22 TL=0.006 !Q-well
LAYER MATSYS=13 XPERC=0.25 YPERC=0.35 TL=0.005 !barrier
LAYER MATSYS=13 XPERC=0.08 YPERC=0.22 TL=0.006 !Q-well
LAYER MATSYS=13 XPERC=0.25 YPERC=0.35 TL=0.005 !barrier

LAYER MATSYS=13 XPERC=0.24 YPERC=0.24 TL=0.16 !sch
LAYER MATSYS=13 XPERC=0.48 YPERC=0.0 TL=1 !p-inner-cladding

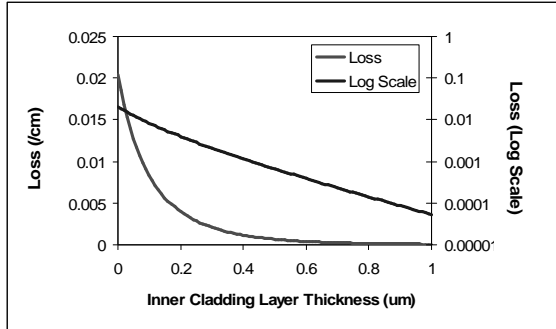
LAYER MATSYS=1 XPERC=0.0 YPERC=0.0 TL=2.0 !p-cladding
LAYER NREAL=3.65 NLOSS=0.0 TL=0.2 !P-cap. InGaAs n from website Adachi's model

OUTPUT PHMO=1 GAMMAO=1 WZRO=1 WZIO=1 QZRO=1 QZIO=0
OUTPUT FWHPNO=0 FWHPFO=1 KMO=1 ITO=1
OUTPUT MODOUT=1 LYROUT=1 SPLTFL=0
GAMOUT LAYGAM=5,7,9,11,13,15 COMPGAM=0 GAMALL=0
```

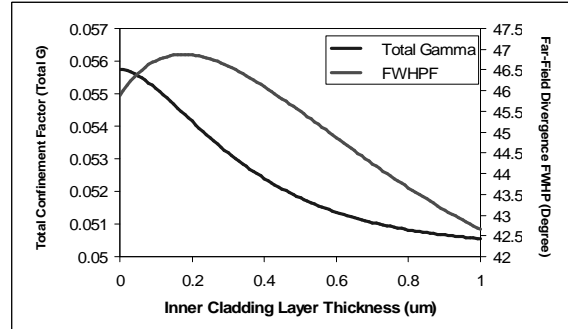
11.2 Simulation details for the design of a ridge waveguide laser using WAVEGUIDE

```

!LOOPZ1 ILZ='WVL' FINV=1.33 ZINC=0.005
!LOOPZ1 ILZ='QZMR' FINV=10.0 ZINC=-0.01
LOOPX1 ILX='TL' FINV=0.0 XINC= -0.01 LAYCH=3
LOOPX1 ILX='TL' FINV=0.0 XINC= -0.01 LAYCH=19
!LOOPX1 ILX='TL' FINV=0.3 XINC=-0.01 LAYCH=40
END
    
```



(a)



(b)

Figure 11.2.2 Plots of (a) loss, (b) the total confinement factor (total Γ) and Far-Field Divergence FWHP (Degree) vs. inner cladding layer thickness

As shown in Figure 11.2.2, as SCH layer thickness increases from 0 to 1 um, loss and confinement factor decreases, and far-field divergence increases first and then drops. Therefore, a compromise among low loss, high confinement factor, and narrow far-field divergence is required to determine the SCH layer thickness. In this example, the layer thickness is chosen to be 0.05 um, when $WZI = 3.141394E-07$, $Loss = 0.012734 /cm$, total $\Gamma = 0.05556$, and $FWHP = 46.41147^\circ$.

Optimization of outer cladding layer thickness

After we chose layer thicknesses of SCH layers and inner cladding layers, the only unknown thicknesses of the laser structure are outer cladding layer thicknesses that need to be simulated in WAVEGUIDE program. Again, we choose the same thickness for outer n-cladding and outer p-cladding layers.

Similar to the step in 11.2.1.2, we can use the QZR of the fundamental mode for inner cladding layer thickness of 0.44 um from the previous .db as an initial guess for QZMR file in the new input file, and then loop the thicknesses of outer cladding layers (layer 2 and layer 20) from 2.0 um to 0.0 um at an increment of -0.01 um simultaneously. A new

Chapter 11 Design a Ridge Waveguide Laser Using WAVEGUIDE Program

input file is generated by modifying the previous input file as listed in Table 11.2.4 with modified parts highlighted.

Table 11.2.4 Input file to determine the outer cladding layer thickness

```

CASE KASE=AlGaInAs (6 wells)
CASE EPS1=1E-8 EPS2=1E-8 GAMEPS=1E-6
CASE QZMR= 10.52369 QZMI=0.0
CASE PRINTF=0 INITGS=0 AUTOQW=0 NFPLT=1 FFPLT=1

!CASE DXIN=0.2
!CASE IL=100 KGSS=1
MODCON KPOL=1 APB1=0.25 APB2=0.25

STRUCT WVL=1.55

LAYER MATSYS=1 XPERC=0.0 YPERC=0.0 TL=200.0 !n-substrate
LAYER MATSYS=1 XPERC=0.0 YPERC=0.0 TL=2.0 !n-cladding

LAYER MATSYS=13 XPERC=0.48 YPERC=0.0 TL=0.05 !n-inner-cladding
LAYER MATSYS=13 XPERC=0.24 YPERC=0.24 TL=0.16 !sch

LAYER MATSYS=13 XPERC=0.25 YPERC=0.35 TL=0.005 !barrier
LAYER MATSYS=13 XPERC=0.08 YPERC=0.22 TL=0.006 !Q-well
LAYER MATSYS=13 XPERC=0.25 YPERC=0.35 TL=0.005 !barrier
LAYER MATSYS=13 XPERC=0.08 YPERC=0.22 TL=0.006 !Q-well
LAYER MATSYS=13 XPERC=0.25 YPERC=0.35 TL=0.005 !barrier
LAYER MATSYS=13 XPERC=0.08 YPERC=0.22 TL=0.006 !Q-well
LAYER MATSYS=13 XPERC=0.25 YPERC=0.35 TL=0.005 !barrier
LAYER MATSYS=13 XPERC=0.08 YPERC=0.22 TL=0.006 !Q-well
LAYER MATSYS=13 XPERC=0.25 YPERC=0.35 TL=0.005 !barrier
LAYER MATSYS=13 XPERC=0.08 YPERC=0.22 TL=0.006 !Q-well
LAYER MATSYS=13 XPERC=0.25 YPERC=0.35 TL=0.005 !barrier
LAYER MATSYS=13 XPERC=0.08 YPERC=0.22 TL=0.006 !Q-well
LAYER MATSYS=13 XPERC=0.25 YPERC=0.35 TL=0.005 !barrier

LAYER MATSYS=13 XPERC=0.24 YPERC=0.24 TL=0.16 !sch
LAYER MATSYS=13 XPERC=0.48 YPERC=0.0 TL=0.05 !p-inner-cladding

LAYER MATSYS=1 XPERC=0.0 YPERC=0.0 TL=2.0 !p-cladding
LAYER NREAL=3.65 NLOSS=0.0 TL=0.2 !P-cap. InGaAs n from website Adachi's model

OUTPUT PHMO=1 GAMMAO=1 WZRO=1 WZIO=1 QZRO=1 QZIO=0
OUTPUT FWHPNO=0 FWHPFO=1 KMO=1 ITO=1
OUTPUT MODOUT=1 LYROUT=1 SPLTFL=0
GAMOUT LAYGAM=5,7,9,11,13,15 COMPGAM=0 GAMALL=0

!LOOPZ1 ILZ='WVL' FINV=1.33 ZINC=0.005
!LOOPZ1 ILZ='QZMR' FINV=10.0 ZINC=-0.01
LOOPX1 ILX='TL' FINV=0.0 XINC= -0.01 LAYCH=2
LOOPX1 ILX='TL' FINV=0.0 XINC= -0.01 LAYCH=20
!LOOPX1 ILX='TL' FINV=0.3 XINC=-0.01 LAYCH=40

END

```

11.2 Simulation details for the design of a ridge waveguide laser using WAVEGUIDE

A plot of loss and far-field divergence FWHP as a function of outer cladding layer thickness is shown in Figure 11.2.3. It is demonstrated that loss and FWHP decrease with the increase of outer cladding layer thickness while the total Γ first increases to a maximum value and then doesn't vary much. The thickness can be determined if there are any requirements on far-field divergence and loss considering a balance between total confinement factor, loss, and far-field divergence.

As can be seen in Figure 11.2.3, loss, far-field divergence, and confinement factor decrease slowly as the outer cladding layer thickness increases to certain values. In other words, up to certain thickness, loss and far-field divergence don't improve much and total confinement factor doesn't decrease much as the thickness is increased. Therefore, in this example, an optimized thickness of 1.87 μm is chosen, where loss = 0.02697 /cm, FWHP = 46.552°, and total $\Gamma = 0.055565$.

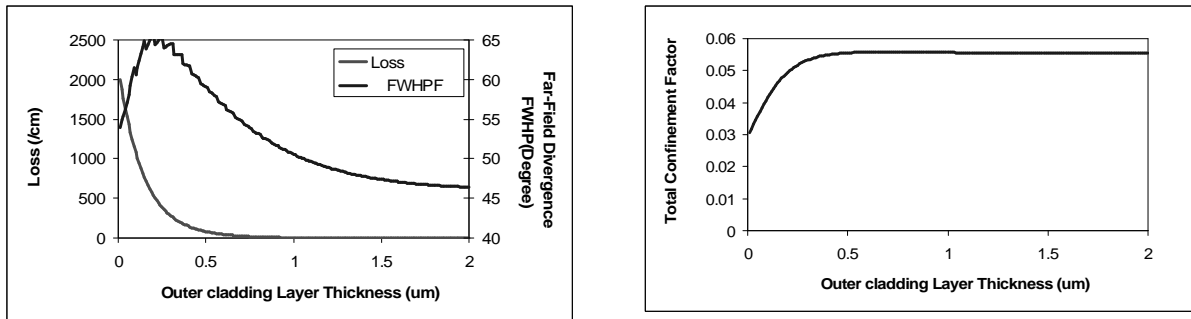


Figure 11.2.3 Plots of (a) loss and far-field divergence FWHP (Degree), (b) the total confinement factor (total Γ) vs. outer cladding layer thickness

11.2.1.4 Summary

A basic waveguide laser has been designed so far with the structure summarized in Table 11.2.5. In the simulations, the thicknesses of SCH layers, inner cladding layers, and outer cladding layers are varied in order to observe variations of loss, far-field divergence, and the total confinement factor as functions of layer thicknesses. In the example, compromises among low loss, narrow far-field divergence, and high confinement factor are made to optimize layer thicknesses.

Table 11.2.5 Layer composition and thickness table for the designed basic waveguide laser

Layer	Material Composition	Layer Thickness (TL) (um)
n-substrate	InP	200
Outer n-cladding	InP	1.87
Inner n-cladding layer	Al _{0.48} In _{0.54} As	0.05
SCH layer	Al _{0.24} In _{0.24} As	0.16
Barrier	Al _{0.25} Ga _{0.35} In _{0.4} As	0.005
Quantum well	Al _{0.08} Ga _{0.22} In _{0.7} As	0.006
Barrier	Al _{0.25} Ga _{0.35} In _{0.4} As	0.005
Quantum well	Al _{0.08} Ga _{0.22} In _{0.7} As	0.006
Barrier	Al _{0.25} Ga _{0.35} In _{0.4} As	0.005
Quantum well	Al _{0.08} Ga _{0.22} In _{0.7} As	0.006
Barrier	Al _{0.25} Ga _{0.35} In _{0.4} As	0.005
Quantum well	Al _{0.08} Ga _{0.22} In _{0.7} As	0.006
Barrier	Al _{0.25} Ga _{0.35} In _{0.4} As	0.005
Quantum well	Al _{0.08} Ga _{0.22} In _{0.7} As	0.006
Barrier	Al _{0.25} Ga _{0.35} In _{0.4} As	0.005
Quantum well	Al _{0.08} Ga _{0.22} In _{0.7} As	0.006
barrier	Al _{0.25} Ga _{0.35} In _{0.4} As	0.005
SCH layer	Al _{0.24} In _{0.24} As	0.16
Inner p-cladding layer	Al _{0.48} In _{0.54} As	0.05
Outer p-cladding	InP	1.87
p-cap	InP	0.2

11.2.2 Position of an etch stop layer, Δn_{eff} vs. p-spacer thickness

As explained in section 11.1.2, an etch stop layer divides p-cladding layer of a basic waveguide laser into p-spacer layer and outer p-cladding layer. Therefore, after defining ridge area through photolithography and etching to the etch stop to form the ridge, a lateral effective refractive index difference exists between the ridge region the wing regions of a ridge waveguide laser, as shown in Figure 11.1.3.

The lateral effective refractive index difference Δn_{eff} is simulated in the waveguide by several steps. We can first (1) calculate the effective refractive index variation as a function of p-spacer layer thickness in the ridge region, (2) calculate that in the wing

11.2 Simulation details for the design of a ridge waveguide laser using WAVEGUIDE region, and then (3) calculate the lateral effective refractive index difference Δn_{eff} and plot Δn_{eff} and far-field divergence FWHP as a function of p-spacer thickness.

- (1) Calculate the effective refractive index variation as a function of p-spacer layer thickness in the ridge region

In the first step, we loop p-spacer layer thickness from 0.1 to 1.85 at an increment of +0.01 and outer p-cladding layer thickness from 1.85 to 0.1 at an increment of -0.01 simultaneously so that the total layer thickness of p-spacer, etch stop, and outer p-cladding layers is constant (1.87 μm) during the loop. We can create a new input file by modifying the previous input file as shown in Table 11.2.6 with changes highlighted in bold.

First, find the initial guess QZMR of the fundamental mode for the initial laser structure with a 0.01- μm p-spacer and a 1.85- μm outer p-cladding as explained in section 2.3 in Chapter 2. Second, change the layer thicknesses of the previous input file according to the results simulated in section 11.2.1.

Next, add an etch stop layer between p-spacer layer and outer p-cladding layer. In this example, an InGaAsP etch stop of 0.1 μm thick is chosen because its different etchant solution is different from that of InP material. Finally, in ‘LOOPX1’, set ‘FINV=1.85 XINC= 0.01 LAYCH=20’ for p-spacer layer, and ‘FINV=0.01 XINC= -0.01 LAYCH=22’ to outer p-cladding layer.

After evaluation of the input file, the effective refractive index (n_{eff}) variation as a function of p-spacer layer thickness in the ridge region is plotted and the .db output file is saved.

Table 11.2.6 input file for the effective refractive index (n_{eff}) variation as a function of p-spacer layer thickness in the ridge region

```

CASE KASE=AlGaInAs (6 wells)
CASE  EPS1=1E-8 EPS2=1E-8 GAMEPS=1E-6
CASE  QZMR= 10.58371 QZMI=0.0
CASE  PRINTF=0 INITGS=0 AUTOQW=0 NFPLT=1  FFPLT=1

!CASE  DXIN=0.2
!CASE  IL=100 KGSS=1
MODCON KPOL=1 APB1=0.25 APB2=0.25

STRUCT WVL=1.55

```

```

LAYER MATSYS=1 XPERC=0.0 YPERC=0.0 TL=200.0 !n-substrate
LAYER MATSYS=1 XPERC=0.0 YPERC=0.0 TL=1.87 !n-cladding

LAYER MATSYS=13 XPERC=0.48 YPERC=0.0 TL=0.05 !n-inner-cladding
LAYER MATSYS=13 XPERC=0.24 YPERC=0.24 TL=0.16 !sch

LAYER MATSYS=13 XPERC=0.25 YPERC=0.35 TL=0.005 !barrier
LAYER MATSYS=13 XPERC=0.08 YPERC=0.22 TL=0.006 !Q-well
LAYER MATSYS=13 XPERC=0.25 YPERC=0.35 TL=0.005 !barrier
LAYER MATSYS=13 XPERC=0.08 YPERC=0.22 TL=0.006 !Q-well
LAYER MATSYS=13 XPERC=0.25 YPERC=0.35 TL=0.005 !barrier
LAYER MATSYS=13 XPERC=0.08 YPERC=0.22 TL=0.006 !Q-well
LAYER MATSYS=13 XPERC=0.25 YPERC=0.35 TL=0.005 !barrier
LAYER MATSYS=13 XPERC=0.08 YPERC=0.22 TL=0.006 !Q-well
LAYER MATSYS=13 XPERC=0.25 YPERC=0.35 TL=0.005 !barrier
LAYER MATSYS=13 XPERC=0.08 YPERC=0.22 TL=0.006 !Q-well
LAYER MATSYS=13 XPERC=0.25 YPERC=0.35 TL=0.005 !barrier
LAYER MATSYS=13 XPERC=0.08 YPERC=0.22 TL=0.006 !Q-well
LAYER MATSYS=13 XPERC=0.25 YPERC=0.35 TL=0.005 !barrier
LAYER MATSYS=13 XPERC=0.24 YPERC=0.24 TL=0.16 !sch
LAYER MATSYS=13 XPERC=0.48 YPERC=0.0 TL=0.05 !p-inner-cladding

LAYER MATSYS=1 XPERC=0.0 YPERC=0.0 TL=0.01 !P-spacer
LAYER MATSYS=12 XPERC=1.1 TL=0.01 !etch stop
LAYER MATSYS=1 XPERC=0.0 YPERC=0.0 TL=1.85 !outer p-cladding
LAYER NREAL=3.65 NLOSS=0.0 TL=0.2 !P-cap. InGaAs n from website Adachi's model

OUTPUT PHMO=1 GAMMAO=1 WZRO=1 WZIO=1 QZRO=1 QZIO=0
OUTPUT FWHPNO=0 FWHPFO=1 KMO=1 ITO=1
OUTPUT MODOUT=1 LYROUT=1 SPLTFL=0
GAMOUT LAYGAM=5,7,9,11,13,15 COMPGAM=0 GAMALL=0

!LOOPZ1 ILZ='WVL' FINV=1.33 ZINC=0.005
!LOOPZ1 ILZ='QZMR' FINV=10.0 ZINC=-0.01
LOOPX1 ILX='TL' FINV=1.85 XINC= 0.01 LAYCH=20
LOOPX1 ILX='TL' FINV=0.01 XINC= -0.01 LAYCH=22
!LOOPX1 ILX='TL' FINV=0.3 XINC=-0.01 LAYCH=40

END

```

- (2) The second step is to calculate the effective refractive index (n_{eff}) variation as a function of p-spacer layer thickness in the wing region.

In the wing region, the p-cap and outer p-cladding layers are etched above the etch stop with p-spacer left, and a dielectric layer SiN_x is deposited on the top of the etch stop for insulation, preventing current injection into the wing region.

Again, we can create a new input file by modifying the previous input file as shown in Table 11.2.7. Similarly, first, find the initial guess QZMR of the fundamental mode for the initial laser structure with a 0.01- μm p-spacer layer

11.2 Simulation details for the design of a ridge waveguide laser using WAVEGUIDE

and a 0.2-um SiNx layer on top of it. Next, delete the outer p-cladding layer, p-cap layer, and 'LOOPX1' for layer 20 which is outer p-cladding layer.

After evaluation of the input file, the effective refractive index (n_{eff}) variation as a function of p-spacer layer thickness in the wing region is plotted and the .db output file is saved.

Table 11.2.7 the input file for the effective refractive index (n_{eff}) variation as a function of p-spacer layer thickness in the wing region

```
CASE KASE=AlGaInAs (6 wells)
CASE EPS1=1E-8 EPS2=1E-8 GAMEPS=1E-6
CASE QZMR= 10.33209 QZMI=0.0
CASE PRINTF=0 INITGS=0 AUTOQW=0 NFPLT=1 FFPLT=1 IL=30

!CASE DXIN=0.2
!CASE IL=100 KGSS=1
MODCON KPOL=1 APB1=0.25 APB2=0.25

STRUCT WVL=1.55

LAYER MATSYS=1 XPERC=0.0 YPERC=0.0 TL=200.0 !n-substrate
LAYER MATSYS=1 XPERC=0.0 YPERC=0.0 TL=1.87 !n-cladding

LAYER MATSYS=13 XPERC=0.48 YPERC=0.0 TL=0.05 !n-inner-cladding
LAYER MATSYS=13 XPERC=0.24 YPERC=0.24 TL=0.16 !sch

LAYER MATSYS=13 XPERC=0.25 YPERC=0.35 TL=0.005 !barrier
LAYER MATSYS=13 XPERC=0.08 YPERC=0.22 TL=0.006 !Q-well
LAYER MATSYS=13 XPERC=0.25 YPERC=0.35 TL=0.005 !barrier
LAYER MATSYS=13 XPERC=0.08 YPERC=0.22 TL=0.006 !Q-well
LAYER MATSYS=13 XPERC=0.25 YPERC=0.35 TL=0.005 !barrier
LAYER MATSYS=13 XPERC=0.08 YPERC=0.22 TL=0.006 !Q-well
LAYER MATSYS=13 XPERC=0.25 YPERC=0.35 TL=0.005 !barrier
LAYER MATSYS=13 XPERC=0.08 YPERC=0.22 TL=0.006 !Q-well
LAYER MATSYS=13 XPERC=0.25 YPERC=0.35 TL=0.005 !barrier
LAYER MATSYS=13 XPERC=0.08 YPERC=0.22 TL=0.006 !Q-well
LAYER MATSYS=13 XPERC=0.25 YPERC=0.35 TL=0.005 !barrier
LAYER MATSYS=13 XPERC=0.08 YPERC=0.22 TL=0.006 !Q-well
LAYER MATSYS=13 XPERC=0.25 YPERC=0.35 TL=0.005 !barrier
LAYER MATSYS=13 XPERC=0.24 YPERC=0.24 TL=0.16 !sch
LAYER MATSYS=13 XPERC=0.48 YPERC=0.0 TL=0.05 !p-inner-cladding

LAYER MATSYS=1 XPERC=0.0 YPERC=0.0 TL=0.01 !P-spacer
LAYER MATSYS=12 XPERC=1.1 TL=0.01 !etch stop
LAYER NREAL=1.8 NLOSS=0.0 TL=0.2 !Dielectric layer: SiNx

LAYER MATSYS=1 XPERC=0.0 YPERC=0.0 TL=1.84 !outer p-cladding
LAYER NREAL=3.65 NLOSS=0.0 TL=0.2 !P-cap. InGaAs n from website Adachi's model

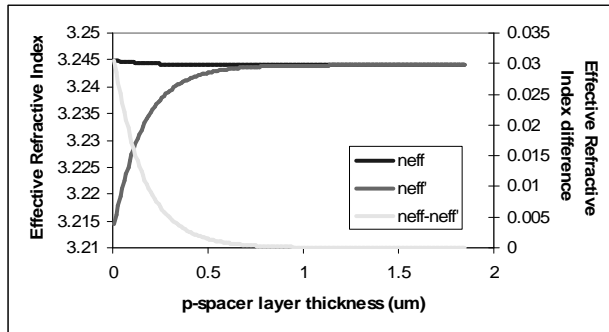
OUTPUT PHMO=1 GAMMAO=1 WZRO=1 WZIO=1 QZRO=1 QZIO=0
OUTPUT FWHPNO=0 FWHPFO=1 KMO=1 ITO=1
OUTPUT MODOUT=1 LYROUT=1 SPLTFL=0
```

```
GAMOUT LAYGAM=5,7,9,11,13,15 COMPGAM=0 GAMALL=0

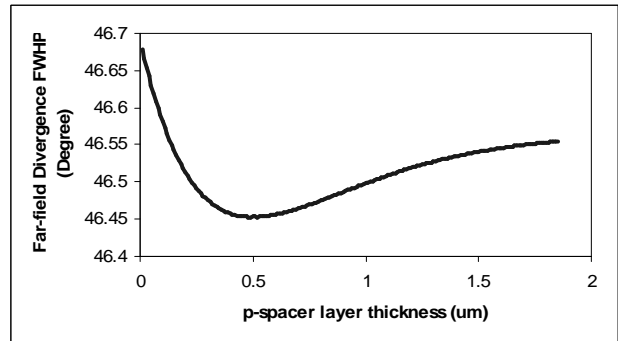
!LOOPZ1 ILZ='WVL' FINV=1.33 ZINC=0.005
!LOOPZ1 ILZ='QZMR' FINV=10 ZINC=-0.01
LOOPX1 ILX='TL' FINV=1.85 XINC= 0.01 LAYCH=20
!LOOPX1 ILX='TL' FINV=0.01 XINC=- 0.01 LAYCH=22
!LOOPX1 ILX='TL' FINV=0.3 XINC=-0.01 LAYCH=40

END
```

- (3) In this step, the two .db output files are combined to calculate lateral effective refractive index difference Δn_{eff} . The plots of n_{eff} , n_{eff}' , and Δn_{eff} and far-field divergence FWHP vs. p-spacer thickness are shown in Figure 11.2.4 (a) and (b).



(a)



(b)

Figure 11.2.4 (a) Plot of n_{eff} , n_{eff}' and Δn_{eff} (b) far-field divergence FWHP as a function of p-spacer layer thickness

From Figure 11.2.4 (b) and the .db file in the ridge region, we can find that the far-field divergence reaches a minimum value of 46.52° when the p-spacer layer thickness equals $0.48 \mu\text{m}$, but Δn_{eff} equals 0.0016 , which is too small a step for a ridge waveguide laser to maintain single lateral mode operation. For an acceptable Δn_{eff} of 0.010 , the p-spacer layer thickness is $0.18 \mu\text{m}$. Therefore, we choose the p-spacer layer thickness to be $0.18 \mu\text{m}$

In summary, the wafer structure of the designed ridge waveguide laser is listed in Table 11.2.8 and Table 11.2.9. Besides, Table 11.2.10 summarizes simulation results of the laser in ridge and wing regions.

11.2 Simulation details for the design of a ridge waveguide laser using WAVEGUIDE

Table 11.2.8 Layer composition and thickness table for the ridge region of the designed ridge waveguide laser.

Layer	Material Composition	Layer Thickness (TL) (um)
n-substrate	InP	200
Outer n-cladding	InP	1.87
Inner n-cladding layer	Al _{0.48} In _{0.54} As	0.05
SCH layer	Al _{0.24} In _{0.24} As	0.16
Barrier	Al _{0.25} Ga _{0.35} In _{0.4} As	0.005
Quantum well	Al _{0.08} Ga _{0.22} In _{0.7} As	0.006
Barrier	Al _{0.25} Ga _{0.35} In _{0.4} As	0.005
Quantum well	Al _{0.08} Ga _{0.22} In _{0.7} As	0.006
Barrier	Al _{0.25} Ga _{0.35} In _{0.4} As	0.005
Quantum well	Al _{0.08} Ga _{0.22} In _{0.7} As	0.006
Barrier	Al _{0.25} Ga _{0.35} In _{0.4} As	0.005
Quantum well	Al _{0.08} Ga _{0.22} In _{0.7} As	0.006
Barrier	Al _{0.25} Ga _{0.35} In _{0.4} As	0.005
Quantum well	Al _{0.08} Ga _{0.22} In _{0.7} As	0.006
Barrier	Al _{0.25} Ga _{0.35} In _{0.4} As	0.005
Quantum well	Al _{0.08} Ga _{0.22} In _{0.7} As	0.006
barrier	Al _{0.25} Ga _{0.35} In _{0.4} As	0.005
SCH layer	Al _{0.24} In _{0.24} As	0.16
Inner p-cladding layer	Al _{0.48} In _{0.54} As	0.05
P-spacer	InP	0.18
etch stop	InGaAsP	0.01
Outer p-cladding	InP	1.68
p-cap	InP	0.2

Table 11.2.9 Layer composition and thickness table for the wing region of the designed ridge waveguide laser.

Layer	Material Composition	Layer Thickness (TL) (um)
n-substrate	InP	200
Outer n-cladding	InP	1.87
Inner n-cladding layer	Al _{0.48} In _{0.54} As	0.05

Chapter 11 Design a Ridge Waveguide Laser Using WAVEGUIDE Program

SCH layer	Al _{0.24} In _{0.24} As	0.16
Barrier	Al _{0.25} Ga _{0.35} In _{0.4} As	0.005
Quantum well	Al _{0.08} Ga _{0.22} In _{0.7} As	0.006
Barrier	Al _{0.25} Ga _{0.35} In _{0.4} As	0.005
Quantum well	Al _{0.08} Ga _{0.22} In _{0.7} As	0.006
Barrier	Al _{0.25} Ga _{0.35} In _{0.4} As	0.005
Quantum well	Al _{0.08} Ga _{0.22} In _{0.7} As	0.006
Barrier	Al _{0.25} Ga _{0.35} In _{0.4} As	0.005
Quantum well	Al _{0.08} Ga _{0.22} In _{0.7} As	0.006
Barrier	Al _{0.25} Ga _{0.35} In _{0.4} As	0.005
Quantum well	Al _{0.08} Ga _{0.22} In _{0.7} As	0.006
barrier	Al _{0.25} Ga _{0.35} In _{0.4} As	0.005
SCH layer	Al _{0.24} In _{0.24} As	0.16
Inner p-cladding layer	Al _{0.48} In _{0.54} As	0.44
P-spacer	InP	0.18
etch stop	InGaAsP	0.01
Dielectric layer	SiNx	0.02

Table 11.2.10 the simulation results of the designed ridge waveguide laser

Confinement factor	0.0554
Far-field divergence FWHP	46.52°
Loss	0.02735 /cm
n _{eff} in ridge region	3.244
n _{eff} ' in wing region	3.234
lateral effective refractive index difference Δn _{eff}	0.010

11.2.3 Determine ridge width and channel width.

11.2.3.1 Ridge Width

As discussed in section 11.1.3.1, the theoretical calculation of maximum ridge width for single-lateral-TE-mode operation is as follows:

$$d < \frac{\lambda}{2\sqrt{n_1^2 - n^2}} = \frac{1.55}{2\sqrt{3.244^2 - 3.234^2}} = 3.0\mu\text{m}$$

11.2 Simulation details for the design of a ridge waveguide laser using WAVEGUIDE

Using WAVEGUIDE program, we can prove the validity of the calculation: for a 3um-ridge, only single lateral mode propagates in the three-layer dielectric slab waveguide, and for a ridge greater than 3um, more than one mode propagate.

As simulated in the previous section and shown in Table 11.2.10, $n_1 = n_{eff} = 3.244$, and $n = n_{eff} = 3.234$. The input file for the three-layer dielectric slab waveguide with $n_1 = 3.244$ and $n = 3.234$ looping QZMR from $n_1^2 (=10.523536)$ to $n^2 (=10.458)$ are listed in Table 11.2.11. After evaluation of the input file, we open .db file and find that only fundamental mode (TE0) with an effective refractive index of 3.240409 is allowed to propagate in the waveguide.

Then we modify the thickness of the core layer of the previous input file into 4um, as listed in Table 11.2.12, and simulate it. We can find that in the .db file that two propagating modes exist with an effective refractive index of 3.241455 (TE0) and an effective refractive index of 3.235244 (TE1) respectively.

Table 11.2.11 the input file for the three-layer waveguide with a core layer thickness of 3 um looping QZMR from n_1^2 to n^2

```
!WIF generated by WIFE (Waveguide Input File Editor)
!-----
!FILENAME: C:\Waveguide\work\input\example.wgi
!DESCRIPTION: WaveGuide Example File
!Last Modified: 3/28/2004 10:34:26 PM
!-----

!CASE Parameter Set
CASE KASE=WIFE
CASE EPS1=1E-9 EPS2=1E-9 GAMEPS=1E-3 QZMR=10.523536 QZMI=0.001
CASE PRINTF=1 INITGS=0 AUTOQW=0 NFPLT=1 FFPLT=1 IL=30

!MODCON Parameter Set
MODCON KPOL=1 APB1=0.25 APB2=0.25

!STRUCT Parameter Set
STRUCT WVWL=1.55
STRUCT XPERC1=0.0 XPERC2=0.0 XPERC3=0.0 XPERC4=0.0
STRUCT YPERC1=0.0 YPERC2=0.0 YPERC3=0.0 YPERC4=0.0

!LAYER Parameter Set
LAYER NREAL=3.234 NLOSS=0.0 TL=10.0
LAYER NREAL=3.244 NLOSS=0.0 TL=3.0
LAYER NREAL=3.234 NLOSS=0.0 TL=10.0

!OUTPUT Parameter Set
OUTPUT PHMO=1 GAMMAO=1 WZRO=1 WZIO=1 QZRO=1 QZIO=1
OUTPUT FWHPNO=1 FWHPFO=1 KMO=1 ITO=1
OUTPUT SPLTFL=0 MODOUT=1 LYROUT=1

!GAMOUT Parameter Set
GAMOUT LAYGAM=3 COMPGAM=0 GAMALL=0
```

Chapter 11 Design a Ridge Waveguide Laser Using WAVEGUIDE Program

```

!LOOPX Parameter Set
!LOOPX1 ILX='TL' FINV=100.0 XINC= 0.1 LAYCH=2
!LOOPX1 ILX='TL' FINV=100.0 XINC= 0.1 LAYCH=4
!LOOPX3 ILX=0 FINV=0 XINC=0.1 LAYCH=2
!LOOPX4 ILX=0 FINV=0 XINC=0.1 LAYCH=2

!LOOPZ Parameter Set
!LOOPZ1 ILZ=17 FINV=10.458 ZINC=-0.001
!LOOPZ2 ILZ=0 FINV=0 ZINC=0.1
!LOOPZ3 ILZ=0 FINV=0 ZINC=0.1
!LOOPZ4 ILZ=0 FINV=0 ZINC=0.1

END

```

Table 11.2.12 the input file for the three-layer waveguide with a core layer thickness of 4 um looping QZMR from n_1^2 to n^2

```

!WIF generated by WIFE (Waveguide Input File Editor)
!-----
!FILENAME:  C:\Waveguide\work\input\example.wgi
!DESCRIPTION: WaveGuide Example File
!Last Modified: 3/28/2004 10:34:26 PM
!-----

!CASE Parameter Set
CASE KASE=WIFE
CASE EPS1=1E-9 EPS2=1E-9 GAMEPS=1E-3 QZMR=10.523536 QZMI=0.001
CASE PRINTF=1 INITGS=0 AUTOQW=0 NFPLT=1 FFPLT=1 IL=30

!MODCON Parameter Set
MODCON KPOL=1 APB1=0.25 APB2=0.25

!STRUCT Parameter Set
STRUCT WV=1.55
STRUCT XPERC1=0.0 XPERC2=0.0 XPERC3=0.0 XPERC4=0.0
STRUCT YPERC1=0.0 YPERC2=0.0 YPERC3=0.0 YPERC4=0.0

!LAYER Parameter Set
LAYER NREAL=3.234 NLOSS=0.0 TL=10.0
LAYER NREAL=3.244 NLOSS=0.0 TL=4.0
LAYER NREAL=3.234 NLOSS=0.0 TL=10.0

!OUTPUT Parameter Set
OUTPUT PHMO=1 GAMMAO=1 WZRO=1 WZIO=1 QZRO=1 QZIO=1
OUTPUT FWHPNO=1 FWHPFO=1 KMO=1 ITO=1
OUTPUT SPLTFL=0 MODOUT=1 LYROUT=1

!GAMOUT Parameter Set
GAMOUT LAYGAM=3 COMPGAM=0 GAMALL=0

!LOOPX Parameter Set
!LOOPX1 ILX='TL' FINV=100.0 XINC= 0.1 LAYCH=2
!LOOPX1 ILX='TL' FINV=100.0 XINC= 0.1 LAYCH=4
!LOOPX3 ILX=0 FINV=0 XINC=0.1 LAYCH=2
!LOOPX4 ILX=0 FINV=0 XINC=0.1 LAYCH=2

!LOOPZ Parameter Set
!LOOPZ1 ILZ=17 FINV=10.458 ZINC=-0.001
!LOOPZ2 ILZ=0 FINV=0 ZINC=0.1
!LOOPZ3 ILZ=0 FINV=0 ZINC=0.1
!LOOPZ4 ILZ=0 FINV=0 ZINC=0.1

END

```


11.2 Simulation details for the design of a ridge waveguide laser using WAVEGUIDE

If the channel width of a ridge waveguide laser is not infinite, the effects of neighboring ridges must be taken into account. Therefore, a five-layer dielectric waveguide shown in Figure 11.1.8 is simulated to prove that only fundamental mode propagates with low loss for a ridge width of 3 μm or less, and more than one modes propagate with low loss for a ridge width greater than 3 μm . The input file is modified as shown in Table 11.2.13, with two outer layers added to the three-layer waveguide with refractive index of 3.244.

Table 11.2.13 the input file for the five-layer waveguide with a core layer thickness of 3 μm , looping QZMR from n_1^2 to n^2

```
!WIF generated by WIFE (Waveguide Input File Editor)
!-----
!FILENAME: C:\Waveguide\work\input\example.wgi
!DESCRIPTION: WaveGuide Example File
!Last Modified: 3/28/2004 10:34:26 PM
!-----

!CASE Parameter Set
CASE KASE=WIFE
CASE EPS1=1E-9 EPS2=1E-9 GAMEPS=1E-3 QZMR=10.523536 QZMI=0.001
CASE PRINTF=1 INITGS=0 AUTOQW=0 NFPLT=1 FFPLT=1 IL=30

!MODCON Parameter Set
MODCON KPOL=1 APB1=0.25 APB2=0.25

!STRUCT Parameter Set
STRUCT WV=1.55
STRUCT XPERC1=0.0 XPERC2=0.0 XPERC3=0.0 XPERC4=0.0
STRUCT YPERC1=0.0 YPERC2=0.0 YPERC3=0.0 YPERC4=0.0

!LAYER Parameter Set
LAYER NREAL=3.244 NLOSS=0.0 TL=100.0
LAYER NREAL=3.234 NLOSS=0.0 TL=10.0
LAYER NREAL=3.244 NLOSS=0.0 TL=3.0
LAYER NREAL=3.234 NLOSS=0.0 TL=10.0
LAYER NREAL=3.244 NLOSS=0.0 TL=100.0

!OUTPUT Parameter Set
OUTPUT PHMO=1 GAMMAO=1 WZRO=1 WZIO=1 QZRO=1 QZIO=1
OUTPUT FWHPNO=1 FWHPFO=1 KMO=1 ITO=1
OUTPUT SPLTFL=0 MODOUT=1 LYROUT=1

!GAMOUT Parameter Set
GAMOUT LAYGAM=3 COMPGAM=0 GAMALL=0

!LOOPX Parameter Set
!LOOPX1 ILX='TL' FINV=100.0 XINC= 0.1 LAYCH=2
!LOOPX1 ILX='TL' FINV=100.0 XINC= 0.1 LAYCH=4
LOOPX3 ILX=0 FINV=0 XINC=0.1 LAYCH=2
LOOPX4 ILX=0 FINV=0 XINC=0.1 LAYCH=2

!LOOPZ Parameter Set
LOOPZ1 ILZ=17 FINV=10.458 ZINC=-0.001
LOOPZ2 ILZ=0 FINV=0 ZINC=0.1
LOOPZ3 ILZ=0 FINV=0 ZINC=0.1
LOOPZ4 ILZ=0 FINV=0 ZINC=0.1

END
```

After evaluation of the input file, we open the .db file, calculate and plot the loss as a function of effective refractive indices of the modes including real and complex solutions to the eigen-equations of the five-layer waveguide. As can be seen in Figure 11.2.5, only fundamental mode with an effective refractive index of 3.240409 propagates with a low loss of 1.07593E-05. All other modes have high losses and cannot propagate long, and the higher order the mode is, the higher loss it propagates with.

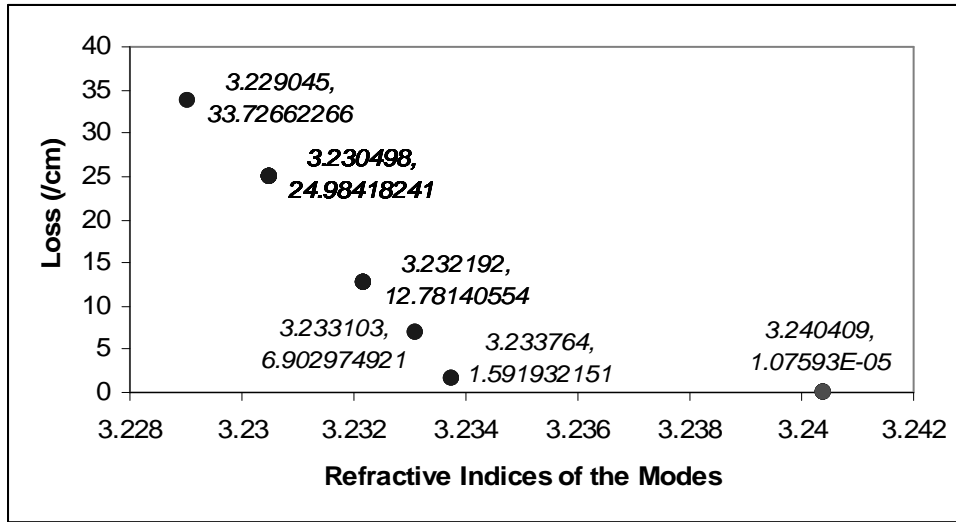


Figure 11.2.5 loss as a function of effective refractive indices of the modes including real and complex solutions for a five-layer dielectric waveguide with a core layer thickness of 3 μm .

Next, we change the core layer thickness from 3 μm to 4 μm , and repeat the previous step. The input file is listed in Table 11.2.14. As shown in Figure 11.2.6, two modes propagate with low loss, TE₀ with effective refractive indices of 3.241455 at a low loss of 1.7709E-06 /cm and 3.235243 at a low loss of 0.04713674 /cm respectively. The near field profiles of the two modes are shown in Figure 11.2.7 (a) and (b).

Table 11.2.14 the input file for the five-layer waveguide with a core layer thickness of 4 μm , looping QZMR from n_1^2 to n^2

```
!WIF generated by WIFE (Waveguide Input File Editor)
!-----
!FILENAME: C:\Waveguide\work\input\example.wgi
!DESCRIPTION: WaveGuide Example File
!Last Modified: 3/28/2004 10:34:26 PM
!-----
```

11.2 Simulation details for the design of a ridge waveguide laser using WAVEGUIDE

```

!CASE Parameter Set
CASE KASE=WIFE
CASE EPS1=1E-9 EPS2=1E-9 GAMEPS=1E-3 QZMR=10.523536 QZMI=0.001
CASE PRINTF=1 INITGS=0 AUTOQW=0 NFPLT=1 FFPLT=1 IL=30

!MODCON Parameter Set
MODCON KPOL=1 APB1=0.25 APB2=0.25

!STRUCT Parameter Set
STRUCT WV=1.55
STRUCT XPERC1=0.0 XPERC2=0.0 XPERC3=0.0 XPERC4=0.0
STRUCT YPERC1=0.0 YPERC2=0.0 YPERC3=0.0 YPERC4=0.0

!LAYER Parameter Set
LAYER NREAL=3.244 NLOSS=0.0 TL=100.0
LAYER NREAL=3.234 NLOSS=0.0 TL=10.0
LAYER NREAL=3.244 NLOSS=0.0 TL=4.0
LAYER NREAL=3.234 NLOSS=0.0 TL=10.0
LAYER NREAL=3.244 NLOSS=0.0 TL=100.0

!OUTPUT Parameter Set
OUTPUT PHMO=1 GAMMAO=1 WZRO=1 WZIO=1 QZRO=1 QZIO=1
OUTPUT FWHPNO=1 FWHPFO=1 KMO=1 ITO=1
OUTPUT SPLTFL=0 MODOUT=1 LYROUT=1

!GAMOUT Parameter Set
GAMOUT LAYGAM=3 COMPGAM=0 GAMALL=0

!LOOPX Parameter Set
!LOOPX1 ILX='TL' FINV=100.0 XINC= 0.1 LAYCH=2
!LOOPX1 ILX='TL' FINV=100.0 XINC= 0.1 LAYCH=4
LOOPX3 ILX=0 FINV=0 XINC=0.1 LAYCH=2
LOOPX4 ILX=0 FINV=0 XINC=0.1 LAYCH=2

!LOOPZ Parameter Set
LOOPZ1 ILZ=17 FINV=10.458 ZINC=-0.001
LOOPZ2 ILZ=0 FINV=0 ZINC=0.1
LOOPZ3 ILZ=0 FINV=0 ZINC=0.1
LOOPZ4 ILZ=0 FINV=0 ZINC=0.1

END

```

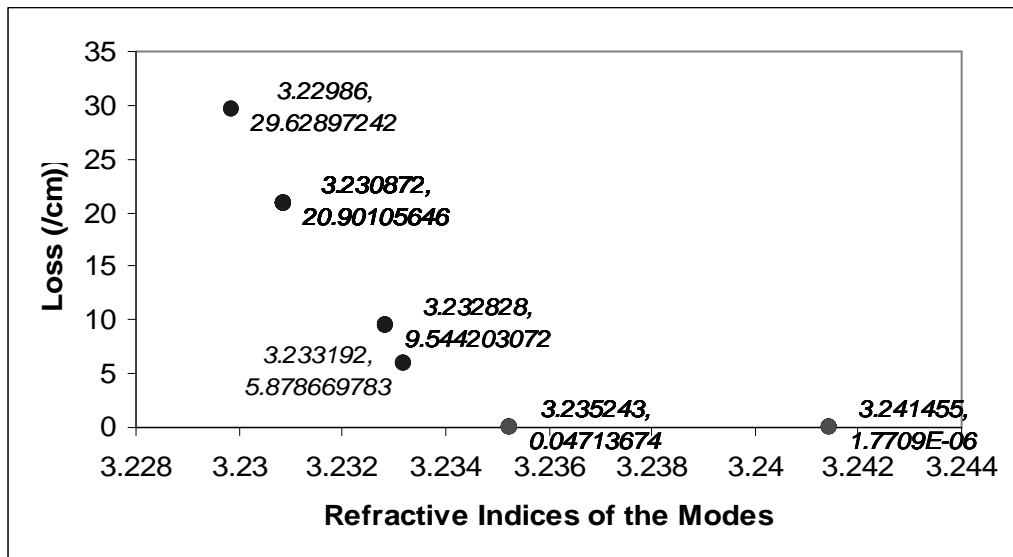
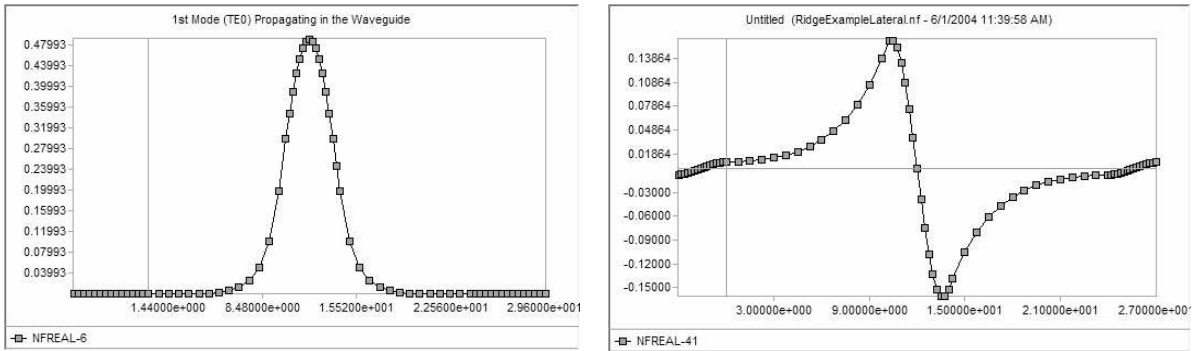


Figure 11.2.6 loss as a function of effective refractive indices of the modes including real and

complex solutions for a five-layer dielectric waveguide with a core layer thickness of 4 μm .



(a)

(b)

Figure 11.2.7 Near field profile of the propagating modes (a) TE₀ and (b) TE₁ with effective refractive indices of 3.241455 and 3.235243 respectively.

In summary, the ridge width of the designed ridge waveguide laser is chosen to be 3 μm to maintain single-lateral-TE₀-mode propagation.

Wing/Channel Width

As explained in section 11.1.3.2, channel width is required to be thick enough so that the effects of neighboring ridges are negligible. In order to optimize the channel width, we vary the channel width and plot the loss as a function of channel width.

First, we modify the previous input file as shown in Table 11.2.15 with changes highlighted. As calculated in the previous section 11.2.3.1 and shown in Figure 11.2.5, the fundamental mode has an effective refractive index of 3.240409, therefore, we change the value of QZMR in previous file to 10.50025, which is the square of 3.240409. Another change is to loop the thicknesses of layer 2 and layer 4 from 10 μm to 0 μm with an increment of -0.01.

Next, we loop the channel width from 10 μm to 100 μm with an increment of 0.1 μm as listed in Table 11.2.16. After the evaluation, we combine the .db file together with the one from the input file in Table 11.2.15, so that we have the data of the waveguide with channel width changing from 0 μm to 100 μm . Then we can calculate and plot loss as a function of channel width as shown in Figure 11.2.8.

11.2 Simulation details for the design of a ridge waveguide laser using WAVEGUIDE

Table 11.2.15 the input file for the five-layer waveguide looping thickness of channel width from 10 um to 0 um with an increment of -0.01.

```

!WIF generated by WIFE (Waveguide Input File Editor)
!-----
!FILENAME: C:\Waveguide\work\input\example.wgi
!DESCRIPTION: WaveGuide Example File
!Last Modified: 3/28/2004 10:34:26 PM
!-----

!CASE Parameter Set
CASE KASE=WIFE
CASE EPS1=1E-9 EPS2=1E-9 GAMEPS=1E-3 QZMR=10.50025 QZMI=0.001
CASE PRINTF=1 INITGS=0 AUTOQW=0 NFPLT=1 FFPLT=1 IL=30

!MODCON Parameter Set
MODCON KPOL=1 APB1=0.25 APB2=0.25

!STRUCT Parameter Set
STRUCT WV=1.55
STRUCT XPERC1=0.0 XPERC2=0.0 XPERC3=0.0 XPERC4=0.0
STRUCT YPERC1=0.0 YPERC2=0.0 YPERC3=0.0 YPERC4=0.0

!LAYER Parameter Set

LAYER NREAL=3.244 NLOSS=0.0 TL=100.0
LAYER NREAL=3.234 NLOSS=0.0 TL=10.0
LAYER NREAL=3.244 NLOSS=0.0 TL=3.0
LAYER NREAL=3.234 NLOSS=0.0 TL=10.0
LAYER NREAL=3.244 NLOSS=0.0 TL=100.0

!OUTPUT Parameter Set
OUTPUT PHMO=1 GAMMAO=1 WZRO=1 WZIO=1 QZRO=1 QZIO=1
OUTPUT FWHPNO=1 FWHPFO=1 KMO=1 ITO=1
OUTPUT SPLTFL=0 MODOUT=1 LYROUT=1

!GAMOUT Parameter Set
GAMOUT LAYGAM=3 COMPGAM=0 GAMALL=0

!LOOPX Parameter Set
LOOPX1 ILX='TL' FINV=0.0 XINC= -0.01 LAYCH=2
LOOPX1 ILX='TL' FINV=0.0 XINC= -0.01 LAYCH=4
LOOPX3 ILX=0 FINV=0 XINC=0.1 LAYCH=2
LOOPX4 ILX=0 FINV=0 XINC=0.1 LAYCH=2

!LOOPZ Parameter Set
!LOOPZ1 ILZ=17 FINV=10.458 ZINC=-0.01
LOOPZ2 ILZ=0 FINV=0 ZINC=0.1
LOOPZ3 ILZ=0 FINV=0 ZINC=0.1
LOOPZ4 ILZ=0 FINV=0 ZINC=0.1

END

```

Table 11.2.16 the input file for the five-layer waveguide looping thickness of channel width from 10 um to 100 um with an increment of 0.1.

```

!WIF generated by WIFE (Waveguide Input File Editor)
!-----
!FILENAME: C:\Waveguide\work\input\example.wgi
!DESCRIPTION: WaveGuide Example File
!Last Modified: 3/28/2004 10:34:26 PM
!-----

!CASE Parameter Set
CASE KASE=WIFE
CASE EPS1=1E-9 EPS2=1E-9 GAMEPS=1E-3 QZMR=10.50025 QZMI=0.001
CASE PRINTF=1 INITGS=0 AUTOQW=0 NFPLT=1 FFPLT=1 IL=30

```

Chapter 11 Design a Ridge Waveguide Laser Using WAVEGUIDE Program

```
!MODCON Parameter Set
MODCON KPOL=1 APB1=0.25 APB2=0.25

!STRUCT Parameter Set
STRUCT WV=1.55
STRUCT XPERC1=0.0 XPERC2=0.0 XPERC3=0.0 XPERC4=0.0
STRUCT YPERC1=0.0 YPERC2=0.0 YPERC3=0.0 YPERC4=0.0

!LAYER Parameter Set
LAYER NREAL=3.244 NLOSS=0.0 TL=100.0
LAYER NREAL=3.234 NLOSS=0.0 TL=10.0
LAYER NREAL=3.244 NLOSS=0.0 TL=3.0
LAYER NREAL=3.234 NLOSS=0.0 TL=10.0
LAYER NREAL=3.244 NLOSS=0.0 TL=100.0

!OUTPUT Parameter Set
OUTPUT PHMO=1 GAMMAO=1 WZRO=1 WZIO=1 QZRO=1 QZIO=1
OUTPUT FWHPNO=1 FWHPFO=1 KMO=1 ITO=1
OUTPUT SPLTFL=0 MODOUT=1 LYROUT=1

!GAMOUT Parameter Set
GAMOUT LAYGAM=3 COMPGAM=0 GAMALL=0

!LOOPX Parameter Set
LOOPX1 ILX='TL' FINV=100.0 XINC= 0.1 LAYCH=2
LOOPX1 ILX='TL' FINV=100.0 XINC= 0.1 LAYCH=4
LOOPX3 ILX=0 FINV=0 XINC=0.1 LAYCH=2
LOOPX4 ILX=0 FINV=0 XINC=0.1 LAYCH=2

!LOOPZ Parameter Set
!LOOPZ1 ILZ=17 FINV=10.458 ZINC=-0.01
LOOPZ2 ILZ=0 FINV=0 ZINC=0.1
LOOPZ3 ILZ=0 FINV=0 ZINC=0.1
LOOPZ4 ILZ=0 FINV=0 ZINC=0.1

END
```

From Table 11.2.17, we can see that for channel width smaller than 0.24 μm , the code doesn't converge in 30 iterations, meaning it couldn't find a root near an initial guess $WZR = 3.240409$. As the channel width increases from 0.25 μm , the loss of the fundamental mode in the waveguide decreases from 78.5444 /cm. When the channel width increases to 5.87 μm , the loss is about $0.009861/\text{cm} \leq 0.01$ /cm, which is an acceptable value for the designed ridge waveguide laser. In other words, as long as the channel width is greater than 5.87 μm , the laser can operate at low loss, resulting in a low threshold current density.

In our example, we choose the channel width to be 50.0 μm , where the loss is close to zero so that effects of the neighboring ridges are negligible.

11.2 Simulation details for the design of a ridge waveguide laser using WAVEGUIDE

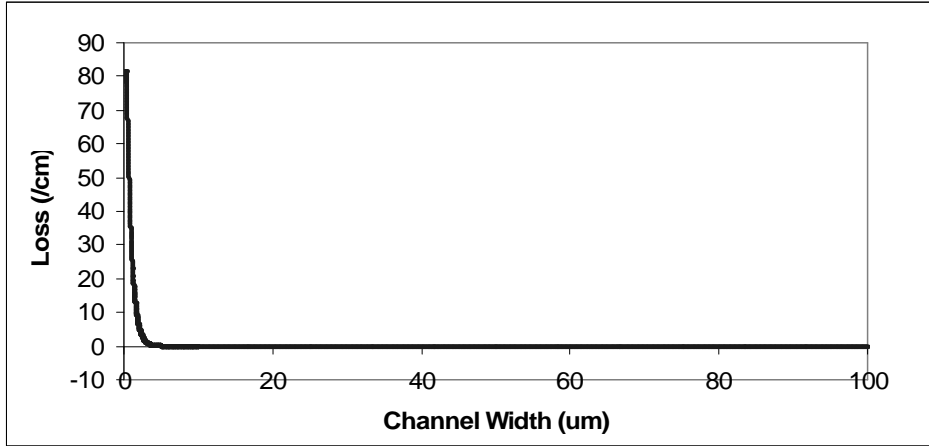


Figure 11.2.8 Plot of loss as a function of channel width

Table 11.2.17 List of loss as a function of channel width

TL(GAMMA	WZR	WZI	Loss	FWHPN	FWHPF	KM	IT
2)	(3)							
1.68								
E-13	0	3.244	8.21E-07	0.033273	0	0	4	30
0.01	0	3.244	2.35E-05	0.951663	0	0	4	30
0.02	0	3.244005	2.22E-05	0.900912	0	0	4	30
0.03	0	3.244001	8.29E-05	3.362192	0	0	4	30
0.04	0	3.244027	4.17E-05	1.6886	0	0	4	30
0.05	0	3.244061	0.000111	4.518944	0	0	4	30
0.06	0	3.244	0.000233	9.452193	0	0	4	30
0.07	0	3.244036	0.000193	7.80655	0	0	4	30
0.08	0	3.244018	0.000279	11.32504	0	0	4	30
0.09	0	3.24402	0.000361	14.61406	0	0	4	30
0.1	0	3.244042	0.000315	12.76496	0	0	4	30
0.11	0	3.244032	0.000282	11.44842	0	0	4	30
0.12	0	3.244118	0.000361	14.64831	0	0	4	30
0.13	0	3.243999	0.00038	15.40404	0	0	4	30
0.14	0	3.24452	0.000316	12.80764	0	0	4	30
0.15	0	3.244012	0.000723	29.32255	0	0	4	30
0.16	0	3.244039	0.000678	27.46385	0	0	4	30
0.17	0	3.243996	0.000671	27.21875	0	0	4	30
0.18	0	3.244074	0.001908	77.34917	0	0	4	30
0.19	0	3.243902	0.002015	81.67387	0	0	4	30
0.2	0	3.243986	0.001914	77.58206	0	0	4	30
0.21	0	3.243912	0.001876	76.04178	0	0	4	30
0.22	0	3.243969	0.001853	75.09517	0	0	4	30
0.23	0	3.243998	0.001857	75.29433	0	0	4	30
0.24	0	3.243978	0.001884	76.37682	0	0	4	30
0.25	0.00021008	3.243921	0.001938	78.5444	0.1735163	2.340376	6	3
0.26	0.00028286	3.243784	0.001968	79.78806	0.1884541	2.552964	6	3

...
...
...
5.83	0.8389797	3.240409	2.6E-07	0.010534	2.542285	13.15553	7	2
5.84	0.8389852	3.240409	2.56E-07	0.010361	2.541595	13.15397	6	1
5.85	0.8389907	3.240409	2.51E-07	0.010192	2.541011	13.15242	7	2
5.86	0.8389961	3.240409	2.47E-07	0.010025	2.540535	13.1509	6	1
5.87	0.8390013	3.240409	2.43E-07	0.009861	2.540164	13.14939	7	2
5.88	0.8390065	3.240409	2.39E-07	0.009699	2.539899	13.14784	6	1
5.89	0.8390115	3.240409	2.35E-07	0.00954	2.53974	13.14633	7	2
5.9	0.8390164	3.240409	2.31E-07	0.009384	2.539687	13.14491	6	1
5.91	0.8390212	3.240409	2.28E-07	0.00923	2.53974	13.14345	7	2
5.92	0.8390259	3.240409	2.24E-07	0.009079	2.539898	13.14201	6	1
5.93	0.8390305	3.240409	2.2E-07	0.00893	2.540162	13.14058	7	2
5.94	0.839035	3.240409	2.17E-07	0.008784	2.540531	13.13915	6	1
5.95	0.8390394	3.240409	2.13E-07	0.00864	2.541008	13.13774	7	2
5.96	0.8390437	3.240409	2.1E-07	0.008499	2.54159	13.13634	6	1
5.97	0.8390479	3.240409	2.06E-07	0.00836	2.54228	13.13498	7	2
5.98	0.839052	3.240409	2.03E-07	0.008223	2.543103	13.13363	6	1
5.99	0.839056	3.240409	2E-07	0.008088	2.544094	13.13229	7	2
6	0.8390599	3.240409	1.96E-07	0.007956	2.545252	13.12969	6	1
6.01	0.8390637	3.240409	1.93E-07	0.007825	2.544093	13.12837	7	2
6.02	0.8390675	3.240409	1.9E-07	0.007697	2.543102	13.12708	6	1
6.03	0.8390711	3.240409	1.87E-07	0.007571	2.542278	13.12581	7	2
6.04	0.8390746	3.240409	1.84E-07	0.007447	2.541587	13.12456	6	1
...
...
...

11.2.4 Summary

As an implementation to section 11.1, section 11.2 has provided an example of how to design a ridge waveguide laser using WAVEGUIDE program. In summary, the optimized wafer structure of the designed laser is again listed in Table 11.2.18 (a) and (b) with a 3- μm ridge width and 50- μm channel width. The laser performance simulation results is shown in Table 11.2.19. The refractive index profiles in the ridge and channel regions are shown in Figure 11.2.9 (a) and (b).

Table 11.2.18 Layer composition and thickness for (a) the ridge region and (b) channel regions of the designed ridge waveguide laser.

(a)

Layer	Material Composition	Thickness (um)
n-substrate	InP	200
Outer n-cladding	InP	1.87

(b)

Layer	Material Composition	Thickness (um)
n-substrate	InP	200
Outer n-cladding	InP	1.87
Inner n-cladding	Al _{0.48} In _{0.54} As	0.05

Figure 11.2.9 (a)

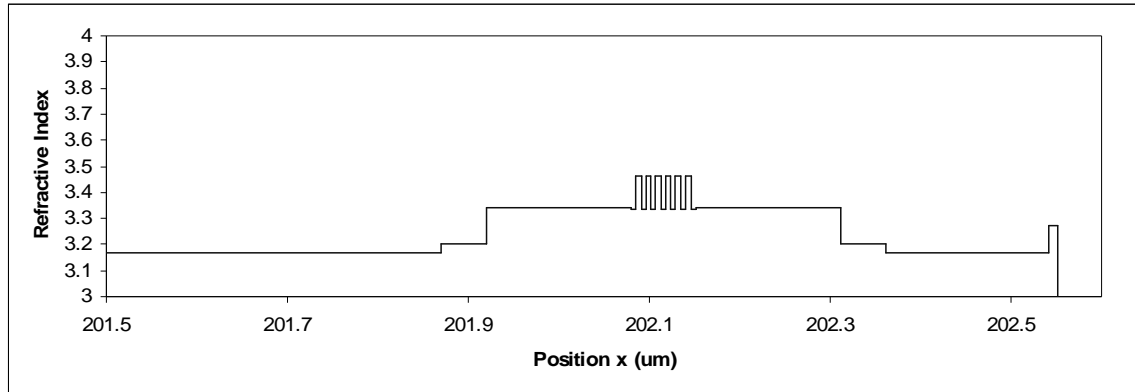


Figure 11.2.9 (b)

Figure 11.2.9 The refractive index profiles in the (a) ridge and (b) channel regions

11.3 Summary of the chapter

This chapter has explained how to design a ridge waveguide MQW laser using WAVEGUIDE program. Simulations details such as input files, output files and plots are provided and the optimization results are interpreted. The example in this chapter demonstrates the flexibility and versatility of the WAVEGUIDE program and how to use it to simulate laser waveguide characteristics such as loss, confinement factor, and far-field divergence. From the example and explanations, users should be able to develop an experience of how to use WAVEGUIDE program for simulation to achieve design requirements.

REFERENCES:

- [1] S.-L. Chuang, *Physics of Optoelectronic Devices*, 1, 421 and 245-246 (1995)
- [2] <http://enr.smu.edu/ee/smuphotonics/GainManualAppendixC/AppendixC.htm>

Chapter 12 Polymer Waveguide Integrated Isolators

12.1 Statement of the problem

Optical Isolators are two-port unidirectional devices that transmit light in one direction and block it in the opposite direction. They are used to eliminate light that is back-reflected, from splices and connectors etc., into lasers or the EDFAs in optical telecommunication systems. Current technology is based on bulk devices, and integrated isolators will provide devices and systems with superior performance than the current technology at reduced cost.

The operation principle of optical isolators is usually based on the nonreciprocal magneto-optic effects, such as Faraday rotation and Kerr effect. All magneto-optic effects are based on the variation of the medium's refractive index with the local magnetization of the material. This anisotropic behavior is the gyroelectric property of the material, which finds expression in the off-diagonal elements of the permittivity tensor $\epsilon(Q)$ of the medium, where Q is called the magneto-optical parameter, and the phase of Q is a measure for the change of ellipticity of the either transmitted or reflected light wave with respect to the incident light wave. Reversing the direction of magnetization results in a 180° -phase shift of Q . The optical behavior of the material is completely determined by the real and imaginary part of ϵ and Q . The absolute value of the complex magneto-optical parameter Q is proportional to the magnetization, which can be caused by an external field or originate from the spontaneous magnetization of the material itself.

Various magneto-optic media have been developed for optical devices, including YIG and $\text{Gd}_{3-x}\text{Bi}_x\text{Fe}_5\text{O}_{12}$. However, it is hard to fabricate these films on glass and semiconductor substrates because they must be grown epitaxially. Evaporated or sputtered continuous ferromagnetic films are easier to fabricate but they have very large optical losses.

The optical losses of the ferromagnetic composite films are much lower than those of bulky ferromagnetic metals. This is mainly caused by reduction of the optical losses due to the free electrons in the metal particles. Ferromagnetic composite films are formed by introducing nanometer-size ferromagnetic particles (such as Fe, Co or Ni) in a host

material (glass or semiconductor). It has been experimentally demonstrated that these composite films show the magneto-optic effects as strong as the conventional films, and have optical losses as low as 30 times when compared to continuous films [1].

In this work, the magneto-optical media is a Ferromagnetic-Plastic Composite (FPC) layer. As shown in Figure 12.1.1, this layer has Fe (alternatively Co or Ni) powder particles of about 30-50 nm size homogeneously dispersed in the polymer solution. Fe powder particles of ~30-50 nm size are mixed with polymer solution, while using an ultrasonic wave in order to homogeneously disperse the particles. The solution is deposited on the cladding using spin coating. Finally step to form the polymer/glass waveguide is to cure the film thermally or using the UV light.

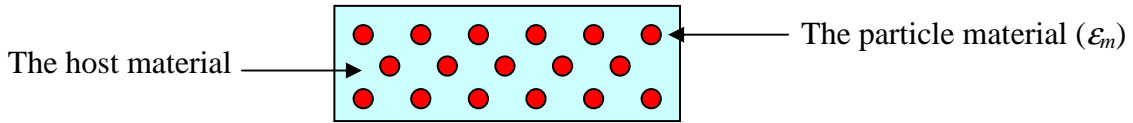


Figure 12.1.1 Ferromagnetic Composite Material

The relative effective dielectric constant of the composite is calculated from Maxwell-Garnet theory [1] as follows.

$$\frac{\epsilon_{eff} - \epsilon_p}{\epsilon_{eff} + 2\epsilon_p} = q \frac{\epsilon_m - \epsilon_p}{\epsilon_m + 2\epsilon_p} \quad (12.1)$$

The complex refractive index of the composite will be calculated from ϵ_{eff} :

$$n_c = n_{real} + i \cdot k \quad (12.2)$$

The real part of n_c in (12.2) will be used in the input file for the waveguide. The loss parameter for waveguide calculations is calculated from the imaginary part of the complex refractive index as follows, and the detailed explanation of n_{loss} parameter is found in Chapter 14:

$$n_{loss} = \frac{2\pi \cdot k}{\lambda} \quad (12.3)$$

Then the optical modal loss for waveguide is calculated from the imaginary part of the complex propagation constant as follows:

$$\alpha = \exp\left(\frac{-4\pi \cdot WZI \cdot z}{\lambda}\right) \quad (12.4)$$

Here WZI is an output parameter and the details can be found in Chapter 6. The unit for α is generally cm^{-1} , and it is power intensity loss. It is typical to talk about the power in dB and this loss quantity is usually converted to dB/cm.

12.2 The RLE Concept

Figure 12.2.1 is a schematic of an integrated isolator based on our approach. A Ferromagnetic Composite layer of thickness t_{RL} is formed on the clad layer of an optical waveguide. A magnetic field applied (H) in the lateral (y) direction results in a non-reciprocal change of the complex propagation constant of the TM like guided mode [2], [3], [4]. This non-reciprocal change is due to the magneto-optic Kerr effect. Thus, the loss for guided light traveling in the plus z direction is different than the loss in the minus z direction. For flow in a single direction, changing the polarity of the magnetic field will have the same effect as that which occurs when the flow direction is reversed and the magnetic field direction is constant.

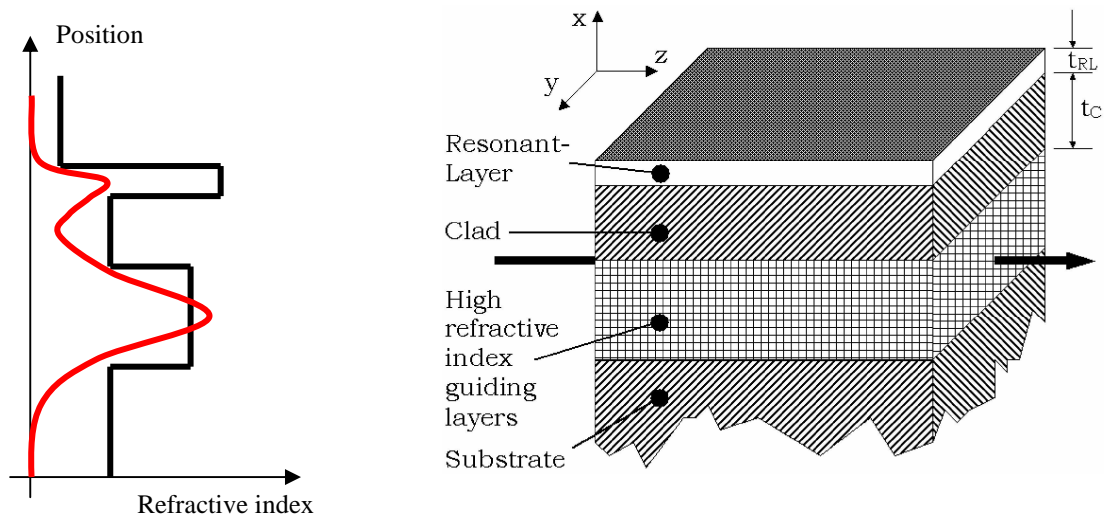


Figure 12.2.1 Fundamental mode near field intensity and isolator schematic

Fundamental modes' confinement in the secondary waveguide layer exhibits Resonance with proper design. The secondary field amplitude is sensitive to the added layer's thickness, location, refractive index, loss, and to the wavelength of operation. This phenomenon is labeled the Resonant-Layer Effect (RLE) [5]. The Ferromagnetic Composite, which is deposited on the clad layer of an optical waveguide (3 layer in this case), is therefore called the Resonant-Layer. A magnetic field applied in the y direction results large difference in loss for TM modes traveling in opposite z directions. This is due to a large confinement of the optical field in the RL layer in one direction, and much smaller confinement in the opposite direction as will be seen in Figure 12.4.1.

12.3 Input File for the Quartz Waveguide Isolator

Consider again the waveguide structure illustrated in Figure 12.2.1. A high-index layer with loss is applied on top of the clad layer of a waveguide consisting of undoped and doped quartz layers (similar to layers used in optical fibers). In this example, the RLE will result in a polarizer and broadband wavelength filter. Each layer of this waveguide is listed in Table 12.3.1. The RL layer is a Polymer, such as perfluorocyclobutyl polymer plastic BP [6], containing a dye that has modest absorption in the 1.55 μm wavelength region and is placed as the Resonant Layer of the waveguide shown in Figure 12.2.1.

The input file for the waveguide is below. The layers are identical to the layers in Table 12.3.1. The second layer (Absorptive Layer Polymer with Iron) is actually one layer and depending on the operation conditions one of the four possibilities will be taken. These are H(+) and H(-) for the isolator or TE or TM for the polarizer/wavelength filter. Also, the parameter KPOL=2 is to set the polarization for TM mode.

Table 12.3.1 Waveguide Layers For An Isolator, Polarizer and Wavelength Filter Using A Quartz Based Waveguide With A Polymer RL Layer

Center Wavelength $\lambda = 1.55 \mu\text{m}$			
Material	Loss, α (cm^{-1})	Refractive Index	Thickness (μm)
Air	0.0	1.0	-
Absorptive Layer Polymer with Iron (H(0))	3.925×10^2	1.53290	TE $t_{\text{RL}} = 0.670$ TM $t_{\text{RL}} = 0.805$
Absorptive Layer Polymer with Iron (H(+))	2.847×10^2	1.52427	$t_{\text{RL}} = 0.765$
Absorptive Layer Polymer with Iron (H(-))	5.543×10^2	1.52427	$t_{\text{RL}} = 0.880$
Quartz (p-) clad	0.0	1.447	$t_{\text{c}} = 4.0$
Doped quartz core	0.0	1.452	10.0
Quartz Substrate	0.0	1.447	-

INPUT FILE:

```
!This structure is for glass waveguide Isolator/Polarizer/Filter.
!The Polymers are with Nclad=1.447 and Ncore=1.452 at 1.55 um.
!FILENAME: isolator.wgi
!DESCRIPTION: Ferromagnetic Plastic Composite on Quartz substrate
!FPC is Polymer has Nhost=1.42 with volume fill factor q=0.08

!CASE Parameter Set
CASE KASE=WIFE
CASE EPS1=1E-9 EPS2=1E-9 GAMEPS=1E-3 QZMR=2.1054 QZMI=0.001
CASE PRINTF=1 INITGS=0 AUTOQW=0 NFPLT=1 FFPLT=1 IL=30

!MODCON Parameter Set
MODCON KPOL=2 APB1=0.25 APB2=0.25

!STRUCT Parameter Set
```

Chapter 12 Polymer Waveguide Integrated Isolater

```
STRUCT WV=1.55

!LAYER Parameter Set
!----- beginning of structure -----
!AIR on top LAY:1
LAYER AIR=1.0                                TL=0.0

!LAYER: 2 is the Resonant-Layer
!Depending on the operation, one of the following layers will be
!activated only. See Table 12.3.1 for layer parameters.
!Isolator layers are for H(+)/H(-)
!LAYER NREAL=1.52427      NLOSS=0.027713      TL=0.765
!LAYER NREAL=1.53967      NLOSS=0.014235      TL=0.880
!Polarizer layers are for TE/TM at H(0)
!LAYER NREAL=1.53290      NLOSS=0.019626      TL=0.670
!LAYER NREAL=1.53290      NLOSS=0.019626      TL=0.805

!quartz sub / doped quartz / quartz (p-) clad LAYS: 3-5
LAYER NREAL=1.447          NLOSS=0.0          TL=4.0
LAYER NREAL=1.452          NLOSS=0.0          TL=10.0
LAYER NREAL=1.447          NLOSS=0.0          TL=0.0
!----- end of structure -----

!OUTPUT Parameter Set
OUTPUT PHMO=1 GAMMAO=1 WZRO=1 WZIO=1 QZRO=0 QZIO=0
OUTPUT FWHPNO=0 FWHPFO=1 KMO=1 ITO=1
OUTPUT SPLTFL=0 MODOUT=0 LYROUT=0

!GAMOUT Parameter Set
GAMOUT LAYGAM=2 LAYGAM=4 COMPGAM=0 GAMALL=0

!LOOPX Parameter Set
!LOOPZ1 ILZ='QZMR'  FINV=1.9    ZINC=-0.001
!LOOPZ1 ILZ='WVL'  FINV=1.5    ZINC=-0.001
!LOOPX1 ILX='TL'    FINV=0.805  XINC=0.005          LAYCH=2
!LOOPX1 ILX='NLOSS' FINV=0.0    XINC=-0.0001       LAYCH=2
```


END

12.4 Quartz Waveguide Isolator

The thickness for the Resonant-Layer for the isolator was set to 0.5 μm initially and for H(+) calculations the layer parameters were set as shown below. The fundamental mode was found for this structure by looping QZMR value from the highest refractive index 2.3 ($\sim 1.52427^2$) to the lowest index 1.9 ($\sim 1.447^2$) in the structure. To confirm the fundamental mode, the QZMR value was set for the fundamental mode (WZR^2) and the near field intensity plot was observed. This time there should be no looping, and the calculation was for a single value of QZMR, which corresponds to the TM_0 mode.

```
!LAYER: 2 is the Resonant-Layer
!Isolator layer is for H(+)
LAYER NREAL=1.52427      NLOSS=0.027713      TL=0.5
```

Next, for the fundamental mode the Layer 2 thicknesses was looped from 0.5 μm initial value to a final value of 1.0 μm . The purpose of this computation is to calculate the Layer 2 (Resonant-Layer) confinement factor as a function of Layer 2 thickness itself.

The same steps were performed for H(-) calculations by setting Layer 2 parameters for this case, as shown below.

```
!LAYER: 2 is the Resonant-Layer
!Isolator layer is for H(-)
LAYER NREAL=1.53967      NLOSS=0.014235      TL=0.5
```

Then, the fundamental mode was found by QZMR looping as before. After that, Layer 2 thickness was varied from 0.5 μm to 1.0 μm and the confinement factor for this layer was calculated.

The dependence of the RL layer confinement factor on the RL layer thickness is shown in Figure 12.4.1. The resonance effect is observed at two values of RL thickness, each corresponding to the propagation direction of light. Changing the propagation direction of light is the same as changing the external applied magnetic field.

For a Ferromagnetic Composite (FC) layer with a thickness t_{RL} in the correct range, the relatively small change in complex refractive index between the positive $H(+)$ and negative $H(-)$ propagation direction causes the modal field of the waveguide to have a large overlap in the Ferromagnetic Composite RL layer in one direction and a much smaller overlap in the reverse direction. This is shown in Figures 12.4.2 and 12.4.3 for a polymer isolator on a quartz waveguide. This in turn results in a large difference in loss between the two directions resulting in a high isolation ratio and low insertion loss. Figures 12.4.2 and 12.4.3 correspond to the resonance conditions which occur for negative and positive applied bias magnetic field directions, respectively (see Figure 12.4.1).

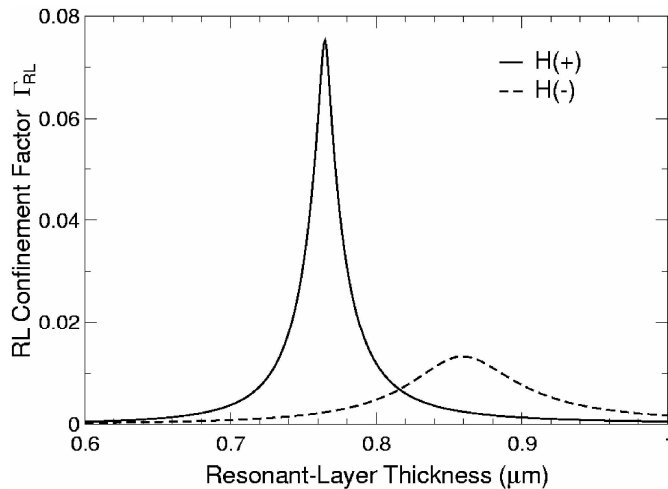


Figure 12.4.1 RL confinement factor vs. RL layer thickness indicates the sensitivity of the thickness of this layer. The resonance is observed at two certain RL thickness values corresponding to the propagation direction of light (equivalently the direction of magnetic field).

The isolation for an optical isolator is defined as the modal loss in the backward propagation direction. Both forward loss (insertion loss) and backward loss (isolation) are calculated by solving for the complex propagation constant of the fundamental mode and Equation (12.4) is used to calculate the cm^{-1} loss. The figure of merit for an isolator is the ratio of backward loss to forward loss. It is called the isolation to loss ratio. The loss values are calculated in dB/cm and the isolation to loss ratio is in dB/dB.

As seen from Figure 12.4.1, there are two resonance peaks, which occur at RL thickness values of $0.765 \mu\text{m}$ for $H(-)$ and $0.88 \mu\text{m}$ for $H(+)$ biasing magnetic fields.

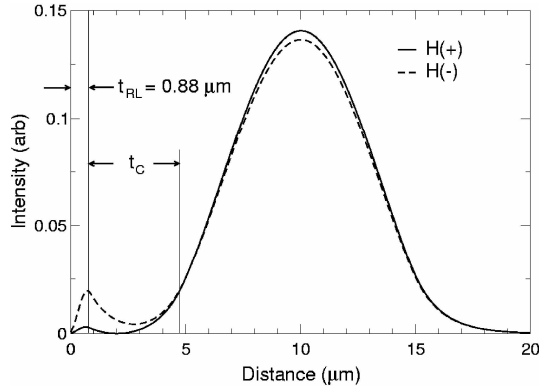


Figure 12.4.2 Near field intensity for an Ferromagnetic Composite RL layer showing the RLE on a quartz waveguide, $t_{\text{RL}} = 0.880 \mu\text{m}$ and $t_{\text{C}} = 4.0 \mu\text{m}$.

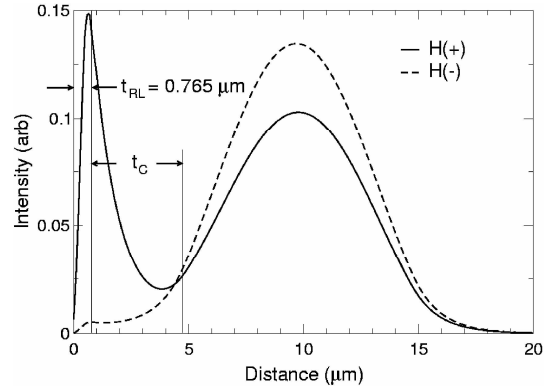


Figure 12.4.3 Near field intensity for an Ferromagnetic Composite RL layer showing the RLE on a quartz waveguide, $t_{\text{RL}} = 0.765 \mu\text{m}$ and $t_{\text{C}} = 4.0 \mu\text{m}$.

For $H(-)$ biasing magnetic field, the forward and backward modal losses are calculated for the fundamental mode. The Resonant-Layer parameters are:

$$N_{\text{REAL}}=1.53967, N_{\text{LOSS}}=0.014235, \text{ and } TL=\text{varied } (0.8 \text{ to } 0.95 \mu\text{m}) \text{ for } H(-), \text{ and}$$

$N_{\text{REAL}}=1.52427, N_{\text{LOSS}}=0.027713, \text{ and } TL=\text{varied } (0.7 \text{ to } 0.8 \mu\text{m}) \text{ for } H(+)$ direction.

The RL thickness was looped from $0.8 \mu\text{m}$ to $0.95 \mu\text{m}$ and the modal loss was calculated for $H(-)$ direction, and again the RL thickness was looped from $0.7 \mu\text{m}$ to $0.8 \mu\text{m}$ and the modal loss was calculated for $H(+)$ direction. The isolation in dB/cm and isolation loss ratio in dB/dB are plotted vs. composite thickness for this case in Figures 12.4.4 and 12.4.5 (corresponding to both negative and positive resonance conditions, respectively).

Next, the optimum layer loss for the Resonant-Layer is calculated using the layer parameters shown below:

$N_{\text{REAL}}=1.53967, N_{\text{LOSS}}=\text{varied } (0 \text{ to } 600 \text{ cm}^{-1}), \text{ and } TL=0.88 \mu\text{m} \text{ for } H(-)$ direction,

$N_{REAL}=1.52427$, $N_{LOSS}=varied (0 \text{ to } 600 \text{ cm}^{-1})$, and $TL=0.765 \mu\text{m}$ for $H(+)$ direction.

For each case, the fundamental mode is found for the RL layer values above by looping for the QZMR value. The initial n_{loss} value is zero (lossless). Next, for the fundamental mode the RL layer loss is looped from 0 to 600 cm^{-1} , which correspond to n_{loss} values from 0 to 0.03. Then, the RL layer confinement factor and the modal loss in dB/cm are calculated and plotted as a function of RL layer loss.

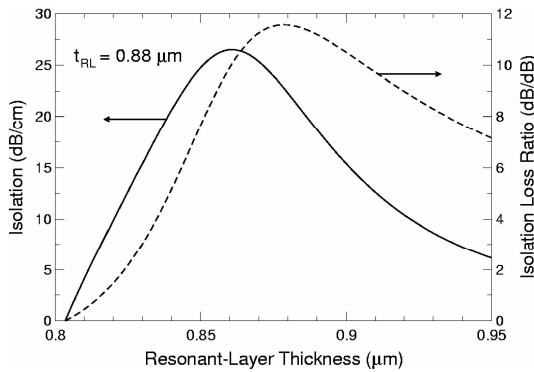


Figure 12.4.4 Resonant-Layer Polymer Isolator. For $H(-)$ biasing magnetic field, insertion loss and Ferromagnetic Composite RL layer confinement factor at $\lambda = 1.55 \mu\text{m}$ as a function of layer loss for Ferromagnetic Composite RL layer. Clad thickness is $t_C = 4.0 \mu\text{m}$ and the optimum RL thickness occurs $t_{RL} = 0.880 \mu\text{m}$.

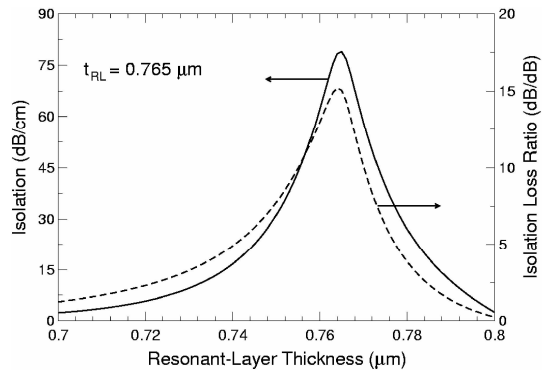


Figure 12.4.5 Resonant-Layer Polymer Isolator. For $H(+)$ biasing magnetic field, insertion loss and Ferromagnetic Composite RL layer confinement factor at $\lambda = 1.55 \mu\text{m}$ as a function of layer loss for Ferromagnetic Composite RL layer. Clad thickness is $t_C = 4.0 \mu\text{m}$ and the optimum RL thickness occurs $t_{RL} = 0.765 \mu\text{m}$.

Figures 12.4.6 and 12.4.7 indicate the optimum amount of loss for the RL layer in order to get the resonance effect and the maximum insertion loss. The amount of loss in the RL layer is critical for good isolator performance.

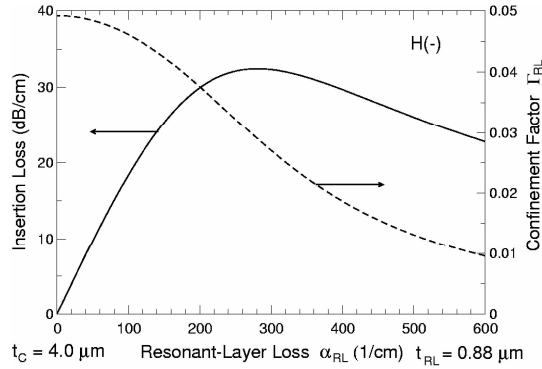


Figure 12.4.6 Insertion loss and RL layer confinement factor as a function of RL layer loss for H(-) biasing magnetic field. The maximum insertion loss occurs around $\alpha_{RL} = 280$ /cm. Here $t_{RL} = 0.880$ μm and $t_C = 4.0$ μm .

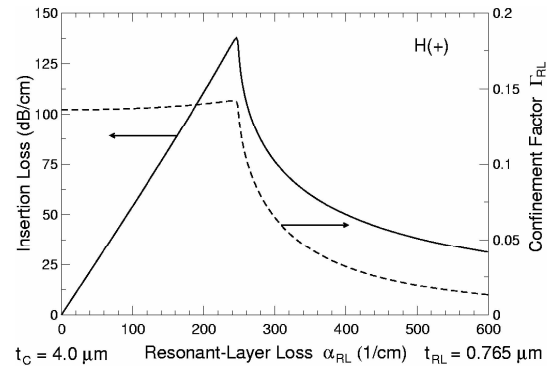


Figure 12.4.7 Insertion loss and RL layer confinement factor as a function of RL layer loss for H(+) biasing magnetic field. The maximum insertion loss occurs around $\alpha_{RL} = 260$ /cm. Here $t_{RL} = 0.765$ μm and $t_C = 4.0$ μm .

12.5 Quartz Waveguide Polarizer

Again for the waveguide structure illustrated in Figure 12.2.1, a high-index layer with loss is applied on top of the clad layer of a waveguide consisting of undoped and doped quartz layers (similar to layers used in optical fibers). In this example, the RLE will result in a polarizer and broadband wavelength filter. The RL layer is a Polymer, such as perfluorocyclobutyl polymer plastic BP [6], containing a dye that has modest absorption in the 1.55 μm wavelength region and is placed as the Resonant-Layer of the waveguide shown in Figure 12.2.1. In our case we use the same Ferromagnetic Composite RL layer as in the isolator case and the layer parameters are shown in Table 12.3.1 for the unbiased (H(0)) magnetic field. Near-field intensities illustrating the secondary peak for the lowest order TE and TM modes are plotted in Figures 12.5.1 and 12.5.2 at a wavelength of 1.55 μm and RL layer loss of $\alpha_{RL}=392.5$ cm^{-1} .

The RL layer parameters for the calculations are as follows:

$N_{REAL}=1.53290$, $N_{LOSS}=0.019625$, and $TL=0.670$ μm for TE polarization, and

$N_{REAL}=1.53290$, $N_{LOSS}=0.019625$, and $TL=0.805$ μm for TM polarization.

In Figure 12.5.1, at an RL layer thickness $t_{RL}=0.805 \mu\text{m}$ a strong secondary peak in the Resonant-Layer occurs for the TM mode and there is no peak for the TE mode. Here maximum absorption of the lowest order TM mode takes place. In Figure 12.5.2 where $t_{RL}=0.670 \mu\text{m}$, the secondary peak occurs for the TE mode, which will result in maximum absorption of this mode. In both figures, the thickness of the cladding layer t_C is $4.0 \mu\text{m}$.

To investigate the effect of polarization status of the light, the polarization parameter was set to TE and then TM. Below are the cases studied:

KPOL=1 corresponds to TE mode,

KPOL=2 corresponds to TM mode, and

The RL layer parameters for the calculations are as follows:

NREAL=1.53290, NLOSS=0.019625, and TL=varied (from 0.5 to 1.0 μm)

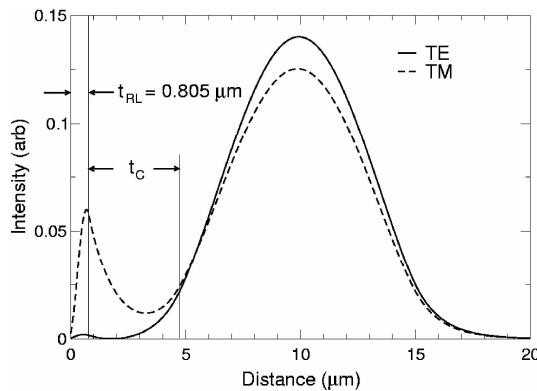


Figure 12.5.1 Near field intensity for an Ferromagnetic Composite RL layer showing the RLE on a quartz waveguide, $t_{RL} = 0.805 \mu\text{m}$ and $t_C = 4.0 \mu\text{m}$.

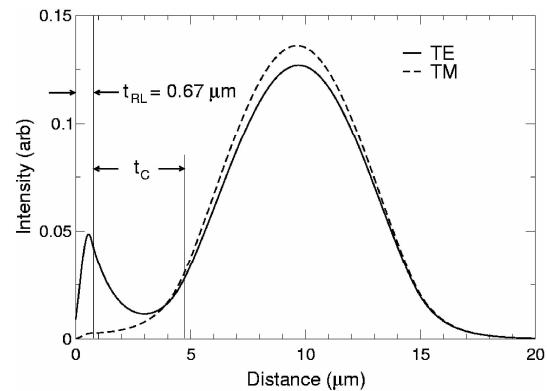


Figure 12.5.2 Near field intensity for an Ferromagnetic Composite RL layer showing the RLE on a quartz waveguide, $t_{RL} = 0.670 \mu\text{m}$ and $t_C = 4.0 \mu\text{m}$.

For both TE and TM polarization cases, the fundamental mode was calculated for RL thickness of $0.5 \mu\text{m}$ by looping for QZMR. Then the RL layer thickness was looped from 0.5 to $1.0 \mu\text{m}$ for the fundamental mode.

The effect of these secondary peaks on the modal transmission is illustrated in Figure 12.5.3, which shows the insertion loss as a function of the RL layer thickness. The solid line is for the TE₀ mode. The dashed line is for the TM₀ mode. At $t_{\text{RL}}=0.670 \mu\text{m}$ the TE shows maximum absorption while at $t_{\text{RL}}=0.805 \mu\text{m}$ the TM mode shows maximum absorption. The absorption passes through a maximum as the thickness of the RL layer is increased. This reflects the magnitude of the secondary peak that also passes through a maximum as the thickness is varied.

To study the optimum absorption value for the RL layer, the loss associated with this layer was varied from 0 to 600 /cm. The insertion loss and the confinement factor for the RL layer were calculated as a function of RL layer loss. First, the fundamental mode was found for zero loss case by looping QZMR. Then for the fundamental mode the RL layer loss was looped. The parameters for the input file are below:

KPOL=1 corresponds to TE mode, and

NREAL=1.53290, NLOSS=varied (from 0 to 0.03), and TL=0.670 μm

There is a limited range of RL layer absorption values over which such “resonant” secondary peaks may be observed, and a maximum value of modal (insertion) loss, which is illustrated in Figure 12.5.4. Figure 12.5.4 shows both the insertion loss and confinement factor of the TE mode at $\lambda=1.55 \mu\text{m}$ as a function of layer loss. In this case the maximum RLE giving rise to the highest insertion loss occurs at a RL layer loss $\alpha_{\text{RL}} \approx 220 \text{ cm}^{-1}$. At this peak value of insertion loss, the confinement factor is still very close to its maximum value which occurs at zero layer loss. In this plot the RL layer thickness t_{RL} is chosen to give strong TE absorption. The TM insertion loss is below 3 dB/cm over the loss range plotted, as suggested by Figure 12.5.3. Similar behavior is observed if the thickness is chosen to give strong TM absorption. In general, there is an optimum value of RL layer loss, which maximizes the modal (or insertion) loss for each particular device.

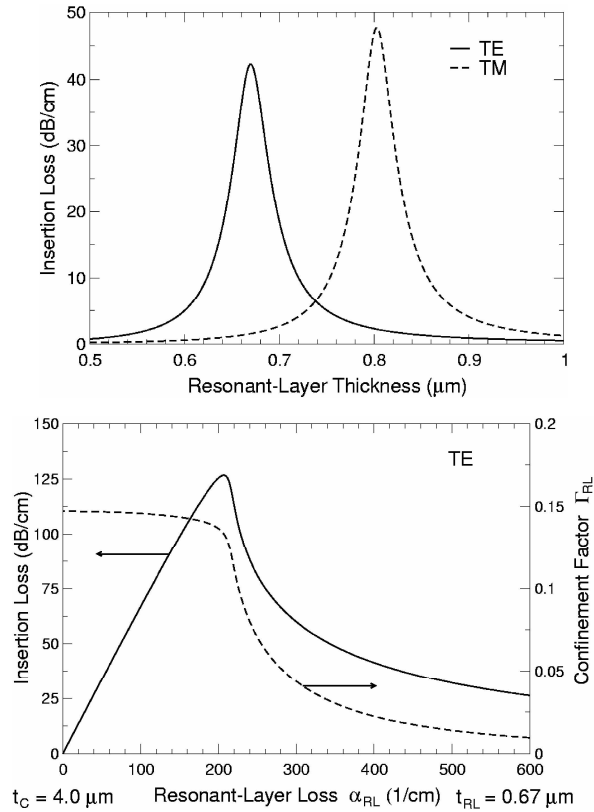


Figure 12.5.3 Insertion loss as a function of the RL layer thickness for a quartz waveguide with Ferromagnetic Composite RL layer. The solid line is the TE₀ mode and the dashed line is the TM₀ mode. RL layer loss is $\alpha_{RL} = 392.5 \text{ cm}^{-1}$ and wavelength of operation is $\lambda = 1.55 \mu\text{m}$.

Figure 12.5.4 Insertion loss and FC RL layer confinement factor of TE₀ mode at $\lambda = 1.55 \mu\text{m}$ as a function of RL layer loss (see Table 12.3.1 and Figure 12.2.1). The RL layer thickness is chosen as $0.670 \mu\text{m}$ to give a TM polarizer. The TM insertion loss is below 3 dB/cm (see Figure 12.5.3).

12.6 Quartz Waveguide Wavelength Filter

Finally, the wavelength dependence of the structure was investigated for both TE and TM polarizations. For both polarization cases, the initial wavelength was set to zero and the fundamental mode for each case was calculated by looping for QZMR. Then, the wavelength was looped from 1.50 to 1.60 μm and the insertion (forward) losses in dB/cm for each polarization were calculated and plotted. The calculations can be done in the reverse wavelength order as well, that is by initially taking wavelength as 1.60 μm and

then looping from 1.60 to 1.50 μm . It is sometimes possible to get the fundamental mode for one case easier than the other.

The RL layer parameters for the calculations are as follows:

STRUCT WV=1.50

NREAL=1.53290, NLOSS=0.019625, and TL=0.670 μm for TE polarization, and

NREAL=1.53290, NLOSS=0.019625, and TL=0.805 μm for TM polarization.

LOOPZ1 ILZ='WV' FINV=1.60 ZINC=0.001

Figure 12.6.1 is a plot of the insertion loss for both the TE_0 and TM_0 modes as a function of wavelength for $t_{\text{RL}}=0.670 \mu\text{m}$ and an RL layer loss of 392.5 cm^{-1} . The strong absorption of the TE mode ($\approx 40 \text{ dB/cm}$) and the weak absorption of the TE mode ($\approx 2 \text{ dB/cm}$) is the behavior of a TM Polarizer. Figure 12.6.2 is a similar plot for $t_{\text{RL}}=0.805 \mu\text{m}$. This case illustrates a good and rather broadband TE Polarizer with $\sim 50 \text{ dB/cm}$ absorption of the TM mode and a very weak absorption of the TE mode ($\approx 2.5 \text{ dB/cm}$). Thus, the Resonant-Layer Effect can be used to make an efficient polarizer and wavelength filter.

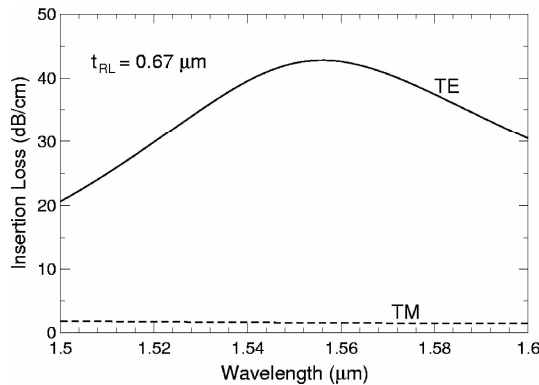


Figure 12.6.1 Band stop characteristic for quartz waveguide with Ferromagnetic Composite RL layer showing RLE. RL layer loss is $\alpha_{\text{RL}} = 392.5 \text{ cm}^{-1}$, $t_{\text{RL}} = 0.670 \mu\text{m}$ and $t_{\text{C}} = 4.0 \mu\text{m}$.

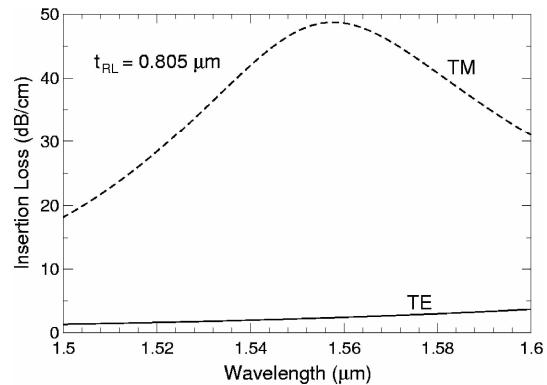


Figure. 12.6.2 Band stop characteristic for quartz waveguide with Ferromagnetic Composite RL layer showing RLE. RL layer loss is $\alpha_{\text{RL}} = 392.5 \text{ cm}^{-1}$, $t_{\text{RL}} = 0.805 \mu\text{m}$ and $t_{\text{C}} = 4.0 \mu\text{m}$.

REFERENCES:

- [1]. K. Baba, F. Takase, M. Miyagi, "Ferromagnetic particle composite polymer films for glass and semiconductor substrates", *Optics Communications*, **139**, 35-38, 15 June 1997.
- [2]. W. Zaets and K. Ando, "Optical waveguide isolator based on nonreciprocal loss/gain of amplifier covered by ferromagnetic layer", *Photon. Tech. Lett.*, **11**, 1012-1014, August 1999.
- [3]. Y. Okamura, T. Negate and S. Yamamoto, "Integrated optical Isolator and circulator using nonreciprocal phase shifters: A proposal", *Appl. Opt.*, **23**, 1866-1889, June 1984. See also T. Mizumoto and Y. Naito, "Nonreciprocal propagation characteristics of YIG thin film", *IEEE Trans. Microwave Theory and Techniques*, **MTT-30**, 922-925, June 1982.
- [4]. T. Mizumoto, K Oochi, T. Harada and Y. Naito, "Measurement of optical nonreciprocal phase shift in Bi-substituted GdFeO film and application to waveguide type optical circulators", *IEEE J. Lightwave Tech.*, **LT-4**, 347-352, March 1986.
- [5]. J. M. Hammer, G. A. Evans, G. Ozgur, and J. K. Butler, "Isolators, polarizers, and other optical waveguide devices using a resonant-layer effect," *IEEE J. Lightwave Tech.*, vol.22, no. 7, pp. 1754-1763, July 2004.
- [6]. J. Ballato, S. Foulger, D. W. Smith, Jr., "Optical properties of perfluorocyclobutyl polymers", *J. Opt. Soc. Am. B.*, vol. 20, in press, September 2003.

Chapter 13 Further Application of WAVEGUIDE ----Leaky Modes Calculation

13.1 Introduction

One of the powerful functions of WAVEGUIDE is the ability to calculate the leaky modes in a waveguide structure. A key to understanding the leaky mode is that the attenuation in a leaky mode is not due to the material absorption, but due to the radiation loss ^{[1], [2]}. In the following discussion, we will assume the materials considered here lossless.

Propagating modes (bounded modes), radiation modes and evanescent modes provide a complete set of orthogonal functions to represent the general field in a waveguide. They have either pure real or pure imaginary propagation constants. For example, in the case of TE mode in the 3-layer waveguide discussed in Chapter 2, the transverse component of electric field E_y and its corresponding modal distribution $\psi(x)$ can be written in the following forms:

$$E_y = F\psi(x)e^{j(\alpha z - \beta z)}$$

$$\psi(x) = \begin{cases} Ce^{-px} & (x \geq d) \\ A \cos(qx) + B \sin(qx) & (d \geq x \geq 0) \\ De^{r(x+d)} & (x \leq 0) \end{cases}$$

The modes here are classified into the propagating modes, radiation modes and evanescent modes, based on the values of propagation constants on both longitudinal (z) and transverse (x) direction.

In the case of propagating modes, the propagation constant along the longitudinal direction β is a pure real value. Therefore, there is no energy loss along the z direction. And the values of p, q, r are all real values too, which correspond to the sinusoidal oscillation in the core layer and the exponential decay in cladding layers. Thus the field is zero at \pm infinity for propagating modes.

Radiation modes have also pure real β values. The difference with the ones in propagating modes is that β here can take continuous value and the number of it is infinite, while in propagating modes β can only take some discrete values which satisfy the boundary conditions and the total number is finite. The conditions of propagation constants on transverse direction of radiation modes are different too. The wave number of q in core layer is still real. However, p and r in the cladding layers change to pure imaginary values. It means that the modes in the cladding region now keep sinusoidal oscillation, and no longer zero at infinity region.

In the case of evanescent modes, propagation constants β along longitudinal direction are pure imaginary and can take continuous values. And the field in the z direction cannot propagate since pure imaginary value β only results in amplitude attenuation but no propagation.

Although the leaky mode has many of the characteristics of the propagating mode, it is a class of “improper” mode since it doesn’t satisfy the radiation condition. Propagation constants of leaky mode on both longitudinal and transverse direction are no longer pure real or imaginary values. All values of β , p , q and r are complex. Therefore, not only does a leaky mode get the amplitude attenuation along the longitudinal direction, but it also loses energy in the transverse direction, that is, the field in the transverse infinity region is not zero. In other words, the power of a leaky mode in a waveguide decays exponentially with distance since it continuously radiates energy through the interfaces of the waveguide. ^[3]

13.2 Calculation of a Three-Layer Waveguide

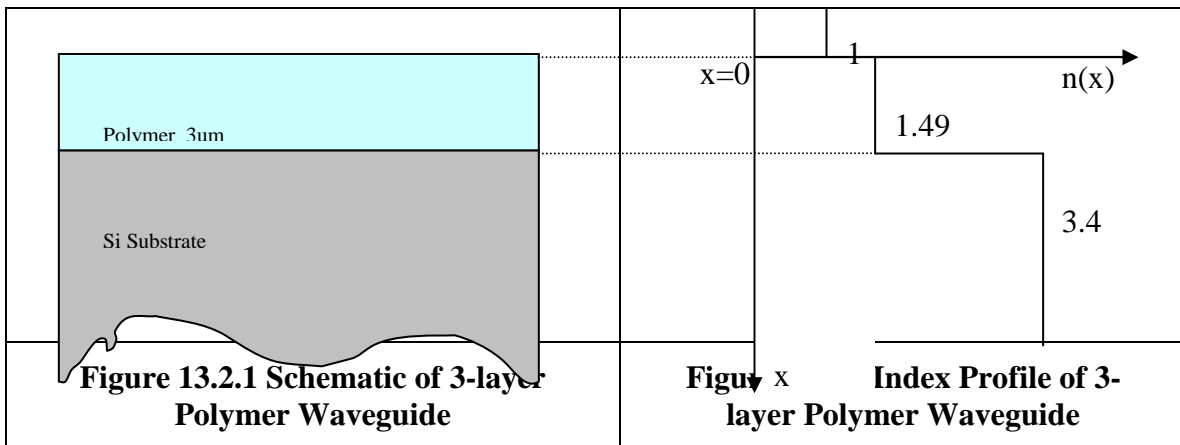
A simple polymer waveguide built on Si substrate is discussed here to demonstrate the calculation of leaky mode propagation. Polymer is becoming a very promising optical material in integrated optics in recent years, since it offers significant advantages, such as low cost, high performance, compatibility with IC and MEMS technologies and ability to be processed rapidly. However, polymer tends to be a low refractive index material (value of refractive index is between 1.3 to 1.7) when comparing with common

13.2 Calculation of a Three-Layer Waveguide

semiconductor substrate materials such as Si, GaAs and InP (their indices of refraction are around 3.4). Due to the high index mismatch in the structure where polymer is adjacent to a semiconductor substrate, leaky modes commonly exist in the waveguide and a significant percent of energy will leak from the polymer film to the semiconductor substrate layer during the light propagation along the waveguide. Table 13.2.1 shows the parameters of such a structure. And Figure 13.2-1 and 13.2-2 give the schematic and index profile of 3-layer polymer Waveguide.

Table 13.2.1 The Parameter of 3-Layer Waveguide

Layer	Thickness (μm)	Refractive Index
1 Superstrate (Air)	Infinity	1
2 Polymer	3	1.49
3 Substrate	Infinity	3.47



13.2.1 Input file

Based on the parameters of this structure, the initial input file is shown as follows

```
!WIF generated by WIFE (Waveguide Input File Editor)
```

Chapter 13 Further Application of WAVEGUIDE –Leaky modes calculation

```
!-----  
!FILENAME:      c:\waveguide\work\input\leaky_eg1.wgi  
!DESCRIPTION:  single Polymer layer on Si_1.55  
!-----  
  
!CASE Parameter Set  
CASE KASE=WIFE  
CASE EPS1=1E-9 EPS2=1E-9 GAMEPS=1E-6 QZMR=2.22 QZMI=0  
CASE PRINTF=0 INITGS=0 AUTOQW=0 NFPLT=1 FFPLT=1 IL=30  
  
!MODCON Parameter Set  
MODCON KPOL=1 APB1=0.25 APB2=0.25  
  
!STRUCT Parameter Set  
STRUCT WVL=1.55  
STRUCT XPERC1=0.0 XPERC2=0.0 XPERC3=0.0 XPERC4=0.0  
STRUCT YPERC1=0.0 YPERC2=0.0 YPERC3=0.0 YPERC4=0.0  
  
!LAYER Parameter Set  
LAYER AIR=1.0 TL=1.0  
LAYER NREAL=1.49 NLOSS=0 TL=3.0  
LAYER NREAL=3.47 NLOSS=0 TL=1.0  
  
!OUTPUT Parameter Set  
OUTPUT PHMO=1 GAMMAO=0 WZRO=1 WZIO=1 QZRO=0 QZIO=0  
OUTPUT FWHPNO=0 FWHPFO=0 KMO=1 ITO=1  
OUTPUT SPLTFL=0 MODOUT=0 LYROUT=1  
  
!GAMOUT Parameter Set  
GAMOUT LAYGAM=2 COMPGAM=0 GAMALL=0  
  
!LOOPX Parameter Set  
LOOPX1 ILX=0 FINV=4.1 XINC=0.1 LAYCH=3  
LOOPX2 ILX=0 FINV=0 XINC=0.1 LAYCH=2  
LOOPX3 ILX=0 FINV=0 XINC=0.1 LAYCH=2  
LOOPX4 ILX=0 FINV=0 XINC=0.1 LAYCH=2
```

13.2 Calculation of a Three-Layer Waveguide

```

!LOOPZ Parameter Set
LOOPZ1 ILZ=17 FINV=1 ZINC=-0.01
LOOPZ2 ILZ=0 FINV=0 ZINC=0.1
LOOPZ3 ILZ=0 FINV=0 ZINC=0.1
LOOPZ4 ILZ=0 FINV=0 ZINC=0.1

END

```

This file loops QZMR (the square of the effective index) from 2.22 to 1 in decrements of -0.01. This will find all TE modes propagating through this given slab polymer waveguide. To find all TM modes, we have to change the value of KPOL to 2 so that the polarization is set to TM.

13.2.2 Output file

We can find that there are 4 TE modes in this structure from the output file named leaky_eg1.db. The modified output files are shown below.

KM	QZMR	IT	PHM	WZR	WZI
6	2.220000E+00		9.296445E-01 6	1.470530E+00	9.552868E-04
6	2.210000E+00		9.296445E-01 6	1.470530E+00	9.552868E-04
6	2.200000E+00		9.296445E-01 5	1.470530E+00	9.552868E-04
6	2.190000E+00		9.296445E-01 5	1.470530E+00	9.552868E-04
6	2.180000E+00		9.296445E-01 4	1.470530E+00	9.552868E-04
7	2.170000E+00		9.296445E-01 4	1.470530E+00	9.552868E-04
6	2.160000E+00		9.296445E-01 3	1.470530E+00	9.552868E-04
6	2.150000E+00		9.296445E-01 4	1.470530E+00	9.552868E-04
...				
5	2.000000E+00		1.855931E+00 3	1.410808E+00	3.933833E-03
...				

```

1.580000E+00      2.773689E+00      1.306542E+00      9.312806E-03
5
...
1.260000E+00      3.669830E+00      1.149822E+00      1.765499E-02
5
...

```

Select the QZMR corresponding to the fundamental TE mode (here we take QZMR = 2.16) to replace the original value 2.22. Then close the loop and run WAVEGUIDE again. Here we only pay attention to the .nf output file since it gives information about the near field of this fundamental mode. Instead of listing the data, we give the plots of the distribution of near field electric field, intensity and phase.

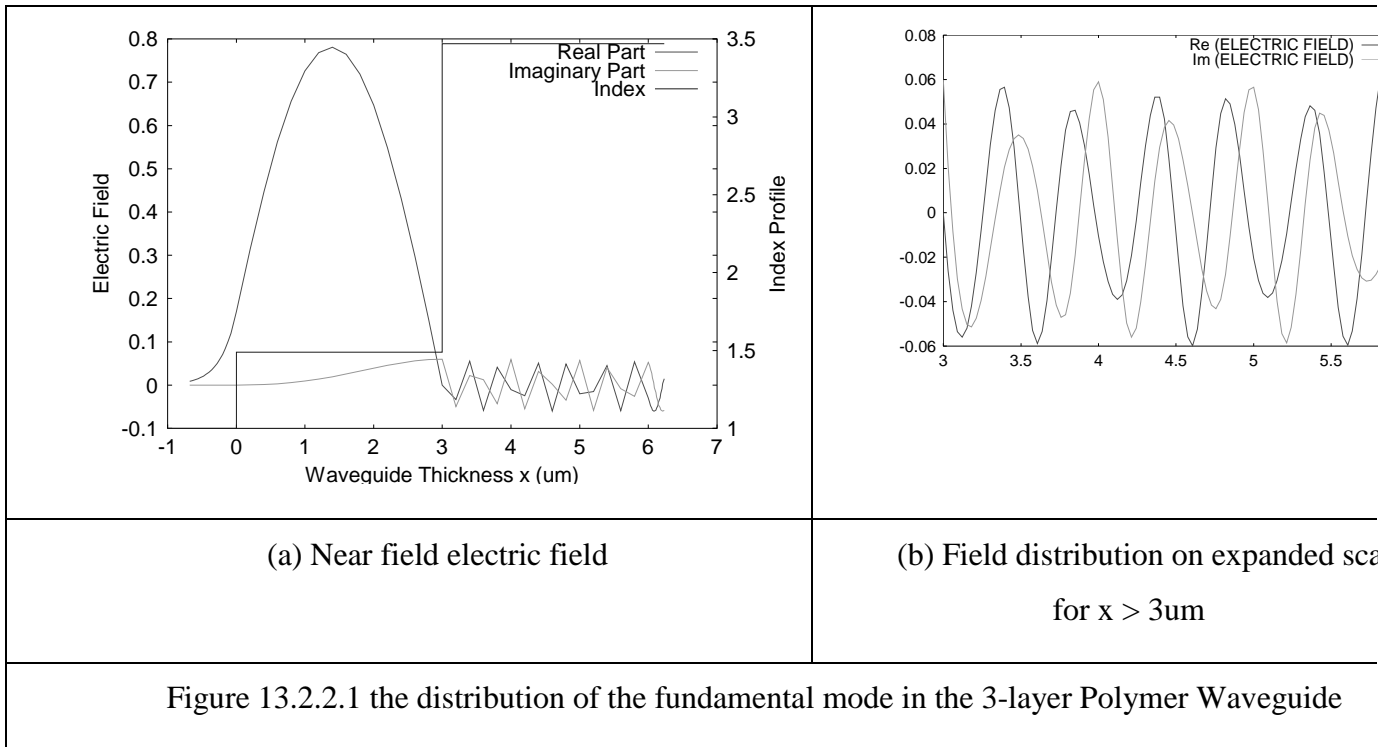
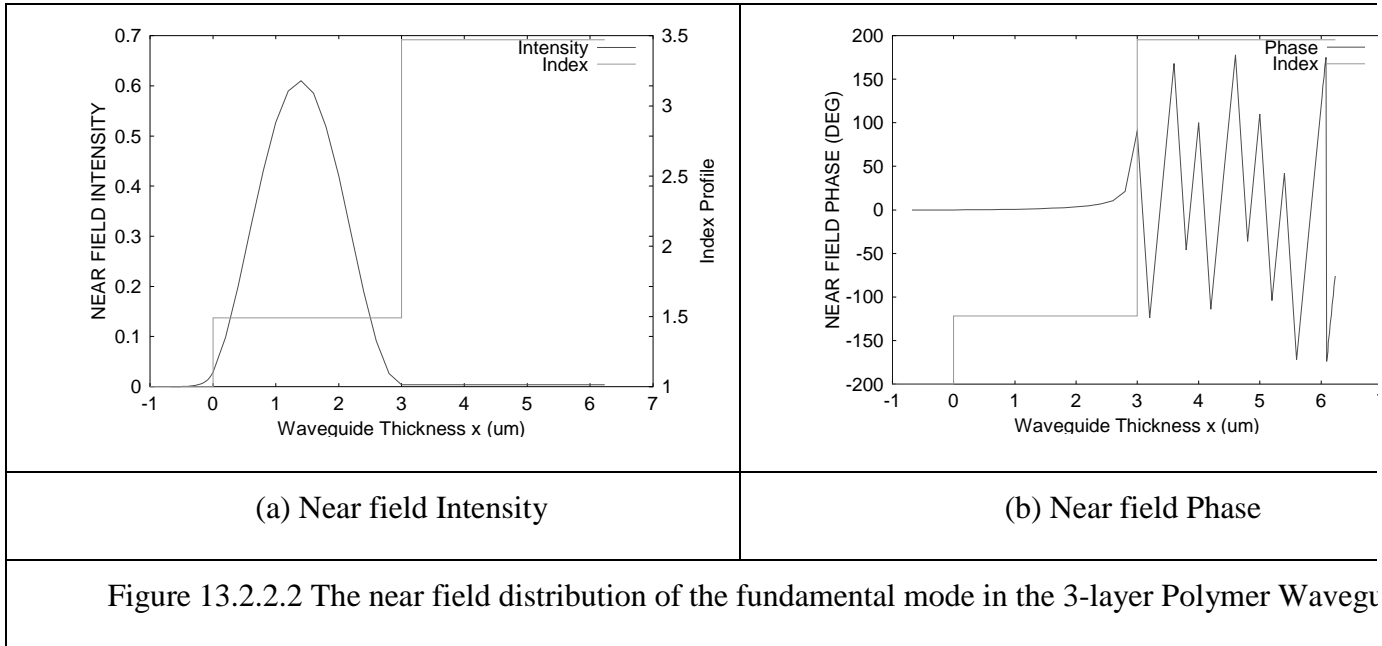


Fig. 13.2.2.1 shows the real and imaginary parts of the near field electric field for the fundamental mode in the 3-layer polymer waveguide (the refractive index profile is shown in the same plot too.) We note that both the real and imaginary parts oscillate in the substrate. Fig. 13.2.2.2 shows the near field intensity and phase of the fundamental mode in this structure. We can see that the phase (i.e. wavefront) curve in the polymer layer is nearly flat. However, it tilted a large angle when it reached to the substrate layer.

Since the wavefront is perpendicular to the propagation direction of the wave, Fig. 13.2.2.2(b) proves that the wave changed its propagation direction at the substrate and radiated part of its energy into the substrate. Therefore, this fundamental mode in the 3-layer waveguide is a leaky mode^{[4] [5]}.



13.2.3 Loss Calculation

In the output .db file, WZI represents the imaginary part of the normalized propagation constant and is corresponding to the amplitude attenuation in the propagation direction. We can calculate the intensity loss with WZI using the following equation:

$$\alpha = WZI \cdot (4\pi/\lambda) \cdot 10^4 \text{ /cm}$$

The loss turns out to be very big (18.89 dB/cm) since we have a large value of WZI (WZI = 9.552868E-04). It means a large number of energy is leaked to the substrate during the propagation of this fundamental mode. Since the loss increases dramatically as the waveguide become thinner, increasing the thickness of polymer film will be a possible solution to lower the loss. For example, the loss decreases to 12.58 dB/cm when

the thickness of polymer film is changed to $5\mu\text{m}$. Figure 13.2.3 shows the modal intensity loss vs. polymer layer thickness.

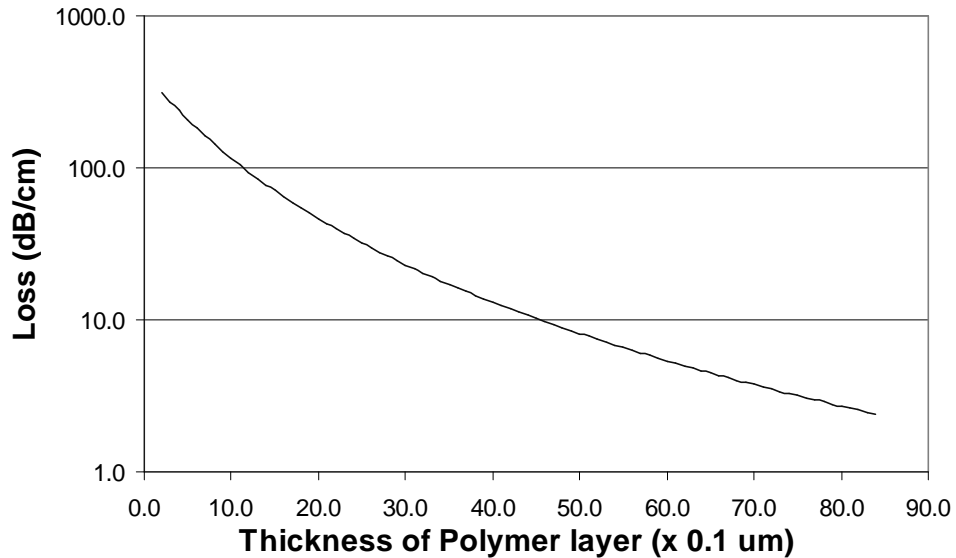


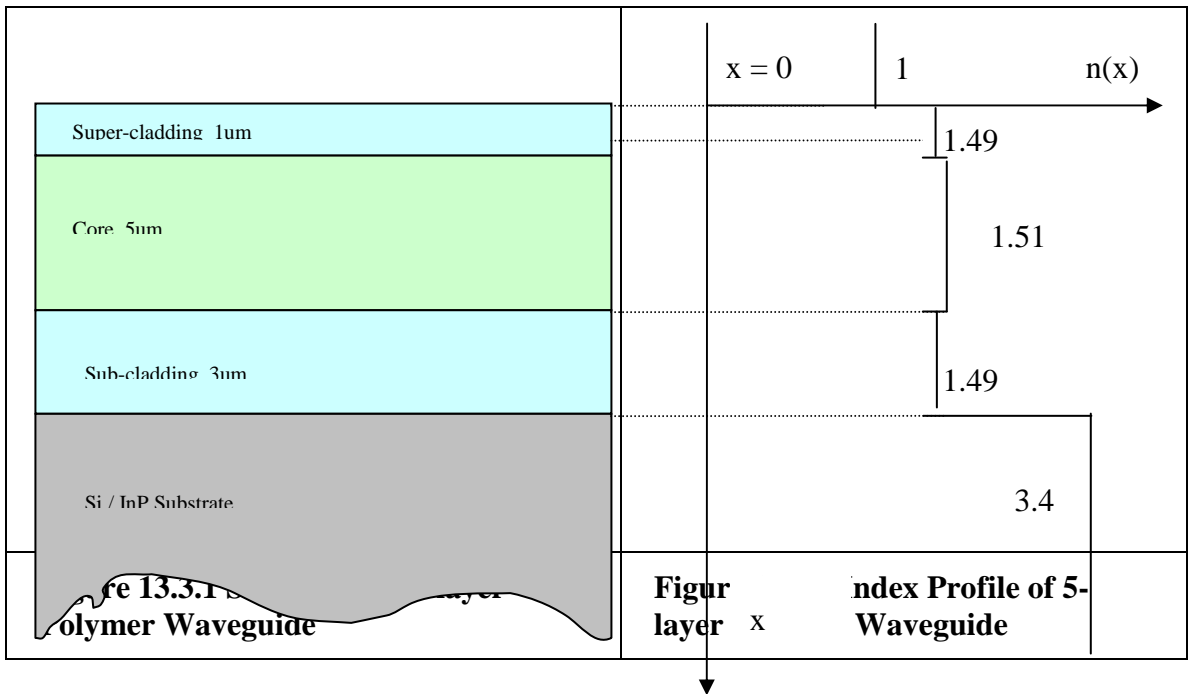
Figure 13.2.3 Loss Vs Polymer layer thickness in the 3-layer Polymer Waveguide

13.3 Calculation of a Five-Layer Waveguide

In the former case, the loss is significant since there is no confinement for the mode in the polymer layer. In this section, we discuss a five-layer waveguide whose indices of refraction of cladding layers are lower than the one of core layer, and thus give some confinement for modes in the core layer, even though the index of core is still much lower than the one of substrate. Table 13.3.1.1 shows the parameters of such a structure. And Figures 13.3.1 and 13.3.2 give the schematic and index profile of 5-layer polymer waveguide.

Table 13.3.1 The Parameters of 3-Layer Waveguide

Layer	Thickness (um)	Refractive Index
1 Superstrate (Air)	Infinity	1
2 Polymer Cladding	1	1.49
3 Polymer Core	5	1.51
4 Polymer Cladding	3	1.49
5 Substrate	Infinity	3.47



Following the same procedures we did in 3-layer waveguide, we got the following results for the fundamental mode in the 5-layer waveguide:

Chapter 13 Futher Application of WAVEGUIDE –Leaky modes calculation

	<i>PHM</i>	<i>WZR</i>	<i>WZI</i>	<i>KM</i>
<i>IT</i>				
	7.257343E-01	1.505805E+00	1.490966E-06	6
	4			

Still, we give the plots of the distribution of near field electric field, intensity and phase of the fundamental mode.

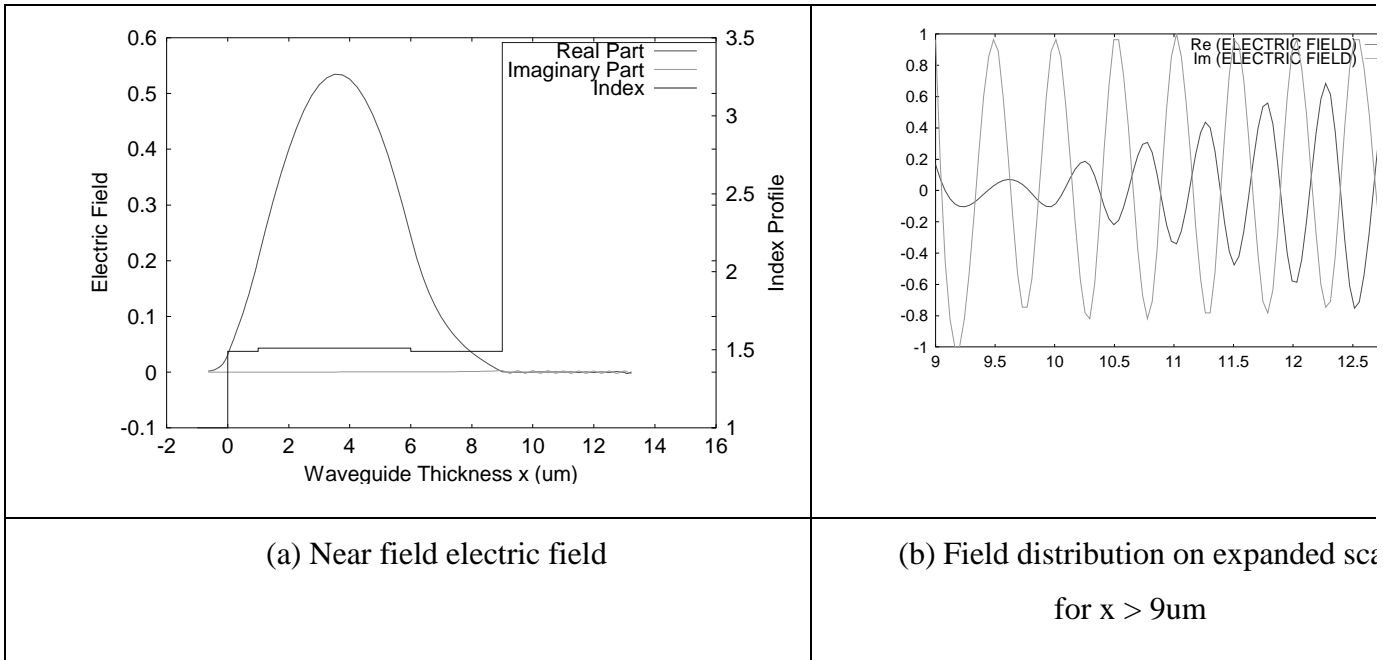
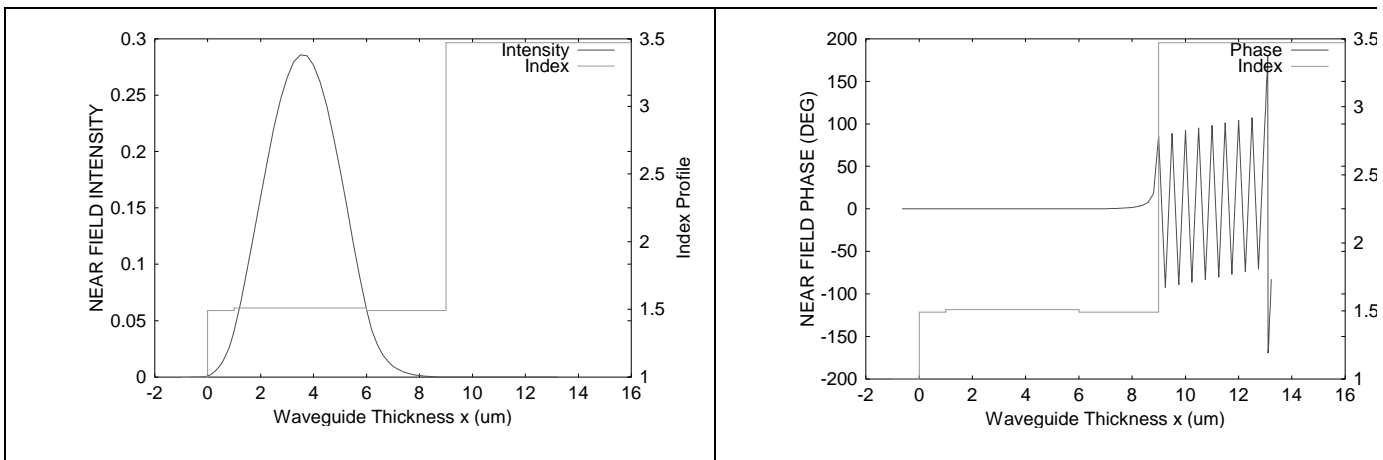


Figure 13.3.2 the distribution of near field electric field of the fundamental mode in the in the 5-layer Polymer Waveguide



13.3 Calculation of a Five-Layer Waveguide

(a) Near field Intensity	(b) Near field Phase
Figure 13.3.3 The near field distribution of the fundamental mode in the 3-layer Polymer Waveguide	

Fig. 13.3.2 shows the real and imaginary parts of the near field electric field. Because of the confinement of sub-cladding, the amplitudes of the electric field oscillations in the substrate are negligible, even though they are still sinusoidal oscillation. (Strictly speaking, the electric field is still complex.) Also, the phase curve in the polymer layers does not tilt until it reaches the substrate. It means the fundamental mode still changes its propagation direction at the substrate. However, the power radiated into the substrate can be negligible since most of its energy is confined into the core layer due to the confinement of the subcladding.

The loss is now reducing to 0.108 dB/cm ($WZI = 1.490966E-06$). It also proves that the loss is negligible for this structure. Figure 13.3.4 shows the modal intensity loss vs. the thickness of polymer core layer.

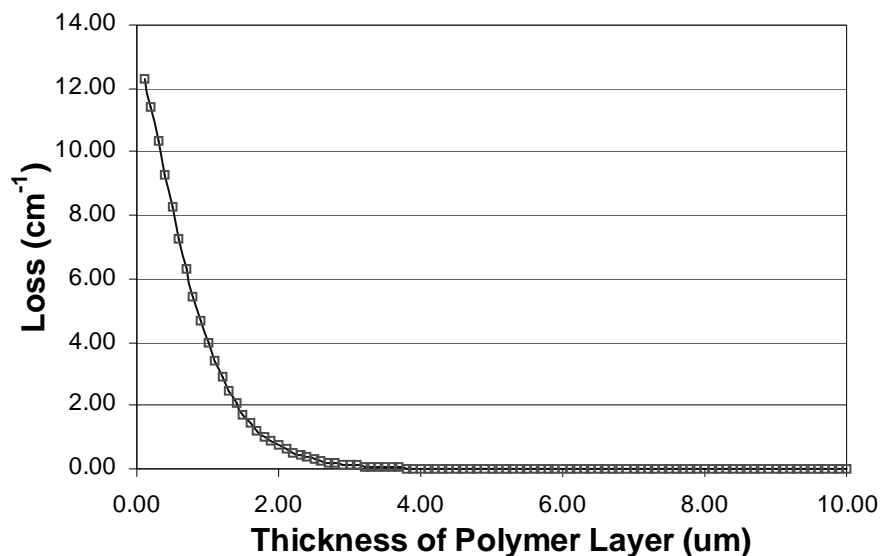


Figure 13.3.4 Loss Vs Polymer layer thickness in the 5-layer Polymer Waveguide

REFERENCES:

- [1]. T. Tamir “Integrated Optics”, Springer Verlag, Berlin (1976)
- [2]. D. Marcuse, IEEE J. Quantum Electronics, QE-8, 661 (1972)
- [3]. N.S. Kapany “Optical Waveguides”, Academic Press, New York, (1972)
- [4]. G. A. Evans, et al, “Lateral Optical Confinement of Channeled-Substrate Planar lasers with GaAs/AlGaAs Substrates”, IEEE J. Quantum Electron., v.24, no.5, pp737-749, 1988
- [5]. G. A. Evans, et al, “Observations and Consequences of Nonuniform Aluminum Concentrations in the Channel Regions of AlGaAs Channeled-Substrate-Planar lasers”, IEEE J. Quantum Electron., v.23, no.11, pp1900-1908, 1987

Chapter 14. Effects of metal cover on semiconductor lasers

14.1. Metal covered slab waveguide in semiconductor lasers

14.1.1. Introduction

Dielectric properties of metals used as electrical contacts in semiconductor lasers are much different from common dielectric materials. Evolving metal layers into semiconductor waveguide can bring different result from laser structure without metal cover.

14.1.2. The input file for wing region

The structure of a 1310nm semiconductor laser with metal layer as contacts is given as table 14.1.1.

In this structure Ni, Pt and Au layers are commonly used metal materials used as electrical contact. QZMR was looped from $n_{QW}^2 = 3.535976^2 \approx 12.50$, $n_{\min}^2 = 10$ to with step size -0.05, which is very small.

```
!CASE Parameter Set
CASE KASE=WIFE
CASE EPS1=1E-9 EPS2=1E-9 GAMEPS=1E-3 QZMR=12.40 QZMI=0.001
CASE PRINTF=1 INITGS=0 AUTOQW=0 NFPLT=0 FFPLT=0 IL=30
!MODCON Parameter Set
MODCON KPOL=0 APB1=0.25 APB2=0.25
!STRUCT Parameter Set
STRUCT WVL=1.31
STRUCT XPERC1=0.0 XPERC2=0.0 XPERC3=0.0 XPERC4=0.0
STRUCT YPERC1=0.0 YPERC2=0.0 YPERC3=0.0 YPERC4=0.0
!LAYER Parameter Set
LAYER NREAL=3.1987 NLOSS=0.0012 TL=1.0      !n-Sub
LAYER NREAL=3.2689 NLOSS=0 TL=0.002      !n-Transition GRIN structure
LAYER NREAL=3.2595 NLOSS=0 TL=0.002
LAYER NREAL=3.2500 NLOSS=0 TL=0.002
LAYER NREAL=3.2405 NLOSS=0 TL=0.002
LAYER NREAL=3.2310 NLOSS=0 TL=0.002
LAYER NREAL=3.2310 NLOSS=0 TL=0.11      !Inner n cladding
LAYER NREAL=3.2310 NLOSS=0 TL=0.02      !n-GRIN
LAYER NREAL=3.2665 NLOSS=0 TL=0.02
LAYER NREAL=3.3019 NLOSS=0 TL=0.02
LAYER NREAL=3.3374 NLOSS=0 TL=0.02
LAYER NREAL=3.3728 NLOSS=0 TL=0.02
LAYER NREAL=3.4850 NLOSS=0 TL=0.005      !QW
LAYER NREAL=3.3728 NLOSS=0 TL=0.01      !barrier
LAYER NREAL=3.4850 NLOSS=0 TL=0.005      !QW
LAYER NREAL=3.3728 NLOSS=0 TL=0.01      !barrier
LAYER NREAL=3.4850 NLOSS=0 TL=0.005      !QW
LAYER NREAL=3.3728 NLOSS=0 TL=0.01      !barrier
LAYER NREAL=3.4850 NLOSS=0 TL=0.005      !QW
LAYER NREAL=3.3728 NLOSS=0 TL=0.01      !barrier
```

Chapter 14 Effect of Metal Cover on Semiconductor Laser

```

LAYER NREAL=3.4850 NLOSS=0 TL=0.005      !QW
LAYER NREAL=3.3728 NLOSS=0 TL=0.02      !p-GRIN
LAYER NREAL=3.3374 NLOSS=0 TL=0.02
LAYER NREAL=3.3019 NLOSS=0 TL=0.02
LAYER NREAL=3.2665 NLOSS=0 TL=0.02
LAYER NREAL=3.2310 NLOSS=0 TL=0.02
LAYER NREAL=3.2310 NLOSS=0 TL=0.11      !Inner p cladding
LAYER NREAL=3.2310 NLOSS=0 TL=0.002     !p transition GRIN
LAYER NREAL=3.2405 NLOSS=0 TL=0.002
LAYER NREAL=3.2500 NLOSS=0 TL=0.002
LAYER NREAL=3.2595 NLOSS=0 TL=0.002
LAYER NREAL=3.2689 NLOSS=0 TL=0.002
LAYER NREAL=3.1987 NLOSS=0 TL=0.05      !p-spacer
LAYER NREAL=1.80 NLOSS=0 TL=0.03        !Si3N4
LAYER NREAL=3.7 NLOSS=18.2415 TL=0.05   !Ti
LAYER NREAL=4.64 NLOSS=26.6731 TL=0.12  !Pt
LAYER NREAL=0.18 NLOSS=41.3474 TL=1.0    !Au
!OUTPUT Parameter Set
OUTPUT PHMO=1 GAMMAO=0 WZRO=1 WZIO=1 QZRO=1 QZIO=0
OUTPUT FWHPNO=0 FWHPFO=0 KMO=1 ITO=1
OUTPUT SPLTFL=0 MODOUT=0 LYROUT=1
!GAMOUT Parameter Set
GAMOUT LAYGAM=8 COMPGAM=0 GAMALL=0
!LOOPX Parameter Set
LOOPX1 ILX=0 FINV=0 XINC=0.1 LAYCH=2
LOOPX2 ILX=0 FINV=0 XINC=0.1 LAYCH=2
LOOPX3 ILX=0 FINV=0 XINC=0.1 LAYCH=2
LOOPX4 ILX=0 FINV=0 XINC=0.1 LAYCH=2
!LOOPZ Parameter Set
LOOPZ1 ILZ=17 FINV=10 ZINC=-0.05      !QZMR
LOOPZ2 ILZ=0 FINV=0 ZINC=0.1
LOOPZ3 ILZ=0 FINV=0 ZINC=0.1
LOOPZ4 ILZ=0 FINV=0 ZINC=0.1
END

```

Table 14.1.1 Input file of 1310nm laser structure with metal cover at wing region

14.1.3. Result of evaluation

The layers information is shown as below:

```

# of layers = 37
LAYER01 NLOSS= 0.00120      NREAL= 3.19870      TL= 1.00000
LAYER02 NLOSS= 0.00000      NREAL= 3.26890      TL= 0.00200
LAYER03 NLOSS= 0.00000      NREAL= 3.25950      TL= 0.00200
LAYER04 NLOSS= 0.00000      NREAL= 3.25000      TL= 0.00200
LAYER05 NLOSS= 0.00000      NREAL= 3.24050      TL= 0.00200
LAYER06 NLOSS= 0.00000      NREAL= 3.23100      TL= 0.00200
LAYER07 NLOSS= 0.00000      NREAL= 3.23100      TL= 0.11000
LAYER08 NLOSS= 0.00000      NREAL= 3.23100      TL= 0.02000
LAYER09 NLOSS= 0.00000      NREAL= 3.26650      TL= 0.02000
LAYER10 NLOSS= 0.00000      NREAL= 3.30190      TL= 0.02000
LAYER11 NLOSS= 0.00000      NREAL= 3.33740      TL= 0.02000
LAYER12 NLOSS= 0.00000      NREAL= 3.37280      TL= 0.02000
LAYER13 NLOSS= 0.00000      NREAL= 3.48500      TL= 0.00500
LAYER14 NLOSS= 0.00000      NREAL= 3.37280      TL= 0.01000
LAYER15 NLOSS= 0.00000      NREAL= 3.48500      TL= 0.01000
LAYER16 NLOSS= 0.00000      NREAL= 3.37280      TL= 0.01000
LAYER17 NLOSS= 0.00000      NREAL= 3.48500      TL= 0.00500
LAYER18 NLOSS= 0.00000      NREAL= 3.37280      TL= 0.01000
LAYER19 NLOSS= 0.00000      NREAL= 3.48500      TL= 0.00500
LAYER20 NLOSS= 0.00000      NREAL= 3.37280      TL= 0.01000
LAYER21 NLOSS= 0.00000      NREAL= 3.48500      TL= 0.00500
LAYER22 NLOSS= 0.00000      NREAL= 3.37280      TL= 0.02000

```


14.1 Metal Covered Slab Waveguide in Semiconductor Lasers

LAYER23	NLOSS= 0.00000	NREAL= 3.33740	TL= 0.02000
LAYER24	NLOSS= 0.00000	NREAL= 3.30190	TL= 0.02000
LAYER25	NLOSS= 0.00000	NREAL= 3.26650	TL= 0.02000
LAYER26	NLOSS= 0.00000	NREAL= 3.23100	TL= 0.02000
LAYER27	NLOSS= 0.00000	NREAL= 3.23100	TL= 0.11000
LAYER28	NLOSS= 0.00000	NREAL= 3.23100	TL= 0.00200
LAYER29	NLOSS= 0.00000	NREAL= 3.24050	TL= 0.00200
LAYER30	NLOSS= 0.00000	NREAL= 3.25000	TL= 0.00200
LAYER31	NLOSS= 0.00000	NREAL= 3.25950	TL= 0.00200
LAYER32	NLOSS= 0.00000	NREAL= 3.26890	TL= 0.00200
LAYER33	NLOSS= 0.00000	NREAL= 3.19870	TL= 0.05000
LAYER34	NLOSS= 0.00000	NREAL= 1.80000	TL= 0.03000
LAYER35	NLOSS=18.24150	NREAL= 3.70000	TL= 0.05000
LAYER36	NLOSS=26.67310	NREAL= 4.64000	TL= 0.12000
LAYER37	NLOSS=41.34740	NREAL= 0.18000	TL= 1.00000

And result of mode searching is:

QZMR	PHM	WZR	WZI	QZR	KM	IT
1.240000E+01	4.227304E+00	1.675837E+00	2.012348E+00	-1.241114E+00	5	20
1.235000E+01	4.227304E+00	1.675837E+00	2.012348E+00	-1.241114E+00	5	20
1.230000E+01	4.227304E+00	1.675837E+00	2.012348E+00	-1.241114E+00	5	20
1.225000E+01	4.227304E+00	1.675837E+00	2.012348E+00	-1.241114E+00	5	20
1.220000E+01	2.964338E+00	2.625931E+00	7.259664E-01	6.368486E+00	5	18
1.215000E+01	2.964338E+00	2.625931E+00	7.259664E-01	6.368486E+00	5	18
1.210000E+01	2.964338E+00	2.625931E+00	7.259664E-01	6.368486E+00	5	18
1.205000E+01	2.964338E+00	2.625931E+00	7.259664E-01	6.368486E+00	5	18
1.200000E+01	2.964338E+00	2.625931E+00	7.259664E-01	6.368486E+00	5	17
1.195000E+01	2.964338E+00	2.625931E+00	7.259664E-01	6.368486E+00	5	17
1.190000E+01	2.964338E+00	2.625931E+00	7.259664E-01	6.368486E+00	5	17
1.185000E+01	2.964338E+00	2.625931E+00	7.259664E-01	6.368486E+00	5	17
1.180000E+01	2.964338E+00	2.625931E+00	7.259664E-01	6.368486E+00	5	17
1.175000E+01	2.964338E+00	2.625931E+00	7.259664E-01	6.368486E+00	5	17
1.170000E+01	2.964338E+00	2.625931E+00	7.259664E-01	6.368486E+00	6	17
1.165000E+01	2.964338E+00	2.625931E+00	7.259664E-01	6.368486E+00	5	16
1.160000E+01	2.964338E+00	2.625931E+00	7.259664E-01	6.368486E+00	5	16
1.155000E+01	2.964338E+00	2.625931E+00	7.259664E-01	6.368486E+00	5	16
1.150000E+01	1.418835E+00	3.223562E+00	1.691319E-03	1.039135E+01	6	7
1.145000E+01	1.418835E+00	3.223562E+00	1.691319E-03	1.039135E+01	6	7
1.140000E+01	1.418835E+00	3.223562E+00	1.691319E-03	1.039135E+01	6	7
1.135000E+01	1.418835E+00	3.223562E+00	1.691319E-03	1.039135E+01	6	7
1.130000E+01	1.418835E+00	3.223562E+00	1.691319E-03	1.039135E+01	6	7
1.125000E+01	1.418835E+00	3.223562E+00	1.691319E-03	1.039135E+01	6	7
1.120000E+01	1.418835E+00	3.223562E+00	1.691319E-03	1.039135E+01	7	7
1.115000E+01	1.418835E+00	3.223562E+00	1.691319E-03	1.039135E+01	7	7
1.110000E+01	1.418835E+00	3.223562E+00	1.691319E-03	1.039135E+01	6	6
1.105000E+01	1.418835E+00	3.223562E+00	1.691319E-03	1.039135E+01	6	6
1.100000E+01	1.418835E+00	3.223562E+00	1.691319E-03	1.039135E+01	6	6
.....						
1.055000E+01	1.418835E+00	3.223562E+00	1.691319E-03	1.039135E+01	6	4
1.050000E+01	1.418835E+00	3.223562E+00	1.691319E-03	1.039135E+01	6	4
1.045000E+01	1.418835E+00	3.223562E+00	1.691319E-03	1.039135E+01	7	4
1.040000E+01	1.418835E+00	3.223562E+00	1.691319E-03	1.039135E+01	6	3
.....						
1.015000E+01	1.418835E+00	3.223562E+00	1.691319E-03	1.039135E+01	7	6
1.010000E+01	1.418835E+00	3.223562E+00	1.691319E-03	1.039135E+01	7	6
1.005000E+01	1.418835E+00	3.223562E+00	1.691319E-03	1.039135E+01	7	6

14.1.4. Fundamental mode in wing region

From the result of mode searching we can see that when $KM > 5$, the WZI value is at the order of 10^{-3} . When $QZMR = 11.15$ gives $KM=7$ and $IT=7$. Then we end the looping and set the QZMR value to 11.15. For this fixed value we run the program and obtain the output parameters db file, near field and profile of indices of each layer. For the TE_0 mode, near field (real part and intensity) is plotted as figures 14.1.1.

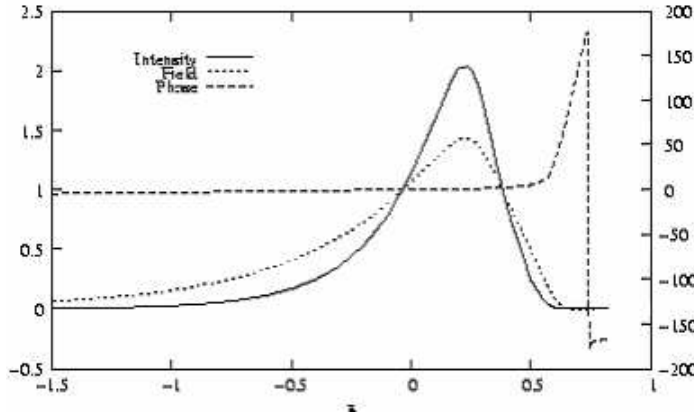


Figure 14.1.1. Fundamental mode near field plots for wing region

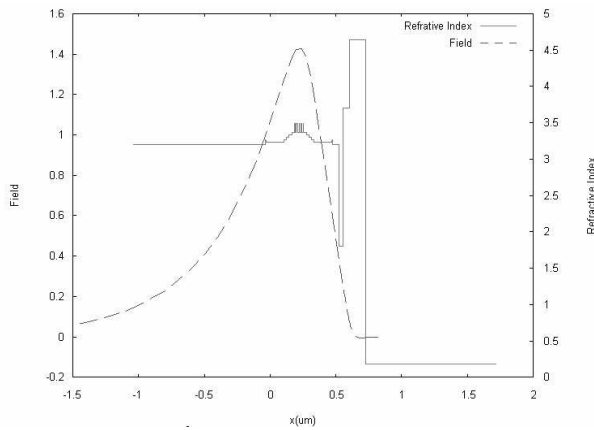


Figure 14.1.2. The comparison of refractive index and field

From the result we note that there is a phase change at the dielectric-metal interface. Because of existence of metal layers, the mode is leaky with WZI to be in order 10^{-3} . Also we can see the 180 degrees phase change at the interface of platinum layer and gold layer.

14.1.5. Fundamental mode in ridge region

The layer structure at ridge region is different from wing region. From the input file of wing region, substitute Si_3N_4 layer by etch stop layer, outer p-cladding layer and p-cap layers as below.

Table 14.1.2 Substitution of nitride layer by the following layers for ridge region

LAYER NREAL=3.3414 NLOSS=0 TL=0.025	!Etch stop
LAYER NREAL=3.1987 NLOSS=0 TL=1.25	!Outer p-cladding
LAYER NREAL=3.0667 NLOSS=0 TL=0.2	!P-cap

14.1 Metal Covered Slab Waveguide in Semiconductor Lasers

Search mode by looping QZMR from 12.50 to 10 with step size -0.05 . The output db field is as follows. And near field of TE_0 mode is plotted as figure 14.1.2.

QZMR	PHM	WZR	WZI	QZR	QZI	KM	IT
1.240000E+01	5.809668E+00	2.817009E+00	6.722267E-02	7.931023E+00	3	30	
1.235000E+01	3.476195E+00	3.102401E+00	1.659044E-02	9.624617E+00	5	28	
1.230000E+01	5.809721E+00	2.816999E+00	6.721301E-02	7.930967E+00	3	30	
1.225000E+01	2.489244E+00	3.173291E+00	3.176866E-03	1.006977E+01	6	25	
1.220000E+01	5.809722E+00	2.816999E+00	6.721296E-02	7.930967E+00	3	30	
1.215000E+01	2.489244E+00	3.173291E+00	3.176866E-03	1.006977E+01	5	24	
.....							
1.115000E+01	4.641235E+00	2.986656E+00	3.844191E-02	8.918637E+00	5	22	
1.110000E+01	4.641235E+00	2.986656E+00	3.844191E-02	8.918637E+00	5	22	
1.105000E+01	3.476195E+00	3.102401E+00	1.659044E-02	9.624617E+00	5	19	
.....							
1.070000E+01	2.489244E+00	3.173291E+00	3.176866E-03	1.006977E+01	5	12	
1.065000E+01	1.317899E+00	3.246359E+00	3.413429E-05	1.053885E+01	7	7	
1.060000E+01	1.317899E+00	3.246359E+00	3.413429E-05	1.053885E+01	6	5	
1.055000E+01	1.317899E+00	3.246359E+00	3.413429E-05	1.053885E+01	7	4	
1.050000E+01	1.317899E+00	3.246359E+00	3.413429E-05	1.053885E+01	7	5	
1.045000E+01	1.317899E+00	3.246359E+00	3.413429E-05	1.053885E+01	6	5	
1.040000E+01	2.489244E+00	3.173291E+00	3.176866E-03	1.006977E+01	6	8	
1.035000E+01	2.489244E+00	3.173291E+00	3.176866E-03	1.006977E+01	5	7	
1.030000E+01	2.489244E+00	3.173291E+00	3.176866E-03	1.006977E+01	6	7	
1.025000E+01	2.489244E+00	3.173291E+00	3.176866E-03	1.006977E+01	6	7	
1.020000E+01	2.489244E+00	3.173291E+00	3.176866E-03	1.006977E+01	5	5	
1.015000E+01	2.489244E+00	3.173291E+00	3.176866E-03	1.006977E+01	6	5	
1.010000E+01	2.489244E+00	3.173291E+00	3.176866E-03	1.006977E+01	5	4	
1.005000E+01	2.489244E+00	3.173291E+00	3.176866E-03	1.006977E+01	6	4	
1.000000E+01	2.489244E+00	3.173291E+00	3.176866E-03	1.006977E+01	6	5	

.....

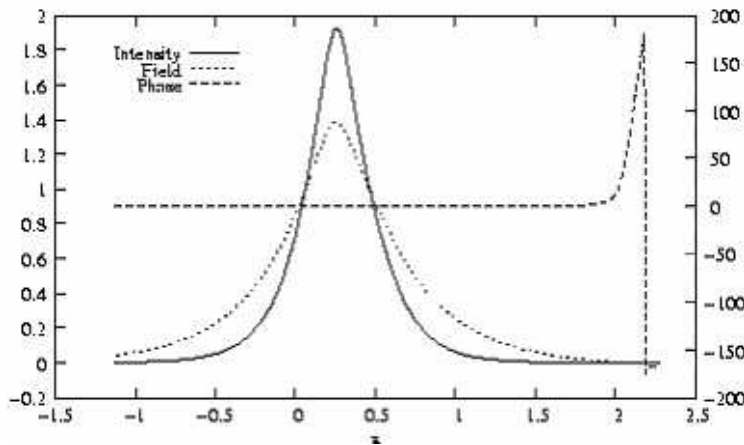


Figure 14.1.3 Fundamental mode near field plots for at ridge region.

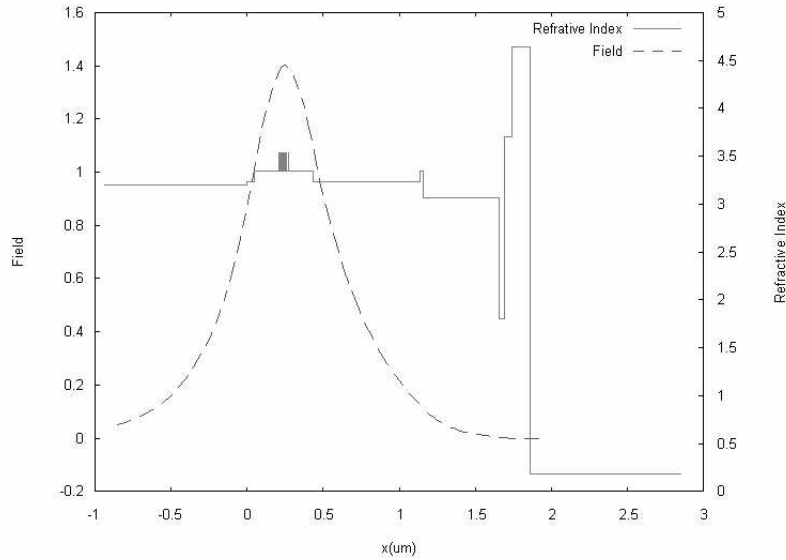


Figure 14.1.4 Comparison of near field and refractive index at ridge region.

14.1.6. Result analysis

14.1.6. Result analysis

From the above calculations we have noticed that leaky mode exists at both ridge and wing region. However, the metal layers play different roles in the leaky phenomenon. In wing region, there is no outer p-spacing but a low refractive index Si_3N_4 layer, we got result as $\text{WZR}=3.22$ and $\text{WZI}=1.69 \times 10^{-3}$. In ridge region, there is a relatively thick outer p-spacing layer but no nitride layer, and we have $\text{WZR}=3.25$ and $\text{WZI}=3.41 \times 10^{-5}$. There is big difference between these two kinds of slab waveguide. It can be seen that the etch stop layer, outer p-spacing and p-cap layers reduce the leak of mode caused by metal covers for two orders. The attenuation in ridge region is mainly caused by the absorption of n-substrate. We will verify this argument in section 14.3, in which calculation was done on almost identical slab waveguides with no metal covers.

14.2 Ridge waveguide with metal covers

Lateral mode of ridge waveguide with metal cover layers is studied in this section. Use the effective refractive indices calculated for wing and ridge region. That is, in wing region, $\text{NREAL}=3.22$ and $\text{NLOSS}=1.69 \times 10^{-3}$, in ridge region, $\text{NREAL}=3.25$ and

14.1 Metal Covered Slab Waveguide in Semiconductor Lasers

$N_{LOSS}=3.41 \times 10^{-5}$. Another difference is that when calculating lateral mode for global TE mode in ridge waveguide device, TM mode should be used [1,2]. The input file for this calculation is shown in table 14.1.3. Because the small difference between two refractive indices of two regions, only a small range of QZMR was looped for mode searching. The db file after looping QZMR is shown below. The result shows for lateral mode $WZR = 3.24$ and $WZI = 1.20 \times 10^{-5}$. The attenuation coefficient is similar to that of ridge region. This is because most energy of light is confined in ridge region. The near field is plotted as figure 14.2.1. From the figure we can see there is no phase change at any interface.

QZMR	PHM	WZR	WZI	QZR	QZI	KM	IT	
1.055000E+01	1.626562E+00	3.239400E+00	2.887700E-05	1.049371E+01	1.870883E-04	6	11	
1.054000E+01	8.199669E-01	3.244622E+00	1.204025E-05	1.052757E+01	7.813211E-05	7	7	
1.053000E+01	8.199669E-01	3.244622E+00	1.204025E-05	1.052757E+01	7.813211E-05	7	4	
1.052000E+01	8.199669E-01	3.244622E+00	1.204025E-05	1.052757E+01	7.813211E-05	7	5	
1.051000E+01	1.626562E+00	3.239400E+00	2.887700E-05	1.049371E+01	1.870883E-04	5	5	
1.050000E+01	1.626562E+00	3.239400E+00	2.887700E-05	1.049371E+01	1.870883E-04	5	4	
1.049000E+01	1.626562E+00	3.239400E+00	2.887700E-05	1.049371E+01	1.870883E-04	5	3	
1.048000E+01	1.626562E+00	3.239400E+00	2.887700E-05	1.049371E+01	1.870883E-04	5	4	
1.047000E+01	2.393875E+00	3.231218E+00	6.935683E-05	1.044077E+01	4.482141E-04	6	6	
1.046000E+01	2.393875E+00	3.231218E+00	6.935683E-05	1.044077E+01	4.482141E-04	5	5	
1.045000E+01	2.393875E+00	3.231218E+00	6.935683E-05	1.044077E+01	4.482141E-04	5	4	
1.044000E+01	2.393875E+00	3.231218E+00	6.935683E-05	1.044077E+01	4.482141E-04	6	3	
1.043000E+01	2.393875E+00	3.231218E+00	6.935683E-05	1.044077E+01	4.482141E-04	5	4	

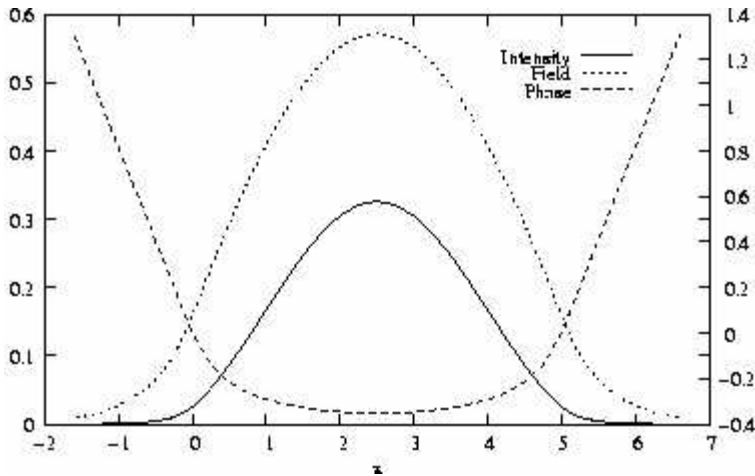


Figure 14.2.1. Fundamental mode near field plots for at ridge waveguide.

Table 14.1.3 Input file for ridge waveguide

14.3

```

!WIF generated by WIFE (Waveguide Input File Editor)
!-----
!FILENAME:      C:\Waveguide\work\input\ridgeguide.wgi
!DESCRIPTION:  RigeGuide
!Last Modified: 5/5/04 PM 6:21:34
!-----

!CASE Parameter Set
CASE KASE=WIFE
CASE EPS1=1E-9 EPS2=1E-9 GAMEPS=1E-3 QZMR=10.55 QZMI=0.001
CASE PRINTF=1 INITGS=0 AUTOQW=0 NFPLT=0 FFPLT=0 IL=30

!MODCON Parameter Set
MODCON KPOL=1 APB1=0.25 APB2=0.25

!STRUCT Parameter Set
LAYER NREAL=3.2235 NLOSS=0.0016913 TL=1.0
LAYER NREAL=3.2464 NLOSS=3.4134E-5 TL=5
LAYER NREAL=3.2235 NLOSS=0.0016913 TL=1.0

!OUTPUT Parameter Set
OUTPUT PHMO=1 GAMMAO=0 WZRO=1 WZIO=1 QZRO=1 QZIO=1
OUTPUT FWHPNO=0 FWHPFO=0 KMO=1 ITO=1
OUTPUT SPLTFL=0 MODOUT=0 LYROUT=0

!GAMOUT Parameter Set
GAMOUT LAYGAM=2 COMPGAM=0 GAMALL=0

!LOOPX Parameter Set
LOOPX1 ILX=0 FINV=0 XINC=0.1 LAYCH=2
LOOPX2 ILX=0 FINV=0 XINC=0.1 LAYCH=2
LOOPX3 ILX=0 FINV=0 XINC=0.1 LAYCH=2
LOOPX4 ILX=0 FINV=0 XINC=0.1 LAYCH=2

!LOOPZ Parameter Set
LOOPZ1 ILZ=17 FINV=10.39 ZINC=-0.01 !QZMR
LOOPZ2 ILZ=0 FINV=0 ZINC=0.1

```

Counterpart ridge waveguide without metal cover

The counterpart ridge waveguide without metal cover is studied in this section. We can see obvious difference from the metal covered structure.

14.3.1 Fundamental mode in wing region

First, remove all three metal layers from the input file of wing region with metal covered slab waveguide. Then do the same loop for QZMR form 13 to 10 with step size – 0.05, the output of QZMR looping is shown as below:

14.1 Metal Covered Slab Waveguide in Semiconductor Lasers

QZMR	PHM	WZR	WZI	QZR	KM	IT
1.300000E+01	2.633446E+00	2.316204E+00	1.619356E+00	2.742489E+00	5	20
1.295000E+01	1.772503E+00	2.684631E+00	5.339300E-01	6.922161E+00	5	19
1.290000E+01	1.772503E+00	2.684631E+00	5.339300E-01	6.922161E+00	6	19
1.285000E+01	1.772503E+00	2.684631E+00	5.339300E-01	6.922161E+00	6	19
1.280000E+01	1.772503E+00	2.684631E+00	5.339300E-01	6.922161E+00	6	19
1.275000E+01	1.772503E+00	2.684631E+00	5.339300E-01	6.922161E+00	6	19
.....						
1.170000E+01	1.772503E+00	2.684631E+00	5.339300E-01	6.922161E+00	5	16
1.165000E+01	1.772503E+00	2.684631E+00	5.339300E-01	6.922161E+00	5	16
1.160000E+01	1.772503E+00	2.684631E+00	5.339300E-01	6.922161E+00	6	16
1.155000E+01	1.772503E+00	2.684631E+00	5.339300E-01	6.922161E+00	5	15
1.150000E+01	1.772503E+00	2.684631E+00	5.339300E-01	6.922161E+00	5	15
1.145000E+01	1.772503E+00	2.684631E+00	5.339300E-01	6.922161E+00	5	15
1.140000E+01	1.772503E+00	2.684631E+00	5.339300E-01	6.922161E+00	5	15
1.135000E+01	1.772503E+00	2.684631E+00	5.339300E-01	6.922161E+00	5	15
1.130000E+01	1.772503E+00	2.684631E+00	5.339300E-01	6.922161E+00	5	15
1.125000E+01	1.772503E+00	2.684631E+00	5.339300E-01	6.922161E+00	5	15
1.120000E+01	3.870541E-01	3.226320E+00	6.758907E-05	1.040914E+01	7	7
1.115000E+01	3.870541E-01	3.226320E+00	6.758907E-05	1.040914E+01	6	6
1.110000E+01	3.870541E-01	3.226320E+00	6.758907E-05	1.040914E+01	6	6
1.105000E+01	3.870541E-01	3.226320E+00	6.758907E-05	1.040914E+01	6	6
1.100000E+01	3.870541E-01	3.226320E+00	6.758907E-05	1.040914E+01	6	6
1.095000E+01	3.870541E-01	3.226320E+00	6.758907E-05	1.040914E+01	6	6
1.090000E+01	3.870541E-01	3.226320E+00	6.758907E-05	1.040914E+01	7	6
1.085000E+01	3.870541E-01	3.226320E+00	6.758907E-05	1.040914E+01	6	5
1.080000E+01	3.870541E-01	3.226320E+00	6.758907E-05	1.040914E+01	6	5
1.075000E+01	3.870541E-01	3.226320E+00	6.758907E-05	1.040914E+01	7	5
1.070000E+01	3.870541E-01	3.226320E+00	6.758907E-05	1.040914E+01	7	5
1.065000E+01	3.870541E-01	3.226320E+00	6.758907E-05	1.040914E+01	7	5
1.060000E+01	3.870541E-01	3.226320E+00	6.758907E-05	1.040914E+01	6	4
1.055000E+01	3.870541E-01	3.226320E+00	6.758907E-05	1.040914E+01	6	4
1.050000E+01	3.870541E-01	3.226320E+00	6.758907E-05	1.040914E+01	7	4
1.045000E+01	3.870541E-01	3.226320E+00	6.758907E-05	1.040914E+01	6	3
1.040000E+01	3.870541E-01	3.226320E+00	6.758907E-05	1.040914E+01	7	3
1.035000E+01	3.870541E-01	3.226320E+00	6.758907E-05	1.040914E+01	7	4
1.030000E+01	3.870541E-01	3.226320E+00	6.758907E-05	1.040914E+01	6	4
1.025000E+01	3.870541E-01	3.226320E+00	6.758907E-05	1.040914E+01	7	6
1.020000E+01	3.870541E-01	3.226320E+00	6.758907E-05	1.040914E+01	6	6
1.015000E+01	3.870541E-01	3.226320E+00	6.758907E-05	1.040914E+01	7	6
1.010000E+01	3.870541E-01	3.226320E+00	6.758907E-05	1.040914E+01	7	6
1.005000E+01	3.870541E-01	3.226320E+00	6.758907E-05	1.040914E+01	7	6
1.000000E+01	3.870541E-01	3.226320E+00	6.758907E-05	1.040914E+01	6	6

Select the fundamental mode with following parameters, near field is plotted as figure 14.2.1

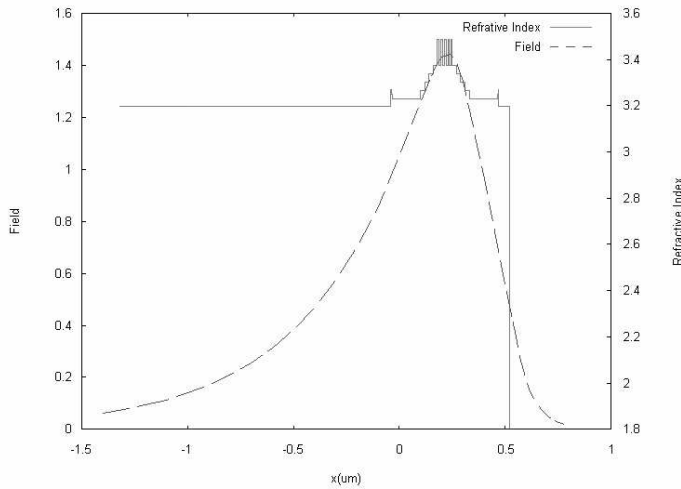


Figure 14.3.1. Near field of fundamental mode at wing region

14.3.2 Fundamental mode in ridge region

First, remove all three metal layers from the input file of ridge region with metal covered slab waveguide. Then do the same loop for QZMR as in 14.1.5, the output of QZMR looping is shown as below.

QZMR	PHM	WZR	WZI	KM	IT
1.200000E+01	3.547135E+00	2.888807E+00	7.113226E-02	5	24

Chapter 14 Effect of Metal Cover on Semiconductor Laser

1.195000E+01	3.547135E+00	2.888807E+00	7.113226E-02	5	24
1.190000E+01	3.547135E+00	2.888807E+00	7.113226E-02	5	24
1.185000E+01	3.547135E+00	2.888807E+00	7.113226E-02	5	23
1.180000E+01	3.547135E+00	2.888807E+00	7.113226E-02	5	23
1.175000E+01	1.414294E+00	3.173920E+00	8.769172E-03	6	18
1.170000E+01	3.547135E+00	2.888807E+00	7.113226E-02	5	23
1.165000E+01	3.547135E+00	2.888807E+00	7.113226E-02	5	22
1.160000E+01	1.414294E+00	3.173920E+00	8.769172E-03	6	16
1.155000E+01	3.547135E+00	2.888807E+00	7.113226E-02	5	22
1.150000E+01	1.414294E+00	3.173920E+00	8.769172E-03	6	16
1.145000E+01	3.547135E+00	2.888807E+00	7.113226E-02	5	22
1.140000E+01	1.414294E+00	3.173920E+00	8.769172E-03	6	15
1.135000E+01	3.547135E+00	2.888807E+00	7.113226E-02	5	21
1.130000E+01	2.593654E+00	3.034025E+00	4.872093E-02	5	18
1.125000E+01	2.593654E+00	3.034025E+00	4.872093E-02	5	18
1.120000E+01	2.593654E+00	3.034025E+00	4.872093E-02	5	17
1.115000E+01	2.593654E+00	3.034025E+00	4.872093E-02	5	17
1.110000E+01	2.593654E+00	3.034025E+00	4.872093E-02	5	16
1.105000E+01	1.414294E+00	3.173920E+00	8.769172E-03	6	12
1.100000E+01	1.414294E+00	3.173920E+00	8.769172E-03	6	12
1.095000E+01	4.439791E-01	3.278437E+00	2.724234E-05	6	7
1.090000E+01	4.439791E-01	3.278437E+00	2.724234E-05	6	6
1.085000E+01	4.439791E-01	3.278437E+00	2.724234E-05	6	5
1.080000E+01	4.439791E-01	3.278437E+00	2.724234E-05	6	4
1.075000E+01	4.439791E-01	3.278437E+00	2.724234E-05	7	3
1.070000E+01	4.439791E-01	3.278437E+00	2.724234E-05	6	4
1.065000E+01	4.439791E-01	3.278437E+00	2.724234E-05	7	5
1.060000E+01	4.439791E-01	3.278437E+00	2.724234E-05	6	5
1.055000E+01	1.414294E+00	3.173920E+00	8.769172E-03	6	8
1.050000E+01	1.414294E+00	3.173920E+00	8.769172E-03	7	8
1.045000E+01	1.414294E+00	3.173920E+00	8.769172E-03	6	7
1.040000E+01	1.414294E+00	3.173920E+00	8.769172E-03	7	7
1.035000E+01	1.414294E+00	3.173920E+00	8.769172E-03	6	6
1.030000E+01	1.414294E+00	3.173920E+00	8.769172E-03	6	7
1.025000E+01	1.414294E+00	3.173920E+00	8.769172E-03	6	7
1.020000E+01	1.414294E+00	3.173920E+00	8.769172E-03	6	5
1.015000E+01	1.414294E+00	3.173920E+00	8.769172E-03	6	4
1.010000E+01	1.414294E+00	3.173920E+00	8.769172E-03	6	4
1.005000E+01	1.414294E+00	3.173920E+00	8.769172E-03	6	4
1.000000E+01	1.414294E+00	3.173920E+00	8.769172E-03	6	4

Select the fundamental mode with parameters as QZMR value highlighted above, near field is plotted as figure 14.3.2.

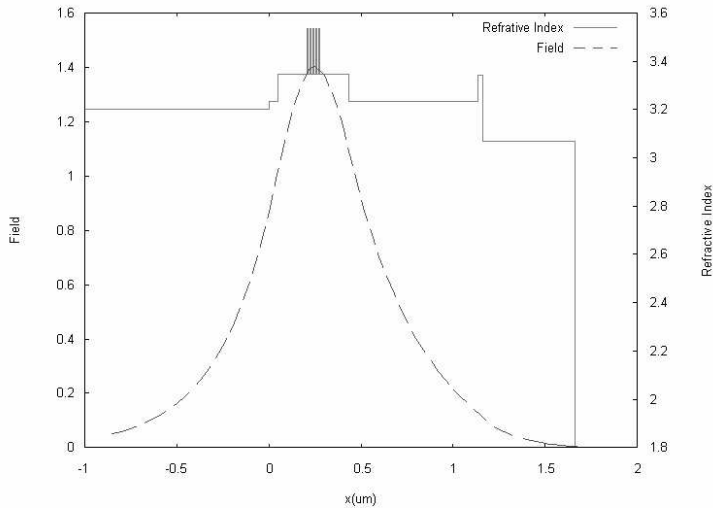


Figure 14.3.2 Near field of fundamental mode at ridge region

14.3.3 Fundamental mode in non-metal covered ridge waveguide

Effective refractive index method should be used for lateral mode search. Another change should be appreciated is that this time should change the polarization to TM mode for lateral direction. Use the following structure:

Wings: NREAL=3.278 NLOSS=2.724E-5

14.1 Metal Covered Slab Waveguide in Semiconductor Lasers

Ridge: NREAL=3.226 NLOSS=6.759E-5

And the ridge width is 5um.

Loop QZMR from $3.278^2 = 10.75$ to $3.226^2 = 19.40$ with step size -0.01 . The results is listed as below:

QZMR	PHM	WZR	WZI	KM	IT
1.075000E+01	8.538662E-01	3.275327E+00	1.304353E-05	6	7
1.074000E+01	8.538662E-01	3.275327E+00	1.304353E-05	6	5
1.073000E+01	8.538662E-01	3.275327E+00	1.304353E-05	6	3
1.072000E+01	8.538662E-01	3.275327E+00	1.304353E-05	6	4
1.071000E+01	8.538662E-01	3.275327E+00	1.304353E-05	6	5
1.070000E+01	1.700590E+00	3.267385E+00	3.381284E-05	5	5
1.069000E+01	1.700590E+00	3.267385E+00	3.381284E-05	5	4
1.068000E+01	1.700590E+00	3.267385E+00	3.381284E-05	5	3
1.067000E+01	1.700590E+00	3.267385E+00	3.381284E-05	5	3
1.066000E+01	1.700590E+00	3.267385E+00	3.381284E-05	5	4
1.065000E+01	1.700590E+00	3.267385E+00	3.381284E-05	5	4
1.064000E+01	2.529195E+00	3.254474E+00	7.697584E-05	5	6
1.063000E+01	2.529195E+00	3.254474E+00	7.697584E-05	5	5
1.062000E+01	2.529195E+00	3.254474E+00	7.697584E-05	5	5
1.061000E+01	2.529195E+00	3.254474E+00	7.697584E-05	5	4
1.060000E+01	2.529195E+00	3.254474E+00	7.697584E-05	5	4
1.059000E+01	2.529195E+00	3.254474E+00	7.697584E-05	5	3
1.058000E+01	2.529195E+00	3.254474E+00	7.697584E-05	5	4
1.057000E+01	2.529195E+00	3.254474E+00	7.697584E-05	5	4
1.056000E+01	2.529195E+00	3.254474E+00	7.697584E-05	5	4
1.055000E+01	2.529195E+00	3.254474E+00	7.697584E-05	5	4
1.054000E+01	3.311859E+00	3.237556E+00	1.783470E-04	5	5
1.053000E+01	3.311859E+00	3.237556E+00	1.783470E-04	5	5
1.052000E+01	3.311859E+00	3.237556E+00	1.783470E-04	5	5
1.051000E+01	3.311859E+00	3.237556E+00	1.783470E-04	5	4
1.050000E+01	3.311859E+00	3.237556E+00	1.783470E-04	5	4
1.049000E+01	3.311859E+00	3.237556E+00	1.783470E-04	5	3
1.048000E+01	3.311859E+00	3.237556E+00	1.783470E-04	5	3
1.047000E+01	3.311859E+00	3.237556E+00	1.783470E-04	5	4
1.046000E+01	3.311859E+00	3.237556E+00	1.783470E-04	5	4
1.045000E+01	3.311859E+00	3.237556E+00	1.783470E-04	5	4
1.044000E+01	3.311859E+00	3.237556E+00	1.783470E-04	5	5
1.043000E+01	3.311859E+00	3.237556E+00	1.783470E-04	5	5
1.042000E+01	3.909935E+00	3.221655E+00	6.027332E-03	5	6
1.041000E+01	3.909935E+00	3.221655E+00	6.027332E-03	5	7
1.040000E+01	3.909935E+00	3.221655E+00	6.027332E-03	5	5

Select the parameters of highlighted line, which corresponds to fundamental mode in lateral mode. Plot near field as figure 14.3.3.

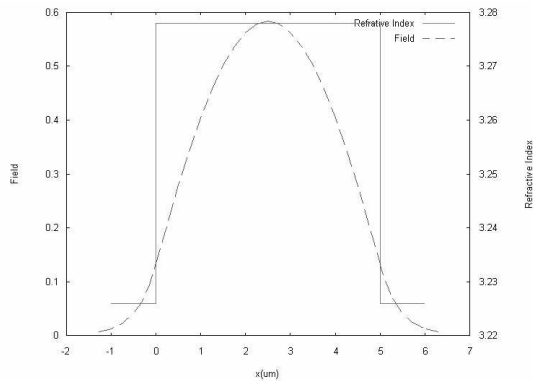


Figure 14.3.3 Near field of fundamental mode at ridge region

14.3.4 Result discussion

We see big difference at wing area in attenuation coefficient. The mode is a leaky mode. But at ridge region, the effect of metal is relatively not obvious. In stead, in ridge region, the lossy n-substrate is the main source of attenuation.

However, the global effect of metal cover to the ridge waveguide is not so big. The lateral mode calculation eventually gives the global attenuation. The attenuation of the device with and without metal is in same order. That is because light is mostly confined in ridge region. And ridge region doesn't give much difference with or without metal cover. So that it is safe for us to add metal cover on ridge laser device.

REFERENCES:

[1] Agrawal G P and Dutta N K, *Semiconductor lasers* 2nd ed, New York: Wan Nostrand-Reinhold S. 1993 R. Selmic et al.

Chapter 15 Field Overlapping Integral Calculation

This chapter uses DBR GSE laser as an example to introduce one important feature of WAVEGUIDE –“field overlapping integral calculation”, through which we can predict the transfer of power between waveguides of different dimensions or material parameters.

15.1 Introduction

Most optoelectronic system contains many components. One commonly occurring feature of optoelectronic devices is the dielectric waveguide discontinuity, such as waveguides of different dimensions as in tapered lasers (figure 15.1.1) or waveguides of different material as in GSE lasers (figure 15.1.2). Inevitably, certain amount of power will lose at such discontinuities by radiation field. The electromagnetic field coupling efficiency between the successive waveguides depends on the overlap integral of the field profiles at both sides of the interface and the normalized intensity overlap integral can be approximated as follows:

$$\frac{\int_{-\infty}^{+\infty} |\phi_1^*(x)\phi_2(x)| dx}{\left(\int_{-\infty}^{+\infty} \phi_1^*(x)\phi_1(x) dx \int_{-\infty}^{+\infty} \phi_2^*(x)\phi_2(x) dx \right)^{1/2}} \quad (15.1)$$

Where $\phi_1(x)$ and $\phi_2(x)$ are the near field distributions at both sides of the discontinuity.

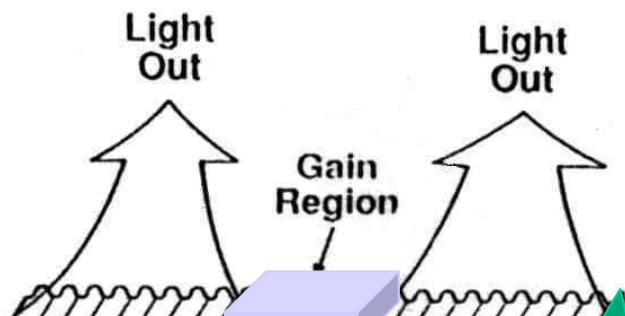
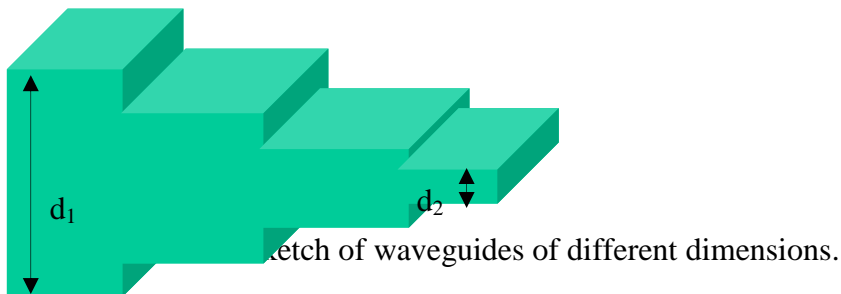
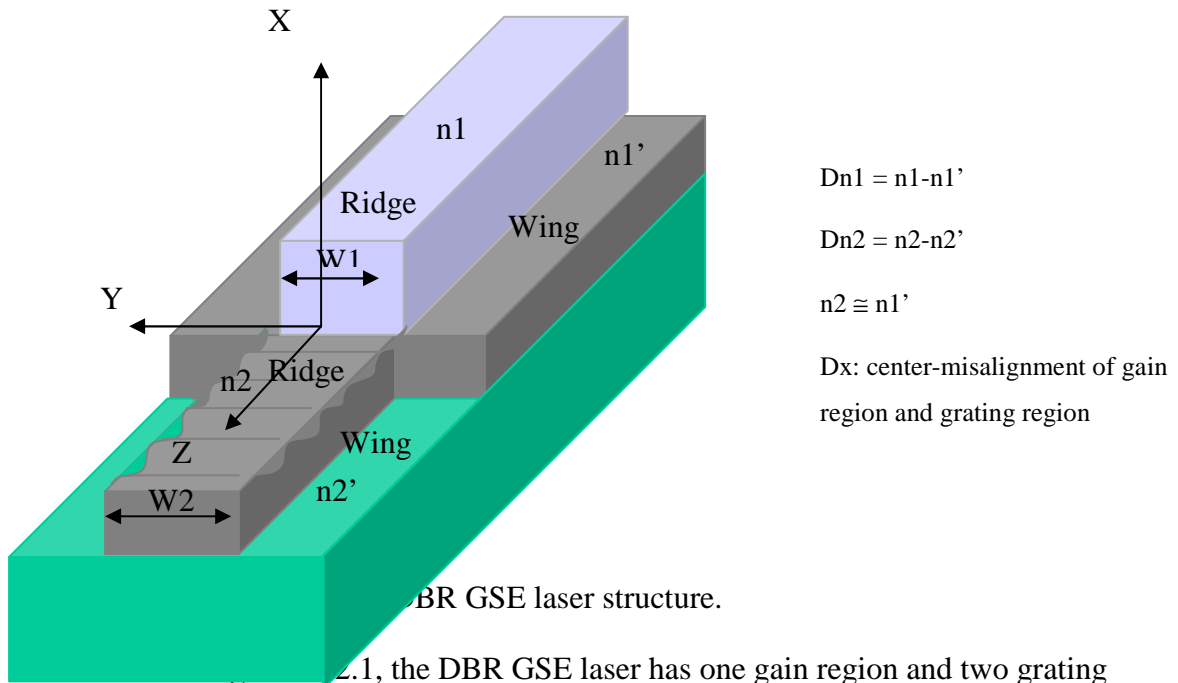


Figure 15.1.2 Sketch of DBR GSE laser structure

15.2 Input File Creation

In this subsection, we'll use a DBR GSE laser structure as an example to show how to calculate the overlap integral of fields using WAVEGUIDE.



In Figure 15.1, the DBR GSE laser has one gain region and two grating regions that are connected to the gain region on both sides. The gain region has the index of $n1$ for the ridge and $n1'$ for the wing and the grating region has the index of $n2$ for the ridge and $n2'$ for the wing. The ridge width is $W1$ in the gain region and $W2$ in the grating region. $Dn1 = n1 - n1'$ is the indices difference of ridge and wing for gain region, $Dn2 = n2 - n2'$ is the indices difference of ridge and wing for grating region, and Dx is the center-misalignment of the ridges in two regions. The index of the ridge for the grating region is approximated to be same as that of the wing for the gain region.

There are several factors that may affect the waveguide and gratings coupling efficiency. In x direction, the grating region has fewer layers than those of the gain region, there'll always be certain amount of difference in their effective indices. This

difference causes the coupling efficiency to be always less than 100%. In y direction, if the ridge width is different as the grating width, or if the ridge and the grating don't align perfectly, the mismatch of the structure in this direction will also cause the power loss.

To analysis how these factors influence the power coupling, we generate following steps:

- (1) Create input file to simulate the lateral structure of the gain region (input_1).
- (2) Create input file to simulate the lateral structure of the grating region (input_2).
- (3) In input_1 files, fix the effective indices of the ridge and the wing ($Dn1 = 0$). Let the center misalignment of two ridges be zero ($Dx = 0$) and the widths of the ridges in two regions be the same ($w1 = w2$). Vary the wing index of input_2 to change the indices difference of the grating region ($Dn2$) and calculate intensity overlap efficiency from WAVEGUIDE for each $Dn2$ value. Plot the intensity overlap efficiency as a function of $Dn2$.
- (4) Fix all the effective indices in both input files (fix $Dn1$ and $Dn2$), let the widths of the ridge and grating be the same ($w1 = w2$). Vary the center misalignment of two ridges (Dx) and calculate the intensity overlap efficiency from WAVEGUIDE for each Dx value. Plot the intensity overlap efficiency as a function of Dx .
- (5) Fix all the effective indices in both input files (fix $Dn1$ and $Dn2$), and fix ridge width in input_1 ($W1$). Let the center misalignment of two ridges be zero ($Dx = 0$). Choose different ridge width in the input_2 ($W2$) and calculate the intensity overlap efficiency from WAVEGUIDE for each $W2$ value. Plot the intensity overlap efficiency as a function of $W2$.

Naturally, we may think to simulate the lateral structure of gain region or grating region with 3-layer waveguide structure. However, in WAVEGUIDE, the outmost two layers are always "seen" as infinite long, and in calculating the near field, the "zero" position of the layer structure always starts from the beginning of the second layer, which is the ridge layer with three layer structure. Because of that, the ridges of two regions will automatically be aligned to each other at their edges in the fields overlapping integral calculation no matter if it is the case in practice. In order for us to have the flexibility in

Chapter 15 Field Overlapping Integral Calculation

adjusting the alignment of two regions, we use 5-layer structure rather than 3-layer structure to simulate both regions. The outmost four layers have the same effective index as the wing, and the middle layer has the index of the ridge. Table 15.2.1 and 15.2.2 give the example input files for the gain region and grating region.

Table 15.2.1 Input file for simulating the lateral structure of gain region for the GSE laser (input_1).

```
CASE KASE=AlGaInAs (5 wells)
CASE   EPS1=1E-8  EPS2=1E-8  GAMEPS=1E-6
CASE   QZMR=10.406  QZMI=0.0
CASE   PRINTF=0    INITGS=0    AUTOQW=0  NFPLT=1    FFPLT=1
!CASE   DXIN=0.2
!CASE   IL=100    KGSS=1

MODCON  KPOL=1    APB1=0.25    APB2=0.25

STRUCT  WVL=1.31
LAYER  NREAL=3.2235  NLOSS=0.0  TL=200.0  !wing
LAYER  NREAL=3.2235  NLOSS=0.0  TL=8.75   !wing
LAYER  NREAL=3.2285  NLOSS=0.0  TL=2.5    !ridge
LAYER  NREAL=3.2235  NLOSS=0.0  TL=8.75   !wing
LAYER  NREAL=3.2235  NLOSS=0.0  TL=200.0  !wing

OUTPUT  PHMO=1    GAMMAO=1  WZRO=1  WZIO=1  QZRO=0    QZIO=0
OUTPUT  FWHPNO=0  FWHPFO=1  KMO=1  ITO=1
OUTPUT  MODOUT=1  LYROUT=1  SPLTF=0
```

Table 15.2.2 Input file for simulating the lateral structure of gain region for the GSE laser (input_2).

```

CASE KASE=AlGaInAs (5 wells)
CASE     EPS1=1E-8  EPS2=1E-8  GAMEPS=1E-6
CASE     QZMR=10.379  QZMI=0.0
CASE     PRINTF=0    INITGS=0    AUTOQW=0  NFPLT=1    FFPLT=1
!CASE    DXIN=0.2
!CASE    IL=100  KGSS=1

MODCON  KPOL=1    APB1=0.25  APB2=0.25
STRUCT  WVL=1.31

LAYER  NREAL=3.221  NLOSS=0.0  TL=200.0  !wing
LAYER  NREAL=3.221  NLOSS=0.0  TL=7.25   !wing
LAYER  NREAL=3.2235 NLOSS=0.0  TL=2.5    !grating
LAYER  NREAL=3.221  NLOSS=0.0  TL=10.25  !wing
LAYER  NREAL=3.221  NLOSS=0.0  TL=200.0  !wing

OUTPUT  PHMO=1    GAMMAO=1  WZRO=1  WZIO=1  QZRO=0  QZIO=0
OUTPUT  FWHPNO=0  FWHPFO=1  KMO=1  ITO=1
OUTPUT  MODOUT=1  LYROUT=1  SPLTFL=0

GAMOUT  LAYGAM=26  COMPGAM=0  GAMALL=0

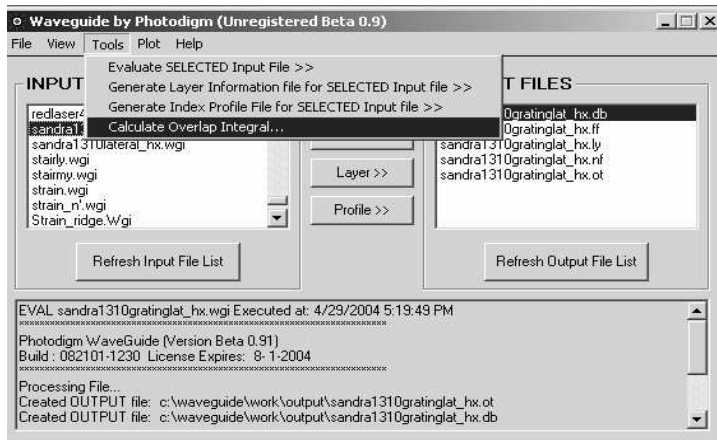
!LOOPZ1 ILZ='QZMR'  FINV=10.2  ZINC=-0.001

END

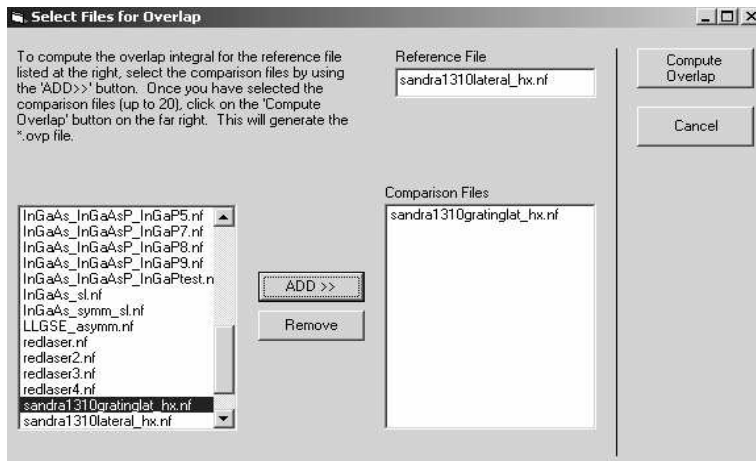
```

15.3 Fields Overlap Analysis with WAVEGUIDE

Before the field-overlap integral calculation, we need to evaluate the two input files to generate “.nf” file. “.nf” file contains the data of the near field for each structure. Then we select one input file and click “Calculate Overlap Integral” tab in the pull down menu “Tools” from the WAVEGUIDE main screen (see figure 15.3.1 (a)), another screen will then be popped up (figure 15.3.1 (a)). The file we’ve selected is shown in the “Reference File” column in this screen. We can easily do the overlap integral calculation by following the instruction shown on the up-left corner of the screen.



(a)



(b)

Figure 15.3.1 Illustration of overlap integral calculation from WAVEGUIDE.

The results of the integral overlap calculation are stored in the “.ovp” file. Table 15.3.1 listed the output “.ovp” file that is obtained by the overlap integral of the near fields from the two input files given in table 15.2.1 and table 15.2.2.

Table 15.3.1 Integral overlap calculation results for the input files in table 15.2.1 and 15.2.2.

```
c:\waveguide\work\output\sandra1310gratinglat_hx.nf vs.
c:\waveguide\work\output\sandra1310lateral_hx.nf

NORMALIZED AMPLITUDE OVERLAP (C)= 0.86371 + j( 0.00000)
NORMALIZED INTENSITY OVERLAP (KAPPA)= 0.74599
AREA OF AMPLITUDE OVERLAP= 0.863709E+00 + j(-0.347384E-09)
AREA OF INTENSITY OVERLAP= 0.745993E+00
AREA UNDER INTENSITY1= 0.999998E+00
AREA UNDER INTENSITY2= 0.100001E+01
```

In the “.ovp” file, the “normalized amplitude overlap” represents the field coupling efficiency and the “normalized intensity overlap” is the square of the former one and represents the intensity (power) coupling efficiency. In study how the intensity coupling efficiency is affected by the structure parameters, we apply the integral overlap calculation to the lateral structure of gain and grating regions in the DBR GSE laser follow the steps 3-5 described in the previous subsection. Table 15.3.5 listed all the parameters in the input file and the calculated results. Figure 15.3.1, 15.3.2 and 15.3.3 shows how the intensity coupling efficiency varies with the indices difference, the center-misalignment and the dimension mismatch of two structures.

Table 15.3.2 Input and output parameters for the overlap integral calculation of grating region and grating region of DBR GSE laser.

Chapter 15 Field Overlapping Integral Caculation

group	n1	n1'	Dn1	n2	n2'	Dn2	Dx (μm)	W1 (μm)	W2 (μm)	Amplitude Overlap	Intensity Overlap
1	3.2335	3.2235	0.01	3.2235	3.2210	0.0025	0	2.5	2.5	0.84805	0.71918
					3.2185	0.005				0.94051	0.88456
					3.2160	0.0075				0.97293	0.9466
					3.2135	0.01				0.98751	0.97517
2	3.2285	3.2235	0.005	3.2235	3.2210	0.0025	0	2.5	2.5	0.97204	0.94486
							0.5			0.9552	0.91241
							1			0.92103	0.8483
							1.5			0.86371	0.74599
3	3.2285	3.2235	0.005	3.2235	3.2210	0.0025	0	2.5	2	0.95807	0.9179
								2.5	0.97204	0.94486	
								3	0.97802	0.95653	
								4	0.97918	0.95878	

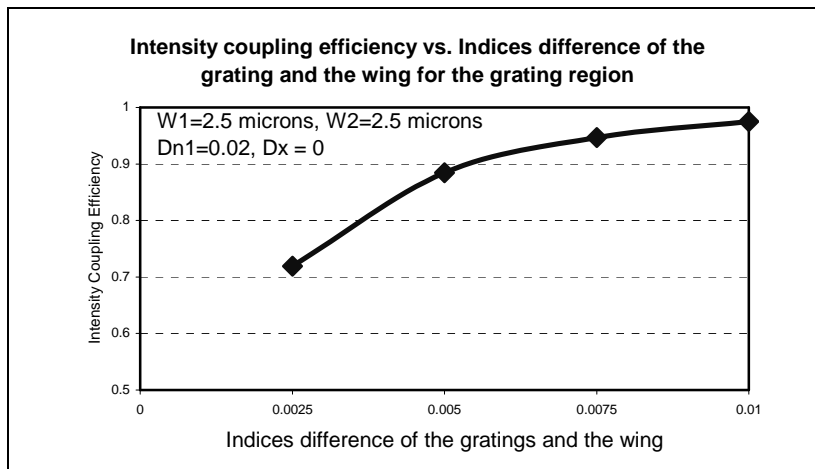


Figure 15.3.3 Intensity coupling efficiency as a function of indices difference of the ridge and the wing in grating region for the DBR GSE laser.

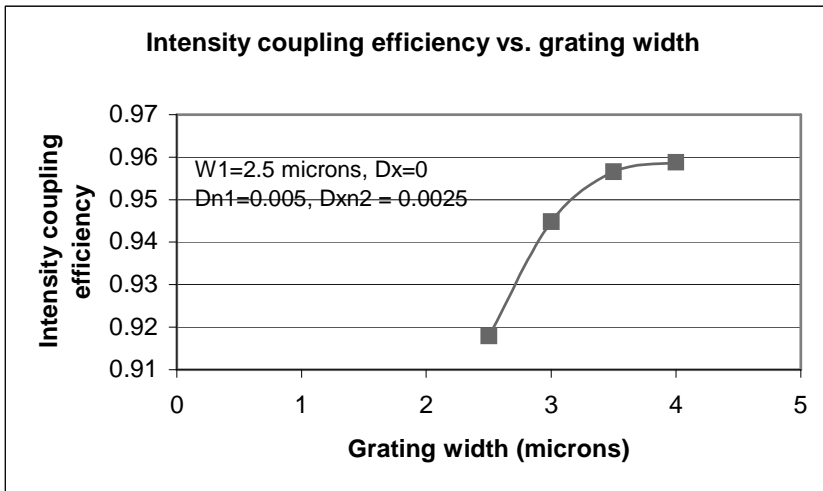
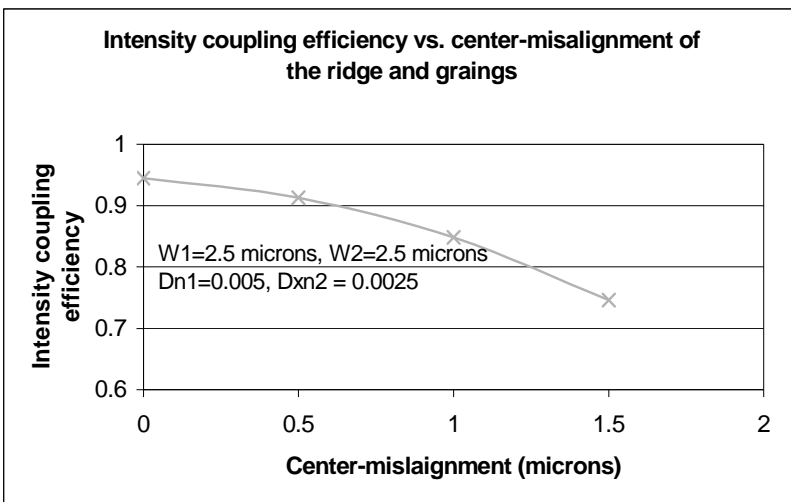


Figure 15.3.4 Intensity coupling efficiency as a function of the center-misalignment of ridges of two regions for the DBR GSE laser.

Figure 15.3.5 Intensity coupling efficiency as a function of ridge width in the grating



region.

Appendix Subprograms for Refractive Indices Calculation

Chapter 3 of this manual describes the material system feature of WAVEGUIDE called Matsys. This appendix lists the software source code from WAVEGUIDE that Matsys uses to calculate the refractive index of a layer given the layer composition defined by the user. The heading of each section listed below corresponds with the drop down list in WAVEGUIDE that shows the available material systems that can be selected.

Al(x)Ga(1-x)As 1

```
SUBROUTINE sALGAAS1(WVL,XPERCENT,EFFINDEX)
```

```
! calculates the effective index given the wavelength (WVL) and  
! the percent (PERC)
```

```
USE INFO_MOD
```

```
IMPLICIT NONE
```

```
REAL(KIND=8), INTENT(IN) :: XPERCENT,WVL
```

```
REAL(KIND=8), INTENT(OUT) :: EFFINDEX
```

```
REAL(KIND=8)          :: X,OMEGA,ENERGY,ENDEL,CHI,CHISO
```

```
REAL(KIND=8)          :: FCHI,FCHISO,AO,BO,EPSI
```

```
REAL(KIND=8) :: C=3.0E+14, PI
```

```
REAL(KIND=8) :: HBAR
```

```
!MM-Notify
```

```
WRITE(STDOUT_RD,*) 'Using AlGaAs-1 Material System'
```

```
!MM-Notify
```

```
PI=4.0*ATAN(1.0)
```

Appendix Subprograms for Refractive Indices Calculation

HBAR=4.14E-15/(2.0*PI)

! !---- finds something (N vs. lamda) ----

X=XPERCENT

OMEGA=2.0*PI*C/WVL

ENERGY=1.425+1.155*X+0.37*X*X

ENDEL=1.765+1.115*X+0.37*X*X

CHI=HBAR*OMEGA/ENERGY

CHISO=HBAR*OMEGA/ENDEL

IF(((1-CHI)<=0.0).OR.((1-CHISO)<=0.0)) THEN

WRITE(STDOUT_RD,*) ' CHI RANGE ERROR!'

ELSE

FCHI=(2-SQRT(1+CHI)-SQRT(1-CHI))/(CHI*CHI)

FCHISO=(2-SQRT(1+CHISO)-SQRT(1-CHISO))/(CHISO*CHISO)

AO=6.3+19.0*X

BO=9.4-10.2*X

EPSI=AO*(FCHI+.5*(FCHISO*((ENERGY/ENDEL)**1.5)))+BO

IF(EPSI<=0) THEN

WRITE(STDOUT_RD,*) 'EPSI RANGE ERROR!'

ELSE

EFFINDEX=SQRT(EPSI)

END IF

END IF

RETURN

END SUBROUTINE sALGAAS1

Al(x)Ga(1-x)As 2

SUBROUTINE sALGAAS2(WVL,P,NEFF)

Appendix Subprograms for Refractive Indices Calculation

! calculates the effective index given the wavelength (WVL) and
! the percent (PERC)

USE INFO_MOD

IMPLICIT NONE

REAL(KIND=8), INTENT(IN) :: P,WVL

REAL(KIND=8), INTENT(OUT) :: NEFF

REAL(KIND=8) :: A,B1,B2,B11,B22,C,D,E1,Ec,Eic,einf,E1c,T,f,fi

REAL(KIND=8) :: E0,Ei,D0,D1

REAL(KIND=8) :: E, G, EE, EEI, EP1E01, EP1E02, EP1E0, EP2E0

REAL(KIND=8) :: EP1E11, EP1E12, EP2E11, EP2E12, EP1E1, EP2E1

REAL(KIND=8) :: EP2EC, EP2EI, EP1EC, EQ1, EPSILON1, EPSILON2

COMPLEX(KIND=8) :: ARG1,ARG2

COMPLEX(KIND=8) :: CE00,CEC,CE,CE0,CEXP0,CEXP00

REAL(KIND=8), PARAMETER :: PI = 3.1415926535898D0

!MM-Notify

WRITE(STDOUT_RD,*) 'Using AlGaAs-2 Material System'

!MM-Notify

! {parameters calculated using equation $Q_i(x)=Q_0+(Q_1*(P-.5))+(Q_2*(P-.5)^2)$

A=4.264374+(4.402701*(P-.5))+(9.160232*((P-.5)*(P-.5)))

B1=8.256268+(-0.585350*(P-.5))+(-1.901850*((P-.5)*(P-.5)))

B2=0.462866+(0.012206*(P-.5))+(1.047697*((P-.5)*(P-.5)))

B11=19.788257+(-3.706511*(P-.5))+(2.990894*((P-.5)*(P-.5)))

B22=0.539077+(-0.172307*(P-.5))+(1.031416*((P-.5)*(P-.5)))

C=3.078636+(-1.598544*(P-.5))+(-0.742071*((P-.5)*(P-.5)))

D=29.803617+(-22.124036*(P-.5))+(-57.863105*((P-.5)*(P-.5)))

E1=3.212414+(0.804397*(P-.5))+(0.228317*((P-.5)*(P-.5)))

Ec=4.724383+(0.024499*(P-.5))+(0.030653*((P-.5)*(P-.5)))

Appendix Subprograms for Refractive Indices Calculation

```

Eic=3.160138+(0.138046*(P-.5))+(1.066214*((P-.5)*(P-.5)))
einf=-0.494941+(-0.030802*(P-.5))+(0.486201*((P-.5)*(P-.5)))
E1c=6.413109+(0.571119*(P-.5))+(-0.735610*((P-.5)*(P-.5)))
T=0.263476+(0.090532*(P-.5))+(-0.254099*((P-.5)*(P-.5)))
G=0.147517+(-0.068764*(P-.5))+(0.047345*((P-.5)*(P-.5)))
f=1.628226+(-1.682422*(P-.5))+(-2.081273*((P-.5)*(P-.5)))
fi=0.507707+(-0.070165*(P-.5))+(-0.122169*((P-.5)*(P-.5)))

```

! {parameters calculated using equation $Q_i(x)=Q_0+(Q_1*P)+(Q_2*P^2)$

```

E0=1.425000+(1.155000*P)+(0.370000*(P*P))
Ei=1.734000+(0.574000*P)+(0.055000*(P*P))
D0=0.340000+(0.0*P)+(0.0*(P*P))
D1=0.230000+(-0.030000*P)+(0.0*(P*P))
E=(4.135701327D-15*2.99792458D14)/WVL

```

EE=E*E

EEI=1.0/EE

! REAL PART OF DIELECTRIC FUNCTION: DIRECT EDGE (E0)

```

ARG1=CMPLX(1.+E/E0,0.0,8)
ARG2=CMPLX(1.-E/E0,0.0,8)
EP1E01=A*EEI*REAL(SQRT(E0)*(2.-SQRT(ARG1)-SQRT(ARG2)))
ARG1=CMPLX(1.+E/(E0+D0),0.0,8)
ARG2=CMPLX(1.-E/(E0+D0),0.0,8)
EP1E02=A*EEI*REAL(.5*SQRT(E0+D0)*(2.-SQRT(ARG1)-
SQRT(ARG2)))

```

EP1E0=EP1E01+EP1E02

! IMAGINARY PART OF DIELECTRIC FUNCTION: DIRECT EDGE (E0)

! TAKING THE REAL PART IS LIKE A HEAVYSIDE FUNCTION

ARG1=CMPLX(E-E0,0.0,8)

Appendix Subprograms for Refractive Indices Calculation

```

ARG2=CMPLX(E-E0-D0,0.0,8)
EP2E0=REAL((2*SQRT(ARG1)+SQRT(ARG2))*EEI)*A/3.0

! REAL PART OF THE DIELECTRIC FUNCTION: L [K=PI/A] (E1)
! ADD A LINEWIDTH GAM
CE00=E*(1.0,0.0)+T*(0.0,1.0)
CEC=1.0/((1.0,0.0)-((CE00/E1c)*(CE00/E1c)))
CE=CE00*CE00
CE0=CE/((E1+D1)*(E1+D1))
CE=CE/(E1*E1)
CEXP0=MIN(EXP(-f*(E-E1)),REAL(1.0,8))/CE
CEXP00=MIN(EXP(-f*(E-E1-D1)),REAL(1.0,8))/CE0
EP1E11=-B1*REAL(LOG(((1.0,0.0)-CE)*CEC)*CEXP0)
EP1E12=-B2*REAL(LOG(((1.0,0.0)-CE0)*CEC)*CEXP00)
EP1E1=EP1E11+EP1E12

! IMAGINARY PART OF DIELECTRIC FUNCTION: L [K=PI/A] (E1)
! DON'T ALLOW A NEGATIVE IMAGINARY PART

!mm ARG1=CMPLX(E1-CE00,0.0,8) - CE00 is already complex...
!mm ARG1=CMPLX(E1-CE00,0.0,8) - CE00 is already complex...

ARG2=E1+D1-CE00
ARG2=E1+D1-CE00
EP2E11=PI*MAX(REAL((B1-B11*SQRT(ARG1))*CEXP0),REAL(0.0,8))

EP2E12=PI*MAX(REAL((B2-B22*SQRT(ARG2))*CEXP00),REAL(0.0,8))
EP2E1=MAX(EP2E11+EP2E12,REAL(0.0,8))

! REAL PART OF DIELECTRIC FUNCTION: (Ec)

```

Appendix Subprograms for Refractive Indices Calculation

CE=(1.0,0.0)-EE/(Ec*Ec)

EP2EC=REAL(C/(CE*CE+EE*((G/Ec)*(G/Ec))))

EP1EC=REAL(CE*EP2EC)

! IMAGINARY PART OF DIELECTRIC FUNCTION: (Ec)

EP2EC=(E*G/Ec)*EP2EC

! IMAGINARY PART OF DIELECTRIC FUNCTION: INDIRECT EDGE

K=[2*PI/A] (X->GAMMA)

EQ1=E-Ei

EP2EI=(D*EEI*(EQ1*EQ1))*MIN(EXP(-fi*(E-Eic)),REAL(1.0,8))

! DO ALL THE HEAVYSIDE FUNCTIONS

IF (E<E0) THEN

EP2E0=0.0

EP2E1=0.0

EP2EC=0.0

EP2EI=0.0

END IF

IF (E<E1) THEN

EP2E1=0.0

END IF

! MULTIPLY THE IMAGINARY PART BY HEAVYSIDE FUNCTION

! INDEX IS THE REAL PART OF THE SQUARE ROOT

! OF THE COMPLEX DIELECTRIC FUNCTION

EPSILON1=einf+EP1E0+EP1E1+EP1EC

Appendix Subprograms for Refractive Indices Calculation

```
EPSILON2=EP2E0+EP2E1+EP2EC+EP2EI
ARG1=EPSILON1*(1.0,0.0) + EPSILON2*(0.0,1.0)
NEFF=REAL(SQRT(ARG1))
RETURN
END SUBROUTINE sALGAAS2
```

In(1-X)Ga(X)As(Y)P(1-Y)

```
SUBROUTINE sInGaAsP(XLAMBDA,X,Y,XN,I)
USE INFO_MOD
implicit none
!mm IMPLICIT REAL*8 (A-H,O-Z)
REAL(8), INTENT(IN) :: X,Y,XLAMBDA
REAL(8), INTENT(OUT) :: XN
INTEGER, INTENT(IN) :: I
REAL(8) :: HV,A,B,EO,EDO,EDD,XO,XSO,F1,F2,X1,X2,X3,X4

!MM-Notify
WRITE(STDOUT_RD,*) 'Using InGaAsP Material System'
!MM-Notify

! 10 WRITE(*,*) ' INPUT X,Y AND PHOTON WAVELENGTH FOR InGaAsP'
! WRITE(*,*) ' X=, Y=, LAMBDA='
! READ (*,*) X,Y,XLAMBDA
! WRITE(*,*) ' InGaAsP'
HV=1.24/XLAMBDA
! WRITE(*,*) ' FOR LATTICE MATCHED, INPUT 1,--STRAIN INPUT 2'
! WRITE(*,*) ' INPUT = ?'
```

Appendix Subprograms for Refractive Indices Calculation

```

!  READ (*,*) I
  IF (I.EQ.1) THEN
    A=8.4-3.4*Y
    B=6.6+3.4*Y
    EO=1.35-0.72*Y+0.12*(Y**2)
    EDD=1.466-0.557*Y+0.129*Y**2
  ELSE IF (I.EQ.2) THEN
    A=(1-X)*Y*5.14+(1-X)*(1-Y)*8.4+X*Y*6.3+X*(1-Y)*22.25
    B=(1-X)*Y*10.15+(1-X)*(1-Y)*6.6+X*Y*9.4+X*(1-Y)*0.9
!c  EO=(1-X)*Y*0.36+(1-X)*(1-Y)*1.35+X*Y*1.424+X*(1-Y)*2.74
    EO=1.35-0.72*Y+0.12*(Y**2)
    EDO=(1-X)*Y*0.38+(1-X)*(1-Y)*0.11+X*Y*0.34+X*(1-Y)*0.08
    EDD=EDO+EO
  ELSE
  END IF
  XO=HV/EO
  XSO=HV/EDD
  F1=(XO**(-2))*(2-((1+XO)**0.5)-((1-XO)**0.5))
  F2=(XSO**(-2))*(2-((1+XSO)**0.5)-((1-XSO)**0.5))
  X1=((EO/(EDD))**(1.5))/2
  X2=F1+X1*F2
  X3=A*X2
  X4=X3+B
  XN=SQRT(X4)
!  WRITE(*,*) ' REFRACTIVE INDEX=', XN
!  WRITE(*,*) ' FOR NEW INPUT I=1, STOP I=2'
!  WRITE(*,*) ' I='
!  READ (*,*) I
!  IF (I.EQ.1) THEN
!  GO TO 10
!  ELSE IF (I.EQ.2) THEN

```

Appendix Subprograms for Refractive Indices Calculation

```
!   GO TO 20
!   ELSE
!   END IF
! 20 RETURN
   RETURN
END SUBROUTINE sInGaAsP
```

Al(X)Ga(Y)In(1-X-Y)As

```
   SUBROUTINE sAlGaInAs(LAMBDA,XX,QY,XN)
   USE INFO_MOD

   implicit none
!mm IMPLICIT REAL*8 (A-H,O-Z)
   REAL(8), INTENT(IN) :: XX,QY,LAMBDA
   REAL(8), INTENT(OUT) :: XN
!   INTEGER :: I
   REAL(8) :: HV,EO,EDO,XO,EDD,XSO,A,B,F1,F2,X1,X2,X3,X4
   !MM-Notify
   WRITE(STDOUT_RD,*) 'Using AlGaInAs Material System'
   !MM-Notify

! 10 WRITE(*,*) ' INPUT XX, QY AND PHOTON WAVELENGTH FOR AlGaInAs'
!   WRITE(*,*) ' XX= , QY=, LAMBDA='

!   READ (*,*) XX,QY,LAMBDA
!C   XLAMBDA=LAMBDA*1000.D0
```

Appendix Subprograms for Refractive Indices Calculation

```

!C  X=XX/0.48
!C  IF ((X.LT.0.3).AND.(LAMBDA.EQ.1.3)) THEN
!C  XN=DSQRT(((1.-XX-QY)*14.6+QY*13.2+XX*10.06)-0.17D0
!C  ELSEIF ((X.LT.0.3).AND.(LAMBDA.EQ.1.55)) THEN
!C  XN=DSQRT(((1.-XX-QY)*14.6+QY*13.2+XX*10.06)-0.31D0
!C  PRINT*, ' XN=',XN
!C  ELSEIF (X.GE.0.3) THEN
!C  A=9.689-1.012*X
!C  B=1.590-0.376*X
!C  C=1102.4-702.0*X+330.4*(X*X)
!C  XN=DSQRT(A+((B*XLAMBDA**2)/(XLAMBDA**2-C**2)))
!C  ELSE
!C  ENDIF

!  WRITE(*,*) ' AlGaInAs'
HV=1.24D0/LAMBDA
EO=0.75D0+1.548D0*XX
EDO=XX*0.28+QY*0.34+(1-XX-QY)*0.38
XO=HV/EO
EDD=EDO+EO
XSO=HV/EDD
A=XX*25.30+QY*6.30+(1-XX-QY)*5.14
B=XX*(-0.80)+QY*9.40+(1-XX-QY)*10.15
F1=(XO**(-2.D0))*(2.D0-((1.D0+XO)**0.5)-((1-XO)**0.5))
F2=(XSO**(-2.D0))*(2.D0-((1.D0+XSO)**0.5)-((1-XSO)**0.5))
X1=((EO/EDD)**(1.5))/2
X2=F1+X1*F2
X3=A*X2
X4=X3+B
XN=SQRT(X4)
!  WRITE(*,*) ' THE REFRACTIVE INDEX IS=', XN

```

Appendix Subprograms for Refractive Indices Calculation

```
! WRITE(*,*) ' FOR NEW INPUT I=1, STOP I=2'  
! WRITE(*,*) ' I='  
! READ (*,*) I  
! IF (I.EQ.1) THEN  
!   GO TO 10  
! ELSE IF (I.EQ.2) THEN  
!   GO TO 20  
! ELSE  
!   END IF  
! 20 RETURN  
   RETURN  
   END SUBROUTINE sAlGaInAs
```

Al(X)Ga(1-X)In(Y)As(1-Y) 2

```
SUBROUTINE sAlGaInAs2(LAMBDA,XX,QY,XN)  
USE INFO_MOD  
  
implicit none  
!mm IMPLICIT REAL*8 (A-H,O-Z)  
REAL(8), INTENT(IN) :: XX,QY,LAMBDA  
REAL(8), INTENT(OUT) :: XN  
!   INTEGER :: I  
REAL(8) :: HV,EO,EDO,XO,EDD,XSO,A,B,C,X,XLAMBDA  
!MM-Notify  
WRITE(STDOUT_RD,*) 'Using AlGaInAs (Mondrys) Material System'  
!MM-Notify  
XLAMBDA=LAMBDA*1000.D0  
X=XX/0.48
```

Appendix Subprograms for Refractive Indices Calculation

```
IF ((X < 0.3d0).AND.(LAMBDA == 1.3d0)) THEN
  XN=SQRT((1.-XX-QY)*14.6+QY*13.2+XX*10.06)-0.17d0
ELSE IF ((X < 0.3d0).AND.(LAMBDA == 1.55d0)) THEN
  XN=SQRT((1.-XX-QY)*14.6+QY*13.2+XX*10.06)-0.31D0
ELSE IF ((X < 0.3d0).AND.(LAMBDA == 1.4d0)) THEN
  XN=SQRT((1.-XX-QY)*14.6+QY*13.2+XX*10.06)-0.226d0
ELSE IF (X >= 0.3) THEN
  A=9.689-1.012*X
  B=1.590-0.376*X
  C=1102.4-702.0*X+330.4*(X*X)
  XN=SQRT(A+((B*XLAMBDA**2)/(XLAMBDA**2-C**2)))
ELSE
  END IF
RETURN
END SUBROUTINE sAlGaInAs2
```

Al(X)Ga(1-X)P(Y)Sb(1-Y)

```
SUBROUTINE sAlGaPSb(XLAMBDA,X,Y,XN)
  USE INFO_MOD
  implicit none
!mm IMPLICIT REAL*8 (A-H,O-Z)
  REAL(8), INTENT(IN) :: X,Y,XLAMBDA
  REAL(8), INTENT(OUT) :: XN
  ! INTEGER :: I

  REAL(8) :: HV,A,B,EO,EDO,EDD,XO,XSO,F1,F2,X1,X2,X3,X4
  !MM-Notify
  WRITE(STDOUT_RD,*) 'Using AlGaPSb Material System'
```


Appendix Subprograms for Refractive Indices Calculation

```

!MM-Notify
! 10 WRITE(*,*) ' INPUT X,Y AND PHOTON WAVELENGTH FOR AlGaPSb'
!  WRITE(*,*) ' X=, Y=, LAMBDA='
!  READ (*,*) X,Y,XLAMBDA
!  WRITE(*,*) ' AlGaPSb'
    HV=1.24/XLAMBDA
    A=(1-X)*Y*22.25+(1-X)*(1-Y)*4.05+X*Y*24.10+X*(1-Y)*59.68
    B=(1-X)*Y*0.9+(1-X)*(1-Y)*12.66+X*Y*(-2.0)+X*(1-Y)*(-9.53)
!c  EO=(1-X)*Y*2.74+(1-X)*(1-Y)*0.72+X*Y*3.58+X*(1-Y)*2.22
    EO=0.885+2.33*X-1.231*(X**2)
    EDO=(1-X)*Y*0.08+(1-X)*(1-Y)*0.82+X*Y*0.07+X*(1-Y)*0.65
    EDD=EDO+EO
    XO=HV/EO
    XSO=HV/EDD
    F1=(XO**(-2))*(2-((1+XO)**0.5)-((1-XO)**0.5))
    F2=(XSO**(-2))*(2-((1+XSO)**0.5)-((1-XSO)**0.5))
    X1=((EO/EDD)**(1.5))/2
    X2=F1+X1*F2
    X3=A*X2
    X4=X3+B
    XN=SQRT(X4)
!  WRITE(*,*) ' REFRACTIVE INDEX=', XN
!  WRITE(*,*) ' FOR NEW INPUT I=1, STOP I=2'
!  WRITE(*,*) ' I='
!  READ (*,*) I
!  IF (I.EQ.1) THEN
!    GO TO 10
!  ELSE IF (I.EQ.2) THEN
!    GO TO 20
!  ELSE
!  END IF

```

Appendix Subprograms for Refractive Indices Calculation

```
! 20 RETURN
  RETURN
  END SUBROUTINE sAlGaPSb
```

Al(X)Ga(1-X)As(Y)Sb(1-Y)

```
  SUBROUTINE sAlGaAsSb(XLAMBDA,X,Y,XN)

  USE INFO_MOD
  implicit none
!mm IMPLICIT REAL*8 (A-H,O-Z)
  REAL(8), INTENT(IN) :: X,Y,XLAMBDA
  REAL(8), INTENT(OUT) :: XN
  ! INTEGER :: I
  REAL(8) :: HV,A,B,EO,EDO,EDD,XO,XSO,F1,F2,X1,X2,X3,X4
  !MM-Notify
  WRITE(STDOUT_RD,*) 'Using AlGaAsSb Material System'
  !MM-Notify
  ! 10 WRITE(*,*) ' INPUT X,Y AND PHOTON WAVELENGTH FOR AlGaAsSb'
  !  WRITE(*,*) ' X=, Y=, LAMBDA='
  !  READ (*,*) X,Y,XLAMBDA
  !  WRITE(*,*) ' AlGaASSb'
  HV=1.24/XLAMBDA
  A=(1-X)*Y*6.30+(1-X)*(1-Y)*4.05+X*Y*25.30+X*(1-Y)*59.68
  B=(1-X)*Y*9.4+(1-X)*(1-Y)*12.66+X*Y*(-0.8)+X*(1-Y)*(-9.53)
!C  EO=(1-X)*Y*1.42+(1-X)*(1-Y)*0.72+X*Y*2.95+X*(1-Y)*2.22
  EO=0.829+1.822*X-0.22*(X**2)
  EDO=(1-X)*Y*0.34+(1-X)*(1-Y)*0.82+X*Y*0.28+X*(1-Y)*0.65
  EDD=EDO+EO
  XO=HV/EO
```

Appendix Subprograms for Refractive Indices Calculation

```
XSO=HV/EDD
F1=(XO**(-2))*(2-((1+XO)**0.5)-((1-XO)**0.5))
F2=(XSO**(-2))*(2-((1+XSO)**0.5)-((1-XSO)**0.5))
X1=((EO/EDD)**(1.5))/2
X2=F1+X1*F2
X3=A*X2
X4=X3+B
XN=SQRT(X4)
! WRITE(*,*) ' REFRACTIVE INDEX=', XN
! WRITE(*,*) ' FOR NEW INPUT I=1, STOP I=2'
! WRITE(*,*) ' I='
! READ (*,*) I
! IF (I.EQ.1) THEN
!   GO TO 10
! ELSE IF (I.EQ.2) THEN
!   GO TO 20
! ELSE
!   END IF
! 20 RETURN
RETURN
END SUBROUTINE sAlGaAsSb
```

Al(X)In(1-X)As(Y)Sb(1-Y)

```
SUBROUTINE sAlInAsSb(XLAMBDA,X,Y,XN)
```

```
USE INFO_MOD
```

```
implicit none
```

Appendix Subprograms for Refractive Indices Calculation

```

!mm IMPLICIT REAL*8 (A-H,O-Z)
    REAL(8), INTENT(IN) :: X,Y,XLAMBDA
    REAL(8), INTENT(OUT) :: XN
!   INTEGER :: I
    REAL(8) :: HV,A,B,EO,EDO,EDD,XO,XSO,F1,F2,X1,X2,X3,X4

!MM-Notify
    WRITE(STDOUT_RD,*) 'Using AlInAsSb Material System'
!MM-Notify

! 10 WRITE(*,*) ' INPUT X,Y AND PHOTON WAVELENGTH FOR AlInAsSb'
!   WRITE(*,*) ' X=, Y=, LAMBDA='
!   READ (*,*) X,Y,XLAMBDA
!   WRITE(*,*) ' AlInAsSb'
    HV=1.24/XLAMBDA
    A=(1-X)*Y*5.14+(1-X)*(1-Y)*7.91+X*Y*25.30+X*(1-Y)*59.68
    B=(1-X)*Y*10.15+(1-X)*(1-Y)*13.07+X*Y*(-0.8)+X*(1-Y)*(-9.53)
!C   EO=(1-X)*Y*0.36+(1-X)*(1-Y)*0.17+X*Y*2.95+X*(1-Y)*2.22
    EO=-0.173+4.014*X-1.418*(X**2)
    EDO=(1-X)*Y*0.38+(1-X)*(1-Y)*0.81+X*Y*0.28+X*(1-Y)*0.65
    EDD=EO+EDO
    XO=HV/EO
    XSO=HV/EDD
    F1=(XO**(-2))*(2-((1+XO)**0.5)-((1-XO)**0.5))
    F2=(XSO**(-2))*(2-((1+XSO)**0.5)-((1-XSO)**0.5))
    X1=((EO/EDD)**(1.5))/2
    X2=F1+X1*F2
    X3=A*X2
    X4=X3+B
    XN=SQRT(X4)
!   WRITE(*,*) ' REFRACTIVE INDEX=', XN

```

Appendix Subprograms for Refractive Indices Calculation

```
! WRITE(*,*) ' FOR NEW INPUT I=1, STOP I=2'  
! WRITE(*,*) ' I='  
! READ (*,*) I  
  
! IF (I.EQ.1) THEN  
!   GO TO 10  
! ELSE IF (I.EQ.2) THEN  
!   GO TO 20  
! ELSE  
!   END IF  
! 20 RETURN  
   RETURN  
   END SUBROUTINE sAlInAsSb
```

Ga(X)In(1-X)P(Y)Sb(1-Y)

```
   SUBROUTINE sGaInPSb(XLAMBDA,X,Y,XN)  
   USE INFO_MOD  
   implicit none  
!mm IMPLICIT REAL*8 (A-H,O-Z)  
   REAL(8), INTENT(IN) :: X,Y,XLAMBDA  
   REAL(8), INTENT(OUT) :: XN  
!   INTEGER :: I  
   REAL(8) :: HV,A,B,EO,EDO,EDD,XO,XSO,F1,F2,X1,X2,X3,X4  
   !MM-Notify  
   WRITE(STDOUT_RD,*) 'Using GaInPSb Material System'  
   !MM-Notify  
! 10 WRITE(*,*) ' INPUT X,Y AND PHOTON WAVELENGTH FOR GaInPSb'  
!   WRITE(*,*) ' X=, Y=, LAMBDA='  
!   READ (*,*) X,Y,XLAMBDA
```

Appendix Subprograms for Refractive Indices Calculation

```

!  WRITE(*,*) ' GaInPSb'
    HV=1.24/XLAMBDA
    A=(1-X)*Y*8.4+(1-X)*(1-Y)*7.91+X*Y*22.25+X*(1-Y)*4.05
    B=(1-X)*Y*6.6+(1-X)*(1-Y)*13.07+X*Y*0.9+X*(1-Y)*12.66
!C  EO=(1-X)*Y*1.35+(1-X)*(1-Y)*0.17+X*Y*2.74+X*(1-Y)*0.72
    EO=1.326-0.018*X-0.34*(X**2)
    EDO=(1-X)*Y*0.11+(1-X)*(1-Y)*0.81+X*Y*0.08+X*(1-Y)*0.82
    EDD=EDO+EO
    XO=HV/EO
    XSO=HV/EDD
    F1=(XO**(-2))*(2-((1+XO)**0.5)-((1-XO)**0.5))
    F2=(XSO**(-2))*(2-((1+XSO)**0.5)-((1-XSO)**0.5))
    X1=((EO/EDD)**(1.5))/2
    X2=F1+X1*F2
    X3=A*X2
    X4=X3+B
    XN=SQRT(X4)

!  WRITE(*,*) ' REFRACTIVE INDEX=', XN
!  WRITE(*,*) ' FOR NEW INPUT I=1, STOP I=2'
!  WRITE(*,*) ' I='
!  READ (*,*) I
!  IF (I.EQ.1) THEN
!    GO TO 10
!  ELSE IF (I.EQ.2) THEN
!    GO TO 20
!  ELSE
!  END IF
! 20 RETURN
    RETURN
    END SUBROUTINE sGaInPSb

```

AlAs(X)Sb(1-X)

```
SUBROUTINE sAlAsSb(XLAMBDA,X,XN)

USE INFO_MOD
implicit none
!mm IMPLICIT REAL*8 (A-H,O-Z)
REAL(8), INTENT(IN) :: X,XLAMBDA
REAL(8), INTENT(OUT) :: XN
! INTEGER :: I
REAL(8) :: HV,A,B,EO,EDO,EDD,XO,XSO,F1,F2,X1,X2,X3,X4
!MM-Notify
WRITE(STDOUT_RD,*) 'Using AlAsSb Material System'
!MM-Notify
! 10 WRITE(*,*) ' INPUT X,Y AND PHOTON WAVELENGTH FOR AlAsSb'
! WRITE(*,*) ' X= ?, LAMBDA='
! READ (*,*) X,XLAMBDA
! WRITE(*,*) ' AlAsSb'
HV=1.24/XLAMBDA
A=(1-X)*59.68+X*25.30
B=(1-X)*(-9.53)+X*(-0.80)
EO=1.7+0.53*X
EDO=(1-X)*0.65+X*0.28
EDD=EDO+EO
XO=HV/EO
XSO=HV/EDD
F1=(XO**(-2))*(2-((1+XO)**0.5)-((1-XO)**0.5))
F2=(XSO**(-2))*(2-((1+XSO)**0.5)-((1-XSO)**0.5))
```

Appendix Subprograms for Refractive Indices Calculation

```
X1=((EO/EDD)**(1.5))/2
X2=F1+X1*F2
X3=A*X2
X4=X3+B
XN=SQRT(X4)
! WRITE(*,*) ' REFRACTIVE INDEX=', XN
! WRITE(*,*) ' FOR NEW INPUT I=1, STOP I=2'
! WRITE(*,*) ' I='
! READ (*,*) I
! IF (I.EQ.1) THEN
!   GO TO 10
! ELSE IF (I.EQ.2) THEN
!   GO TO 20
! ELSE
!   END IF
! 20 RETURN
RETURN
END SUBROUTINE sAlAsSb
```

Al(x)Ga(1-x)0.5In(0.5)P

```
SUBROUTINE sAlGaInP(XLAMBDA,X,XN)
USE INFO_MOD
implicit none
!mm IMPLICIT REAL*8 (A-H,O-Z)
REAL(8), INTENT(IN) :: X,XLAMBDA
REAL(8), INTENT(OUT) :: XN
! INTEGER :: I
REAL(8) :: HV,EO,ED
```


Appendix Subprograms for Refractive Indices Calculation

```
!MM-Notify
WRITE(STDOUT_RD,*) 'Using AlGaInP Material System'
!MM-Notify
! 10 WRITE(*,*) '(AlxGa(1-x))0.5In0.5P--Eg=1.9+0.6*X'
! WRITE(*,*) ' INPUT X AND PHOTON WAVELENGTH FOR AlGaInP'
! WRITE(*,*) ' X= ?, LAMBDA='
! READ (*,*) X,XLAMBDA
! WRITE(*,*) '(AlxGa(1-x))0.5In0.5P--Eg=1.9+0.6*X'
HV=1.24/XLAMBDA
EO=3.39+0.62*X
ED=28.07+1.72*X
XN=SQRT((EO*ED/(EO**2-HV**2))+1)
! WRITE(*,*) ' REFRACTIVE INDEX=', XN
! WRITE(*,*) ' FOR NEW INPUT I=1, STOP I=2'
! WRITE(*,*) ' I='
! READ (*,*) I
! IF (I.EQ.1) THEN
! GO TO 10
! ELSE IF (I.EQ.2) THEN

! GO TO 20
! ELSE
! END IF
! 20 RETURN
RETURN
END SUBROUTINE sAlGaInP
```

In(1-x)Ga(x)As [matched to InP]

```
SUBROUTINE sInGaAs1(XLAMBDA,X,XN)
```

Appendix Subprograms for Refractive Indices Calculation

```

USE INFO_MOD
implicit none
!mm IMPLICIT REAL*8 (A-H,O-Z)
REAL(8), INTENT(IN) :: X,XLAMBDA
REAL(8), INTENT(OUT) :: XN
! INTEGER :: I
REAL(8) :: A,B,HV,EO,EDO,EDD,XO,XSO,F1,F2,X1,X2,X3,X4
!MM-Notify
WRITE(STDOUT_RD,*) 'Using InGaAs-1 Material System'
!MM-Notify
! 10 WRITE(*,*) ' In(1-x)Ga(x)As/InP'
! WRITE(*,*) ' INPUT X AND PHOTON WAVELENGTH FOR In(1-x)Ga(x)As'
! WRITE(*,*) ' X= ?, LAMBDA='
! READ (*,*) X,XLAMBDA
! WRITE(*,*) ' In(1-x)Ga(x)As/InP'
A=(1-X)*5.14+X*6.30
B=(1-X)*10.15+X*9.40
HV=1.24/XLAMBDA
EO=0.324+0.7*X+0.4*(X**2)
EDO=(1-X)*0.38+X*0.34
EDD=EDO+EO
XO=HV/EO
XSO=HV/EDD
F1=(XO**(-2))*(2-((1+XO)**0.5)-((1-XO)**0.5))
F2=(XSO**(-2))*(2-((1+XSO)**0.5)-((1-XSO)**0.5))
X1=((EO/(EDD))**(1.5))/2
X2=F1+X1*F2
X3=A*X2
X4=X3+B
XN=SQRT(X4)
! WRITE(*,*) ' REFRACTIVE INDEX=', XN

```

Appendix Subprograms for Refractive Indices Calculation

```
!  WRITE(*,*) ' FOR NEW INPUT I=1, STOP I=2'  
!  WRITE(*,*) ' I='  
  
!  READ (*,*) I  
!  IF (I.EQ.1) THEN  
!    GO TO 10  
!  ELSE IF (I.EQ.2) THEN  
!    GO TO 20  
!  ELSE  
!    END IF  
! 20 RETURN  
    RETURN  
    END SUBROUTINE sInGaAs1
```

In(1-x)Ga(x)As [matched to GaAs]

```
    SUBROUTINE sInGaAs2(XLAMBDA,X,XN)  
    USE INFO_MOD  
    implicit none  
!mm  IMPLICIT REAL*8 (A-H,O-Z)  
    REAL(8), INTENT(IN) :: X,XLAMBDA  
    REAL(8), INTENT(OUT) :: XN  
!  INTEGER :: I  
    REAL(8) :: A,B,HV,EO,EDO,EDD,XO,XSO,F1,F2,X1,X2,X3,X4  
    !MM-Notify  
    WRITE(STDOUT_RD,*) 'Using InGaAs-2 Material System'  
    !MM-Notify  
! 10 WRITE(*,*) ' In(1-x)Ga(x)As/GaAs'  
!  WRITE(*,*) ' INPUT X AND PHOTON WAVELENGTH FOR In(1-x)Ga(x)As'  
!  WRITE(*,*) ' X= ?, LAMBDA='
```

Appendix Subprograms for Refractive Indices Calculation

```
! READ (*,*) X,XLAMBDA
! WRITE(*,*) ' In(1-x)Ga(x)As/GaAs'
A=(1-X)*5.14+X*6.30
B=(1-X)*10.15+X*9.40
HV=1.24/XLAMBDA
EO=0.36+0.509*X+0.555*(X**2)
EDO=(1-X)*0.38+X*0.34
EDD=EDO+EO
XO=HV/EO
XSO=HV/EDD
F1=(XO**(-2))*(2-((1+XO)**0.5)-((1-XO)**0.5))
F2=(XSO**(-2))*(2-((1+XSO)**0.5)-((1-XSO)**0.5))
X1=((EO/(EDD))**(1.5))/2
X2=F1+X1*F2
X3=A*X2
X4=X3+B
XN=SQRT(X4)
! WRITE(*,*) ' REFRACTIVE INDEX=', XN
! WRITE(*,*) ' FOR NEW INPUT I=1, STOP I=2'
! WRITE(*,*) ' I='
! READ (*,*) I
! IF (I.EQ.1) THEN
!   GO TO 10
! ELSE IF (I.EQ.2) THEN
!   GO TO 20
! ELSE
!   END IF
! 20 RETURN
RETURN
END SUBROUTINE sInGaAs2
```

Ga(x)In(1-x)P [matched to GaAs]

```
SUBROUTINE sGaInP(XLAMBDA,X,XN)
USE INFO_MOD
implicit none
!mm IMPLICIT REAL*8 (A-H,O-Z)
REAL(8), INTENT(IN) :: XLAMBDA, X
REAL(8), INTENT(OUT) :: XN
! REAL(8) :: X,XLAMBDA
! INTEGER :: I
REAL(8) :: A,B,HV,EO,EDO,EDD,XO,XSO,F1,F2,X1,X2,X3,X4
!MM-Notify
WRITE(STDOUT_RD,*) 'Using GaInP Material System'
!MM-Notify
! 10 WRITE(*,*) ' GaxIn(1-x)P/GaAs'
! WRITE(*,*) ' INPUT X AND PHOTON WAVELENGTH FOR GaxIn(1-x)P'
! WRITE(*,*) ' X= ?, LAMBDA='
! READ (*,*) X,XLAMBDA
! WRITE(*,*) ' GaxIn(1-x)P/GaAs'
A=(1-X)*8.4+X*22.25
B=(1-X)*6.6+X*0.9
HV=1.24/XLAMBDA
!c EO=1.351+0.643*X+0.786*(X**2)
EO=1.35*(1-X)+2.74*X
EDO=(1-X)*0.11+X*0.08
EDD=EDO+EO
XO=HV/EO
XSO=HV/EDD
```

Appendix Subprograms for Refractive Indices Calculation

```
F1=(XO**(-2))*(2-((1+XO)**0.5)-((1-XO)**0.5))
F2=(XSO**(-2))*(2-((1+XSO)**0.5)-((1-XSO)**0.5))
X1=((EO/(EDD))**(1.5))/2
X2=F1+X1*F2
X3=A*X2
X4=X3+B
!c EO=(3.39+0.62*X)
!c ED=(28.07+1.72*X)
!c X4=(EO*ED/(EO**2-HV**2))+1
XN=SQRT(X4)
! WRITE(*,*) ' REFRACTIVE INDEX=', XN
! WRITE(*,*) ' FOR NEW INPUT I=1, STOP I=2'
! WRITE(*,*) ' I='
! READ (*,*) I
! IF (I.EQ.1) THEN
!   GO TO 10
! ELSE IF (I.EQ.2) THEN
!   GO TO 20
! ELSE
!   END IF
! 20 RETURN
RETURN
END SUBROUTINE sGaInP
```

InGaAsP using PL [matched to InP]

(See reference 8 in Section 3.3)

```
SUBROUTINE sInGaAsPPL(WVL,XPERCENT,EFFINDEX)
  implicit none
```

Appendix Subprograms for Refractive Indices Calculation

```
REAL(8), INTENT(IN) :: WVL, XPERCENT
REAL(8), INTENT(OUT) :: EFFINDEX

REAL(8)          :: e1,e2,ep,e,a1,a2,xtemp
xtemp=0.0000000000000000
xtemp=XPERCENT
e1=2.5048
e2=0.1638
ep=1.24/xtemp
e =1.24/WVL

a1=13.3510-5.4554*ep+1.2332*(ep**2)
a2=0.7140-0.3606*ep

EFFINDEX=(1+(a1/(1-((e/(ep+e1))**2)))+(a2/(1-((e/(ep+e2))**2))))**0.5
RETURN
END SUBROUTINE sInGaAsPPL
```

InGaAsP [matched to InP]

```
SUBROUTINE sInGaAsPInP(WVL, XPERCENT, EFFINDEX)

USE INFO_MOD
implicit none

REAL(8), INTENT(IN) :: WVL, XPERCENT
REAL(8), INTENT(OUT) :: EFFINDEX
!
REAL(8) :: H,A1,A2,EP,E1,E2,C,EC,TERM1,TERM2
REAL(8) :: EPSILON,E
```

Appendix Subprograms for Refractive Indices Calculation

```
!MM-Notify
WRITE(STDOUT_RD,*) 'Using InGaAsPInP Material System'
!MM-Notify
IF (WVL <= XPERCENT) THEN
  WRITE(STDOUT_RD,*) ' ERROR: This Material System not valid for lambda <=
lambdapl'
WRITE(STDOUT_RD,*) WVL, XPERCENT
  WRITE(STDOUT_RD,*) ' ERROR: Please use the InGaAsP MatSys '
  RETURN
END IF
```

! All energies are in Electron Volts

! Speed of light 'C', Plank's constant 'H' and electron charge 'EC'

```
C = 2.9979E8
H = 6.6261E-34
EC = 1.6022E-19
EP = (H*C)/(XPERCENT*1E-6*EC)
A1 = 13.3510 - (5.4554*EP) + 1.2332*(EP**2)
A2 = 0.7140 - 0.3606*EP
E1 = 2.5048
E2 = 0.1638
E = (H*C)/(WVL*1E-6*EC)
TERM1 = A1/(1 - ((E/(EP + E1))**2))
TERM2 = A2/(1 - ((E/(EP + E2))**2))
EPSILON = 1 + TERM1 + TERM2
EFFINDX = SQRT(EPSILON)
RETURN
END SUBROUTINE sInGaAsPInP
```


Appendix Subprograms for Refractive Indices Calculation